

*recd with letter dtd
1/15/97*

9701210068 970115

NUREG/CR-6513, NO.1
CNWRA 96-01A

**NRC HIGH-LEVEL RADIOACTIVE WASTE PROGRAM
ANNUAL PROGRESS REPORT
FISCAL YEAR 1996**

Budhi Sagar (Editor)

**Center for Nuclear Waste Regulatory Analyses
Southwest Research Institute**

**Prepared for
U.S. Nuclear Regulatory Commission**

102. D

9701210090 970115
PDR WASTE
WM-11 PDR

NUREG/CR-6513, NO.1
CNWRA 96-01A

**NRC HIGH-LEVEL RADIOACTIVE WASTE PROGRAM
ANNUAL PROGRESS REPORT
FISCAL YEAR 1996**

Manuscript Completed: November 1996
Data Published:

B. Sagar (Editor)

Center for Nuclear Waste Regulatory Analyses
Southwest Research Institute
6220 Culebra Road
San Antonio, TX 78228-0510

M.V. Federline, Deputy Director
Division of Waste Management

Prepared for
Division of Waste Management
Office of Nuclear Material Safety and Safeguards
U.S. Nuclear Regulatory Commission
Washington, DC 20555
NRC FIN D1035

FOREWORD

This is the first in a series of annual reports prepared jointly by the Nuclear Regulatory Commission (NRC) staff from the Division of Waste Management (DWM) and staff from the Center for Nuclear Waste Regulatory Analyses (CNWRA). Each Key Technical Issue team was headed by two principal investigators: one each from the DWM and the CNWRA. Primary authors of each chapter were responsible for writing the text that describes the work of many investigators. Names of the primary authors, technical contributors, and principal investigators are given below, and are also included at the beginning of each chapter. This report was edited by B. Sagar (CNWRA).

PRIMARY AUTHORS

NRC: T.M. Ahn, J.W. Bradbury, R.B. Codell, N.M. Coleman, B.N. Jagannath, R.L. Johnson, P.S. Justus, M.P. Lee, B.W. Leslie, T.J. McCartin, M.S. Nataraja, J.S. Trapp, and R.G. Wescott

CNWRA: P.J. Angell, R.G. Baca, A.C. Bagtzoglou, R. Chen, A.H. Chowdhury, C.B. Connor, G.A. Cragnolino, A.R. DeWispelare, D.S. Dunn, D.A. Ferrill, A. Ghosh, R.T. Green, B.E. Hill, S.M. Hsiung, M.S. Jarzemba, P.C. Lichtner, P.C. Mackin, H.K. Manaktala, R.D. Manteufel, S. Mohanty, W.M. Murphy, G.I. Ofoegbu, R.T. Pabalan, E.C. Percy, D.A. Pickett, B. Sagar, N. Sridhar, J.A. Stamatakos, S.A. Stothoff, D.R. Turner, and G.W. Wittmeyer

TECHNICAL CONTRIBUTORS

NRC: R. Abu-Eid, J.H. Austin, M.J. Bell, J.W. Bradbury, R.E. Cady, R.B. Codell, N.M. Coleman, B.J. Davis, M.V. Federline, J.R. Firth, B.N. Jagannath, J. Kotra, M.P. Lee, B.W. Leslie, T.J. McCartin, S.M. McDuffie, M.S. Nataraja, R.B. Neel, C.W. Reamer, J.S. Trapp, and R.G. Wescott

CNWRA: M.P. Ahola, M.G. Almendarez, P.J. Angell, R.G. Baca, A.C. Bagtzoglou, D.P. Cederquist, R. Chen, A.H. Chowdhury, C.B. Connor, F.M. Conway, A.R. DeWispelare, D.A. Ferrill, A. Ghosh, S.L. Greenan, D.B. Henderson, B.E. Hill, M.E. Hill, S.M. Hsiung, A.M. Hoh, K.M. James, R.W. Janetzke, M.S. Jarzemba, H. Karimi, R.V. Klar, P.L. LaFemina, P.A. LaPlante, P.C. Lichtner, H.L. McKague, P.C. Mackin, S.B. Magsino, R.D. Manteufel, R.H. Martin, S. Mohanty, M.A. Muller, W.M. Murphy, G.I. Ofoegbu, R.T. Pabalan, W.C. Patrick, E.C. Percy, D.A. Pickett, J.D. Prikryl, B.R. Rahe, K.J. Smart, N. Sridhar, J.A. Stamatakos, G.L. Stirewalt, S.A. Stothoff, T.L. Tolley, D.R. Turner, and G.W. Wittmeyer

CONSULTANTS: F.P. Bertetti, S. Larose, Y.-M. Pan, R.A. Rapp, G. Rice, and D.A. Woolhiser

KEY TECHNICAL ISSUE CO-LEADS

NRC: J.W. Bradbury, K.C. Chang, N.M. Coleman, B.N. Jagannath, P.S. Justus, B.W. Leslie, T.J. McCartin, J.A. Pohle, J.S. Trapp, and R.G. Wescott

CNWRA: R.G. Baca, A.H. Chowdhury, H.L. McKague, E.C. Percy, and N. Sridhar

ABSTRACT

This annual status report for fiscal year 1996 documents technical work performed on ten key technical issues (KTI) that are most important to performance of the proposed geologic repository at Yucca Mountain. This report has been prepared jointly by the staff of the Nuclear Regulatory Commission (NRC) Division of Waste Management and the Center for Nuclear Waste Regulatory Analyses. The programmatic aspects of restructuring the NRC repository program in terms of KTIs is discussed and a brief summary of work accomplished is provided in chapter 1. The other ten chapters provide a comprehensive summary of the work in each KTI. Discussions on probability of future volcanic activity and its consequences, impacts of structural deformation and seismicity, the nature of the near-field environment and its effects on container life and source term, flow and transport including effects of thermal loading, aspects of repository design, estimates of system performance, and activities related to the U.S. Environmental Protection Agency standard are provided.

CONTENTS

Section	Page
FIGURES	xiii
TABLES	xvii
ACKNOWLEDGMENTS	xviii
QUALITY OF DATA	xviii
ANALYSES AND CODES	xviii
EXECUTIVE SUMMARY	xix
1 DESCRIPTION OF THE NUCLEAR REGULATORY COMMISSION FY96 REPOSITORY PROGRAM AND ACCOMPLISHMENTS	1-1
1.1 INTRODUCTION	1-1
1.2 EVENTS IMPACTING THE NRC REPOSITORY PROGRAM	1-1
1.3 THE NRC REFOCUSED PRELICENSING PROGRAM	1-3
1.3.1 Revised Prelicensing Objectives	1-3
1.3.2 Refocused Approach	1-4
1.3.3 Prioritized Activities	1-5
1.3.4 Reduced Staff, Restructured Organizations, and Responsibilities	1-5
1.3.5 Advantages and Disadvantages of Refocused Approach	1-6
1.3.6 Importance of Maintaining a Credible Prelicensing Program	1-7
1.4 HIGHLIGHTS OF FY96 TECHNICAL ACCOMPLISHMENTS	1-7
1.5 CONCLUSIONS	1-21
1.6 REFERENCES	1-22
2 IGNEOUS ACTIVITY	2-1
2.1 INTRODUCTION	2-1
2.2 OBJECTIVES AND SCOPE OF WORK	2-2
2.3 SIGNIFICANT TECHNICAL ACCOMPLISHMENTS	2-3
2.3.1 Stabilize Database	2-3
2.3.2 Probability Estimates of Volcanic Disruption	2-6
2.3.2.1 Gravity Data	2-8
2.3.2.2 Fault Dilation-Tendency	2-9
2.3.2.3 Method of Using Structural Data in the Hazard Analysis	2-9
2.3.2.4 Results	2-13
2.3.2.5 Discussion	2-15
2.3.3 Dispersion of Tephra from Basaltic Eruptions	2-16
2.3.3.1 Introduction	2-16
2.3.3.2 Model Parameters	2-18
2.3.3.3 Analog Volcano Data	2-18
2.3.3.4 Sensitivity Analysis	2-19
2.3.3.5 Discussion	2-24
2.3.4 Conclusions	2-25

CONTENTS

Section	Page
2.4	ASSESSMENT OF PROGRESS TOWARD MEETING OBJECTIVES 2-26
2.5	INTEGRATION WITH OTHER KEY TECHNICAL ISSUES 2-28
2.6	REFERENCES 2-28
3	STRUCTURAL DEFORMATION AND SEISMICITY 3-1
3.1	INTRODUCTION 3-1
3.2	OBJECTIVES AND SCOPE OF WORK 3-4
3.3	SIGNIFICANT TECHNICAL ACCOMPLISHMENTS 3-4
3.3.1	Tectonic Models 3-4
3.3.2	Analog Modeling of Pull-Apart Basins 3-5
3.3.2.1	Sequential Development of Pull-Apart Basins 3-6
3.3.2.2	Implications to Seismic Hazard Analyses 3-8
3.3.3	Mechanical (Numerical) Analyses of Faulting at Bare Mountain and Yucca Mountain 3-9
3.3.4	Type I Faults 3-13
3.3.5	Dilation-Tendency of Faults and Fractures and Implications for Groundwater Flow in the Yucca Mountain Region 3-14
3.3.5.1	Dilation-Tendency 3-15
3.3.5.2	Dilation-Tendency Analysis of Yucca Mountain Area Faults and Fractures 3-16
3.3.5.3	Sensitivity Analysis of Transmissivity Anisotropy on Groundwater Flow 3-16
3.3.6	Hangingwall Deformation from Normal Faulting—UDEC (v.2.01) Modeling Calculations 3-18
3.3.7	Summary 3-22
3.4	ASSESSMENT OF PROGRESS TOWARD MEETING OBJECTIVES 3-24
3.4.1	Resolution of Main Key Technical Issue 3-24
3.4.2	Evaluation of U.S. Department of Energy Testable Hypotheses 3-25
3.4.3	Evaluation of Selected U.S. Department of Energy Assumptions 3-26
3.5	INTEGRATION WITH OTHER KEY TECHNICAL ISSUES 3-27
3.6	REFERENCES 3-27
4	EVOLUTION OF THE NEAR-FIELD ENVIRONMENT 4-1
4.1	INTRODUCTION 4-1
4.2	OBJECTIVES AND SCOPE OF WORK 4-3
4.3	SIGNIFICANT TECHNICAL ACCOMPLISHMENTS 4-4
4.3.1	Sensitivity Analyses Using MULTIFLO 4-4
4.3.1.1	Introduction 4-4
4.3.1.2	Description of the Code MULTIFLO 4-5

CONTENTS

Section	Page
4.3.1.3	Application to the Proposed Nuclear Waste Repository at Yucca Mountain, Nevada 4-5
4.3.1.4	Results 4-5
4.3.2	Effects of Manmade Materials: Cement-Water Interactions 4-7
4.3.3	Effect of Microorganisms in the Near Field 4-16
4.4	SUMMARY OF TECHNICAL ACCOMPLISHMENTS 4-17
4.5	ASSESSMENT OF PROGRESS TOWARD MEETING OBJECTIVES 4-18
4.6	INTEGRATION WITH OTHER KEY TECHNICAL ISSUES 4-19
4.7	REFERENCES 4-20
5	CONTAINER LIFE AND SOURCE TERM 5-1
5.1	INTRODUCTION 5-1
5.2	OBJECTIVES AND SCOPE OF WORK 5-2
5.3	SIGNIFICANT TECHNICAL ACCOMPLISHMENTS 5-3
5.3.1	Sensitivity Analyses Using the Engineered Barrier System Performance Assessment Code 5-3
5.3.2	Thermal Embrittlement of Carbon Steel 5-6
5.3.3	Dry Oxidation of Carbon Steel Overpack 5-10
5.3.4	Long-Term Corrosion Prediction 5-11
5.3.4.1	Effect of Solution Composition on Repassivation Potential for A516 Grade 60 and Alloy 825 5-12
5.3.4.2	Long-Term Testing of Alloy 825 5-12
5.3.5	Effects of Microbial Growth on High-Level Nuclear Waste Containers . . 5-13
5.3.6	Factors Affecting Radionuclide Release from Spent Fuel 5-15
5.3.7	Future Developments 5-16
5.4	ASSESSMENT OF PROGRESS TOWARD MEETING OBJECTIVES AND PATHS TO RESOLUTION 5-18
5.5	INTEGRATION WITH OTHER KEY TECHNICAL ISSUES 5-19
5.6	REFERENCES 5-20
6	THERMAL EFFECTS ON FLOW 6-1
6.1	INTRODUCTION 6-1
6.2	OBJECTIVES AND SCOPE OF WORK 6-1
6.3	SIGNIFICANT TECHNICAL ACCOMPLISHMENTS 6-2
6.3.1	Review and Evaluation of the Department of Energy Thermohydrology Program 6-2
6.3.2	Benchmark Testing of Computer Codes 6-4
6.3.3	Sensitivity Analysis 6-4
6.3.3.1	Effects of Backfill on Temperature and Saturation 6-5
6.3.3.2	Effect of Media Properties on Prediction of Moisture Redistribution at Yucca Mountain 6-12
6.3.3.3	Effects of Ventilation on Rock Dryout and Drift Humidity 6-12

CONTENTS

Section	Page	
6.3.3.4	Effects of Geologic Structure and Features on the Evolution of Perched Water Bodies	6-15
6.3.3.5	Effects of High Permeability Features on Temperature and Saturation . . .	6-18
6.3.3.6	Summary of Sensitivity Analyses	6-21
6.4	ASSESSMENT OF PROGRESS TOWARD MEETING OBJECTIVES	6-23
6.5	INTEGRATION WITH OTHER KEY TECHNICAL ISSUES	6-24
6.6	REFERENCES	6-25
7	REPOSITORY DESIGN AND THERMAL-MECHANICAL EFFECTS	7-1
7.1	INTRODUCTION	7-1
7.2	OBJECTIVES AND SCOPE OF WORK	7-2
7.3	SIGNIFICANT TECHNICAL ACCOMPLISHMENTS	7-2
7.3.1	Repository Seismic Design	7-2
7.3.2	Design Control Process	7-3
7.3.2.1	Background	7-3
7.3.2.2	Regulatory Compliance	7-4
7.3.2.3	Exploratory Studies Facility Design	7-4
7.3.3	<i>In Situ</i> Heater Test	7-5
7.3.4	Parametric Study of Drift Stability—Phase I: Discrete Element Thermal-Mechanical Analysis of Unbackfilled Drifts	7-6
7.3.4.1	Study Method and Model Setup	7-6
7.3.4.2	Discussion of Modeling Results	7-8
7.3.4.3	Summary	7-11
7.3.5	Development of Rock Joint Model	7-11
7.4	ASSESSMENT OF PROGRESS TOWARD MEETING OBJECTIVES	7-14
7.5	INTEGRATION WITH OTHER KEY TECHNICAL ISSUES	7-16
7.6	REFERENCES	7-17
8	TOTAL SYSTEM PERFORMANCE ASSESSMENT AND INTEGRATION	8-1
8.1	INTRODUCTION	8-1
8.2	OBJECTIVES AND SCOPE OF WORK	8-2
8.3	SIGNIFICANT TECHNICAL ACCOMPLISHMENTS	8-3
8.3.1	Audit Review of the U.S. Department of Energy Total System Performance Assessment-95	8-3
8.3.1.1	Infiltration and Deep Percolation	8-4
8.3.1.2	Groundwater Dilution	8-6
8.3.1.3	Temperature and Humidity	8-7
8.3.1.4	Waste Package Failure Modes	8-10
8.3.1.5	Subsystem Abstractions	8-10
8.3.2	Expert Elicitation	8-13
8.3.3	Consolidated Document Management System	8-13
8.3.4	Licensing Support System Pilot Program	8-14

CONTENTS

Section	Page
8.4	ASSESSMENT OF PROGRESS TOWARD MEETING OBJECTIVES 8-15
8.5	INTEGRATION WITH OTHER KEY TECHNICAL ISSUES 8-17
8.6	REFERENCES 8-18
9	ACTIVITIES RELATED TO DEVELOPMENT OF THE U.S. ENVIRONMENTAL PROTECTION AGENCY YUCCA MOUNTAIN STANDARD 9-1
9.1	INTRODUCTION 9-1
9.2	OBJECTIVES AND SCOPE OF WORK 9-3
9.3	SIGNIFICANT TECHNICAL ACCOMPLISHMENTS 9-5
9.3.1	Scoping Calculations for Interactions with the Environmental Protection Agency 9-5
9.3.1.1	Relative Hazards of High-Level Waste Over Long Time Periods 9-5
9.3.1.2	Preliminary Calculations of Expected Dose from Extrusive Volcanic Events at Yucca Mountain 9-7
9.3.1.3	Dilution Analyses 9-10
9.3.1.4	Human Intrusion 9-15
9.3.1.5	Annual Individual Dose Estimates 9-15
9.3.2	Reference Biosphere/Critical Groups 9-22
9.3.3	Background Information and Recommendations for a Stylized Human Intrusion Calculation at Yucca Mountain 9-23
9.4	ASSESSMENT OF PROGRESS TOWARD MEETING OBJECTIVES 9-23
9.5	INTEGRATION WITH OTHER KEY TECHNICAL ISSUES 9-24
9.6	REFERENCES 9-25
10	UNSATURATED AND SATURATED FLOW UNDER ISOTHERMAL CONDITIONS . . 10-1
10.1	INTRODUCTION 10-1
10.2	OBJECTIVES AND SCOPE OF WORK 10-2
10.3	SIGNIFICANT TECHNICAL ACCOMPLISHMENTS 10-3
10.3.1	Progress Toward Resolving Technical Issues at Yucca Mountain 10-3
10.3.1.1	Climate Change, Future Precipitation, and Water Table Rise 10-3
10.3.1.2	Infiltration 10-5
10.3.2	Perched Water Bodies at the Yucca Mountain Site and Inferences for Recharge Rates 10-6
10.3.2.1	Perched Water Body Occurrences at Yucca Mountain 10-7
10.3.2.2	Perched Water Body Modeling 10-7
10.3.2.3	Results and Discussion 10-11
10.3.2.4	Conclusions 10-13
10.3.3	Estimates of Infiltration at Yucca Mountain 10-13
10.3.3.1	One-Dimensional Simulator Description 10-14
10.3.3.2	Deep-Alluvium Response Function Abstractions 10-14
10.3.3.3	Colluvium/Fracture Response Function Abstractions 10-15

CONTENTS

Section	Page
10.3.3.4 Refined Surface-Cover Model	10-16
10.3.3.5 Sensitivities of Spatial Distributions of Infiltration	10-16
10.3.4 Progress Toward Development of a Distributed Watershed Model of Solitario Canyon	10-19
10.4 ASSESSMENT OF PROGRESS TOWARD MEETING OBJECTIVES	10-23
10.5 INTEGRATION WITH OTHER KEY TECHNICAL ISSUES	10-24
10.6 REFERENCES	10-25
11 RADIONUCLIDE TRANSPORT	11-1
11.1 INTRODUCTION	11-1
11.2 OBJECTIVES AND SCOPE OF WORK	11-2
11.3 SIGNIFICANT TECHNICAL ACCOMPLISHMENTS	11-3
11.3.1 Chlorine-36 at the Yucca Mountain Site and Evaluation of Conceptual Models	11-3
11.3.2 Using Uranium Transport at Peña Blanca to Constrain Radionuclide Transport	11-4
11.3.3 Geochemical Parameters Controlling Radionuclide Sorption	11-7
11.3.4 Evaluating Saturated Zone Mixing Using Existing Hydrochemical Data	11-18
11.3.5 Development of Preferred Pathway Model	11-22
11.3.6 Conclusions	11-26
11.4 ASSESSMENT OF PROGRESS TOWARD MEETING OBJECTIVES	11-27
11.5 INTEGRATION WITH OTHER KEY TECHNICAL ISSUES	11-28
11.6 REFERENCES	11-28

FIGURES

Figure	Page
2-1 Distribution of post-12 Ma basalts of the YMR. Dotted line defines boundary of the YM-Death Valley isotopic province of Yogodzinski and Smith (1995) and Hill and Connor (1996)	2-5
2-2 Map of horizontal gravity-gradient, faults, and volcanoes near the proposed repository site	2-7
2-3 Maps illustrating the steps in calculation of the probability estimate.	2-14
2-4 Range of probability estimates of dike intersection of the proposed repository, based on Epanechnikov and near-neighbor estimates, and amplitude of the horizontal gravity-gradient weighted by w (Eq. 2-8) for $\lambda_t = 2$ to 10 v/m.y.	2-16
2-5 Range of probability estimates of dike intersection of the proposed repository based on Epanechnikov and near-neighbor estimates and density of high dilation-tendency faults weighted $0 < w < 4.5$ (Eq. 2-8) for $\lambda_t = 2$ (circles) to 10 v/m.y. (squares)	2-17
2-6 Dispersal characteristics for analog basaltic eruptions. Data sources in text. Thickness measured along main dispersal axis as reported in original isopach maps	2-20
2-7 Variations in deposit thicknesses with distance from the vent as a function of wind speed using the tephra dispersal model of Suzuki (1983) and data from the 1995 Cerro Negro eruption	2-21
2-8 Sensitivity of the Suzuki (1983) model to variations in a) Average particle diameter; b) Particle sorting	2-22
2-9 a) Distribution of tephra modeled using Suzuki (1983) optimized to conditions from the 1995 Cerro Negro eruption compared with measured deposit thicknesses	2-24
3-1 Photographs and corresponding line drawings showing evolution of a pull-apart basin from analog modeling experiments	3-7
3-2 Contour of horizontal (left column) and vertical (right column) components of ground accelerations in m/s^2 for model case sc03	3-11
3-3 Dilation-tendency analysis of faults in and around YM based on fault maps (Frizzell and Schulters, 1990; Monsen et al., 1992; and Sawyer et al., 1995)	3-17
3-4 Contours representing potentiometric surface based on interpreted steady-state water levels (after Wittmeyer et al. 1995) overlaid on Landsat Thematic Mapper image	3-19
3-5 Geometry of YM fault used in UDEC (v.2.01) modeling	3-21
4-1 Temperature plotted as a function of distance above the water table at times ranging from 10 to 10,000 yr.	4-8
4-2 Liquid saturation [(a) and (b)] and pH [(c) and (d)] plotted as a function of distance above the water table at times ranging from 10 to 10,000 yr	4-9
4-3 Chloride [(a) and (b)] and silica concentration [(c) and (d)] plotted as a function of distance above the water table at times ranging from 10 to 10,000 yr	4-10
4-4 Reaction rate of quartz [(a) and (b)] for times of 25 and 250 yr for a repository heat load of 80 MTU/acre, and pH and chloride concentration [(c) and (d)] at 25 yr for heat loads of 40, 60, 80, and 100 MTU/acre plotted as a function of distance above the water table.	4-11

FIGURES

Figure	Page
5-1 Effect of galvanic coupling on the waste package failure time for two values of areal mass loading in the absence of ventilation and backfilling	5-6
5-2 Temperature of the waste package and remaining wall thickness as a function of time for the lowest areal mass loading in the absence of galvanic coupling	5-7
5-3 Schematic diagram of the effect of embrittlement on the ductile-brittle transition temperature as a function of test temperature	5-8
5-4 Embrittlement as a function of phosphorus segregation in A 533B-Class 1 simulated coarse-grained heat affected zone	5-9
5-5 Grain boundary concentration of phosphorus at various temperatures calculated on the basis of the values of the diffusion coefficient given by Eq. (5-2) and upper and lower bounds obtained at each temperature by multiplying such values by 5 and 0.2, respectively	5-9
5-6 Effect of potential on initiation and repassivation of localized (pitting and crevice) corrosion of alloy 825 in 1,000 ppm Cl ⁻ solution at 95 °C using potentiostatic and zero resistance ammeter measurements	5-14
5-7 Corrosion potential of alloy 825 (creviced specimen) as a function of time in an air saturated 1,000 ppm Cl ⁻ solution at 95 °C	5-14
6-1 Effects of backfill on temperature at the waste package	6-6
6-2 Waste package temperature as a function of initial saturation of backfill for initial saturations of 0.01 (dotted line), 0.5 (solid line), and 0.99 (dashed line)	6-6
6-3 Schematic of bulk thermal conductivity measurement apparatus	6-9
6-4 Thermal conductivity of dry bulk tuff from the Apache Leap Test site as a function of temperature	6-10
6-5 Waste package as a function of backfill thermal conductivity of 0.2 (solid line), 0.6 (dotted line), 2.0 (short dash), and 10.0 W/m-K (long dash)	6-10
6-6 Temperature at waste package (solid line), drift roof (dotted line), drift sidewall (short dash), and pillar center (long dash) for backfill with a thermal conductivity	6-11
6-7 Thermal output of waste package for no ventilation (reference scheme, 30 yr old fuel) and two ventilation schemes	6-14
6-8 Maximum drift wall temperature for three schemes	6-14
6-9 Results of nonisothermal flow analyses after 1 yr of repository heating with isothermal analyses steady-state results as initial conditions	6-17
6-10 Saturation after 100 yr of heating. Dashed black lines correspond to steady-state saturation values obtained from isothermal analyses	6-19
6-11 Saturation after 250 yr of heating. Dashed black lines correspond to steady-state saturation values obtained from isothermal analyses	6-19
6-12 Time history of water volume for parts of the domain with saturations higher or equal to 0.998, 0.9998, and 1.00	6-20
6-13 Liquid-phase velocity magnitude contours and direction vectors at 10,000 yr	6-21
6-14 Maximum temperature before backfill and after backfill at waste package and drift roof as a function of the width of a vertically oriented fracture zone	6-22

FIGURES

Figure	Page
6-15 Maximum waste package temperature with no fracture, a 10-cm wide fracture zone, and a 140-cm wide fracture zone	6-22
7-1 UDEC model showing block geometry for one particular joint set pattern and thermal loading	7-8
7-2 Distribution and magnitude of joint shear displacements after 100 yr of heating for Case 12	7-10
7-3 Failure distribution after 100 yr of heating for Case 26	7-10
7-4 Distribution of joint opening and closure after 100 yr of heating for typical UDEC run ..	7-12
7-5 Schematic diagrams of rock surface conceptual model	7-13
7-6 Schematic diagram of rock joint model	7-15
7-7 Plot of shear stress versus shear displacement curves showing results from test no. 20	7-15
8-1 Comparison of process-level simulations with abstractions for an infiltration flux of 2 mm/yr	8-5
8-2 Two and three-dimensional computational models near the waste package	8-9
8-3 Comparison for 25 MTU/acre areal mass loading	8-9
8-4 Comparison of complementary cumulative distribution functions for cumulative release ..	8-12
8-5 CDOCS architecture	8-15
8-6 Licensing Support System Test Bed	8-16
9-1 Comparison of spent nuclear fuel repository and hypothetical uranium ore body hazards accounting for uncertainties in radionuclide solubilities and release rates	9-8
9-2 Streamlines (solid lines), particle travel times (dashed lines), and plume for lateral flow model (solid lines with arrows)	9-13
9-3 Streamlines (solid lines with arrows) and contaminant plume for vertical cross section model	9-14
9-4 Uncertainty analysis of dose for one hundred vectors at a point 5 km down gradient from the proposed repository	9-17
9-5 Uncertainty analysis of dose for one hundred vectors (all dose pathways) in the Amargosa Desert region 30 km down gradient from the proposed repository	9-18
9-6 Annual individual dose from all radionuclides total effective dose equivalent and for selected radionuclides for the drinking water pathway at a distance of 5 km	9-19
9-7 Annual individual dose from all radionuclides total effective dose equivalent and for selected radionuclides for the drinking water pathway at a distance of 30 km	9-20
10-1 Schematic of perched water volume as a function of time for complete drainage and steady-state attainment simulations	10-10
10-2 Temporal evolution of perched water volume for draining and $q=6.2$ and 8.0 mm/yr simulations	10-12

FIGURES

Figure	Page
10-3 Depletion of perched water ^{14}C as a function of time for $q=6.2$ mm/yr and three areal extent values	10-13
10-4 Example spatial distribution of AAI accounting for depth of alluvium, underlying bedrock, and meteorological effects	10-18
11-1 $^{234}\text{U}/^{238}\text{U}$ versus $^{230}\text{Th}/^{238}\text{U}$ plot of Nopal I traverse bulk rock samples, with preferred model for evolution. Symbols denote separate traverses away from the ore deposit	11-6
11-2 Uranium(6+) sorption (expressed as K_d in ml/g) on common rock-forming minerals.	11-9
11-3 a) Uranium(6+) sorption on montmorillonite as a function of M/V expressed as percent U(6+) sorbed versus pH	11-11
11-4 CNWRA experimental results for U(6+) sorption on montmorillonite, clinoptilolite, α -alumina, and quartz expressed as K_d	11-12
11-5 U(6+) sorption results shown previously in figure 11-4 and normalized to the measured N_2 -BET surface area (S_a)	11-13
11-6 U(6+) sorption results shown previously in figure 11-4 and normalized to the effective surface area (S_a'). S_a' was assumed to be 10 percent of measured N_2 -BET surface area for montmorillonite and clinoptilolite	11-14
11-7 Sorption of Np(5+) on (a) clinoptilolite and (b) montmorillonite under conditions in equilibrium with atmospheric PCO_2 and with initial Np(5+) concentration of 1×10^{-6} M.	11-15
11-8 CNWRA experimental results for Np(5+) sorption on montmorillonite, clinoptilolite, α -alumina, and quartz expressed as K_d	11-17
11-9 Np(5+) sorption results shown previously in figure 11-7, and normalized to the measured N_2 -BET surface area (S_a)	11-18
11-10 Np(5+) sorption results shown previously in figure 11-7 and normalized to the effective surface area (S_a'). S_a' was assumed to be 10 percent of measured N_2 -BET surface area for montmorillonite and clinoptilolite	11-19
11-11 Geology coverage generated using ArcView (Version 2.0b) based on the geologic map of Frizzell and Shulters (1990)	11-21
11-12 Schematic diagram of a conceptual model for flow through intersecting fracture planes	11-24
11-13 Schematic diagram of conceptual model of fracture controlled flow system with diffusion of water into the matrix.	11-25

TABLES

Table	Page
1-1 Overview of the Nuclear Regulatory Commission program activities in FY96	1-23
3-1 BMF displacement, down-dip rupture length, and earthquake magnitudes	3-12
3-2 Fault displacements on YM faults triggered by slip on BMF	3-13
4-1 Chemical species used in MULTIFLO calculations	4-6
4-2 Initial fluid composition corresponding to that of J-13 well water	4-7
4-3 Composition of Type II Portland cement	4-13
4-4 Predicted solid and porewater composition for hydrated Type II Portland cement with initial composition given in table 4-3: water/cement ratio of 0.38 and setting time of 90 d.	4-14
4-5 Predicted solid and porewater composition for hydrated alkali-free Type II Portland cement.	4-15
5-1 Candidate materials in the advanced conceptual design	5-3
6-1 Classification of thermal/mechanical units at Yucca Mountain	6-8
6-2 Measured and estimated values of thermal conductivity, K_t	6-8
6-3 Unsaturated thermal conductivity measurements of ALTS tuff	6-11
6-4 Saturation and unsaturated hydraulic conductivity (m/s) in the CHnv at 100, 1,000, and 10,000 yr for the TSPA-95	6-13
7-1 Upper and lower value for UDEC final analysis	7-7
7-2 Effects of parameters studied on selected performance measures	7-9
8-1 Dilution factors computed using conservative values for transverse dispersivity and saturated zone flux	8-7
9-1 Expected values and standard deviations as a function of position and the time period of interest	9-11
10-1 Parameter values used for sensitivity coefficient estimation	10-20
10-2 Relative change in AAI used to calculate base-case sensitivity coefficients and the AAI sensitivity coefficient values for the base case and cases resulting from systematically changing parameters	10-21
10-3 Statistics of simulated storms	10-23

ACKNOWLEDGMENTS

The quality of the report was enhanced through editorial, technical, and programmatic reviews. Efforts of these Nuclear Regulatory Commission (NRC) and Center for Nuclear Waste Regulatory Analyses (CNWRA) reviewers are gratefully acknowledged. Skillful editorial review was provided by B. Long (CNWRA). Two technical reviews were obtained for each chapter. The CNWRA technical reviewers were R.G. Baca, A.C. Bagtzoglou, A.H. Chowdhury, R.T. Green, R.D. Manteufel, W.M. Murphy, W.C. Patrick, E.C. Percy, J.L. Russell, N. Sridhar, and J.A. Stamatakos; and the NRC reviewers were J.W. Bradbury, R.B. Codell, N.A. Eisenberg, B.W. Leslie, C.H. Lui, K.I. McConnell, T.J. McCartin, S.M. McDuffie, and J.A. Pohle. Each chapter was also reviewed for programmatic context. The programmatic reviews were provided by the High-Level Waste Management Review Board members: J.H. Austin, M.J. Bell, M.V. Federline, W.C. Patrick, and B. Sagar.

Finally, the help from L.F. Gutierrez in coordinating the production of this document and able secretarial support provided by E.F. Cantu, B.P. Caudle, B.L. Garcia, C. Garcia, L.G. Hearon, Y.C. Lozano, A. Ramos, R.A. Sanchez, and L. Selvey are appreciated. Quality Assurance (QA) oversight was provided by B. Mabrito. Obviously, this report would not be possible without the wholehearted cooperation from key technical issue teams who kept to the tight schedule of the editor. Names of primary authors, technical contributors, and principal investigators are given at the front of the report and are also included at the beginning of each chapter.

QUALITY OF DATA: Sources of data are referenced in each chapter. CNWRA-generated laboratory and field data contained in this report meet QA requirements described in the CNWRA QA Manual. Data from other sources, however, are freely used. Sources for other data should be consulted for determining the level of quality for those data.

ANALYSES AND CODES: Scientific/engineering computer software used in analyses contained in this report are: 3DStress, Version 1.2 (chapters 2, 3), controlled, release date 11/13/96; PVHVIEW, Version 1.0 (chapter 2), in development, not released; UDEC, Version 2.01 (chapter 3), leased commercial version under CNWRA configuration control; ABAQUS, Version 5.5 (chapter 3), leased commercial version under CNWRA configuration control; MULTIFLO, Version 1.0 (chapters 4, 6), in development, not yet released; EBSPAC, Version 1.0 β (chapter 5), in development, not yet released; CTOUGH, Version 1.0 (chapter 6), controlled, release date 2/08/96; TPA, Version 2.0 (chapter 8), in development, not released; CHAINT, Version 2.3 (chapter 9), documentation in final stage, not released; MAGNUM, Version 3.2 (chapter 9), documentation in final stage, not released; BREATH 1.2 (chapter 10), in development, not released; SUFLAT, Version 1.0 (chapter 10), documentation in process, not released; and MINTEQA2, Version 3.10/3.11 (chapter 11), release date 8/02/96. These computer software are being configured under the CNWRA Technical Operating Procedure Development and Control of Scientific and Engineering Software (TOP-018, Revision 4, Change 1). The software SIMUL (chapter 4), created by the University of Waterloo and not under CNWRA control, was utilized for preliminary, nonquality affecting scoping analyses, although its use is described in a CNWRA scientific notebook.

Other software, ARCVIEW, Version 2.0 β , and ARCINFO, Version 6.1, are commercial codes and only the object codes are available to the CNWRA.

EXECUTIVE SUMMARY

ES.1 INTRODUCTION AND GENERAL PROGRAM ACCOMPLISHMENTS

Early in 1995, the Nuclear Regulatory Commission (NRC) staff recognized the need to refocus its preclicensing repository program on resolving issues most significant to repository performance. Since that time, three major events have driven a significant restructuring of the NRC repository program: (i) a reduction in Congressional appropriations for the repository program for both the NRC and the U.S. Department of Energy (DOE), (ii) a reorganization of the DOE high-level waste (HLW) work in what became known as the Program Approach in 1994 and its modification in 1995, and (iii) a report issued to the U.S. Environmental Protection Agency (EPA) by the National Academy of Sciences (NAS) that contained recommendations for setting a safety standard for a proposed HLW repository at Yucca Mountain (YM). The scope of the NRC preclicensing program was adjusted to focus on only those topics most critical to repository performance; these topics are called the key technical issues (KTIs). This was done with a recognition that items not on the current list of KTIs may be found to be important to repository performance in the future, carrying some risk of either (i) having to make overly conservative assumptions about such items or (ii) causing a delay in regulatory actions.

This report was jointly produced by the NRC and Center for Nuclear Waste Regulatory Analyses (CNWRA) staffs. The CNWRA, located in San Antonio, Texas, is a Federally Funded Research and Development Center sponsored by the NRC to provide technical assistance for the repository program. This report provides a status of NRC-HLW work conducted in fiscal year (FY) 96, as well as assessments of progress toward resolution of the KTIs. Chapter 1 describes the restructured NRC program and provides a programmatic context for the remaining ten chapters. Chapters 2 through 11 provide succinct summaries of work accomplished for each of the ten KTIs considered to be critical to repository performance. It should be noted that details of the activities summarized here are available in separate reports and technical papers, noted in the references at the end of each chapter. Highlights of program accomplishments for FY96 are given in the following pages.

The NRC revised approach focuses on resolving ten KTIs. Other activities necessary for licensing have been deferred as a result of FY96 budget reductions. The ten KTIs are as follows.

- 1) Igneous activity
- 2) Structural deformation and seismicity
- 3) Evolution of the near-field environment
- 4) Container life and source term
- 5) Thermal effects on flow
- 6) Repository design and thermal-mechanical effects
- 7) Total system performance assessment and integration
- 8) Activities related to development of the U.S. Environmental Protection Agency Yucca Mountain Standard
- 9) Unsaturated and saturated flow under isothermal conditions
- 10) Radionuclide transport

Because each of the ten KTIs encompasses a number of important subissues and resources are severely limited, the NRC staff is using a vertical slice or audit approach that has been successfully used in other areas of NRC responsibility, including reactor licensing. To further focus the work within each

KTI, the NRC staff will evaluate a few narrow slices or topics (focused, well-defined scope) in depth; while conclusions about resolution of the broader issue will be inferred from examining these topics in detail. Within a particular vertical slice, the NRC staff plans to conduct appropriate activities such as evaluating alternate conceptual models, including underlying data and assumptions; conducting independent modeling for use in sensitivity and importance analyses; performing limited technical investigations, including laboratory tests, to develop an independent understanding of relevant processes; reviewing the DOE data and independent literature; establishing acceptance criteria, to guide reviews and issue resolution; and establishing clear objectives for each interaction with the DOE and others to ensure progress toward issue resolution.

The NRC approach is to focus all activities on resolution of the ten KTIs at the staff level. Issue resolution is achieved when the NRC staff has no further questions or comments regarding how the DOE is addressing the issue in its program. However, it is recognized that there may be some cases where reaching a common understanding regarding differences in the NRC and the DOE points of view may be all that can be achieved. The NRC staff will prepare periodic issue resolution status reports to document significant progress and give the DOE timely feedback regarding specific issues or subissues. In addition, an annual report, such as this document, is intended to summarize the significant technical work completed for all KTIs during the preceding FY. To the extent that the NRC and the DOE can resolve issues before the Viability Assessment (VA), there would be greater confidence that the potential licensing vulnerabilities have been properly addressed by the DOE in its VA.

Numerous advantages are apparent in refocusing the NRC program on KTIs using the vertical slice approach. Scarce resources are keyed on those issues most significant to repository performance, thus enhancing attention to safety. Issue resolution is facilitated by acknowledging the appropriate bounding of less significant effects and aiming interactions with the DOE on those factual or interpretative differences with the greatest significance to performance. The audit nature of the vertical slice approach effectively evaluates a wide range of the DOE activities and identifies how well they are integrated. Integration of the NRC program is improved by coordinating necessary activities and technical disciplines in the review of each issue. Stressing issues that are potential licensing vulnerabilities is a robust approach that is not highly dependent on the DOE products and thus less likely to be seriously impacted by potential future changes in the DOE program. Finally, the approach is flexible enough to allow necessary changes to the issues or priority of activities based on new site information or new insights regarding repository performance.

As with any approach, there are some disadvantages. The audit nature of focusing only on the ten KTIs and selected vertical slices within each issue will result in areas of the DOE program not being examined in detail during prelicensing. Also, if some vulnerabilities are not recognized as KTIs and effectively addressed during prelicensing, the licensing review could be extended.

Significant progress has been made in developing paths to resolution for various subissues in the ten KTIs. The path to resolution takes into consideration the DOE data and analyses, non-DOE data and analyses available in the literature, the NRC independent data and analyses, future investigations proposed by the DOE, and an understanding of the impact of the subissue on the overall performance of the repository. It should be understood that the DOE is ultimately responsible for developing an integrated safety case for the repository, and the DOE may choose to adopt a different path to issue resolution than would be developed by the NRC.

For each individual KTI, the specific path to resolution is unique and reflects both the nature of the issue and progress of the DOE and the NRC technical work to date. Overall, for most of the KTIs, activities in FY96 concentrated on establishing a sound technical basis for future issue resolution during FY97. For a few KTIs, this involved data collection to improve the understanding of parameters or processes thought to be important to various analyses and for which data were not available. Activities also emphasized refining or in some cases completing development of models and associated computer codes representing various subsystems or processes of the repository. These models were then used to conduct sensitivity/importance analyses in FY96 at the repository subsystem or process level to help focus further resolution work on those factors having a dominant effect on the subsystem or specific processes. Subsystem or process models will provide additional value by either calculating parameter input for use in the total performance assessment (TPA) code or being abstracted as modules in the TPA code during FY97. The resulting updated TPA code will be used for sensitivity/importance analyses in FY97 that integrate the various subsystems and processes that can then be used to confirm the importance of various parameters and processes to the total system performance measure of dose. Such integrated analyses are necessary to support resolution of individual issues or subissues that cannot be resolved in isolation of the total system. These analyses will also help develop acceptance criteria during FY97. In FY96, various approaches were evaluated on how acceptance criteria could be identified and used to support the issue resolution process. Presently, they are envisioned to be part of the technical basis for issue resolution.

While the resolution of many KTIs is dependent on additional work in FY97, some important progress was made this past year. Interactions between the NRC and the DOE during FY96 were successful in achieving informal agreements to be documented in issue resolution status reports in FY97. Examples include narrowing the range of tectonic models, identifying an acceptable seismic design methodology, and resolving design control process concerns. Another major step toward issue resolution was made in the total system performance assessment (TSPA) area. An NRC and DOE interaction identified differences between the NRC and the DOE TSPAs, causes, and potential future resolution actions. Finally, the staff completed a Branch Technical Position (BTP) giving an acceptable methodology for the use of expert elicitation. This guidance resolved questions of when and how to use expert elicitation for areas of major uncertainty, and currently is being used by the DOE to conduct and plan future expert elicitation. Progress made in each KTI is described very briefly in the following. More detailed abstracts of KTI technical activities are included in chapter 1.

ES.2 IGNEOUS ACTIVITY

In this KTI, work focused on determining an upper bound for the probability of repository disruption by future volcanic eruptions. The probability estimates obtained from historical data were conditioned by knowledge about the geologic structure. The range of this probability was determined to be between 10^{-7} to 10^{-8} per year, similar to the range determined by the DOE through elicitation of an expert panel. Sensitivity analyses of consequences of such disruptions indicated that the number of waste packages (WPs) impacted in a volcanic event, the resulting fuel particle size, and the incorporation ratio of fuel into the volcanic ash were critical to determining dose to a postulated critical group.

ES.3 STRUCTURAL DEFORMATION AND SEISMICITY

Two subissues found to be most critical to performance in this KTI are: (i) potential impact of faulting and seismicity on WPs and (ii) effect of structure and tectonic stresses on groundwater flow. Understanding of the regional tectonic setting is required to resolve both subissues. Work in this KTI has

reduced the number of conceptual tectonic models to five and has shown that seismicity along the Bare Mountain fault is critical. Analyses of the effects of stress and deformation on groundwater flow indicate that discrete networks of fractures and faults may strongly influence both local and regional flow patterns. Further refinements of these models will lead to technically supported estimates of future faulting, seismicity, and structural influence on flow and their effect on repository performance.

ES.4 EVOLUTION OF THE NEAR-FIELD ENVIRONMENT

Rates of WP failures and waste dissolution are affected by evolution of the environment close to WPs. The work in this KTI was directly focused on investigating several components of the DOE Waste Containment and Isolation Strategy (WCIS)¹ (e.g., low water flux through the repository, slow corrosion of waste containers, and low waste dissolution rates). An equivalent porous medium model that coupled thermal, hydrological, and chemical processes was completed. Analyses using this model indicated a wide variation in pH and salinity, strong functions of the repository thermal loading. The effect of these changes on total repository system performance (i.e., on dose to a critical group) will be investigated in FY97. It was concluded that for bounding the near-field environment, approaches other than the equivalent porous medium may need to be considered.

ES.5 CONTAINER LIFE AND SOURCE TERM

An assessment tool called the Engineered Barrier System Performance Assessment Code (EBSPAC) was developed in this KTI. Through a sensitivity analysis using EBSPAC, it was concluded that galvanic coupling between the inner and outer overpacks was perhaps the most important factor in determining container life. Higher galvanic efficiency caused an increase in container life. In the absence of galvanic protection, intermediate heat loads tended to produce lower container lives than either the low or the high heat loads. Work on this KTI has been eliminated at the CNWRA in FY97 due to further reduction in appropriations.

ES.6 THERMAL EFFECTS ON FLOW

Work in this KTI focused on estimating the effect of thermal load on water and vapor flow through the repository. Results of sensitivity analyses showed that backfill initially lowered the WP temperature as thermal energy was consumed in evaporating pore water in the backfill. Once the backfill was dry, however, it acted as an insulator and increased WP temperature. Depending on heat load, the insulation effect may persist for hundreds of years. Another analysis indicated that ventilation during the preclosure phase can lower the drift wall temperature by tens of degrees. The effects of these and other thermal-hydrologic factors on total system performance will be evaluated in FY97.

ES.7 REPOSITORY DESIGN AND THERMAL-MECHANICAL EFFECTS

Thermal effects on design of the underground facility was the primary subissue considered for resolution in this KTI. Phase I of a sensitivity analysis was undertaken to bound the effects of key

¹U.S. Department of Energy. 1996. *Highlights of the U.S. Department of Energy's Updated Waste Containment and Isolation Strategy for the Yucca Mountain Site*. DOE Concurrence Draft. July 1996. Washington, DC: U.S. Department of Energy.

parameters on drift stability. Thermal loading, and properties and patterns of rock joints were found to significantly influence drift stability. Efforts at developing a suitable rock-joint constitutive equation that will apply to the situation of multiple reversals of shear displacements resulting from seismic events is incomplete at this time. The NRC, however, was able to resolve several methodology subissues regarding seismic design of the repository. The NRC staff will continue to evaluate the DOE design control process but no further work on this KTI will be undertaken at the CNWRA in FY97 in response to budget reductions.

ES.8 TOTAL SYSTEM PERFORMANCE ASSESSMENT AND INTEGRATION

An audit and detailed review of the latest DOE iteration of TSPA-95 (TRW Environmental Safety Systems, Inc., 1995) was performed in this KTI. Based on the audit review, five topics were selected for detailed review: (i) water flux through the repository, (ii) dilution in the saturated zone, (iii) temperature and humidity in the near-field environment, (iv) WP failure modes, and (v) model abstraction. A comparison of the cumulative complementary distribution function in TSPA-95 (TRW Environmental Safety Systems, Inc., 1995) and the one obtained using the NRC/CNWRA code TPA together with TSPA-95 data indicated significant differences attributable to differences in model abstraction. These differences, their causes, and potential resolution were discussed with the DOE. Also included in this KTI was the completion of a BTP on expert elicitation. Finally, a licensing support system test bed accessible through the Internet was brought on line. The test bed allows for searching, retrieving, and downloading documents, and obtaining user feedback.

ES.9 ACTIVITIES RELATED TO DEVELOPMENT OF THE U.S. ENVIRONMENTAL PROTECTION AGENCY YUCCA MOUNTAIN STANDARD

With the goal of contributing to the development of reasonable and implementable standards for YM, activities in this KTI focused on analyses of critical components of the standard. These analyses can also be applied to future development of the NRC regulations to implement these standards. These critical components included (i) definition of the compliance period, (ii) determination of critical groups, (iii) establishment of methods to deal with human intrusion scenarios, and (iv) provision of details to which other disruptive scenarios would be specified. Comparing hazard assessment of a uranium ore body with a HLW repository indicated that hazards were comparable at 10,000 yr, providing a rationale for adopting 10,000 yr as the compliance period. Stylized analysis of human intrusion showed that exploratory drilling was an unlikely event and that its consequences were low. It was concluded that consequences of human intrusion should be analyzed separately from other scenarios and its consequences need not be incorporated into the overall risk assessment. In addition to the scoping calculations, numerous interactions conducted with EPA achieved the following: a consistent understanding of NAS recommendations and implementation complexities; general acceptance in many areas of appropriate approaches for the proposed standard; and clear identification of where significant differences remain, such as groundwater protection.

ES.10 UNSATURATED AND SATURATED FLOW UNDER ISOTHERMAL CONDITIONS

Based on analyses of paleoclimatic data in the YM region, this KTI concluded that an upper bound on future precipitation can be estimated at two to three times the present rate. Efforts were also

made to bound the rate of shallow infiltration under present day conditions. Considering space-time variability of climatic and subsoil conditions, the average shallow infiltration was estimated to lie between 10 to 20 mm per yr. This study will be extended to estimate bounds on deep percolation. In FY96, the preliminary modeling study of existing perched waters indicated a possible average rate of deep percolation of about 6 to 8 mm/yr.

ES.11 RADIONUCLIDE TRANSPORT

Radionuclide sorption was studied in this KTI. Although part of the DOE WCIS², the importance of geochemical sorption has been reduced in comparison to dilution in the saturated zone and retardation provided by matrix diffusion. The aim of this KTI was to determine the lower bounds for geochemical sorption of important radionuclides. Laboratory and natural analog studies combined with modeling indicate strong dependence of sorption on pH. For example, the sorption coefficient for uranium can vary between 0.1 to 1,000 as pH varies between 2 to 9. Similar results were also obtained for neptunium. Work on this KTI has been eliminated at both the NRC and the CNWRA in FY97 as a result of further budget reductions.

ES.12 REFERENCE

TRW Environmental Safety Systems, Inc. 1995. *Total System Performance Assessment—1995: An Evaluation of the Potential Yucca Mountain Repository*. B00000000-01717-2200-00136. Las Vegas, NV: TRW Environmental Safety Systems, Inc.

²U.S. Department of Energy. 1996. *Highlights of the U.S. Department of Energy's Updated Waste Containment and Isolation Strategy for the Yucca Mountain Site*. DOE Concurrence Draft. July 1996. Washington, DC: U.S. Department of Energy.

1 DESCRIPTION OF THE NUCLEAR REGULATORY COMMISSION FY96 REPOSITORY PROGRAM AND ACCOMPLISHMENTS

1.1 INTRODUCTION

Early in 1995, the Nuclear Regulatory Commission (NRC) staff recognized the need to refocus its prelicensing repository program on resolving issues most significant to repository performance. Since that time, three major events have driven a significant restructuring of the NRC repository program: (i) a reduction in Congressional appropriations for the repository program for both the NRC and the U.S. Department of Energy (DOE), (ii) a reorganization of the DOE high-level waste (HLW) work in what became known as the Program Approach in 1994 and its modification in 1995, and (iii) a report issued to the U.S. Environmental Protection Agency (EPA) by the National Academy of Sciences (NAS) that contained recommendations for setting a safety standard for a proposed HLW repository at Yucca Mountain (YM). The scope of the NRC prelicensing program was adjusted to focus on only those topics most critical to repository performance; these topics are called the key technical issues (KTIs). This was done with a recognition that items not on the current list of KTIs may be found to be important to repository performance in the future, carrying some risk of either (i) having to make overly conservative assumptions about such items or (ii) causing a delay in regulatory actions.

This report was jointly produced by the NRC and Center for Nuclear Waste Regulatory Analyses (CNWRA) staffs. The CNWRA, located in San Antonio, Texas, is a Federally Funded Research and Development Center sponsored by the NRC to provide technical assistance for the repository program. This report provides a status of NRC-HLW work conducted in fiscal year (FY) 96, as well as assessments of progress toward resolution of the KTIs. Chapter 1 describes the restructured NRC program and provides a programmatic context for the remaining ten chapters. Further details and rationales for the NRC restructured program are available in SECY-96-120.¹ Chapters 2 through 11 provide succinct summaries of work accomplished for each of the ten KTIs considered to be critical to repository performance. It should be noted that details of the activities summarized here are available in separate reports and technical papers, noted in the references at the end of each chapter.

1.2 EVENTS IMPACTING THE NRC REPOSITORY PROGRAM

The first major event impacting the NRC program was the reduction of Congressional appropriations for the NRC HLW program in FY96—\$22 million to \$11 million (a 50 percent reduction). Use of previous year funds to supplement the FY96 appropriation resulted in a \$17 million funding level for the overall HLW program.²

¹Nuclear Regulatory Commission's Refocused Prelicensing High-Level Waste Repository Program, Division of Waste Management, Office of Nuclear Material Safety and Safeguards.

²The FY97 appropriation for the NRC HLW program remains at \$11 million. Adding \$3 million from previous year funds, the overall HLW program at the NRC for FY97 is funded at \$14 million. This further reduction by \$3 million led to the decision to defer a majority of work on three of the ten KTIs that were the focus of the FY96 program. Thus, the NRC will sponsor work at the CNWRA on only seven KTIs in FY97. The NRC staff, to the extent limited resources permit, will monitor the DOE program and address only the most urgent regulatory issues for the deferred KTIs.

Second, the DOE FY96 budget for the repository program at YM was reduced from \$375 million in FY95 to \$250 million in FY96 (a reduction of 33 percent). In 1994, the DOE issued a Program Approach for streamlining its HLW activities and demonstrating clear measurable progress. The cornerstone of the Program Approach was preparation of the Site Suitability Analysis in 1998. FY96 budget reductions, together with Congressional guidance, led the DOE to revise its Program Approach in early FY96 addressing the critical unanswered technical questions leading to an assessment (in late FY98) of the viability of licensing the proposed repository at YM. This Viability Assessment (VA) is intended to provide a better understanding of the repository design and its performance in the geologic setting, a better appreciation of the remaining work needed to prepare a license application, and a more accurate cost estimate for licensing and developing a repository. Completion of the VA by June 1998 is included as a milestone in the Energy and Water Appropriations Act of 1997 (H.R. 3816). The VA, which is not a regulatory document, is anticipated to be somewhat less rigorous technically than the Site Suitability Analysis originally incorporated in the Program Approach.

Congressional guidance and severe budget constraints resulted in the DOE reducing its site characterization activities to those core scientific activities necessary to determine suitability of the site and to complete conceptual designs for the repository and waste package (WP). These remaining activities will be further focused by the DOE Waste Containment and Isolation Strategy (WCIS)³ that is currently being refined. Hypotheses making up this strategy comprise an integrated safety case for YM that the DOE intends to test, using existing data, together with additional data from limited future testing. In June 1996, the DOE released a revised program plan including a revised schedule. Although preparing the VA remains the major near-term mission, the DOE announced schedules for several additional activities that had been eliminated from earlier plans or were not previously scheduled. Of particular importance to the NRC program are a revision to the Siting Guidelines (10 CFR Part 960) in FY97, which requires Commission concurrence; a final Environmental Impact Statement (EIS) in FY99; a site recommendation report in FY2001 (including the NRC sufficiency comments); and a license application in FY2002. The DOE also described a phased approach to preparing the repository design and the project integrated safety assessment, which will integrate data, assumptions, designs, and assessments into one common document, to support the VA, site recommendation report, EIS, and the license application. DOE plans on preparing important sections of this document in FY97-98, including data synthesis and site process models that, together with the designs, will be the major input to the DOE total system performance assessment (TSPA). As the DOE continues to implement its revised program approach, more detailed information will become available.

A third event impacting the NRC program was the issuance of the August 1995 NAS report, containing findings and recommendations for YM standards. This was the first in a series of actions under the Energy Policy Act of 1992 (EnPA), which also requires EPA to develop YM specific standards and the NRC to amend its technical criteria consistent with these standards. Under EnPA, EPA and the NRC must establish standards and regulations consistent with NAS recommendations. Although the NAS provides thoughtful and studied recommendations, a number of areas will require additional efforts from EPA and the NRC to formulate reasonable and implementable regulations: definition of an appropriate level of risk, compliance period, exposure scenarios, reference biosphere, and composition of a critical

³U.S. Department of Energy. 1996. *Highlights of the U.S. Department of Energy's Updated Waste Containment and Isolation Strategy for the Yucca Mountain Site*. DOE Concurrence Draft. July 1996. Washington, DC: U.S. Department of Energy. For ease of reading, the reference to DOE WCIS is omitted from all subsequent citations.

group. EPA is expected to issue a proposed standard for public comment in late 1996 and a final standard in 1997.

1.3 THE NRC REFOCUSED PRELICENSING PROGRAM

1.3.1 Revised Prelicensing Objectives

Staff recognition of the need to refocus its prelicensing program, as well as the impacts described, resulted in a revised prelicensing schedule and objectives for the prelicensing period. Although new HLW authorizing legislation is being considered, enactment is uncertain.⁴ Therefore, the refocused program is based on the NRC current statutory responsibilities under the Nuclear Waste Policy Act (NWPA) as amended and the EnPA.

- Cooperate with EPA to ensure development of reasonable and implementable HLW standards. Implement these standards through a simplified, risk-informed performance-based, regulation specific to YM.
- Review and advise the Commission on concurrence with the DOE Siting Guidelines in Part 960.
- Establish program priorities based on KTIs that are most important to repository performance. Achieve agreement with the DOE on KTIs. Make progress toward KTI resolution at the staff level.
- Provide timely feedback to the DOE on potentially significant site, design, or assessment vulnerabilities for the DOE consideration in preparing its 1998 VA. Review the DOE VA to identify licensing vulnerabilities.
- Develop and exercise independent technical assessment capability necessary to implement EPA Standards, evaluate significance of KTIs and develop paths to resolution, test hypotheses and assumptions of the DOE WCIS, provide feedback to the DOE for consideration in preparing the VA, provide sufficiency comments for incorporation into the DOE site recommendation report, and eventually review a license application.
- Improve program efficiency by streamlining integration of the NRC activities and simplifying procedures for the NRC interactions with the DOE and others.
- Review and provide comments on the DOE draft EIS so the NRC can adopt the final EIS to the extent practicable as provided in the NWPA.
- Prepare comments on sufficiency of at-depth site characterization and waste form for the DOE to include in its site recommendation report.

⁴S. 1936 — Nuclear Waste Policy Act was passed in the U.S. Senate on July 31, 1996. The House of Representatives failed to complete action on the bill in the 104th Congress. New bill(s) may be introduced in the 105th Congress.

1.3.2 Refocused Approach

To achieve the revised objectives in a resource-constrained environment, NRC has also revised its approach during FY96 to focus on resolving ten KTIs the staff considers to be the most important to repository performance and, therefore, licensing. Other activities necessary for licensing have been deferred as a result of FY96 budget reductions.⁵ The ten KTIs are as follows.

- 1) Igneous activity
- 2) Structural deformation and seismicity
- 3) Evolution of the near-field environment
- 4) Container life and source term
- 5) Thermal effects on flow
- 6) Repository design and thermal-mechanical effects
- 7) Total system performance assessment and integration
- 8) Activities related to development of the U.S. Environmental Protection Agency Yucca Mountain Standard
- 9) Unsaturated and saturated flow under isothermal conditions
- 10) Radionuclide transport

These issues were identified through the NRC iterative performance assessments, previously conducted exploratory and confirmatory research, a systematic analysis of 10 CFR Part 60, review of the DOE draft WCIS, and the NRC understanding of relevant processes and events at the YM site, based on independent studies, evaluations, reviews of the DOE work, and other experience. The NRC will periodically re-evaluate the significance of the KTIs considering new information and performance assessments. In a November 1995 technical exchange, the DOE and the NRC agreed on the potential significance to repository performance of eight of the ten KTIs. The DOE questioned the technical basis for two KTIs dealing with the significance of igneous activity and structural deformation and seismicity. The NRC staff is evaluating data, conducting analyses, and interacting with DOE and others to clarify differences on these issues.

Because each of the ten KTIs encompasses a number of important subissues and resources are severely limited, the NRC staff is using a vertical slice or audit approach that has been successfully used in other areas of NRC responsibility, including reactor licensing. To further focus the work within each KTI, the NRC staff will evaluate a few narrow slices or topics (focused, well-defined scope) in depth; while conclusions about resolution of the broader issue will be inferred from examining these topics in detail. Within a particular vertical slice, the NRC staff plans to conduct appropriate activities such as evaluating alternate conceptual models, including underlying data and assumptions; conducting independent modeling for use in sensitivity and importance analyses; performing limited technical investigations, including laboratory tests, to develop an independent understanding of relevant processes; reviewing the DOE data and independent literature; establishing acceptance criteria, to guide reviews and issue resolution; and establishing clear objectives for each interaction with the DOE and others to ensure progress toward issue resolution.

⁵Nuclear Regulatory Commission's Refocused Prelicensing High-Level Waste Repository Program, Division of Waste Management, Office of Nuclear Material Safety and Safeguards.

The NRC approach is to focus all activities on resolution of the ten KTIs at the staff level.⁶ Issue resolution is achieved when the NRC staff has no further questions or comments regarding how the DOE is addressing the issue in its program. However, it is recognized that there may be some cases where reaching a common understanding regarding differences in the NRC and the DOE points of view may be all that can be achieved. The NRC staff will prepare periodic issue resolution status reports to document significant progress and give the DOE timely feedback regarding specific issues or subissues. In addition, an annual report, such as this document, is intended to summarize the significant technical work completed for all KTIs during the preceding FY. To the extent that the NRC and the DOE can resolve issues before the VA, there would be greater confidence that the potential licensing vulnerabilities have been properly addressed by the DOE in its VA.

1.3.3 Prioritized Activities

To focus its limited resources most effectively on issue resolution, the staff prioritized all the activities (i.e., technical assistance and research) believed necessary to resolve each of the KTIs before licensing. Priorities were established by considering significance of the work to repository performance and issue resolution; appropriate timing of feedback to the DOE; lead times necessary to conduct activities; likelihood of success; and efficiency. During the budget cycle, the NRC staff intends to revisit defined activities and prioritization each year and consider new information and results of performance assessments. Table 1-1 (located at the end of this chapter) provides an overview of funded and unfunded KTI activities for FY96.

Activities funded for resolving the Total System Performance Assessment and Integration KTI are particularly important to the NRC approach. Integrated assessments conducted as part of this KTI will provide the basis for continuing confirmation or revision of significance of the NRC KTIs to repository performance and identifying new issues that might need to be considered. It will also provide a systems perspective for evaluating the DOE WCIS, including the DOE performance assessment—the centerpiece of the DOE VA and ultimately the license application. Sensitivity and importance analyses will also facilitate an understanding of the relative significance of processes and events to repository performance and provide a basis for concluding that certain effects are appropriately bounded. This information is vitally important to issue resolution and compliance determination. Analyses will also indicate where additional detailed analyses or data may be necessary to narrow uncertainties. Finally, integration activities under this KTI are essential for ensuring that interfaces among the NRC activities are identified and consistent and appropriate information flows among these activities.

1.3.4 Reduced Staff, Restructured Organizations, and Responsibilities

Refocusing the HLW repository program within the \$17 million funding level resulted in a 27 percent total staff reduction among over the Office of Nuclear Material Safety and Safeguards (NMSS), Office of Nuclear Regulatory Research (RES), Office of Information Resources Management (IRM), and

⁶The FY97 appropriation for the NRC HLW program remains at \$11 million. Adding \$3 million from previous year funds, the overall HLW program at the NRC for FY97 is funded at \$14 million. This further reduction by \$3 million led to the decision to defer a majority of work on three of the ten KTIs that were the focus of the FY96 program. Thus, the NRC will sponsor work at the CNWRA on only seven KTIs in FY97. The NRC staff, to the extent limited resources permit, will monitor the DOE program and address only the most urgent regulatory issues for the deferred KTIs.

the Advisory Committee on Nuclear Waste (ACNW). The direct sponsorship of work by RES was eliminated and the critical parts of various research projects were incorporated into the KTI plans. These reductions were accomplished through reassigning NRC staff to other programs. At the CNWRA, the funding level led to a 20 percent staff reduction accommodated by attrition as well as elimination of some temporary positions and subcontractors. Additional reductions resulted from the FY97 HLW \$11 million appropriations.

Staff reductions, improved efficiency, and integration of staff activities led to restructuring organizations and responsibilities. In February 1996, the Division of Waste Management (DWM) reorganized, consolidating its HLW activities in two branches instead of three. This action was taken to improve coordination and to better direct management attention. Additional changes were made within DWM branches and at the CNWRA to redistribute supervisory responsibilities and facilitate multidisciplinary interaction. In addition, the HLW Management Review Board (Board) was established to support the DWM Director by providing direct management oversight of the refocused program. The Board is comprised of DWM management representatives and senior management representatives from the CNWRA. The intent of this Board is to improve the overall integration of the program by coordinating policy and implementation guidance and providing a focus for decisionmaking on recommendations to upper management.

The NRC and the CNWRA staffs were also reorganized into ten KTI teams with the necessary technical and regulatory expertise for resolving each KTI. With oversight from the Board, each KTI team is responsible for planning and conducting those activities needed to resolve its issue within the established schedule and budget. The ten multidisciplinary teams represent the core technical expertise needed for the refocused program under the \$17 million funding level. Sustaining this expertise was a key consideration in management decisions regarding staff reductions. Reductions in NMSS, RES, and CNWRA staff expertise occurred in a broad range of skills including geology, hydrology, engineering, project management, quality assurance, and systems engineering. These areas of expertise were chosen to minimize the impact on the core technical expertise required to resolve the KTIs. Many of these areas, however, are unique disciplines with specialized experience regarding repository issues that will be difficult and time-consuming to replace.

1.3.5 Advantages and Disadvantages of Refocused Approach

Numerous advantages are apparent in refocusing the NRC program on KTIs using the vertical slice approach. Scarce resources are keyed on those issues most significant to repository performance, thus enhancing attention to safety. Issue resolution is facilitated by acknowledging the appropriate bounding of less significant effects and aiming interactions with the DOE on those factual or interpretative differences with the greatest significance to performance. The audit nature of the vertical slice approach effectively evaluates a wide range of the DOE activities and identifies how well they are integrated. Integration of the NRC program is improved by coordinating necessary activities and technical disciplines in the review of each issue. Stressing issues that are potential licensing vulnerabilities is a robust approach that is not highly dependent on the DOE products and thus less likely to be seriously impacted by potential future changes in the DOE program. Finally, the approach is flexible enough to allow necessary changes to the issues or priority of activities based on new site information or new insights regarding repository performance.

As with any approach, there are some disadvantages. The audit nature of focusing only on the ten KTIs and selected vertical slices within each issue will result in areas of the DOE program not being examined in detail during preclicensing. Also, if some vulnerabilities are not recognized as KTIs and effectively addressed during preclicensing, the licensing review could be extended.

1.3.6 Importance of Maintaining a Credible Preclicensing Program

A sustained and credible preclicensing program is important to the success of the national program for several reasons. First, the NRC must ensure that practical and implementable safety standards and regulations are developed. Second, the NRC must be prepared to comment on the DOE VA for YM. Although it is recognized that the DOE VA is not a regulatory document, it certainly will be the basis for decisions about the future of the national program for storage and disposal of HLW and spent fuel. The NRC comments on the potential vulnerabilities of the YM site from a licenseability viewpoint and the technical assumptions underlying the DOE cost estimates are essential input to what will undoubtedly be a complex and controversial decisionmaking process. Finally, a credible preclicensing program is essential for identifying potential licensing issues early in the repository development process, rather than later after substantial investments have been made. As the DOE prepares its WCIS and supporting program plan, critical decisions are being made to focus the program on issues important to repository performance. Although commendable, such decisions will be the basis for identifying those site characterization and design activities that can be eliminated, reduced, or delayed to stay within the budget. As the NRC, the DOE, and others work toward resolution of the KTIs, it will be essential for the NRC to advise the DOE if these reductions will pose a risk to licensing. If so, these resolutions might be the basis for comments on the sufficiency of the DOE at-depth site characterization and waste form proposal.

1.4 HIGHLIGHTS OF FY96 TECHNICAL ACCOMPLISHMENTS

As discussed in more detail in chapters 2 through 11, significant progress has been made in developing paths to resolution for various subissues in the ten KTIs. The path to resolution takes into consideration the DOE data and analyses, non-DOE data and analyses available in the literature, the NRC independent data and analyses, future investigations proposed by the DOE, and an understanding of the impact of the subissue on the overall performance of the repository. It should be understood that the DOE is ultimately responsible for developing an integrated safety case for the repository, and the DOE may choose to adopt a different path to issue resolution than would be developed by the NRC. In each chapter, general program accomplishments are summarized first, followed by specific accomplishments for each individual KTI.

General Program Accomplishments

As described in the previous sections of this chapter, a major accomplishment in FY96 was refocusing the entire NRC repository program after a thorough evaluation of important external events including the NRC budget reductions, the DOE program revisions, and NAS recommendations for YM standards. The program was refocused on resolving ten KTIs most important to repository performance. Activities were reprioritized and organizations were restructured to support issue resolution and improve integration of technical work. An initial step in this program was to discuss the ten KTIs and the issue resolution process with the DOE and others. As a result, agreement was achieved with the DOE on the potential significance to repository performance of eight of the ten KTIs. For the two remaining issues on

igneous activity and structural deformation and seismicity, the DOE has been responsive by revising its WCIS to include evaluations of these issues.

For each individual KTI, the specific path to resolution is unique and reflects both the nature of the issue and progress of the DOE and the NRC technical work to date. Overall, for most of the KTIs, activities in FY96 concentrated on establishing a sound technical basis for future issue resolution during FY97. For a few KTIs, this involved data collection to improve the understanding of parameters or processes thought to be important to various analyses and for which data were not available. For example, state-of-the-art ground magnetic surveys of buried igneous features in the YM region (YMR) and studies of an actively erupting basaltic volcano were conducted to help construct scenarios and conceptual models of potential volcanic processes.

Activities emphasized refining or in some cases completing development of models and associated computer codes representing various subsystems or processes of the repository such as engineered barriers; near-field coupled thermal, hydrological, and chemical processes; volcanic processes; and fault deformation. These models were used to conduct sensitivity/importance analyses in FY96 at the repository subsystem or process level. Examples include thermal effects on moisture flow, drift stability, and radionuclide transport. Results of these analyses help focus further resolution work on those factors having a dominant effect on the subsystem or on processes.

Subsystem or process models will provide additional value by either calculating parameter input for use in the total performance assessment (TPA) code or being abstracted as modules in the TPA code during FY97. The resulting updated TPA code will be used for sensitivity/importance analyses in FY97 that integrate the various subsystems and processes that can then be used to confirm the importance of various parameters and processes to the total system performance measure of dose. Such integrated analyses are necessary to support resolution of individual issues or subissues that cannot be resolved in isolation of the total system. These analyses will also help develop acceptance criteria during FY97. In FY96, various approaches were evaluated on how acceptance criteria could be identified and used to support the issue resolution process. Presently, they are envisioned to be part of the technical basis for issue resolution.

While the resolution of many KTIs is dependent on additional work in FY97, some important progress was made this past year. Interactions between the NRC and the DOE during FY96 were successful in achieving informal agreements to be documented in issue resolution status reports in FY97. Examples include narrowing the range of tectonic models, identifying an acceptable seismic design methodology, and resolving design control process concerns. Another major step toward issue resolution was made in the TSPA area. An NRC and DOE interaction identified differences between the NRC and the DOE TSPAs, causes, and potential future resolution actions. Finally, the staff completed a Branch Technical Position giving an acceptable methodology for the use of expert elicitation. This guidance resolved questions of when and how to use expert elicitations for areas of major uncertainty, and currently is being used by the DOE to conduct and plan future expert elicitations.

Igneous Activity KTI

The Igneous Activity (IA) KTI is directed toward evaluating the significance of IA to repository performance by reviewing and independently confirming the data, and evaluating and developing alternative conceptual models for the probability and consequences of IA at YM. Technical investigations conducted in FY96 provide quantitative information to assess the DOE WCIS for IA—that volcanic events

within the controlled area will be rare and consequences of volcanism will be acceptable. The CNWRA staff developed probability models that cast volcano distribution and structural models as continuous probability density functions. This approach results in a probability estimate for volcanic eruptions at the proposed repository that does not rely on subjectively defined source zones, a feature common to all previous probability estimates that attempt to incorporate structural models into the analysis. These new models show that the probability of future basaltic volcanic eruptions at the proposed repository site is 10^{-8} to 10^{-7} per year. This probability range will likely form the basis for issue resolution with the DOE as it is unlikely that new information, such as changes in volcano recurrence rate or structural setting of the proposed repository, will result in order of magnitude changes in this probability range.

Although not considered a significant hazard at this time, the character of approximately 6 Ma silica volcanic material is being re-evaluated because of evidence that silicic activity occurred in the YMR well after caldera-forming eruptions ceased.

Field data and modeling show that basaltic volcanic eruptions are capable of dispersing considerably more material over much greater areas than assumed in the DOE performance models. Based on observations of modern basaltic eruptions, current CNWRA models of volcanic dispersion may underestimate deposit thicknesses by up to 50 percent at distances of tens of kilometers from the source. Issue resolution on IA consequences will address the interpreted dispersal capabilities of YMR basaltic volcanoes, in addition to assumptions regarding incorporation and transport of waste material, which are key parameters for assessing dose to a critical group. Based on current technical investigations, the consequences of basaltic IA on proposed repository performance may be greater than indicated in the DOE WCIS.

Structural Deformation and Seismicity KTI

The primary objective of the Structural Deformation and Seismicity (SDS) KTI is to evaluate potential SDS hazards relevant to safe containment and isolation of HLW at the DOE proposed repository at YM. SDS KTI technical investigations were carried out in FY96 to evaluate four aspects of the overall YM SDS program: (i) hypotheses outlined in the DOE WCIS, (ii) conclusions regarding SDS in the DOE 1995 TSPA (TSPA-95) (TRW Environmental Safety Systems, Inc., 1995), (iii) the DOE probabilistic and deterministic seismic hazard analyses (PSHA and DSHA), and (iv) controlled design assumptions concerning faults and fractures. In this report, SDS KTI technical investigations in four areas are presented: (i) analyses and evaluations of viable tectonic models and present conditions of crustal-scale stresses and strains describing the structural setting of the YM, (ii) identification of faults in the YMR that pose significant seismic risk to repository performance (Type I Faults), (iii) numerical models that describe the attenuation of seismic energy from nearby (near-field) seismic sources such as Bare Mountain fault (BMF), and (iv) investigations of the potential effects of structural deformation on groundwater flow and infiltration. As a result of these technical investigations, the effects of SDS on repository performance appear to be greater and more complex than indicated in the DOE WCIS and TSPA-95 (TRW Environmental Safety Systems, Inc. 1995).

Based on detailed analysis of Basin and Range tectonism and discussions during an NRC and CNWRA hosted Appendix 7 Meeting on tectonic models with the DOE, U.S. Geological Survey (USGS), ACNW, Nuclear Waste Technical Review Board (NWTRB), Electric Power Research Institute (EPRI), and representatives of the State of Nevada, it was concluded that only 5 conceptual tectonic models of the more than 12 proposed for the YMR are presently supported by existing data. Of these five, two of the models (proposed by representatives of the State of Nevada and the USGS) envision Crater Flat (CF) as

part of a tectonic (pull-apart) basin that formed from regional strike-slip or transtensional deformation. These strike-slip dominated models appear to pose the greatest seismic risk because of the potential for significant blind or buried faults currently not accounted for in the DOE PSHA. The CNWRA investigations examined the development of pull-apart basins through a series of analog sandbox experiments. Results of the experiments confirm earlier suggestions that pull-apart basins evolve in four stages (incipient, early, early mature, and late mature). Of these four, the risk for large magnitude and damaging earthquakes is greatest in the late mature stage; a pull-apart stage that closely resembles the conceptualization of CF in the State of Nevada tectonic model.

Fifty-two faults that pose significant seismic risk to the proposed repository (Type I faults) were differentiated from the catalog of more than 400 mapped faults in the YMR using the deterministic approach established in NUREG-1415 (McConnell et al., 1992). In this approach, seismic risk is evaluated in terms of ground motion a given fault could potentially generate (gauged as a peak horizontal acceleration assuming the fault's maximum-magnitude earthquake (the largest earthquake a fault could generate because of its size). Maximum magnitude and peak acceleration derive from empirical scaling and attenuation functions based on fault length and source-to-site distance. Two important assumptions in this type of analysis are fault ruptures are confined to single fault segments and attenuation functions properly extrapolate the seismic energy of near-site earthquakes (i.e., earthquakes close enough to the site that they no longer behave as point sources). Numerical modeling of faulting and seismicity on a stylized cross section of CF and YM, consisting of a listric BMF and two antithetic YM faults, indicates that the single rupture assumption is reasonable (at least for this fault geometry). Only minimal displacement is triggered on the antithetic YM faults from an initial rupture on the BMF. The latter assumption, however, may not be valid. Empirical attenuation functions, like those used in current DOE PSHA, appear to underestimate ground motions (horizontal accelerations) at the YM site from slip on the BMF. The numerical models predict anisotropic seismic energy propagation from the rupture point on the BMF to the surface.

The potential influence of structural features on groundwater flow and infiltration was investigated at two scales of observation. Regional groundwater flow patterns in the fractured aquifer around YM were modeled based on results of dilation-tendency analyses. Results from this analysis suggest a convergence of groundwater flow paths near the eastern boundary of the proposed repository, which could potentially limit lateral spreading of contaminant plumes emanating from the repository and thereby reduce dilution. This effect needs to be considered in assessments of the DOE WCIS hypothesis regarding dilution as a favorable condition. Local variations in fracture and fault dilation were examined by numerical modeling of hangingwall deformation above a series of normal faults akin to the geometry of faults in the proposed repository block. Faults were steeply dipping and each faulting event consisted of 1 m of displacement parallel to the fault plane. The results suggest significant dilation of vertical fractures and joints in the hangingwall block (with concomitant increases in porosity and permeability) after each faulting episode. This observation is counter to the DOE hypothesis that future tectonic events are unlikely to significantly alter current hydrologic characteristics of the site.

Further investigation of the effects of alternate tectonic models on future faulting activity and structural control on flow provide the foundation for resolution of several aspects of this KTI in FY97.

Evolution of Near-Field Environment KTI

The DOE updated WCIS for the proposed repository at YM has the primary goals of near complete containment of radionuclides within WPs for several thousand years and acceptably low annual

doses to a member of the public living near the site. Among the system attributes recognized in this strategy to be most important in accomplishing these goals are the rate of seepage of water into the proposed repository, WP lifetime (containment), release rate of radionuclides from breached WPs, and radionuclide transport through engineered and natural barriers. Of potential importance to the WP lifetime and radionuclide release from the engineered barrier system is the chemical composition of groundwater in the near-field region that could come in contact with the WP. This includes environmental variables defining the oxidation state, pH, chloride concentration, and other compositional variables of ingressing fluid that may affect the waste container and waste form. Depending on composition of this fluid, the rate of corrosion and leaching of spent fuel could be either greatly accelerated or inhibited. Additionally, chemical changes in the near-field environment can affect radionuclide transport characteristics such as speciation, sorption, and permeability. The objective of the Evolution of the Near-Field Environment (ENFE) KTI is to evaluate these characteristics of the evolving near-field environment and provide input to the TSPA.

In the DOE TSPA-95 (TRW Environmental Safety Systems, Inc., 1995), effects of waste emplacement on the near-field temperature and relative humidity were considered. These considerations led to determination of the time the WPs got wet, considered to trigger the aqueous corrosion processes, radionuclide release from the waste form, and radionuclide transport out of the WPs. However, in studying corrosion and radionuclide release, the chemistry of the near-field environment was not considered. Rather, assumptions were made relating corrosion behavior of waste containers to corrosion in humid industrial atmosphere or river water. Similarly, parametric equations relating the dissolution of spent fuel to environmental species were used, but no explicit justification was made regarding concentrations of these environmental species. A similar approach may be adopted in the viability assessment. The tools developed in the ENFE KTI can be used to assess the validity of using these environmental parameters. While the evolution of the near-field environment can occur by a variety of processes, three effects were investigated this FY: (i) effect of evaporation and condensation, (ii) effect of interactions between cementitious materials and groundwater, and (iii) effect and viability of microbiological activity.

The MULTIFLO code was used to determine the range of possible near-field environments due to evaporation and condensation processes as a function of thermal loading of the proposed repository. Calculations show that significant changes in pH and salinity could occur with moderate thermal loading of the proposed repository. With increasing heat load, higher concentrations of dissolved solutes are expected. At the extreme case of complete dryout, salts are expected to precipitate during the heating regime and dissolve during the cooling phase as the proposed repository rewets. It is expected that for the higher heat loads where complete dryout occurs, an evaporite deposit will form in the near-field with the deposition of salts occurring throughout the dryout zone. The effect of evaporite deposition on fluid composition during the rewetting stage is being investigated.

A primary limitation of the present calculation is use of the equivalent continuum model (ECM). In this model, fractured porous medium is represented as a single average continuum. Capillary equilibrium is assumed to be maintained between the fracture and matrix. As a consequence of this assumption, it is not possible for flow to take place in the fracture network without the matrix becoming fully saturated at the same time. This assumption of the model is fundamental to the formation of a capillary barrier sandwiched between the zone of enhanced moisture content and the proposed repository horizon preventing liquid water from reaching the waste during the heating regime. Consequently, gravity driven flow such as dripping, which may be an important process for container life and source term evaluations, cannot be described within the confines of the ECM. Alternate conceptualizations, such as multiple interacting continua, may provide a better description of fracture flow. Validation of the

thermal-hydrologic-chemical coupling may be attempted through an analysis of field samples in the vicinity of YM originating from paleohydrothermal sources. Field samples have been collected and are being analyzed.

The effects of cementitious materials on the near-field environment have been estimated using available data mainly at near-ambient temperatures. However, considerable uncertainties exist regarding stability of the calcium silicate hydrate gel phase that may determine the pH of the fluid contacting the cement. If the gel phase recrystallizes at higher temperatures, the pH may not attain as high a value as calculated from room temperature data. It is also important to couple these essentially batch calculations with a transport model such as MULTIFLO to estimate the spatial extent of the change in pH due to cement water interactions.

The investigation of microbiological activity has shown that bacterial colonies native to the host rock at YM are viable even after exposure to 120 °C for a short period of time. However, activity and the effects on near-field environment through interaction with cementitious materials may be limited by the concentration of oxidizable sulfur species.

The primary focus of resolving this KTI will be on bounding the environment around WPs sufficiently well so that WP performance can be estimated. Time to wetting and the effects of aqueous chemistry on container life appear to be critical factors. Adequacy of ECM models for estimating these factors remains to be investigated.

Container Life and Source Term KTI

The DOE updated WCIS for the proposed repository at YM has the primary goals of near-complete containment of radionuclides within WPs for several thousand years and acceptably low annual doses to a member of the public living near the site. Among the system attributes recognized in the DOE strategy to be most important in accomplishing these goals are the WP lifetime (containment), rate of release of radionuclides from breached WPs, and radionuclide transport through engineered and natural barriers. The objective of the Container Life and Source Term (CLST) KTI is to evaluate these attributes independently and provide input to the performance assessment (PA) of the overall proposed repository.

Several subissues delineated within the CLST KTI directly address the DOE WCIS: (i) evaluating methodologies for extrapolating short-term laboratory data to long-term performance; (ii) evaluating factors affecting waste form alteration products and the release of radionuclides; (iii) determining effect of long-term thermal exposure and mechanical loads on the mechanical stability of the container materials; (iv) assessing the effect of microbiological organisms on the performance of container materials; and (v) performing sensitivity analyses on the effects of thermal loading, near-field environment, and galvanic coupling on container life using the Engineered Barrier System Performance Assessment Code (EBSPAC). The DOE performed a probabilistic analysis of container life in TSPA-95 (TRW Environmental Safety Systems, Inc., 1995) using the Waste Package Degradation (WAPDEG) code. Similar methodologies may be used in the DOE VA through TSPA-VA. The sensitivity analyses performed in this KTI will enable the NRC and the CNWRA staffs to evaluate methodologies used by the DOE in TSPA-95 (TRW Environmental Safety Systems, Inc., 1995) and compare the container life cumulative distribution curves predicted by EBSPAC and WAPDEG. These analyses will also facilitate evaluating the significance of these subissues to the overall system performance.

In the most common WP design proposed by the DOE, 21 pressurized water reactor or 40 boiling water reactor spent fuel (SF) assemblies are contained in a type 316L stainless steel multi-purpose canister (MPC) (3.5-cm thick wall). The MPC is surrounded by an inner overpack of corrosion-resistant alloy (2.5-cm thick wall), contained in an outer overpack of corrosion-allowance material (10-cm thick wall). The container life evaluations in this KTI focused on the inner and outer overpacks.

Calculations of container life using EBSPAC indicated that two parameters are of great importance to container life: (i) the areal mass loading (AML), as defined by the thermal loading strategy, which determines the near-field temperature as well as the chemistry of the environment contacting the WP; and (ii) the degree of galvanic coupling between the outer carbon steel overpack, once it is breached, and the inner nickel-base alloy overpack, which determines the failure time of the inner overpack. In the absence of galvanic coupling, the container life exhibits a minimum at an intermediate AML. At high AML, the container remains dry for long periods of time and the overall life of the container is long. At low AML, container wetting occurs shortly after emplacement but corrosion processes are not as severe and life is extended just beyond 10,000 yr. For example, the critical potential above which localized corrosion occurs increases with decreasing temperature so the likelihood of localized corrosion for a given chemical environment decreases with decreasing temperature. These two competing factors lead to a minimum container life at an intermediate AML. If efficient galvanic coupling occurs, calculated container life can exceed 10,000 yr, regardless of the AML value.

The effect of long-term thermal exposure on susceptibility to mechanical failure of the steel outer overpack (thermal embrittlement) was evaluated on the basis of a review of the literature. Thermal embrittlement may occur due to segregation of phosphorus (an incidental impurity in steel) to grain boundaries. It was concluded that the candidate steels considered for the outer overpack are susceptible to thermal embrittlement if the WP surface temperature exceeds 200 °C for significant periods (thousands of years). The investigation also revealed that low-alloy steels are more susceptible to thermal embrittlement than plain carbon steels.

Even if the container surface remains dry and aqueous corrosion is obviated, dry oxidation may be a determining factor in container performance. Literature on the kinetics of dry oxidation of plain carbon and low-alloy steels at temperatures anticipated in the proposed repository was evaluated critically. It appears that dry oxidation and intergranular penetration of these steels are not important factors at the predicted temperatures. Further but limited investigation may be necessary to resolve this issue.

The DOE strategy in extending the life of containers is to use two dissimilar metals so the outer overpack protects the inner overpack from corrosion through a galvanic coupling effect. Implicit in this strategy is the assumption that a critical potential exists for a given environment/material combination below which localized corrosion does not occur. This critical potential is identified as the repassivation potential, E_p . Long-term corrosion tests, ongoing for over 2 yr, have shown that when the potential is maintained below E_p for Alloy 825, localized corrosion has not occurred.

A factor that often affects corrosion of materials exposed to natural environments is microbiological activity. Microbiological organisms can adversely affect the susceptibility to localized corrosion of a material by either increasing the corrosion potential, E_{corr} , (called ennoblement) or decreasing the E_p . Investigations conducted using a model organism, *Shewanella putrefaciens*, originally

isolated from a corroded oil supply line, show that the bacterium has no significant effect on E_{corr} of stainless steel but decreases E_{p} in an anaerobic environment containing thiosulfate.

The literature on dry oxidation and fracturing of SF was evaluated because these phenomena could enhance radionuclide release rate by increasing the surface area and solid-state diffusion of relatively volatile radionuclides, followed by dissolution or colloid formation under aqueous conditions. It was concluded that higher oxides (i.e., greater than UO_2) may not form below 150 °C due to slow diffusion of oxygen. Although colloids are formed by oxidative dissolution of SF, there are uncertainties regarding the significance of colloids to the source term. Natural analog, experimental, and thermodynamic studies indicate that the properties of secondary uranyl minerals such as uranophane will control the source term. Experimental studies were initiated to determine fundamental thermodynamic properties of uranophane to reduce the uncertainties in solubility calculations. Pure uranophane was synthesized for this purpose.

The subissue of extrapolating short-term laboratory tests on corrosion can be resolved by using repassivation potential as a bounding value for onset of localized corrosion. Efficiency of galvanic corrosion remains to be investigated.

Thermal Effects on Flow KTI

Prediction of thermally driven redistribution of moisture through partially saturated, fractured porous media caused by the emplacement of heat-generating HLW with acceptable uncertainty is the focus of the Thermal Effects on Flow (TEF) KTI. It is necessary to understand the spatial and temporal effects of the thermal load on temperature as well as liquid and gas phase flux in the vicinity of the proposed repository to have confidence in predictions of containment and long-term waste isolation. The DOE is developing a strategy to demonstrate that waste can be contained and isolated at the proposed YM repository site. Evaluating this strategy necessitates a detailed understanding of thermally driven moisture flow through partially saturated, fractured porous media. This KTI was divided into three resolvable subissues in pursuit of this understanding: (i) is the DOE thermal testing program sufficient to assess the likelihood of gravity driven refluxing occurring in the near field, (ii) is the DOE thermal modeling approach adequate for assessing the nature and bounds of thermally induced flux in the near-field, and (iii) will the DOE thermal loading strategy result in thermally induced flux in the near-field and humidity at the WP surface to meet the performance objectives? Resolution of these subissues establishes the knowledge base necessary to predict with acceptable uncertainty thermally driven redistribution of moisture through partially saturated, fractured porous media.

The objective of this KTI is to resolve the subissues to a level of acceptable uncertainty. Activities designed to reduce uncertainties in these subissues in FY96 were both reactive and proactive: (i) reviewing and evaluating the DOE thermohydrology program, including the DOE peer review activity; (ii) benchmark testing of computer codes; (iii) providing sensitivity analyses; and (iv) evaluating conceptual models. Results from the DOE and the NRC activities (i), (ii), and (iii) are summarized here. Evaluations of alternative conceptual models are only preliminary and will be reported in future documents.

The review and evaluation concluded that the DOE Thermohydrologic Testing and Modeling Program adequately addresses most, but not all, critically relevant technical issues. It was noted in the DOE peer review team (PRT) report, and supported here, that the DOE has not demonstrated that it has plans to evaluate the conceptual models as rigorously as needed. The importance of near-field flow and

transport calculations will depend upon the degree to which WP performance is affected. The current DOE models may not adequately include all important transport mechanisms. Either the current models will need to be modified or different models used if these mechanisms are to be included. Additionally, in neither the PRT recommendations nor the DOE response to the PRT report was it demonstrated that the DOE bounding assumptions and analyses of the thermal-hydrological-chemical coupled effects are conservative. The review noted that the discontinuance of surface based hydrologic testing may result in unacceptably high uncertainty in infiltration estimates. The importance of acceptable predictions of infiltration rates is manifested in thermohydrologic flow models whose predictions are highly sensitive to prescribed infiltration rates at the upper boundary.

Benchmark testing (i.e., code-to-code comparisons) was conducted on four general thermohydrologic codes: TOUGH2, FEHM, CTOUGH, and MULTIFLO; the first two codes are currently being used by the DOE while the latter two are NRC codes. Primary differences among the codes were in computational efficiency—the MULTIFLO code was substantially faster than the other three codes. The FEHM code experienced computational difficulties in two test cases; one with high infiltration rates and the other with flow in fractured porous media. With respect to computational precision, simulation results from all codes were sufficiently similar that differences in future predictions from either of the codes can be attributed to differences in input and not computational inconsistencies.

Sensitivity and numerical scoping analyses helped identify the relative importance of specific types of information that contribute to the evaluation of thermally driven moisture flow through partially saturated fractured porous rock. This is of interest because the presence of liquid water or water vapor in the repository environment is important in corrosion analyses of the WP and transport of radionuclides once released from the WP. These sensitivity analyses indicate that (i) placement of backfill materials can lead to increased temperatures at the WP and decreased temperatures at the drift wall; (ii) varying the hydraulic properties of the PTn and CHnv within reasonable limits can produce a factor of 10^4 change in the unsaturated hydraulic conductivity of the CHnv located below the proposed repository horizon; (iii) vertically oriented fracture zones that intersect the emplacement drifts can decrease peak temperatures by 20 °C at the WP and 15 °C at the drift wall; (iv) ventilation can reduce drift wall temperatures by as much as 45 °C and induce dryout 5 m into the drift wall; and (v) geologic structures at YM are capable of forming perched water bodies; heating within these structures can lead to increased saturation in, above, and below the proposed repository horizon during early times after the onset of heating.

FY96 activities of the TEF KTI made significant progress toward resolution of subissues. Comments and recommendations made on the DOE Thermohydrologic Testing and Modeling Program provide input to the basis for the resolution in FY97 of the subissue on the sufficiency of the DOE thermal testing program to assess the likelihood of gravity driven refluxing occurring in the near-field. The identification, through sensitivity study of important parameters, features, and processes that may significantly affect the moisture flow and postclosure performance of the repository, will provide additional input for the resolution in FY97 of the subissue on the sufficiency of the DOE thermal testing program to assess the likelihood of gravity driven refluxing occurring in the near-field. There remain two areas that still contribute to the uncertainty in resolving the subissues in the TEF KTI. High levels of uncertainty exist regarding the effect of heterogeneities and geologic structure on thermally driven moisture movement, even though insight has been gained in this area. A second major contributor to the high level of uncertainty in this KTI is the absence of evidence to support a conceptual model adequately representative of the heat and mass transfer mechanisms present in partially saturated fractured rock. These are two target areas for future evaluation and resolution in FY98 of the subissue on the adequacy of the DOE thermal modeling approach for assessing the nature and bounds of thermally induced flux in the near-field.

Repository Design and Thermal-Mechanical Effects KTI

The main focus of the Repository Design and Thermal-Mechanical Effects (RDTME) KTI is the evaluation of time-dependent thermal-mechanical (TM) coupled effects on the heated rock mass near the repository horizon for repository design and preclosure and postclosure repository performance. There are three resolvable subissues associated with this KTI: (i) design of a proposed repository to meet preclosure and postclosure performance objectives, (ii) evaluation of thermal effects on design of the underground facility, and (iii) role of repository seals in meeting performance objectives. In addition, this KTI also supports examination of two of the DOE hypotheses regarding the ability of the proposed YM repository to isolate wastes: (i) flow of water into the repository will be low and (ii) engineered barriers, possibly including backfill, will limit migration of radionuclides into the host rock and any sources of groundwater. The objective of the RDTME KTI during FY96 was to address certain components of the first and second subissues. The associated activities included (i) review of the DOE repository design program with emphasis on technical reviews of DOE seismic design methodology, regulatory compliance review report, and Exploratory Studies Facility (ESF) design report; (ii) a TM parametric study of drift stability to identify important parameters that may affect repository design; and (iii) development of a prediction tool for TM analysis.

Review of the DOE Seismic Topical Report No. 2 (TR2) *Seismic Design Methodology for a Geologic Repository at Yucca Mountain* indicated that the proposed seismic performance categories are not consistent with the NRC categories 1 and 2 design basis events in the proposed rule changes to 10 CFR Part 60. This inconsistency could potentially pose a problem during license review of repository design. This topical report did not adequately link proposed preclosure seismic methodology and postclosure performance considerations. The proposed treatment of repeated seismic loadings as low-probability/low-consequence events is not justifiable given that limited information is available regarding seismic activity at YM. Furthermore, the proposed methodology did not provide sufficient details regarding fault-specific investigations needed to define set-back distance for fault avoidance. These concerns are currently being addressed by the DOE in its revised topical report. These concerns will be resolved if the revised topical report is found acceptable by the NRC.

As a part of the activity for resolving the NRC concerns on the DOE design control process—an integral part of the DOE repository design program—a DOE regulatory compliance review report was reviewed during early FY96. The focuses of the review were to verify that the DOE identified applicable 10 CFR Part 60 design requirements to be addressed in ESF design and assess if these design requirements were correct and if the flow-down to the design specifications was objective and traceable. Review of the document made it possible to conclude that the NRC concerns related to the DOE design control process can be considered resolved. The only outstanding item remaining is to assess the DOE implementation of the improved design control process. The NRC recommendations made on DOE design of the ESF Main Drift will provide guidelines to the DOE in its future repository design considerations.

An enhanced model has been developed to simulate the response of natural rock joints under cyclic loads taking into account the primary, secondary, and higher-order asperities present on the joint surfaces. This model will provide review tools to the NRC and the CNWRA staffs to assess stability of drifts in the context of preclosure safety and retrievability. Review of seismic TR2, ESF design package, and DOE regulatory compliance review report, and development of a rock joint model provided a basis for resolving the subissue on design of the proposed repository to meet preclosure and postclosure performance objectives.

The first phase TM parametric study of drift stability investigated the potential effects of inherent variation of thermal and mechanical properties of the rock mass and site characteristics on emplacement drift stability without backfill during the operation period. The range of properties used in the study are those currently considered to be representative of the site. Various combinations of nine rock mass parameters were included in the parametric study using numerical modeling with the Universal Distinct Element Code. Statistical analyses of the parametric study results based on certain performance measures were conducted. These performance measures include maximum and minimum principal stress, maximum joint shear displacement, maximum joint closure and separation, convergence of excavated openings, and extent of yield zone around the excavation. Results indicate that thermal load and thermal expansion coefficient are important parameters that affect most of the performance measures studied while other rock mass properties affect drift stability to various degrees of significance. Among them, intact rock cohesion and friction angle were found to have less significant effects on the performance measures related to joint behavior. However, they have a relatively significant effect on the extent of yield zone. These findings will bring necessary focus in development of review procedures and acceptance criteria for resolution of RDTME KTI and in review of the DOE ESF design packages.

The NRC and CNWRA staffs reviewed the DOE ESF thermal tests program through DOE/NRC technical interactions and a site visit to the ESF thermal testing alcove. Objectives related to the RDTME KTI in the first ESF Thermal Test are developing information on rock mass thermal and mechanical properties at elevated temperature through the single heater test, and investigating interactions between the rock mass and various ground support systems through the drift-scale heater test. The locations for both tests are in a relatively competent rock mass. The NRC and the CNWRA anticipate that the mechanical properties and responses obtained from these tests will be near the high end of the range encountered in the emplacement area. The TM parametric study and review of the DOE ESF heater tests led to identification of thermal load and site specific rock mechanical and thermal parameters that may significantly affect emplacement drift stability and waste retrievability. These will provide input to the basis for resolution of the subissue on consideration of thermal effects in underground facility design.

Total System Performance Assessment and Integration KTI

Licensing decisions regarding the proposed HLW repository at YM will be largely based on the quantitative determination of compliance over relatively long time periods (e.g., 10,000 yr). This determination of compliance will be made by the NRC through a predictive analysis referred to as a TSPA. Simply stated, TSPA is a broad based engineering analysis that (i) considers the features, events, and processes (FEPs) that significantly affect the proposed repository; (ii) examines the effects of these FEPs on the proposed repository system (composed of engineered and natural barriers); and (iii) estimates the probability and consequences in terms of dose (or risk). Results of the TSPA are expressed in a probabilistic context because of the broad uncertainties associated with the large spacial scale of the complex geologic setting and the long compliance period.

The primary objective of the Total System Performance Assessment and Integration (TSPAI) KTI is to assess compliance of the proposed repository with regulatory standards. Such assessments must identify and analyze the features, processes, and events relevant to the site, as well as account for uncertainties in conceptual models, abstracted mathematical models, future system states, and model parameters. The resolution of this issue will, in part, be accomplished by completing development of the TPA code. Full resolution will be achieved with application of the TPA code to evaluations of the DOE TSPA-VA and review of the TSPA for license application.

A number of subissues were identified that are essential to resolution of the primary issue: (i) do the hypotheses described in the DOE WCIS adequately represent the major performance characteristics of the YM repository, (ii) what is the relative importance of the individual NRC KTIs and is there is a need for change in emphasis, and (iii) are major components of the DOE TSPA methodology (e.g., model abstractions, probability and consequences of relevant FEPs, parameter and model uncertainties, and bounding assumptions) sufficiently comprehensive to provide a defensible safety case? In addition to these subissues, work performed under this KTI involved conducting independent assessments for prelicensing review, developing guidance on the use of expert judgment, promoting integration among KTIs, and assisting the NRC with maintenance of the advanced computer system and Consolidated DOCUMENT System (CDOCS).

Significant progress was made this FY in addressing a number of the TSPAI KTI tasks. Through the conduct of an audit (i.e., prelicensing) review of the DOE TSPA-95 (TRW Environmental Safety Systems, Inc., 1995) report, the NRC and the CNWRA staffs made substantive progress on the subissue dealing with the DOE TSPA methodology. The KTI teams conducting the audit review identified a number of significant vulnerabilities in the DOE TSPA-95 (TRW Environmental Safety Systems, Inc., 1995) primarily associated with nonconservative assumptions, inadequate model abstractions, inconsistencies with field data, and inconsistencies with previous DOE TSPA analyses. Specific recommendations for improving analyses were made to the DOE and support contractors at a technical exchange meeting on TSPA-95. Regarding the use of expert judgment, a branch technical position was prepared and published for public review and comment. In addition, the CDOCS software was documented and successfully installed on the NRC advanced computer system.

Activities Related to Development of the U.S. Environmental Protection Agency Yucca Mountain Standard KTI

The primary objectives for this KTI are to (i) support the NRC in interactions with the EPA regarding development of an EPA Standard for the YM site and (ii) subsequent to promulgation of the EPA Standard, assist in developing the technical bases for future revisions to the NRC regulations to conform with the new EPA Standard. A number of subissues were defined that must be addressed to constrain exposure scenarios for TSPA: (i) defining a compliance period and method, (ii) selecting a critical group(s), (iii) evaluating results of potential human intrusion, and (iv) considering disruptive events. Results of the analyses conducted during FY96 on these subissues are summarized briefly in the following paragraphs.

The relative radiological hazard of a repository containing only SF is initially about four orders of magnitude greater than that of an equivalent hypothetical ore body. The hazard diminishes rapidly over the first few hundred to few thousand years—by 90 percent at 100 yr; 99 percent at 1,000 yr; and 99.9 percent at 10,000 yr. An apparent increase in hazard at 100,000 to 500,000 yr is due to the ingrowth of radionuclides such as ^{230}Th , ^{229}Th , ^{226}Ra , and ^{210}Pb . By 10,000 yr the relative radiological hazard will be within an order of magnitude of the hypothetical ore body. A time period of regulatory interest (TPI) for a repository of about 10,000 yr would, therefore, focus attention on the period when the waste hazard has a significant man-made component that is readily discernible from an equivalent hypothetical ore body, even after considering uncertainties associated with solubilities and release rates. The findings of this study are consistent with those of earlier studies (U.S. Environmental Protection Agency, 1982, 1985).

Calculations were made of expected peak dose to a hypothetical member of a critical group residing in the Amargosa Valley region for an extrusive volcanism scenario, assuming a lifestyle as

described in NUREG-1538⁷. These calculations considered doses for different locations of this individual on the earth surface (i.e., 20, 25, and 30 km directly south of the proposed repository) immediately after the event. These analyses show that increasing the TPI has the effect of increasing the importance of low-probability, high-consequence events such as extrusive volcanism when compared with scenarios that are certain to occur regardless of the TPI (e.g., undisturbed repository). The magnitude of this increase was found to be about a factor of 4, although this estimate is somewhat uncertain due to large variances in the expected dose values.

A scoping analysis on dilution effects found that dilution at the YM site is not likely to produce large reductions in groundwater concentrations of radionuclides (or the associated radiologic doses). In the immediate vicinity of the proposed repository, dilution factors (DF) on order of 2 to 10 are expected based on model calculations. Relatively low DFs are likely if the plume is confined to fracture zones that are pervasive in the tuff aquifer (Geldon, 1993). Alternatively, if the plume spreads vertically, as a result of flow through vertical fractures or faults, the DFs will tend toward the higher end of the range. Passive mixing along the long flow path (from the proposed repository site to the Amargosa Valley region) will contribute to dilution but is unlikely to increase DFs by many orders of magnitude. This scoping analysis did not identify any methodology issues with regard to implementation of an individual dose-based requirement. Characterization of the local and regional groundwater system is more important for demonstrating compliance with a dose-based standard than for a derived standard based on integrated releases to the accessible environment (i.e., the containment requirements of 40 CFR Part 191). This increased emphasis on characterizing the groundwater system will hold for individual risk-based requirements as well. Additional tracer tests, such as those being conducted by the DOE in the C-Well complex (Geldon, 1995), may be needed to acquire data on transport parameters (e.g., mass dispersivities and effective porosities).

The NRC staff concluded from preliminary analyses of the consequences of a stylized human intrusion at YM that exploratory drilling appears to be an unlikely, low consequence event, if restricted to reasonable assumptions. The staff also found that such an analysis need not be directly incorporated into a total system performance demonstration. If the revised EPA Standard requires such stylized calculations, the NRC staff recommends that analysis be constrained to specific reasonable scenarios identified in the regulatory framework.

General conclusions from the peak dose analysis presented in this report are that (i) a relatively small number of long-lived, mobile radionuclides will be important to performance; (ii) there do not appear to be any major technical difficulties that might preclude estimating an annual individual dose; and (iii) assumptions concerning critical group location and lifestyle could be very important in determining an appropriate approach for establishing radionuclide concentrations at receptor locations.

Sections of this report also describe continuing efforts for this KTI to determine appropriate critical group(s), reference biosphere assumptions, and parameter values for a stylized human intrusion scenario.

⁷Nuclear Regulatory Commission. 1996. *Preliminary Performance Assessment Analyses Relevant to Dose-Based Performance Measures*. In preparation. NUREG-1538. Washington, DC: Nuclear Regulatory Commission.

Unsaturated and Saturated Flow Under Isothermal Conditions KTI

Yucca Mountain was selected as a potential HLW repository site in part due to the favorable hydrogeologic conditions provided by an unsaturated zone up to 700 m thick. Low moisture fluxes and water contents reduce the likelihood of waste canister corrosion, SF dissolution, and rapid transport to the water table. It has also been postulated that dissolved radionuclides that reach the water table will be rapidly diluted by relatively large saturated zone flow rates. The Unsaturated and Saturated Flow Under Isothermal Conditions (USFIC) KTI is responsible for assessing aspects of the ambient hydrogeologic regime of YM that have the potential to compromise performance of the proposed repository. The DOE developed a WCIS for YM that defines low seepage and saturated zone dilution as two of three key natural barriers for a geologic repository at YM. The primary goal of the USFIC KTI is to develop technical procedures and conduct technical investigations to assess the adequacy of the DOE strategy for characterizing and modeling hydrogeologic processes and features at YM. Three subissues related to shallow infiltration, unsaturated zone conditions above the repository, and ambient flow condition through the repository were identified in the KTI, whose resolution will aid in assessing the DOE low seepage hypothesis. One subissue addresses the saturated zone and the dilution hypothesis. During FY96, efforts were primarily focused on those FEPs that most strongly affect shallow infiltration, unsaturated zone conditions above the repository and flow conditions from the repository horizon to the water table.

Progress was made toward resolving differences with the DOE on methods for bounding the effects of climate changes on hydrogeologic conditions and on estimates of shallow infiltration. It appears likely that changes in climate at YM may be bounded using available paleoclimatic data to establish temporal patterns, likely limits on precipitation, and expected changes in water table elevation. Estimates for net infiltration have been made for an area including YM using a numerical simulator. Resulting distributions are similar to those made by the DOE using different codes and somewhat different modeling assumptions.

Technical investigations related to the formation of perched water zones, the spatial distribution of infiltration, and focused recharge were conducted. These investigations were designed to address subissues related to the shallow infiltration, unsaturated zone conditions above the repository, and flow conditions from the repository horizon to the water table and accordingly evaluate the low seepage WCIS hypotheses. Numerical models were developed to investigate the formation and persistence of perched water bodies at YM and whether simulated perched zones were consistent with measured ^{14}C residence times. An average deep recharge rate of 6.2 mm/yr was estimated to sustain a perched water body and application of hydrologic and geochemical constraints suggests that perched zones may contain a combination of older pluvial water and younger water from more recent infiltration. The spatial distribution of infiltration at YM was estimated by abstracting detailed one-dimensional simulations into a response surface for annual-average infiltration (AAI) as a function of hydraulic properties, annual average meteorologic input, and depth of surficial cover. Analyses indicate that after precipitation and temperature, AAI is most sensitive to colluvium depth. Development of a distributed watershed model was initiated to evaluate the possibility for focused recharge in the YM area. Calculations were made for a portion of the northern end of Solitario Canyon. Preliminary results indicate that channel recharge can be calculated for Solitario Canyon but better estimates for key hydraulic and infiltration parameters are required.

Based on paleoclimate data, an upper bound on future precipitation can be estimated to be 2–3 times the present rate. This bound will help resolve the subissue of estimating deep percolation through the repository horizon. The near agreement between the range of near-surface infiltration estimated through modeling by the CNWRA and measured in the field by the DOE will also contribute to resolution of this KTI.

Radionuclide Transport KTI

The Radionuclide Transport (RT) KTI was designed to conduct technical investigations of processes that affect radionuclide transport from the proposed YM repository to the accessible environment and thereby affect the overall system performance. Matrix diffusion, sorption, and dilution that may reduce radionuclide concentrations during transport are key attributes of the DOE WCIS. The primary goals of the RT KTI are to determine which processes are critical to meeting overall system performance objectives and develop criteria with respect to data sufficiency, process representation in system models, and parameter values to resolve this KTI.

Technical investigations were conducted to address a subset of radionuclide transport issues. Fast transport paths at YM have been indicated by the presence of bomb-pulse ^{36}Cl in data collected by the DOE in the ESF. Available data and associated interpretations were evaluated. The consensus interpretation is that groundwater moved from the surface to the proposed repository horizon, mainly along faults and fractures within the last 50 yr. Data from the Nopal I deposit within the Peña Blanca District, an analog site, were measured and interpreted to evaluate radionuclide transport at tens of meters scale in hydrologically unsaturated tuffs. These interpretations indicate that long-term (hundreds of thousands of years) radionuclide transport is affected by changes in hydrologic conditions and document the role of fracture transport in unsaturated tuffs. Furthermore, observations of the incorporation of uranium (U) within fracture minerals suggest that retardation is not a fully reversible process.

Retardation processes were evaluated by interpreting a combination of U and neptunium (Np) sorption data from the CNWRA experiments and from the literature to show that the magnitude of sorption of a given actinide is similar for different minerals if normalized to the number of available sorption sites. Additionally, these studies indicate that U and Np sorption coefficients can be constrained using approaches that account for changes in aqueous and surface speciation over wide ranges of geochemical conditions. To study regional-scale flow and mixing, hydrochemistry data for the YM region have been gathered and entered into a geographic information system database. This system will allow analysis of hydrochemical signatures for different aquifers to evaluate the possibility of dilution of radionuclide-contaminated groundwater upon mixing with the regional groundwater system as postulated by the DOE. A conceptual model of hydrologic flow has been outlined to test the DOE simulations of transport through fractures and matrix. This conceptual model may allow development of a numerical approach for fracture and matrix transport that can be compared with site data.

The path to resolution for this KTI includes estimating the effects of geochemical conditions on retardation through TSPA. This will help identify those radionuclides that require retardation, in addition to dilution, for the site and proposed repository to comply with applicable standards. The resolution will then focus on estimating lower bounds for retardation of these radionuclides.

1.5 CONCLUSIONS

The refocused program is expected to provide an efficient and effective way to streamline the NRC precicensing program and enhance the emphasis on safety of the proposed repository program in an environment of constrained resources. This program provides the essential technical basis for fulfilling NRC responsibilities independent of the DOE, including establishing implementable regulations consistent with EnPA direction and evaluating the sufficiency of at-depth site characterization and the proposed waste forms during the precicensing period in accordance with the NWPA. Focusing on KTIs that are potential

licensing vulnerabilities is a robust approach that is not highly dependent on DOE products and thus less likely to be impacted by potential future changes to the DOE program. Finally, the approach is flexible enough to allow necessary changes to issues or priority of activities based on new site information or insights about repository performance.

This report provides a summary of the progress made in FY96 on developing paths to resolution for various subissues in the ten KTIs. The NRC work is clearly keyed to those issues that most impact repository performance. Recognizing the uncertainties in description of the natural system and processes that lead to release from the engineered system, migration through the geosphere, and eventual dose to humans in the biosphere, the effort is directed toward estimating appropriate bounds for factors that are important to performance.

1.6 REFERENCES

- Geldon, A.L. 1993. *Preliminary Hydrogeologic Assessment of Boreholes UE-25c #1, UE-25c #2, and UE-25c #3, Yucca Mountain, Nye County, Nevada*. Denver, CO: U.S. Geological Survey.
- Geldon, A.L. 1995. *Results and Interpretation of Preliminary Aquifer Tests in Boreholes UE-25c #1, UE-25c #2, and UE-25c #3, Yucca Mountain, Nevada*. United States Geological Survey Water-Resources Investigations Report 94-4177. Washington, DC: U.S. Geological Survey.
- McConnell, K.I., M.E. Blackford, and A.K. Ibrahim. 1992. *Staff Technical Position on Investigations to Identify Fault Displacement Hazards and Seismic Hazards at a Geologic Repository*. NUREG-1451. Washington, DC: Nuclear Regulatory Commission.
- TRW Environmental Safety Systems, Inc. 1995. *Total System Performance Assessment—1995: An Evaluation of the Potential Yucca Mountain Repository*. B00000000-01717-2200-00136. Las Vegas, NV: TRW Environmental Safety Systems, Inc.
- U.S. Environmental Protection Agency. 1982. *Population Risks from Disposal of High-Level Radioactive Wastes in Geologic Repositories*. EPA 520/3-80-006. Washington, DC: U.S. Environmental Protection Agency.
- U.S. Environmental Protection Agency. 1985. *High-Level and Transuranic Radioactive Wastes—Background Information Document for Final Rule*. EPA 520/1-85-023. Washington, DC: U.S. Environmental Protection Agency.

Table 1-1. Overview of the Nuclear Regulatory Commission program activities in FY96

Key Funded NRC Activities

- Work cooperatively with the EPA to develop a YM-specific HLW standard consistent with NAS recommendations. Perform independent analyses to evaluate the implementability of these standards.
- Review the DOE data related to KTIs and conduct modeling and sensitivity analyses to independently evaluate whether the issues pose a risk to repository licensing.
- Continue interactions with DOE and other parties through use of video conferencing and enhanced role of on-site representatives.
- Use TSPA to provide the framework for both verifying and resolving the NRC KTIs, and for evaluating the DOE WCIS.
- Develop acceptance criteria and review procedures necessary to evaluate KTI resolution.
- Conduct independent investigations for specific KTIs most significant to repository performance and having a high likelihood of success before licensing.

Reduced NRC Program Activities

- NRC quality assurance observation audits and in-field verifications significantly reduced.
- Oversight of DOE field work reduced.
- Review of DOE study plans and test procedures for collection of data eliminated.
- Review of DOE Site Characterization Plan progress reports not planned.
- Reviews of DOE designs limited.
- Peer reviews of CNWRA work conducted through peer-review journal publications and limited review by external experts.
- Use of CNWRA consultants reduced.
- License Application Review Plan development deferred.
- Research efforts eliminated (including field investigations, laboratory testing, and model development for KTIs on igneous activity, unsaturated flow, container life, and radionuclide transport).

2 IGNEOUS ACTIVITY

Primary Authors: B.E. Hill, C.B. Connor, and J.S. Trapp

Technical Contributors: C.B. Connor, F.M. Conway, D.A. Ferrill, S.L. Greenan, D.B. Henderson, B.E. Hill, M.S. Jarzempa, P.L. LaFemina, S.B. Magsino, R.H. Martin, J.A. Stamatakos, and J.S. Trapp

Key Technical Issue Co-Leads: H.L. McKague (CNWRA) and J.S. Trapp (NRC)

2.1 INTRODUCTION

The Igneous Activity (IA) Key Technical Issue (KTI) has been defined by the Nuclear Regulatory Commission (NRC) as "Predicting the probability and consequences of IA affecting the repository in relationship to the overall system performance standard." The hypothesis to be evaluated by the U.S. Department of Energy (DOE) Waste Containment and Isolation Strategy (WCIS) is "Volcanic events within the controlled area will be rare and the consequences of volcanism will be acceptable";¹ subsurface IA is not thought by the DOE to demonstrably affect repository performance (e.g., Wilson et al., 1994). In addition to directly releasing waste material into the accessible environment, IA could alter groundwater flow paths and initiate mechanical, chemical, and thermal effects that could cause degradation of the waste package and other engineered barriers. A concern with the DOE IA program and WCIS is that a reasonable range of probability and consequences of future IA have not been bounded by the DOE. Data and models developed by the NRC, the Center for Nuclear Waste Regulatory Analyses (CNWRA), and others provide an independent technical basis for defining the concern and data to support resolution of this issue.

IA has been factored by the NRC into three subissues that contain numerous technical foci. The first subissue, probability, focuses on definition of igneous events, determination of recurrence rates, and examination of geologic factors that control timing and location of IA. A recent expert elicitation by the DOE concluded "the aggregate expected annual frequency of intersection of the repository footprint by a volcanic event is 1.5×10^{-8} , with a 90 percent confidence interval of 5.4×10^{-10} to 4.9×10^{-8} ." (U.S. Department of Energy, 1996a). Based on additional qualitative arguments, DOE² suggests the probability of volcanism could be even less than currently estimated. Technical investigations presented in Connor and Hill (1995) and in this chapter will show that the geologic evidence supports most annual probability estimates between 1×10^{-7} and 1×10^{-8} per yr. In addition, a new probability model incorporating structural control of volcanic events is presented.

The second subissue consists of the range of expected consequences for IA within the proposed repository setting. Primary focus areas are definition of the physical characteristics of igneous events, determination of the eruption characteristics for modern and ancient basaltic igneous features in undisturbed geologic settings, models of the effects of the disturbed geologic setting of the proposed repository on igneous processes, evaluation of waste and repository characteristics with regard to behavior during igneous events, and determination of geologic system characteristics. Historically, small-volume

¹U.S. Department of Energy. 1996. *Highlights of the U.S. Department of Energy's Updated Waste Containment and Isolation Strategy for the Yucca Mountain Site*. DOE Concurrence Draft, July 1996.

²*Ibid.*

basaltic volcanism has not been studied in the same detail as large-volume volcanic systems, primarily because of a relatively low level of hazards and lack natural resources associated with cinder cone systems. Of primary importance in performance models is determining the ability of cinder cone eruptions to fragment and transport subsurface material. Detailed sensitivity analyses have been performed on a model routinely used to simulate ash transport in volcanic eruptions (Suzuki, 1983).³ Results of these analyses are presented in this chapter. These analyses provide an alternative interpretation to a critical assumption in the DOE performance models regarding limited tephra dispersion (Link et al., 1982) which is a primary basis for the conclusion that "the consequences of volcanism will be acceptable."⁴

The third subissue is the viability of data sets used to make probability and consequence analyses. In essence, this subissue is designed to evaluate the precision and accuracy of data used in the characterization program and licensing process. At times, multiple sources provide contradictory data regarding age, location, and characteristics of the Yucca Mountain region (YMR) volcanoes. Recent CNWRA field technical investigations in the YMR will be presented in this report to document there is an insufficient technical basis to conclude the probability of future silicic eruptions in the YMR is negligible. Ground magnetics surveys (Connor et al., 1996)⁵ and ongoing technical investigations show that buried igneous features continue to be discovered and characterized within 25 km of the proposed repository site. Analysis of the DOE characterization program consisted of two Appendix 7 meetings; one on geophysics in December 1995 to review and better understand the status of the DOE geophysics program, and one on tectonic models in May 1996 to evaluate various tectonic models and determine which models can still be considered viable. Results of these meetings are presented in the respective trip reports. In addition, staff observed the DOE Quality Assurance (QA) audit of the Los Alamos program on September 16-20, 1996. Further details on this audit can be found in the DOE audit report.

2.2 OBJECTIVES AND SCOPE OF WORK

The main objective of work within this KTI is to evaluate the significance of IA to repository performance by reviewing and independently confirming the data, and evaluating and developing alternative conceptual models for the probability and consequence of IA at YM. The scope of work includes review of various DOE documents as well as applicable documents in the open literature, participation in meetings with the DOE to discuss issues related to the KTI, observation of QA audits of the DOE, and independent technical investigations. This technical investigation is designed to address key licensing issues regarding IA in the YMR. Although none have been published to date, issue resolution reports are intended to be an important programmatic aspect starting in FY97.

CNWRA technical investigation is designed to provide an independent assessment of the probability and consequences of future IA in the YMR using physical data from YMR and analog

³Jarzemba, M.S. 1996. Stochastic radionuclide distributions after a basaltic eruption for performance assessments of Yucca Mountain. *Nuclear Technology*. In press.

⁴U.S. Department of Energy. 1996. *Highlights of the U.S. Department of Energy's Updated Waste Containment and Isolation Strategy for the Yucca Mountain Site*. DOE Concurrence Draft, July 1996.

⁵Stamatakos, J.A., C.B. Connor, and R.H. Martin. 1996. Quaternary basin evolution and basaltic volcanism of Crater Flat, Nevada, from detailed ground magnetic surveys of the Little Cones. *Journal of Geology*. In press.

volcanoes applied to empirical, deterministic, and probabilistic models that link directly into iterative performance assessment. For example, physical volcanological data and samples were collected during the 1995 eruption of Cerro Negro volcano in Nicaragua. These data and subsequent laboratory analyses are used in this report to test the accuracy of tephra dispersion models currently used in Performance Assessment (PA). Theoretical studies regarding the sensitivity of ground magnetic measurements to detect buried igneous features (Connor and Sanders, 1994) prompted field studies to better define known buried igneous features in the YMR (Connor et al., 1996) and to investigate igneous features that are present but uncharacterized by previous site characterization work.

Issue resolution regarding probability will be achieved by gaining agreement on reasonable mechanisms and realistic ranges of the critical parameters necessary to evaluate the likelihood and character of future IA at or near the proposed repository. This will require an evaluation of existing data and models from the DOE, CNWRA, and others to arrive at a reasonably conservative range for the probability of future IA at the proposed repository site. Probability models will need to reflect the resolution capabilities of YMR characterization activities along with the uncertainties associated with understanding igneous processes. In accordance with regulatory requirements, there must be reasonable assurance that values used do not underestimate possible effects of IA on the proposed repository site. The activities described in the following sections provides the basis for resolving this issue.

Issue resolution for the consequences of IA will be more difficult to achieve, as the direct and indirect effects of igneous intrusion through a waste repository have no known geological analog. In addition, the physical, chemical and thermal effects of magma on engineered systems are poorly understood and often are well beyond the design limits of these systems. Thus, expert opinions are likely to vary widely on how the proposed repository might be affected by future IA. Resolution of consequences will be achieved through comparison of results from independently derived data and models with those from the DOE program and through agreement on reasonable mechanisms and realistic ranges of parameters necessary to evaluate IA on repository total system performance. Critical to this resolution is the ability of performance models to reasonably reproduce igneous processes measured directly at active and historically active basaltic volcanoes.

IA KTI subissues on probability and consequences require that available data are correctly presented and used as part of the characterization and licensing process. Inherent in this use is an evaluation of the precision and accuracy of the data. At times, multiple sources provide contradictory data regarding age, location, and characteristics of YMR volcanoes. These contradictions must be evaluated and incorrect data removed from consideration to achieve issue resolution in this area.

2.3 SIGNIFICANT TECHNICAL ACCOMPLISHMENTS

2.3.1 Stabilize Database

Probability models are critically dependent on accurately determining age, location, and characteristics of igneous features. In order to achieve issue resolution on the probability of future IA in the YMR, this KTI evaluates several aspects of IA that are factors in assessing the probability of future volcanism in the YMR.

Age and location of basalts younger than about 12 Ma and currently thought by CNWRA staff to be part of the YMR magma system through time are shown in figure 2-1.⁶ Recent work has shown that the YMR magma system may extend south and west into the Death Valley area (Yogodzinski and Smith, 1995; Hill and Connor, 1996). Mid-Pliocene basalts of the Funeral Formation in the Greenwater Range, California, rest unconformably on volcanic and volcanoclastic rocks of the Miocene Greenwater Formation (figure 2-1). The timing of volcanism of the Funeral Formation is poorly constrained by several K-Ar ages and is considered to have erupted between 4 and 4.8 Ma (e.g., Wright et al., 1991). Geochemical data from Yogodzinski and Smith (1995) and Hill and Connor (1996) show that Funeral Formation basalts have the same, relatively unique isotopic signature as YMR basalts. The Funeral Formation is, however, in a different structural setting than most YMR basalts and immediately follows a period of distributed silicic volcanism (e.g., Wright et al., 1991).

Few vent structures in the Funeral Formation in the Greenwater Range are identified on regional and local geologic maps (e.g., McAllister, 1970). Satellite imagery (multispectral Landsat Thematic Mapper (TM) images and high-resolution panchromatic images) and high-altitude, side-looking airborne radar indicate that more than 20 vents crop out within the Funeral Formation. Vents are predominantly cinder cones, but at least one shield volcano consisting of more than 20 cooling units is present in the northern part of the Greenwater Range. Additionally, well-log data from more than 150 wells drilled by U.S. Borax Corporation show a number of vents buried beneath late-stage lava flows. Well-log data indicate an average thickness of 130 m for basaltic lava flows and interbedded conglomerates. Preliminary calculations suggest a minimal volume of about 11 km³ for Funeral Formation basalt.

The immediate significance of the Funeral Formation to proposed repository performance is that inclusion of these vents would increase Pliocene recurrence rates to about seven volcanoes per m.y. (v/m.y.), which is equal to Quaternary recurrence rates. Weibull-process probability models used by, for example, Ho (1991) are extremely sensitive to the timing of past volcanic events. Maintaining a relatively constant Plio-Quaternary recurrence rate of seven v/m.y. would lower most probability estimates from Weibull-process models that assume volcanic recurrence rates have increased in the Quaternary (e.g., Ho, 1991; U.S. Department of Energy, 1996a). In addition, inclusion of the Funeral Formation basalts into the YMR igneous system gives a more northerly trend to many of the statistically defined zones used in the probability models in U.S. Department of Energy (1996a). Funeral Formation vents are too old and too distant from the proposed repository site to significantly affect the results of nonhomogeneous Poisson spatio-temporal probability models (e.g., Connor and Hill, 1995) that will form the basis for issue resolution. Other classes of probability models, however, that place more reliance on volcano timing (e.g., Ho, 1991) or source-zone definition (e.g., U.S. Department of Energy, 1996a) can be affected to varying degrees by inclusion of Funeral Formation vents in the YMR system. Because of uncertainty about the relationship of Funeral Formation basalts to basalts closer to YM, including Funeral Formation basalts into recurrence calculations appears prudent.

Silicic volcanoes can erupt much more explosively than basaltic volcanoes. In addition, the geologic processes that produce basaltic magmatism are significantly different from those that produce silicic magmatism. DOE investigations indicate that there has been no silicic activity in the YMR since 7.5 Ma at the Stonewall Mountain caldera (more than 100 km northwest of Crater Flat) or 9 Ma at the Black Mountain caldera (60 km northwest of Crater Flat) (U.S. Department of Energy, 1993; Crowe et al.,

⁶Fleck, R.J., U.S. Geological Survey, Menlo Park. Unpublished K-Ar dates for basalt lava in MSH-C drill core and Dome Mountain. Personal communication to B. Hill, 1996.

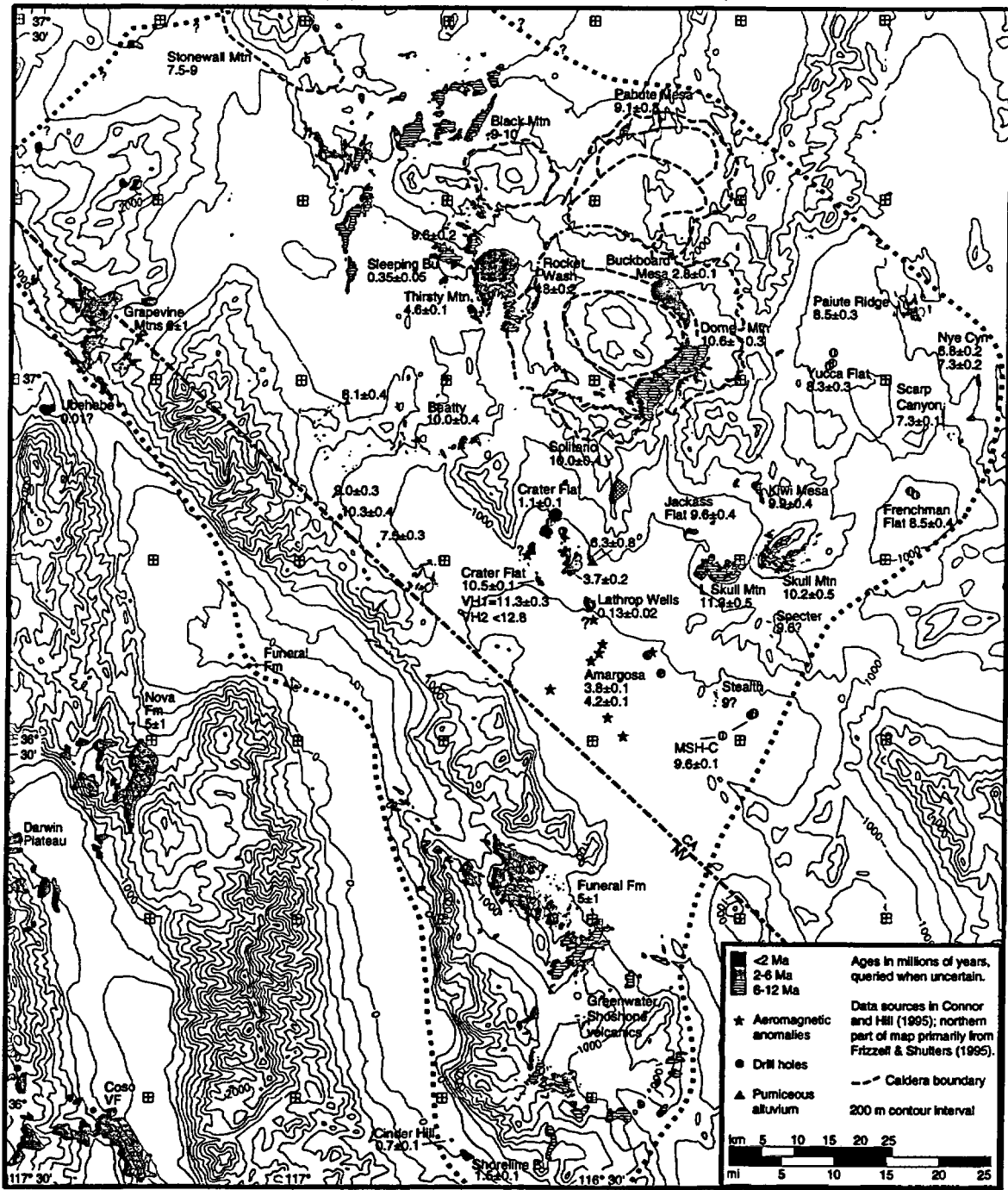


Figure 2-1. Distribution of post-12 Ma basalts of the YMR. Dotted line defines boundary of the YMR-Death Valley isotopic province of Yogodzinski and Smith (1995) and Hill and Connor (1996). Unpublished dates for MSH-C and Dome Mountain from R. Fleck.¹ Other data sources in Connor and Hill (1995), Fleck et al. (1996), and this report.

1995; U.S. Department of Energy, 1996a,b). These analyses form the basis of the DOE conclusion that "the potential for future silicic volcanism . . . is considered to be negligible for the post-closure period of the repository." (U.S. Department of Energy, 1996b). The DOE investigations, however, have not considered all available data.

Carr (1982) described silicic pumice beneath the easternmost 3.7 ± 0.2 Ma basalts of Crater Flat (figure 2-1). This pumice has a zircon fission-track date of 6.3 ± 0.8 Ma and does not correlate petrographically or chronologically with known Miocene pyroclastic deposits in the Crater Flat area (Carr, 1982). Recent CNWRA work shows that the pumice is relatively pristine, subangular to subrounded lapilli ranging in size from 2-to-6 cm in diameter, with an average maximum diameter of 4.4 cm. The pumice is disseminated in massive, medium to coarse-grained sandy alluvium that is extensively bioturbated. Pumice abundances increase downwards from trace amounts at the basalt contact to roughly 30 percent at 2 m below the basalt. At least two 10–15 cm beds of generally matrix-free reworked pumice occur within 2 m of the base of the overlying 3.7 ± 0.2 Ma basalt. The deposit is only weakly indurated and shows no evidence of thermal or chemical alteration that could reset a zircon fission-track date. The deposit most likely represents a pumice-fall tuff that has been locally reworked and buried by alluvium in Crater Flat. At present, silicic volcanism is not considered a concern at YM, based on a lack of nearby Pliocene or younger eruptions. The CNWRA will, however, continue to perform some confirmatory investigations of the uncertainties represented by this post-caldera silicic deposit. These investigations will examine the age and petrogenesis of the Crater Flat pumice deposit and should lead to either resolution of the issue or definition of a potential concern.

2.3.2 Probability Estimates of Volcanic Disruption

In an area of active volcanism such as the YMR, a probabilistic hazard analysis starts with the null hypothesis that the site will be affected by volcanic activity during the expected performance period and an alternate hypothesis that the site will not be affected by volcanic activity. The primary goal of the probabilistic hazard analysis is to estimate the confidence with which the null hypothesis can be accepted or rejected. The sensitivity of probability estimates to uncertainty about volcanological and volcanotectonic processes, such as structural control on dike propagation and the distribution of volcanic events, must therefore be assessed as part of a probabilistic hazard assessment (e.g., Smith et al., 1990; Sheridan, 1992; Crowe et al., 1995). The following analyses explore the bounds of probability estimates of volcanic disruption using models based on spatial patterns of basaltic volcanism, regional recurrence rates of volcanic activity, and structural control on volcanism in the YMR.

In areas where magma is available, the crust is being extended and dike injection can accommodate crustal strain. In this sense, dikes and faults play the same role in responding to extension (Parsons and Thompson, 1991). Faults with a high dilation-tendency in the current stress state of the crust can act as conduits for magma transport through the crust. The abundance of these faults may indicate areas that, because they are extending, are likely areas of dike injection, given a magma supply. Thus, the frequency of faults may be an indicator of future volcanism. In this sense basin bounding faults such as the Bare Mountain fault (BMF) may provide low energy pathways for magma ascent to the surface (McDuffie et al., 1994). A comparison of the distribution of Miocene and younger basalts and faults in the YMR supports this hypothesis. For example, one way to view basaltic volcanism in Crater Flat is that this volcanism is localized in the hangingwall of the BMF. Other basalts in the YMR are associated with major mapped faults with significant vertical displacements: the Miocene Beatty basalts along the Fluorspar Canyon fault and the Little Skull Mountain and Kiwi Mesa basalts along the Rock Valley and Wahmonie faults (figure 2-2).

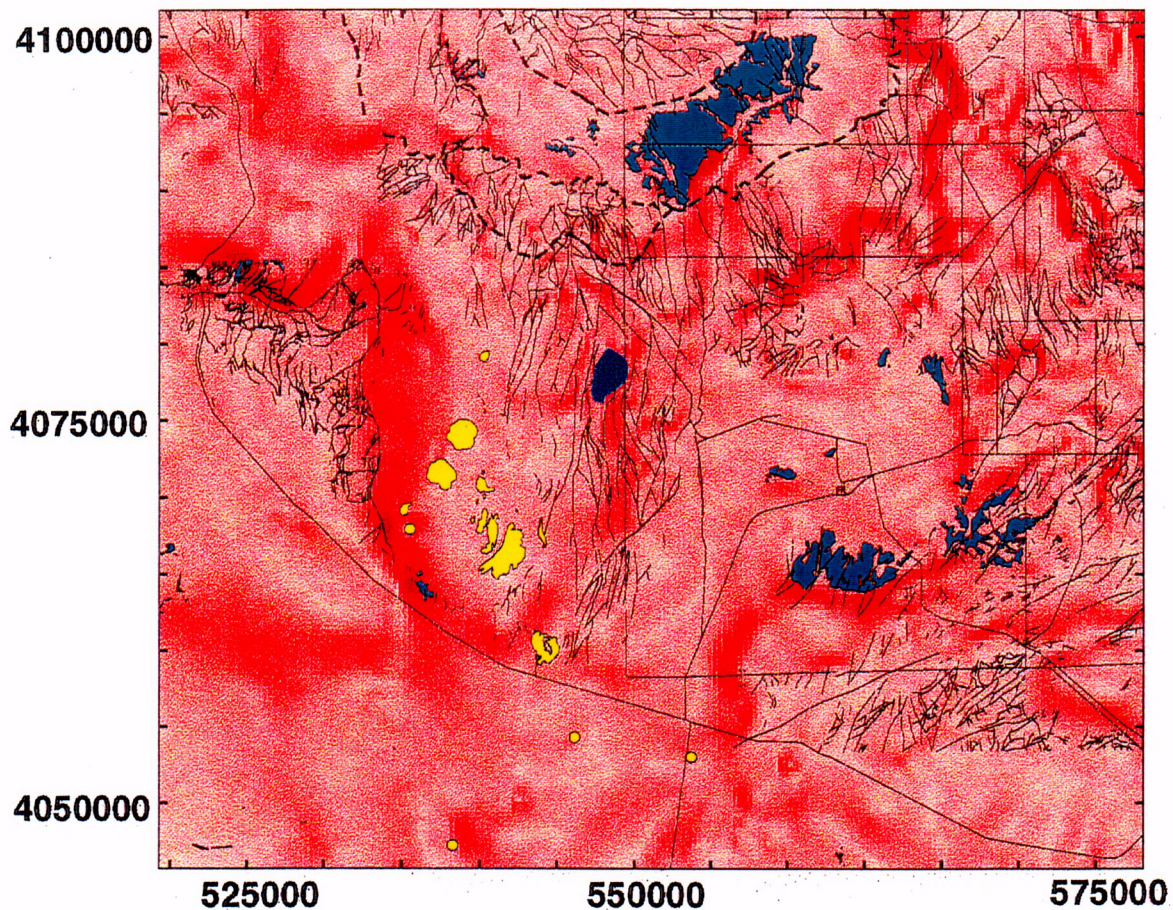


Figure 2-2. Map of horizontal gravity-gradient, faults, and volcanoes near the proposed repository site. Plio-Quaternary basalt in yellow, Miocene basalt in cyan, and mapped caldera boundaries outlined by dashed lines. Areas of high-amplitude horizontal gravity-gradient are shown in dark shading; low gradient is indicated by light shading. Faults from Frizzell and Shulters (1990) gravity data are summarized in Oliver et al. (1995).

This relationship between structure and volcanism has been used to suggest both higher and lower probabilities of volcanic disruption of the proposed repository than are predicted using spatio-temporal patterns alone. A wide variation in probability estimates is a direct result of the varying ways in which these source zones have been drawn. Smith et al. (1990) suggested that a narrow NE-trending structurally controlled zone of potential volcanism extends through Lathrop Wells and the proposed repository site, resulting in probabilities much greater than indicated by spatio-temporal patterns (e.g., Connor and Hill, 1995). Sheridan (1992) also incorporated NE-trending dikes into a probabilistic model but did not restrict these dikes to a narrow zone. Alternatively, some structure models exclude the repository from zones of potential volcanism. For example, Crowe and Perry (1989) proposed the Crater Flat Volcanic Zone (CFVZ), a NNW-trending zone through the Crater Flat and Sleeping Butte volcanoes with the eastern boundary located west of the proposed repository site. Similar source-zone models that exclude the proposed repository site have been used elsewhere (Crowe et al., 1995; U.S. Department of Energy, 1996a). Because these models exclude the repository from the potential source-zone of volcanism,

their application results in low estimates for the probability of volcanic disruption of the proposed repository compared with spatio-temporal models.

Analyses presented here avoid the source-zone concept altogether by casting structural information as a discretized density distribution, readily comparable to spatial and spatio-temporal probability distributions. Two data sets are used in this analysis: (i) gravity data, which reveal large-scale variations in crustal density and hence basin development and extension and (ii) distribution of high dilation-tendency faults, which indicates areas of past extension and areas where crustal strain may be accommodated by dike injection.

2.3.2.1 Gravity Data

Yucca Mountain and Crater Flat are part of a structural half-graben, bounded on the west by the BMF, an eastwardly dipping master fault, and on the east by a diffuse set of westward dipping normal faults. Variations in the intensity of the earth's gravitational field, reflecting major changes in the density of subsurface rocks, can be used to define the structural boundaries of the Crater Flat basin. A large volume of gravity data have been collected in the YMR during the last 40 yr. This data set, summarized in Oliver et al. (1995), consists of approximately 16,000 gravity stations. A subset of these complete Bouguer gravity data, consisting of approximately 8,000 gravity stations, was obtained from the Lawrence Berkeley Laboratory where these data are archived.

Langenheim and Ponce (1995) interpreted the depth to pre-Cenozoic basement in the YMR from gravity data by iterative calculation of expected gravity using density-depth estimates. Their preliminary results suggest that the depth to pre-Cenozoic basement in southern Crater Flat is approximately 2.5 km. The gravity data suggest that anomalously deep pre-Cenozoic basement (greater than 0.5 km) extends south into the Amargosa Desert from Crater Flat. The amplitude of the horizontal gravity-gradient indicates the position of the boundaries of this basement low (figure 2-2). For example, the BMF produces a steep gravity-gradient on the western edge of Crater Flat. The amplitude of the horizontal gravity-gradient increases and the width of the anomaly decreases from north to south along the BMF. This is consistent with an increasing dip of the BMF from north to south, a geometry supported by additional modeling of gravity data (e.g., Oliver et al., 1995) and structural models of the evolution of the Bare Mountain block (Ferrill et al., 1996). The eastern boundary of Crater Flat basin is less distinct, but it is clear from the gravity-gradient map (figure 2-2) that the steepest gravity-gradients lie east of the topographic edge of the basin beneath YM and the proposed repository site. The southern topographic margin of Crater Flat basin also correlates with a rapid change in depth to basement. Comparatively steep gravity-gradients, however, also continue south of Crater Flat along the projection of the BMF into Amargosa Desert. Steep N-trending gradients are found on the eastern margin of Amargosa Desert that likely indicate a major N-trending fault in the northern part of Amargosa Desert (Healey and Miller, 1971; Oliver et al., 1995).

These observations are important to volcanic hazard assessment because many of the known Plio-Quaternary volcanoes in the YMR lie within or at the margins of this basement low. Plio-Quaternary volcanoes in Crater Flat all lie within or near high gravity-gradient areas associated with the Crater Flat basin. Two episodes of volcanism, the eruption of the Little Cones⁷ and the eruption of Miocene basalt

⁷Stamatakis, J.A., C.B. Connor, and R.H. Martin. 1996. Quaternary basin evolution and basaltic volcanism of Crater Flat, Nevada, from detailed ground magnetic surveys of the Little Cones. *Journal of Geology*. In press.

south of the Little Cones (figure 2-2), and a possible third episode suggested by the presence of a shallowly buried body of highly magnetized rock in southern Crater Flat, all occur very close to the steepest gravity-gradient in the region. The repetition of volcanic activity in this small area of the basin suggests that the BMF may provide a pathway for ascending magmas. Topographically, Lathrop Wells cinder cone lies outside Crater Flat but, based on the gravity data, is within the larger N-trending basin and at the margin of the prominent basement low in southernmost Crater Flat. Aeromagnetic anomalies A-E (Langenheim et al., 1993) in the Amargosa Desert also lie within or at the margins of the southern extension of this basin. The largest of these anomalies, (B), is the easternmost Plio-Quaternary volcano in the Crater Flat area and lies close to N-trending gravity anomaly demarcating the eastern edge of Amargosa Desert. Thus, the horizontal gravity-gradient appears to adequately represent crustal structures that have controlled past volcanism, especially the Plio-Pleistocene. It has been used here as a discrete density function to add structural data to the overall probability estimates.

2.3.2.2 Fault Dilation-Tendency

The ability of any fault or fracture to dilate is directly related to the normal stress acting across the fault or fracture surface. The relative tendency for a fault of a given orientation to dilate in a given stress state can be expressed by comparing the normal stress acting across the fault with the differential stress. Dilation tendency of the fault can be expressed as (Morris et al., 1996)

$$T_d = \frac{(\sigma_1 - \sigma_n)}{(\sigma_1 - \sigma_3)} \quad (2-1)$$

where σ_1 and σ_3 are the maximum and minimum compressional stresses and σ_n is the normal stress acting across the fault or fracture surface. In the YMR, σ_1 is vertical, σ_2 is horizontal and oriented 28° , and σ_3 is horizontal and oriented 300° . The relative magnitudes of $\sigma_1:\sigma_2:\sigma_3$ are 10:9:1.8 (Stock et al., 1985; Morris et al., 1996). As a result of this stress pattern, NE-trending vertical or steeply dipping faults have a greater tendency to dilate than faults of other orientations and there is a good correlation between the density of high dilation-tendency faults and extended terrains. Areas with higher concentrations of high dilation-tendency faults also may be more likely sites for future volcanic activity. Thus, in addition to the gravity data, the effect of structure on potential volcanic hazards can be further assessed by casting the distribution of high dilation-tendency faults as a density distribution and comparing this distribution to patterns of past volcanic activity.

2.3.2.3 Method of Using Structural Data in the Hazard Analysis

Incorporation of structural data into the probability estimate proceeds in several steps. First, an estimate of the spatial recurrence rate is made based on distribution and timing of past volcanic events. Connor and Hill (1995) reviewed patterns in volcanic activity in basaltic volcanic fields and found that nonhomogeneous methods provide estimated spatial and spatio-temporal recurrence rates that capture the clustered nature of volcanism and shifts in the location of volcanism through time within these volcanic fields.

The following equation shows an $m = 8$ near-neighbor spatio-temporal estimate of recurrence rate

$$\lambda_n(x,y) = \frac{m}{\sum_{i=1}^n u_i t_i} \quad (2-2)$$

where t_i is the time elapsed since formation of volcano i , m the number of near-neighbor volcanoes, and u_i the area of a circle having a radius equal to the distance between the point x,y and the i^{th} volcano. The resulting map of recurrence rate is normalized using a constant, k_1 , so that

$$\int_X \int_Y \frac{1}{k_1} \lambda_n(x,y) dy dx = 1 \quad (2-3)$$

where the limits X and Y correspond to the geographic extent of the map, well beyond the boundaries of the volcanic field and the area of the probability assessment. The resulting map of $\lambda_n(x,y)$ shows expected volcanic events/km² based on distribution and timing of past volcanic events.

Other methods of estimating $\lambda_n(x,y)$ are discussed in Connor and Hill (1995) and U.S. Department of Energy (1996a). These include use of the Epanechnikov kernel estimate of the density distribution (Connor and Hill, 1995). The near-neighbor and Epanechnikov kernel models produce a range of probability estimates and both approaches are used in the following bounding analysis.

In the second step, this map of $\lambda_n(x,y)$ based on either the near-neighbor or Epanechnikov kernel methods is multiplied with a map having the distribution of structural features represented by a surface, $s(x,y)$, calculated over the same geographic area, X,Y , and at the same grid spacing as the recurrence rate map. In the case of gravity data, a grid of complete Bouguer corrected gravity values was first constructed by minimum-tension bicubic spline interpolation. The amplitude of the horizontal gravity-gradient is then given by

$$s(x,y) = \sqrt{\left[\frac{\partial g}{\partial x}\right]^2 + \left[\frac{\partial g}{\partial y}\right]^2} \quad (2-4)$$

where g is the complete Bouguer gravity anomaly interpolated at location x,y .

Alternatively, $s(x,y)$ can be calculated based on distribution of faults with high dilation-tendency. To accomplish this, mapped faults in the YMR (Frizzell and Shulters, 1990) were discretized at 50 m intervals along their lengths. The number of fault segments within a circle of radius r about a grid node at point x,y is $n_f(x,y)$; the number of high dilation-tendency fault segments within the same area is $n_d(x,y)$. Here, r is chosen to be 4,850 m and the threshold for high dilation-tendency faults is chosen to be $T_d > 0.8$. Then

$$t(x,y) = \frac{n_i(x,y)}{\sum_x \sum_y n_i} - \frac{n_f(x,y)}{\sum_x \sum_y n_f} \quad (2-5)$$

Map areas where $t(x,y) < 0$ correspond to uplifted Paleozoic basement, resurgent areas within Timber Mountain caldera, and similar zones where bedrock that was not faulted predominantly in the current crustal stress-state is exposed. In contrast, terrains extended in the Neogene and Quaternary have predominantly high dilation-tendency faults and $t(x,y) > 0$. One of the central difficulties in using mapped fault distribution in hazard analysis is that in areas covered by Quaternary alluvium, both $n_f(x,y)$ and $n_i(x,y) = 0$. High dilation-tendency fault density is likely to be high, and is possibly greatest, in alluvial basins because these regions have experienced extension in the Neogene and Quaternary. Mapped fault density, however, is very low in these areas because of alluvial cover, resulting in low values of $t(x,y)$ that do not reflect true crustal-scale structure. For example, a detailed ground magnetic survey of Northern Cone⁸ reveals a large number of high dilation-tendency faults associated with the cone, although mapped fault density in the alluvium is low. Unfortunately, such detailed geophysical data are not available for much of Crater Flat or for other alluvial basins in the region. One means of addressing a lack of understanding of the fault density in alluvial basins is to assign a minimum value of $t(x,y)$ to areas of alluvial cover. This minimum value, n_k , was chosen so that $0 \leq n_k < \max [t(x,y)]$. Then

$$s(x,y) = \begin{cases} t(x,y), & t(x,y) > n_k \\ n_k, & 0 < t(x,y) < n_k \\ 0, & t(x,y) < 0 \end{cases} \quad (2-6)$$

Choosing a large value for n_k assumes that fault density is high in alluvial areas and heavily weights these areas in the probability analysis. Choosing a small value of n_k assumes that fault density is low in alluvial basins and letting $n_k \rightarrow 0$ results in $s(x,y)$ depending solely on mapped fault distribution.

To cast $s(x,y)$, calculated from either the horizontal gravity-gradient or the relative distribution of high dilation-tendency faults, as a probability density distribution, a constant, k_2 , is determined so that

$$\int_x \int_y \frac{1}{k_2} s(x,y) dy dx = 1 \quad (2-7)$$

The resulting probability density distribution is multiplied by the near-neighbor model or any other probability density distribution based on location and timing of past volcanic events. The resulting map can be renormalized so that probability of volcanism across the region is unity. The resulting

⁸Connor, C.B., LaFemina, P.L., Magsino, S.B., Hill, B.E. Unpublished ground magnetic survey on Northern Cone, August 1996.

expected recurrence rate of volcanism in a particular small area, $\Delta x \cdot \Delta y$, is $\lambda_s(x,y)$ given that volcanism will recur in the region X, Y .

It is important to note that s may be weighted in a variety of ways. For example, assigning a low weight to s by attenuating this matrix yields a solution that approaches the results of the near-neighbor analysis alone (i.e., λ_n). Conversely, assigning a large weight to s diminishes the role of the near-neighbor analysis, essentially suggesting that spatial distribution of volcanic events is well-represented and predicted by the distribution of crustal structure. Thus, both geologic interpretation and uncertainty are reflected in the relative weighing of λ_n and s in the calculation of λ_s . A simple weighing scheme commonly used in risk analysis (e.g., Griesmeyer and Okrent, 1981) is

$$\lambda_s(x,y) = \frac{1}{k_3} (\lambda_n(x,y) \cdot s(x,y)^w), \quad 0 < w \quad (2-8)$$

where w is the weight assigned to $s(x,y)$ and k_3 is a proportionality constant so that the integral of $\lambda_s(x,y)$ across the region is unity.

In the fourth step of the spatial analysis, the likelihood that a volcanic event at a given location will result in disruption of the proposed repository is assessed. One way to do this is to use an effective repository area, such as the actual area of the proposed repository, currently estimated to be approximately 5.6 km², plus some buffer area (e.g., Connor and Hill, 1995). A second approach, adopted here, is to estimate the probability that an event at a given location will produce a dike that will intersect the repository (e.g., Sheridan, 1992; U.S. Department of Energy, 1996a). In this analysis it is assumed that dike length has a uniform random probability distribution $U[d_1, d_2]$, $d_1 = 1,000$ m and $d_2 = 5,000$ m, and that dikes will be oriented at an azimuth of 28°, perpendicular to the regional minimum horizontal compressional stress. Other distributions for dike length and dike orientation can be used (U.S. Department of Energy, 1996a) and yield similar probability distributions. The volcanic event is assumed to be centered on the dike, thus

$$\begin{aligned} h_1 &= \frac{\min\{U[d_1, d_2]\}}{2} \\ h_2 &= \frac{\max\{U[d_1, d_2]\}}{2} \end{aligned} \quad (2-9)$$

then

$$d_L(x,y) = \frac{(h_2 - d(x,y))}{(h_2 - h_1)} \quad (2-10)$$

where $d(x,y)$ is the distance from a grid point at location x, y to the proposed repository boundary along a 28° azimuth. The frequency of dike intersection becomes

$$\lambda_d(x,y) = \begin{cases} 1, & d(x,y) \leq h_1 \\ d_L, & h_1 < d(x,y) < h_2 \\ 0, & h_2 \leq d(x,y) \text{ or } d(x,y) \text{ is undefined} \end{cases} \quad (2-11)$$

The probability of one or more volcanic events disrupting the repository is given by

$$P[N \geq 1] = 1 - \exp \left[-t \lambda_r \int_X \int_Y \lambda_s(x,y) \cdot \lambda_d(x,y) dy dx \right] \quad (2-12)$$

where X and Y are the limits of integration across the region of interest, λ_r is the regional recurrence rate of volcanic events, and t is the time interval of interest (e.g., 10,000 yr). The regional recurrence rate of volcanism is taken to be a constant in this analysis. U.S. Department of Energy (1996a) and Ho (1991) have explored the possibility of time-dependence of λ_r in detail.

2.3.2.4 Results

Two examples of spatial analysis and the resulting distribution of λ_s are shown in figures 2-3a–e. The calculation of λ_n using $m=8$ near-neighbor volcanoes results in a high probability of volcanism in southern Crater Flat and a zone of lower probability that extends along a NNW-trend. Connor and Hill (1995) present a full range of probability estimates based on different nonparametric estimates of λ_n . Application of the Epanechnikov kernel method results in a similar overall map pattern, but probability is more uniform in high probability areas, where distances to nearby volcanoes are less than h and uniformly low outside these zones (Connor and Hill, 1995).

The gravity-gradient map is normalized so that the sum of $s(x,y)$ across the map is unity (figure 2-3). Multiplying the two maps (figures 2-3a,b) with $w=1$ [Eq. (2-8)] produces a map of λ_s (figure 2-3c) that is considerably different from probability maps based on the near-neighbor model alone (e.g., figure 2-3a). High gravity-gradients along the BMF elongate and narrow the probability distribution in Crater Flat. The highest probabilities are located within 5 km of the surface expression of the BMF and are limited to the BMF hangingwall in Crater Flat. Conversely, probabilities based on λ_s are less than those based on λ_n across most of Bare Mountain because of the low gravity-gradients within this block. The pattern is slightly more complicated on the eastern margin of Crater Flat at YM. Gravity-gradients are relatively high at YM and south of YM along the Stagecoach fault delimiting the eastern boundary of the structural basin. This structure increases the probability of volcanism at YM. The calculated probability is, however, also more variable in this area than elsewhere in the basin.

An example of s calculated using high dilation-tendency fault density [Eq. (2-6)] is given in figure 2-3d with n_k equal to the average $t(x,y)$ across YM and $w = 1$ [Eq. (2-8)]. An important feature of this map is that $s(x,y)$ is zero where Paleozoic rocks crop out and in the Timber Mountain caldera

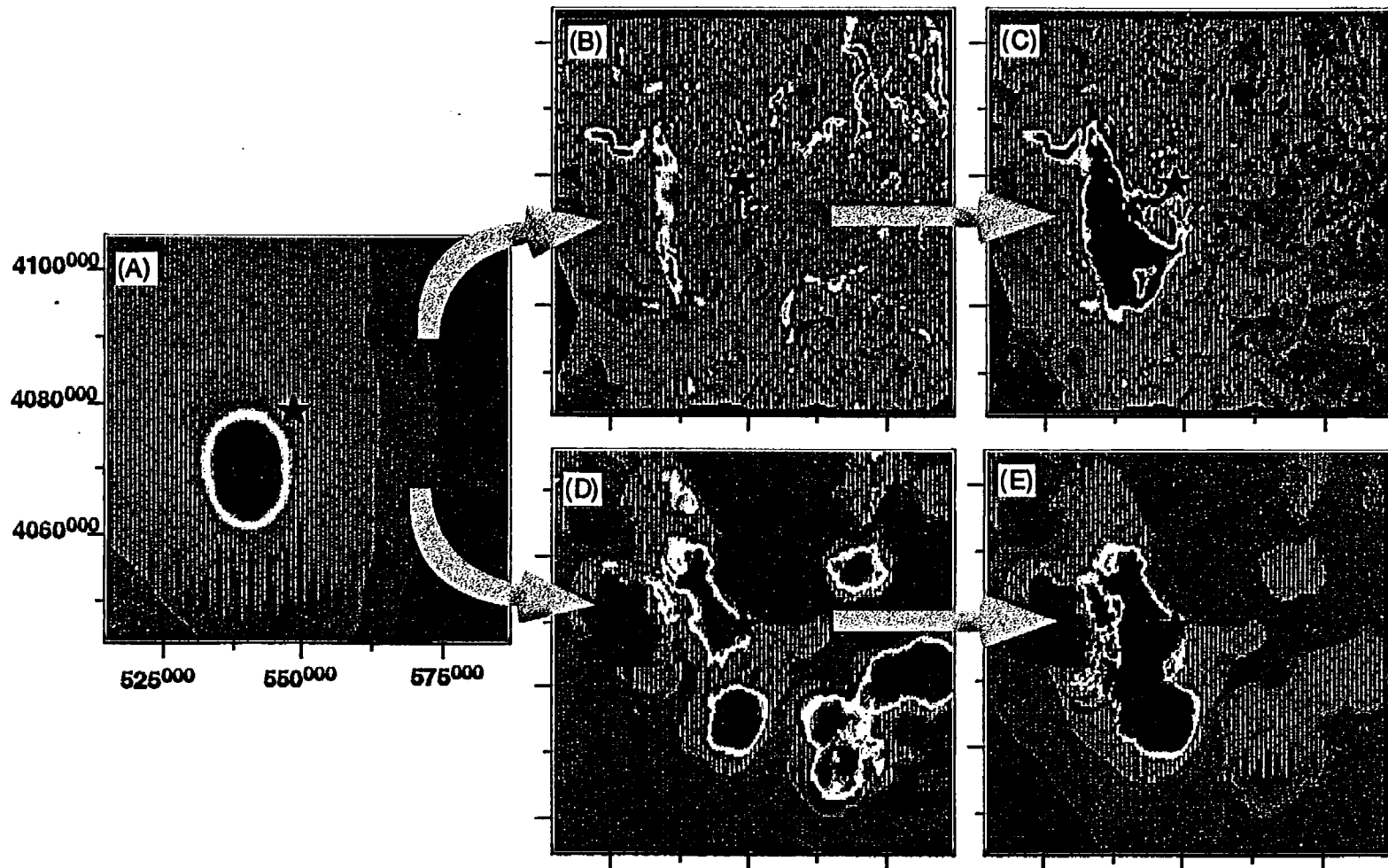


Figure 2-3. Maps illustrating the steps in calculation of the probability estimate. (a) Spatio-temporal model based on a near-neighbor model [Eq. (2-2)]; (b) Normalized horizontal gravity-gradient and (c) Resulting map with $w = 1$; (d) Normalized density of high dilation-tendency faults with n_k equal to the average of $t(x,y)$ across YM, and (e) Resulting probability map with $w=1$. Proposed repository location indicated by star (exact boundary used in analysis shown in figure 2-2).

complex—areas that have not extended significantly in the Quaternary. Multiplying the high dilation-tendency fault density map with λ_n results in an estimate of λ_s , which is quite similar to that obtained from the horizontal gravity-gradient. Probabilities are highest in Crater Flat and this high probability zone extends in a NNW direction. The proposed repository site is located at the eastern edge of this relatively high probability zone.

Results of the spatial probability analysis depend on assumptions made about the relative weight given to s and λ_n and the type of spatio-temporal model used to estimate λ_n . Sensitivity of the probability estimates to these assumptions was explored using various weights, w , in Eq. (2-8) for both the near-neighbor and Epanechnikov models. Eight near-neighbor volcanoes were chosen for the near-neighbor model and a smoothing parameter of $h=20$ was selected for the Epanechnikov model because the resulting maps provide lower and upper bounds on spatio-temporal recurrence rate in the site vicinity. With $w=0$, the probability of dike intersection with the proposed repository is that obtained from the spatio-temporal recurrence rate model alone, and ranges from approximately $P[N \geq 1] = 0.005$ to 0.0075 with $\lambda_s = 1$. Letting w vary from 0 to 4.5 increases the probability of dike intersection with maximum probabilities between $w=2$ and 2.5. Varying λ_s between 2 and 10 v/m.y. gives a probability of volcanic disruption between $1 \times 10^{-8}/\text{yr}$ and $1.4 \times 10^{-7}/\text{yr}$ (figure 2-4).

The effect of n_k and w on the probability calculated using the high dilation-tendency fault model is shown in figure 2-5. If the distribution of faults in alluvium is estimated to be the same as the average fault density at YM, the effect on probability is minimal. Although the probability of volcanism decreases in areas like Bare Mountain, probability is not significantly redistributed over large regions of the map. Probabilities are greatest for $n_k=0$ when analysis is restricted to mapped faults. In this case, probability values are higher at YM because of the high density of high dilation-tendency faults mapped on and around YM. Assigning $w=1-1.5$ gives the highest probability of dike intersection of the proposed repository, with probabilities ranging from 0.014 for the $m=8$ near-neighbor model to 0.019 for the $h=20$ km Epanechnikov kernel model, given that a volcanic event will occur in the area ($\lambda_s = 1$). Using $\lambda_s = 2-10$ v/m.y., probability estimates of volcanic disruption of the proposed repository that incorporate fault dilation-tendency vary between $1 \times 10^{-8}/\text{yr}$ and $1.9 \times 10^{-7}/\text{yr}$ (figure 2-5), essentially the same range estimated from the horizontal gravity-gradient.

2.3.2.5 Discussion

Results of this analysis indicate that structural models increase probability of volcanic disruption of the proposed repository site compared to models that do not incorporate structure explicitly. This result primarily reflects that fact that YM is structurally part of the Crater Flat basin (Ferrill et al., 1996) with geophysical data suggesting a rapid change in the depth to Paleozoic basement beneath the eastern edge of YM and high dilation-tendency faults bounding and penetrating YM itself. Because of the presence of these structures, a lower limit on probability estimates is represented by the spatio-temporal recurrence rate models that do not incorporate structure (e.g., Connor and Hill, 1995). This result is contrary to numerous source-zone models that suggest the presence of structure decreases the probability of volcanism at YM (Crowe et al., 1995; U.S. Department of Energy, 1996a). For example, the CFVZ as proposed by Crowe and Perry (1989), is a distinctive feature on the maps of λ_s calculated using both gravity and fault dilation-tendency models. However, the same structural features that tend to enhance the probability of volcanism within this zone occur at YM, albeit possibly to a lesser degree.

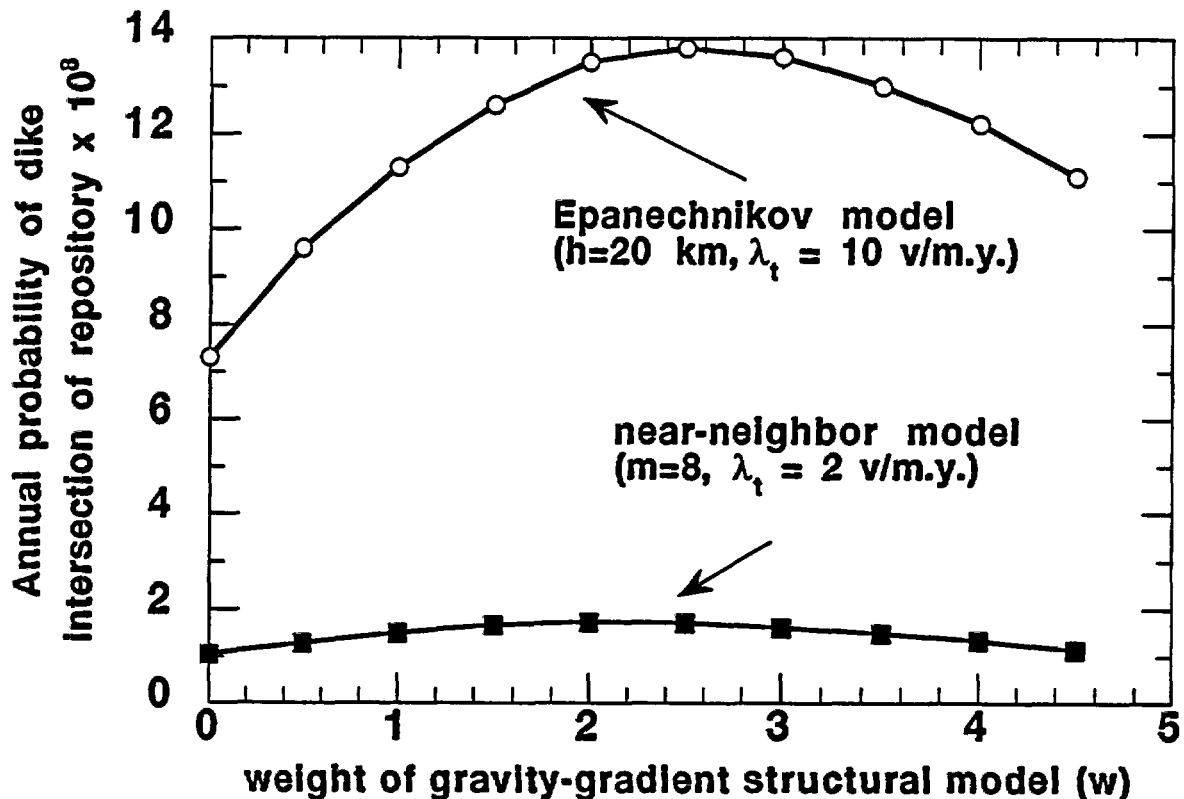


Figure 2-4. Range of probability estimates of dike intersection of the proposed repository, based on Epanechnikov and near-neighbor estimates, and amplitude of the horizontal gravity-gradient weighted by w (Eq. 2-8) for $\lambda_t = 2$ to 10 v/m.y.

Data sets other than the horizontal gravity-gradient and distribution of high dilation-tendency faults can be used to calculate s and λ_s . Estimators of s might include depth to Paleozoic basement based on integrated geological and geophysical models, improved models of fault distribution, or stress maps based on *in situ* stress measurements or microseismicity. Such estimates of s may provide further insight into the sensitivity of probability estimates to alternative conceptual models of the relationship between volcanism and structure. It is anticipated, however, that the range of probability estimates identified here (i.e., $1 \times 10^{-8} - 2 \times 10^{-7}$) will not change substantially given uncertainties associated with the regional recurrence rate of volcanism, λ_r , and the area affected by dike injection represented by λ_d .

2.3.3 Dispersion of Tephra from Basaltic Eruptions

2.3.3.1 Introduction

One of the key parameters in calculating risks associated with basaltic volcanic activity is accurately modeling how far erupted material can be transported from the vent into the accessible environment. For basaltic volcanic eruptions, the primary mode of dispersal is through aerial transport commonly extending tens of kilometers from the vent. Additional material accumulates at the vent through ballistic transport with lava flows commonly extending for several kilometers from the source. This section

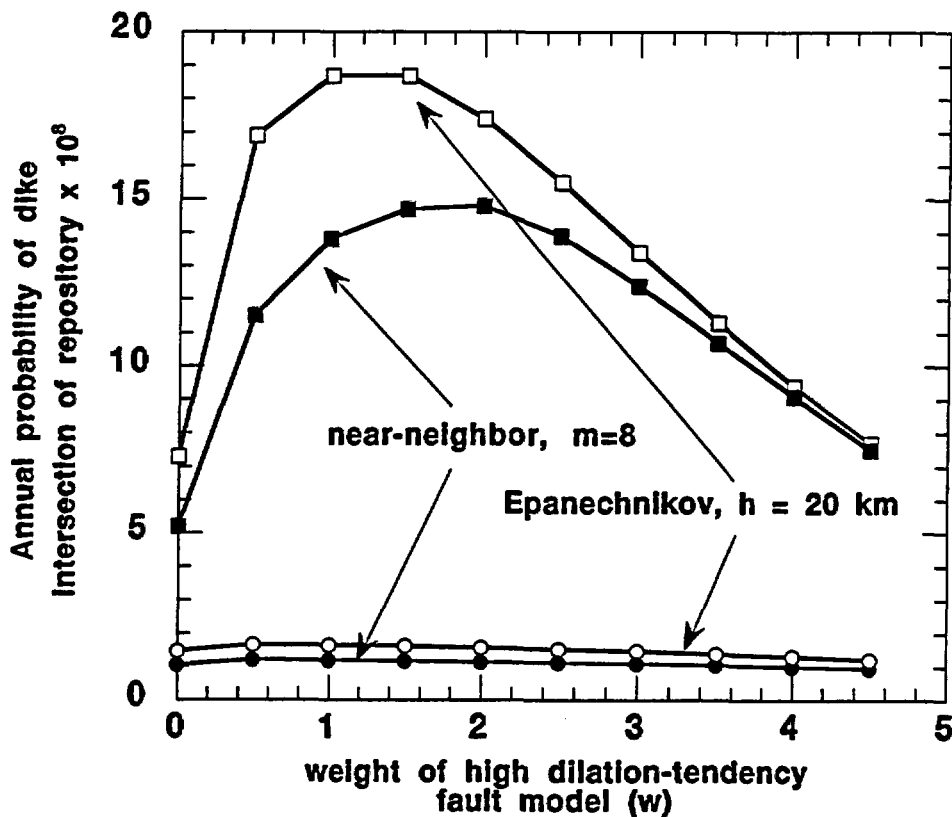


Figure 2-5. Range of probability estimates of dike Intersection of the proposed repository based on Epanechnikov and near-neighbor estimates and density of high dilation-tendency faults weighted $0 < w < 4.5$ (Eq. 2-8) for $\lambda_t = 2$ (circles) to 10 v/m.y. (squares)

examines recent work on modeling the dispersion of basaltic tephra using the model of Suzuki (1983) as implemented in Jarzempa.⁹ The primary emphasis of this section is to determine Suzuki (1983) model sensitivities to a range of input parameters that are derived from the literature and recent CNWRA field studies at active analog volcanoes. The results of the Suzuki (1983) model are then compared to tephra distribution patterns for the 1995 Cerro Negro eruption in Nicaragua, which has the detailed volcanological and granulometric data necessary for model evaluation.

The DOE efforts at modeling tephra distribution are described in Link et al. (1982). In summary, tephra with diameters greater than 0.06 mm are assumed to remain within 8 km of the vent with deposit thicknesses less than 1 cm beyond 8 km (Link et al., 1982). Work presented in this section will show that basaltic eruptions comparable or smaller in volume to Quaternary events in the YMR are capable of transporting tephra greater than 0.1 mm in diameter tens of kilometers from the vent and producing deposits centimeters thick. Link et al. (1982) modeled tephra with diameters less than 0.06 mm using a

⁹Jarzempa, M.S. 1996. Stochastic radionuclide distributions after a basaltic eruption for performance assessments of Yucca Mountain. *Nuclear Technology*. In press.

modified Gaussian plume equation. Jarzempa¹⁰ notes that a Gaussian plume model may not be appropriate for volcanic eruptions because the eruption column is a distributed source rather than a point source of particulates release. This may overestimate the dispersal capability of a basaltic eruption and thus underestimate radiation exposure to persons in a critical group.¹¹

2.3.3.2 Model Parameters

The Suzuki (1983) dispersal model is described in detail in Jarzempa.¹² In summary, Suzuki (1983) simulates the dispersal of tephra using a two-dimensional diffusion model in the atmosphere and relates the accumulation of tephra on the ground to the total mass of the tephra, grain size and density characteristics, height of the eruption column, and eruption and wind velocity. The Suzuki (1983) model successfully reproduced distribution patterns of tephra from the 1977 eruption of Usu volcano in Japan (Suzuki, 1985) and the 1986 eruption of Lascar volcano in Chile (Glaze and Self, 1991), both of which are short-duration plinian style eruptions from composite volcanoes.

Many of the input parameters for the Suzuki (1983) model can be sampled stochastically using a range of values for basaltic volcanic eruptions¹³ or entered directly for eruptions with detailed data. Critical parameters are (i) height of the eruption column, (ii) eruption duration, (iii) total tephra mass, (iv) mean particle diameter for the entire deposit, (v) standard deviation of particle diameter, (vi) average particle density, (vii) particle shape, and (viii) wind velocity. In addition, Suzuki (1983) uses constants for eddy diffusivity (C) and diffusion within the eruption column (β). Sensitivity of the Suzuki (1983) model to each of these input parameters is discussed in section 2.3.4.4.

2.3.3.3 Analog Volcano Data

The tephra deposits from YMR volcanoes have been removed by erosion and thus their dispersal characteristics must be inferred. Comparison with historically active basaltic volcanoes of similar size and eruption style provides a means to evaluate the tephra dispersal characteristics of ancient YMR volcanoes and to construct accurate models for use in PA. Using computer-assisted cartography, Quaternary volcanoes of the YMR have density-corrected volumes of roughly 0.002 km³ for Northern Cone and NE Little Cone, 0.02 km² for Hidden Cone, Little Black Peak and SW Little Cone,¹⁴ and 0.08 km³ for Lathrop Wells, Red and Black Cones. Historically active analog volcanoes (Connor, 1993; Hill, 1995) have density corrected volumes of 0.52 km³ for 1975 Tolbachik (Budinkov et al., 1983), 0.92 km³ for

¹⁰Jarzempa, M.S. 1996. Stochastic radionuclide distributions after a basaltic eruption for performance assessments of Yucca Mountain. *Nuclear Technology*. In press.

¹¹*Ibid.*

¹²*Ibid.*

¹³*Ibid.*

¹⁴Stamatakis, J.A., C.B. Connor, and R.H. Martin. 1996. Quaternary basin evolution and basaltic volcanism of Crater Flat, Nevada, from detailed ground magnetic surveys of the Little Cones. *Journal of Geology*. In press.

1943 Parícutin (Luhr and Simkin, 1993), 0.18 km³ for 1973 Heimaey (Self et al., 1974), 0.015 km³ for 1968 Cerro Negro (Taylor and Stoiber, 1973), 0.025 km³ for 1971 Cerro Negro (Rose et al., 1973), 0.012 km³ for 1992 Cerro Negro (McKnight, 1995), and 0.008 km³ for 1995 Cerro Negro (Global Volcanism Network, 1995).

The dispersal characteristics of these analog volcanoes are shown in figure 2-6. With the exception of Heimaey volcano, all of the analog volcanoes have deposit thicknesses greater than 1 cm at distances greater than 10 km from the vent. Heimaey volcano, which is a mantle hot-spot volcano located on a mid-oceanic ridge, represents the lower range of possible dispersion from a low-energy basaltic eruption. In addition to the dispersal characteristics, grain-size data are available for several of these eruptions. For the 1995 Cerro Negro eruption, 82.9 percent of the fall deposit is coarser than 0.1 mm at 20.1 km from the volcano. This percent increases to 86.1 at 6 km from Cerro Negro. The 1975 eruption of Cone 1 at Tolbachik volcano produced fall deposits with 70 percent of the material coarser than 0.1 mm (Budinkov et al., 1983). These data and figure 2-6 show that significant thicknesses and material coarser than 0.1 mm extends tens of kilometers from the vent and there is an insufficient technical basis to truncate volcanic dispersion models at 8 km (i.e., Link et al., 1982).

Data from the 1995 eruption of Cerro Negro was chosen as an initial test for the Suzuki (1983) model because the data were collected during and immediately after the eruption and all parameters necessary for detailed modeling were obtained. One fundamental problem in modeling basaltic volcanism is that eruption duration commonly is greater than the period of intense activity that produced the tephra fall deposits. Although these differences are well recognized in observed eruptions (e.g., Self et al., 1974; Budinkov et al., 1983; Luhr and Simkin, 1993), eruption durations reported in the literature rarely distinguish between total duration and duration of the main tephra producing phase. In addition, column heights vary significantly during the eruption and often are visually estimated from distant locations. These problems do not occur with the 1995 Cerro Negro eruption data. Errors introduced through erosion and diagenesis of the tephra deposits also were avoided.

2.3.3.4 Sensitivity Analysis

Before conducting the sensitivity analyses, the CNWRA computer code of the Suzuki (1983) model was tested by using the model parameters in Suzuki (1983) to reproduce the reported dispersal patterns. Small deviations (less than 10 percent) between output from the code and values reported in Suzuki (1983) were deemed acceptable and can be accounted for by the level of precision under which the code is routinely run. Slightly higher precision is possible, but involves an order of magnitude increase in computational time that was not judged effective for these analyses.

The Suzuki (1983) model calculates mass of basalt per unit area with distance from the vent. Calculating deposit thicknesses requires that the *in situ* bulk density of the deposit is known. Because of systematic changes in the size and sorting of the deposit with distance from the vent, deposit density will also vary systematically in pyroclastic falls (e.g., Cas and Wright, 1987). For the 1995 Cerro Negro eruption, proximal (i.e., less than 5 km) fall deposits have a measured bulk density of 1,100 kg m⁻³. Distal deposits (i.e., greater than 5 km) have a measured bulk density of 600 kg m⁻³. These values are used to calculate deposit thicknesses in the following analyses.

Deterministic parameters from the 1995 Cerro Negro eruption used in the sensitivity analyses are a column height of 2.0 km, eruption duration of 3.456×10⁶ s, total ash mass of 1.667×10⁹ kg, mean particle diameter for the entire deposit of 0.5 mm, standard deviation of particle diameter of 0.5 mm,

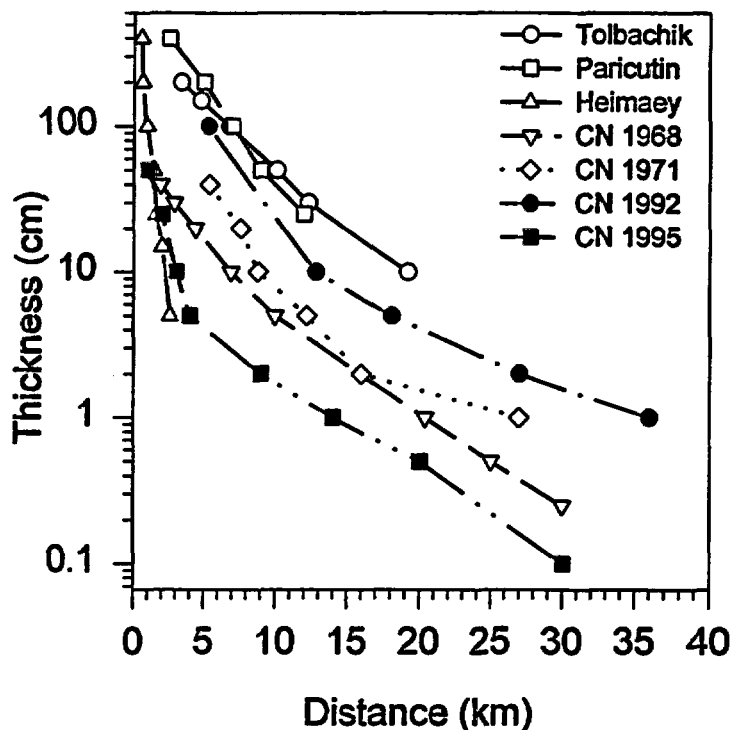


Figure 2-6. Dispersal characteristics for analog basaltic eruptions. Data sources in text. Thicknesses measured along main dispersal axis as reported in original isopach maps. Note significant thicknesses extend beyond 8 km from the vent, even for eruptions much smaller than those of the YMR.

particle shape factor of 0.5, β of 0.01, and C of 400. Average particle density ranged from 800 to 1,200 kg m^{-3} with a log-triangular distribution that was sampled stochastically (Jarzempa and LaPlante, 1996).

Wind speed is the most sensitive parameter in the Suzuki (1983) model, with a 100 percent increase in wind speed resulting in 200 percent increases in deposit thicknesses for lower wind velocities. During the 1995 eruption of Cerro Negro, wind speeds at ground level were estimated at 9 m s^{-1} (i.e., 20 mi hr^{-1}). Satellite imagery also shows wind speeds between 8 and 10 m s^{-1} during the eruption (Global Volcanism Network, 1995). Although the Suzuki (1983) model accurately calculates deposit thicknesses within 5 km of the vent using observed wind speeds and eruption characteristics, it underestimates distal thicknesses (i.e., greater than 5 km) by approximately 60 percent (figure 2-7a). A wind speed of 18 m s^{-1} (40 mi hr^{-1}) agrees well with observed distal thicknesses but overestimates proximal thicknesses by 100 percent (figure 2-7a). Analyses presented later in this section will show that this sensitivity to wind speed cannot be overcome by selecting reasonable values for other critical parameters. This discrepancy may be important as the distal component of a repository-penetrating eruption will transport most of the waste material into the accessible environment (e.g., Jarzempa and LaPlante, 1996). The remaining analyses will show a range of wind speeds, to present a sense of scale to model parameter sensitivities.

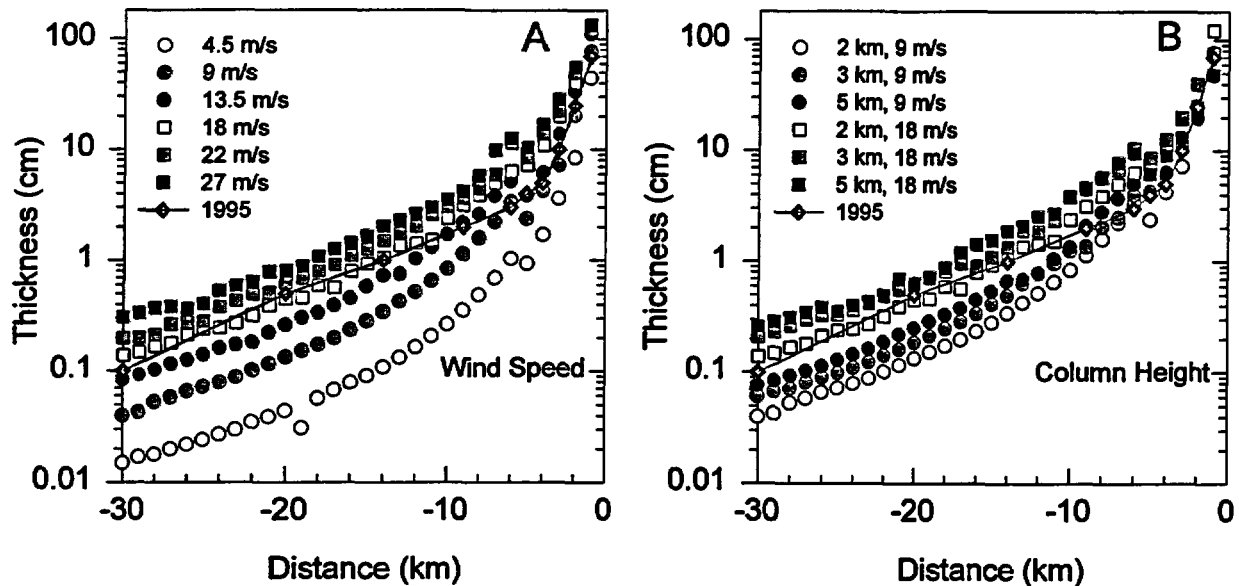


Figure 2-7. a) Variations in deposit thicknesses with distance from the vent as a function of wind speed using the tephra dispersal model of Suzuki (1983) and data from the 1995 Cerro Negro eruption. Observed wind speeds were 9 m s^{-1} during the eruption; 1995 deposits shown by symbol 1995. b) Variations in deposit thicknesses with distance from the vent as a function of column height. Observed column heights were 2 km during the eruption.

Variations in the eruption column height also have a demonstrable effect on modeled deposit thicknesses, although this effect is significantly less than the effect of wind speed. Increasing the column height from 2 to 5 km, while maintaining a constant eruption volume, increases distal deposit thicknesses by roughly 50 percent (figure 2-7b). To maintain mass balance, however, the eruption duration must decrease to 3 hr to sustain a 5 km high column. Similarly, a 3-km-high column could only be sustained for 1 d given the observed eruption mass. Direct observation and calculation of mass accumulation rates show the main tephra-producing phase of the eruption must have lasted 3.5–4 d. Thus, small variations in column height (i.e., $\pm 0.5 \text{ km}$) cannot account for discrepancies between modeled and measured deposit thicknesses beyond 5 km from the vent.

Order of magnitude variations in the median particle diameter can produce less than 50 percent variations in deposit thicknesses using the Suzuki (1983) model. For the 1995 Cerro Negro eruption, 50 percent of the tephra volume is contained within the 5 cm isopach which extends to 5 km from the vent and has a bulk deposit median grain-size diameter of about 0.5 mm. For comparison, 50 cm thick deposits 1 km from the vent have median diameters of 2 mm, whereas deposits at 20 km from the vent are 0.5 cm thick with median diameters of only 0.2 mm. Varying particle diameter between 0.5 and 2 mm produces only minor variations in deposit thicknesses (figure 2-8a) and cannot account for the discrepancies between observed and calculated dispersal for the 1995 Cerro Negro eruption.

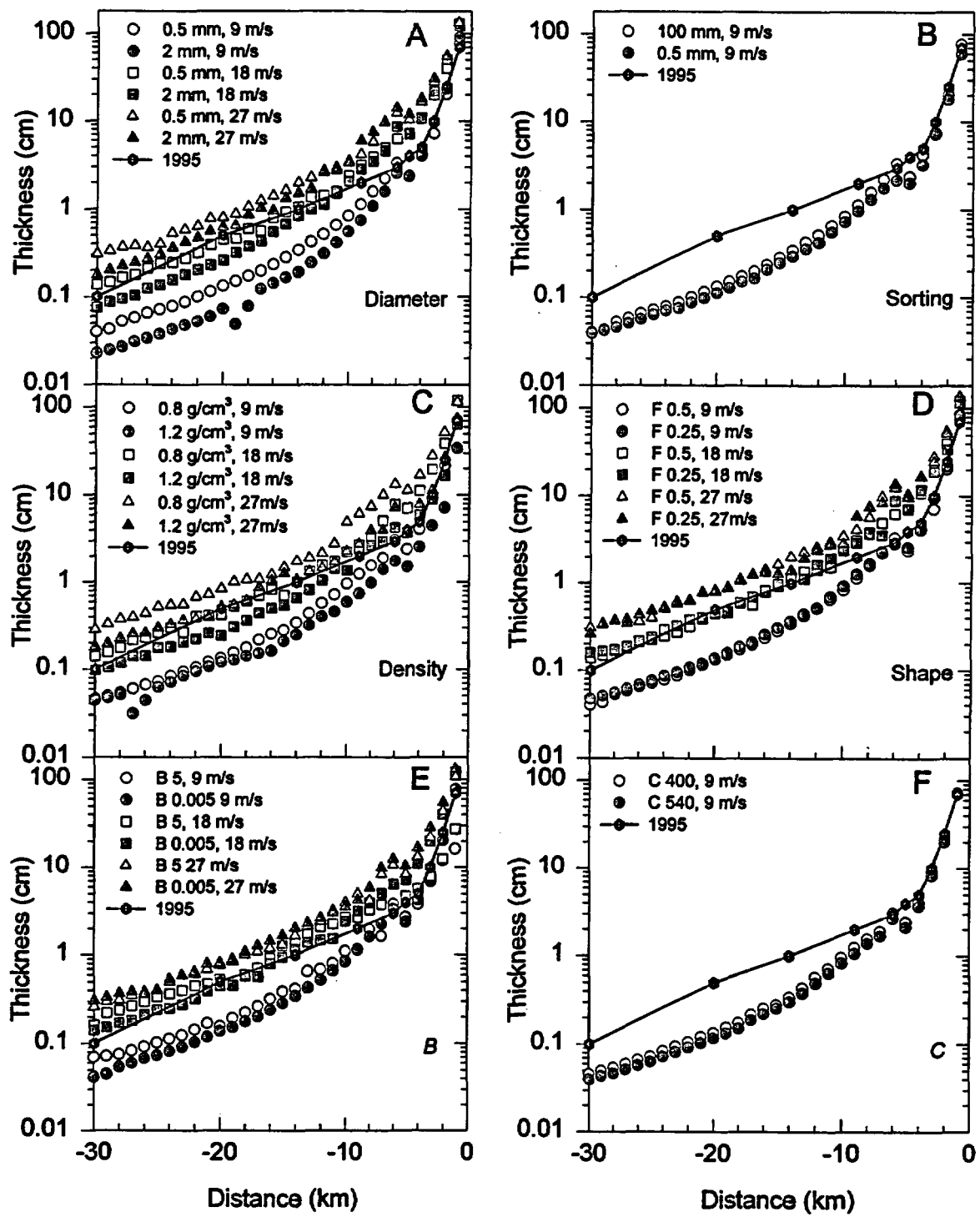


Figure 2-8. Sensitivity of the Suzuki (1983) model to variations in a) Average particle diameter; b) Particle sorting; c) Particle density; d) Particle shape; e) Constant β for vertical diffusion; and (f) Constant C for eddy diffusivity. Models are shown for a range of wind speeds and compared with data from the 1995 Cerro Negro eruption.

Other particle size and shape characteristics have even less effect on dispersal patterns using the Suzuki (1983) model. With clast density fixed at 800 kg m^{-3} , sorting (i.e., the distribution of different particle sizes within a deposit) has only a minor effect on deposit thicknesses (figure 2-8b). Deposits from the 1995 Cerro Negro eruption have a relatively narrow range of grain sizes and are thus considered well sorted (i.e., sorting = 0.5 mm). Increasing the range of grain sizes (i.e., sorting) within the deposit to 100 mm only results in a roughly 10 percent increase in deposit thicknesses. Changes in particle density have variable but small effects on deposit thicknesses (figure 2-8c), although these variations are less systematic than those associated with most other parameters. Decreasing particle density from $1,200 \text{ kg m}^{-3}$ to 800 kg m^{-3} increases deposit thicknesses about 20 percent for 9 m s^{-1} wind speeds, with a roughly 40 percent increase for 27 m s^{-1} wind speeds (figure 2-8c). Changing the shape of the tephra has a negligible effect on thickness distributions (figure 2-8d). Decreasing the shape parameter F from 0.5 (roughly equant) to 0.25 (roughly tabular) increases the cross-sectional area of the particle and thus increases particle settling times. This increase in settling times, however, results in a less than 5 percent increase in deposit thicknesses.

Several important physical constants are used in the Suzuki (1983) model of tephra dispersion. Suzuki (1983) uses the constant β to control the mass diffusion pattern from the eruption column. Variations of β in Suzuki (1983) between 0.5 and 0.02 produce very different diffusion patterns, with broader and greater dispersion of material for larger values of β . It is important to note that the CNWRA computer code successfully reproduced the distribution patterns reported in Suzuki (1983) when using his eruption conditions. In contrast, similar variations in β produced barely discernable variations in deposit thicknesses for the 1995 Cerro Negro eruption conditions (figure 2-8e). Increasing β from 0.005 to 0.5 results only in a 10 percent average increase in deposit thicknesses for all wind speeds. Increasing β to 5 results in a 24 percent increase in distal deposit thicknesses, relative to β equal to 0.005. This value of β , however, results in an approximately 50 percent underestimation of thicknesses within several kilometers of the vent (figure 2-8e). Increasing β to 0.5 results in the maximum tephra mass per unit area occurring at a significant distance from the vent (Suzuki, 1983) rather than immediately at the vent as observed in basaltic eruptions. Thus, values of β above 0.5 do not appear justified.

The relative insensitivity of β likely results from the small column-height for basaltic cinder cone eruptions. Because these eruptions columns ascend to only around 5 km or less, there is limited opportunity for lateral diffusion or spreading within the rising column. Thus, particles are released from essentially a point-source at the top of the column rather than from a broad area as commonly observed for larger eruptions [cf. Suzuki, 1983 figures (2-3)–(2-4)]. Suzuki (1983) uses another constant, C , in equations governing eddy diffusivity (i.e., horizontal transport). Data presented in Suzuki (1983) for a range of eruption sizes result in a value for C of 400. Restricting these data to only relatively small eruptions results in a value of 540 for C . As shown in figure 2-8, using a value of 540 for C results in a less than 10 percent decrease in deposit thicknesses.

A final set of simulations were run for conditions that best represent the 1995 Cerro Negro eruption: column height of 2.0 km, eruption duration of $3.456 \times 10^6 \text{ s}$, total ash mass of $1.667 \times 10^9 \text{ kg}$, mean particle diameter for the entire deposit of 0.5 mm, standard deviation of particle diameter of 0.5 mm, particle shape factor of 0.25, average particle density of 800 kg m^{-3} , β of 0.5 and C of 400. These conditions were used with wind speeds of 9 m s^{-1} (i.e., observed) and 18 m s^{-1} . The latter results in the best apparent fit of the model to observed tephra distributions (figure 2-9a) although this wind velocity

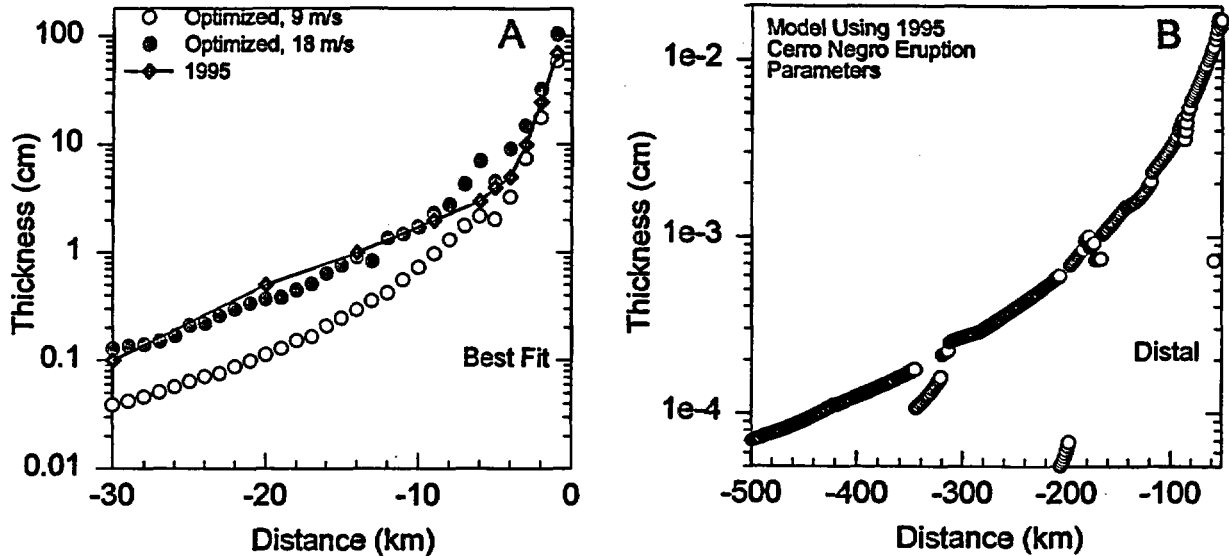


Figure 2-9. a) Distribution of tephra modeled using Suzuki (1983) optimized to conditions from the 1995 Cerro Negro eruption compared with measured deposit thicknesses. Wind speed during the eruption was 9 m s^{-1} , whereas speeds of approximately 18 m s^{-1} are required to generate measured deposit thicknesses at 5–30 km from the vent. b) Deposit thicknesses to 500 km from the vent, using same conditions as 1995 Cerro Negro eruption including wind speeds of 9 m s^{-1} .

is twice that observed during the eruption. Using measured wind velocities, the model underestimates deposit thicknesses by 50 percent at distances of 5 to 30 km from the vent.

2.3.3.5 Discussion

The Suzuki (1983) model successfully produces tephra-fall thicknesses observed for the 1995 Cerro Negro eruption at distances less than 5 km from the vent. Optimizing the Suzuki (1983) model for parameters measured during the 1995 Cerro Negro eruption, or at the reasonable upper bounds of these parameters, underestimates deposit thicknesses by 50 percent at distances 5–30 km from the vent. In addition, the volume of the 1995 Cerro Negro eruption is significantly smaller than most Quaternary YMR volcanoes and mass discharge rate also is relatively low (about $4 \text{ m}^3 \text{ s}^{-1}$). This eruption thus should not overestimate the dispersal characteristics for YMR-type eruptions. The sensitivity of key parameters in the Suzuki (1983) model has been examined in detail. The model is highly sensitive to wind velocity, moderately sensitive to column height, particle diameter and density, and relatively insensitive to the degree of sorting, particle shape, and constants related to column diffusivity and eddy diffusivity. The sensitivity to wind speed is especially important to repository performance models, where average wind

speeds of 3–7 m s⁻¹ are used.¹⁵ Current versions of the Suzuki (1983) model likely underestimate deposit thicknesses, and thus volume of waste material dispersed, by 50 percent in regions critical to determining radiation releases within the accessible environment (Jarzemba and LaPlante, 1996).¹⁶

The implementation of the Suzuki (1983) model on the CNWRA systems has been checked and found to accurately reproduce distribution patterns and parameter sensitivities shown in the original reference. Currently, the cause for underestimation of deposit thicknesses is speculative, but presumably relates to a conceptual problem with the Suzuki (1983) model as applied to small column height, low mass-flow basaltic eruptions. Apparently, mass distribution is not accurately accounted for in these small-volume eruptions and there is insufficient horizontal transport of material along the depositional axis. To test for mass conservation, tephra dispersal was modeled over a 50×50 km area. This area contains nearly all of the deposit down to thicknesses of 0.1 mm. The material modeled within this area underestimates the mass deposited from the 1995 Cerro Negro eruption by 36 percent (i.e., 1×10¹² g), which is in relative agreement with the 50 percent underestimation of deposit thicknesses solely along the main fall axis. In addition, deposit thicknesses down to 0.001 mm were modeled to a distance of 500 km from the vent (figure 2-9b). Construction of reasonable isopachs from these data can only account for about 25 percent of the missing mass.

For comparison, calculations using the well-recognized exponential thinning of fall deposits with distance from the vent (e.g., Fierstein and Nathenson, 1992) show that only 25 percent of the 1995 Cerro Negro fall deposits should be present in deposits thinner than 1 mm. One of the characteristics of basaltic eruptions, however, is that magma fragmentation is relatively weak, resulting in a lack of ≤1 mm tephra (e.g., Walker, 1973; 1981). It is thus highly unlikely that 25 percent of the Cerro Negro deposits are contained in deposits thinner than 1 mm, whereas such volumes are possible for more highly fragmented silicic eruptions (e.g., Fierstein and Nathenson, 1992).

2.3.4 Conclusions

Calculations of the probability of future igneous activity at the proposed repository site are dependent on accurate identification and characterization of igneous features within the YMR. Pliocene volcanism in the Funeral Formation suggests that Plio-Quaternary recurrence rates may be relatively constant through time. This is an alternative interpretation to that used in many Weibull-process probability models which assume volcanism recurrence rates increase during the Quaternary (e.g., Ho, 1991; U.S. Department of Energy, 1996a). In addition, Funeral Formation volcanoes may affect probability models that use vent location to control definition of spatial trends to the YMR volcanic field, so that the probability of future igneous activity at the proposed repository site could be greater than calculated by some models in U.S. Department of Energy (1996a). Reworked, coarse-grained 6.3±0.8 Ma silicic pumice in Crater Flat alluvium cannot be correlated with any known silicic eruption in the YMR and likely indicates a previously unrecognized episode of silicic magmatism in the YMR. The risk of future silicic igneous activity was thought to be negligible based on the absence of post-caldera silicic eruptions in the YMR (U.S. Department of Energy, 1993). The post-caldera Crater Flat pumice shows that determining

¹⁵Jarzemba, M.S. 1996. Stochastic radionuclide distributions after a basaltic eruption for performance assessments of Yucca Mountain. *Nuclear Technology*. In press.

¹⁶*Ibid.*

the risks presented by future silicic eruptions requires an additional evaluation of the YMR geologic setting to see if the conditions that led to the production of this pumice are present or could be present during future periods of interest.

Integration of fault dilation-tendency with spatio-temporal Poisson probability models shows that many of the faults in and proximal to the proposed repository site are in high dilation orientations, which favors magma ascent. Other areas, such as Bare Mountain, lack such faults. The probability of future igneous activity should be lower in areas lacking high dilatancy faults than calculated strictly by spatio-temporal methods but proportionally higher in areas of high dilation-tendency. Integrated dilation-tendency probability models show that the probability of future volcanic disruption of the proposed repository site ranges between 1×10^{-8} and 2×10^{-7} per year. In contrast, U.S. Department of Energy (1996a) concluded, based in large part on the definition of preferred structural zones, that this probability is 1.5×10^{-8} with a 90 percent confidence interval of 5.4×10^{-10} to 4.9×10^{-8} .

Data from basaltic volcanoes analogous to those of the YMR and modeling shows that significant amounts of material can be transported tens of kilometers from a small-volume basaltic eruption. In contrast, the DOE models assume that only material with diameters less than 0.06 mm can be transported more than 8 km from the vent, forming deposits less than 1 cm thick. Current models being used in the CNWRA research underestimate tephra deposit thicknesses by about 50 percent at distances of 5–30 km. These distances are important to evaluating releases of radioactive material into the accessible environment. Tephra dispersion models are highly sensitive to wind speed and a lesser extent to eruption column height, particle diameter, and density. Whereas wind speed can be sampled stochastically, the other eruption parameters will need to be estimated accurately for the poorly preserved to absent deposits at YMR volcanoes. Data from historically active analog volcanoes will be critical to constraining these parameters.

The DOE WCIS concludes "Volcanic events within the controlled area will be rare and the consequences of volcanism will be acceptable." Based on information presented herein, the current understanding of the YMR volcanic and structural setting indicates the probability of future basaltic volcanic events at the proposed repository site ranges between 10^{-8} and 10^{-7} per year. The probability of future silicic volcanic events is unknown, but the available data shows that silicic pyroclastic eruptions likely occurred in the YMR at least several million years after cessation of caldera-forming activity. The consequences of volcanism on repository performance are incompletely bounded, but the current understanding of small-volume basaltic eruption processes is sufficient to show that significant amounts of material can be transported tens of kilometers from the vent into the accessible environment.

2.4 ASSESSMENT OF PROGRESS TOWARD MEETING OBJECTIVES

Work completed in FY96 continued to provide independent assessments of the probability of future igneous activity in the YMR and of processes important to consequence analyses. Detailed field investigations have shown that significant igneous features remained present but undetected or poorly characterized including post-caldera silicic eruptions. These activities will ensure that all relevant information is used in assessing risks associated with igneous activity including the quantification of uncertainty associated with these analyses. Important progress also was made through the integration of fault dilation-tendency into spatio-temporal probability models, which provides a significantly different interpretation of the effects of structure on igneous activity than presented in many DOE models (e.g., U.S. Department of Energy, 1996a). Work on probability issues not reported herein also has continued on

understanding the petrogenetic evolution of the YMR volcanic field and integrating field and geochronological data from other western U.S. volcanic fields to construct robust tests of probability model accuracies.

Understanding the consequences of igneous activity on proposed repository performance also has progressed well during FY96. Data from analog basaltic volcanoes, most importantly from the December 1995 Cerro Negro eruption, continue to provide an independent means to develop and test consequence models. The sensitivity analysis of the Suzuki (1983) dispersion model shows that accurately quantifying the column height and grain-size characteristics for YMR volcanoes is important to calculating risks of radiological releases into the accessible environment. Additional major work during FY96 related to consequences included integration of data from analog volcanoes on thermal and degassing effects associated with basaltic igneous activity, field and laboratory analyses to determine critical eruption characteristics from tephra deposits, and studies of wall-rock fragmentation and entrainment processes at historically active and YMR volcanoes.

In addition to the technical accomplishments, significant progress was made on closure of open items. Between the Site Characterization Analysis and study plan reviews, the NRC generated 57 open items of which six had been closed prior to FY96. During FY96, the NRC closed an additional 18 open items and a re-analysis of the open items based on information contained within the new DOE Program Plan suggests that review of U.S. Department of Energy (1996a), along with the proposed DOE Geophysical Synthesis report, should allow the closure of a significant number of other open items during FY97.

Work in FY97 will shift to greater emphasis on consequence analyses, primarily related to waste fragmentation, entrainment mechanisms, and dispersal modeling. Previous and ongoing PA analyses (e.g., Jarzempa and LaPlante, 1996) have shown these to be critical processes to determining risks associated with igneous activity. In FY97 resources will need to be devoted to review of the DOE reports and planned documents including U.S. Department of Energy (1996a) and a volcanism synthesis report.

Although the DOE mean probability value is within the range reported in section 2.3.3, significant differences in approach to consideration of processes that control location of igneous activity, including shallow and deep structural setting, topography, and definition of "source zones." One example is the detailed ground magnetic studies by CNWRA staff, which revealed north-trending faults in eastern Crater Flat that offset tuff beneath a thin carapace of alluvium. These faults apparently localized volcanism at Northern Cone at a stratigraphic level above the repository horizon. Many DOE source-zone models, which form the basis for the DOE WCIS, are inconsistent with these volcano-fault relationships. Understanding the processes that control volcanism is important because the probability of future igneous activity is low but may be large enough to influence repository performance. Regardless of these differences and because of the proposed revisions to the U.S. Environmental Protection Agency standard, from a regulatory perspective issue resolution is possible in FY97. Both DOE and NRC agree that while volcanic activity affecting the repository is a low probability event, probability is sufficiently high that the consequences of such activity must be considered in PA. Although technical differences apparently exist, an Issue Resolution Report is planned for FY97 to attempt to resolve the probability subissue. This report will evaluate existing data and models from the DOE, CNWRA, and others to arrive at a reasonably conservative range on the probability of future igneous activity at the proposed repository site.

2.5 INTEGRATION WITH OTHER KEY TECHNICAL ISSUES

IA has relied heavily on input from the Structural Deformation and Seismicity (SDS) KTI in developing fault dilation-tendency probability models and understanding the structural and geophysical setting of the YMR. Output from igneous activity to SDS include the integration of geophysical data that constrains the structural setting of the YMR and the timing and nature of post-caldera volcanism as tectonic indicators. IA also is strongly linked with the Total System Performance Assessment and Integration (TSPA) KTI, providing input on volcanic processes and probabilities for performance models, review of DOE TSPA-95 (TRW Environmental Safety Systems, Inc., 1995), and development and testing of the tephra dispersal model. These links will strengthen in FY97, especially for model development and integration with TSPA. In addition, some integrated study is expected with Container Life and Source Term KTI staff to better understand the effects of igneous activity on waste package integrity.

2.6 REFERENCES

- Budinkov, V.A., Ye.K. Markhinin, and A.A. Ovsyannikov. 1983. The quantity, distribution and petrochemical features of pyroclastics of the great Tolbachik fissure eruption. S.A. Fedotov and Ye.K. Markhinin, eds. *The Great Tolbachik Fissure Eruption*. New York, NY: Cambridge University Press: 41-56.
- Carr, W.J. 1982. *Volcano-Tectonic History of Crater Flat, Southwestern Nevada, as Suggested by New Evidence from Drill Hole USU-VH-1 and Vicinity*. U.S. Geological Survey Open-File Report 82-457. Reston, VA: U.S. Geological Survey.
- Cas, R.A.F., and J.V. Wright. 1987. *Volcanic Successions*. Winchester, MA: Unwin Hyman Inc.
- Connor, C.B. 1993. *Technical and Regulatory Basis for the Study of Recently Active Cinder Cones*. San Antonio, TX: Center for Nuclear Waste Regulatory Analyses.
- Connor, C.B., and B.E. Hill. 1995. Three nonhomogeneous Poisson models for the probability of basaltic volcanism: Application to the Yucca Mountain region, Nevada, U.S.A. *Journal of Geophysical Research* 100(B6): 10,107-10,125.
- Connor, C.B., and C.O. Sanders. 1994. *Geophysics Review Topical Report: Application of Seismic Tomographic and Magnetic Methods to Issues in Basaltic Volcanism*. CNWRA 94-013. San Antonio, TX: Center for Nuclear Waste Regulatory Analyses.
- Connor, C.B., R.H. Martin, P.G. Hunka, J.A. Stamatakos, D.B. Henderson, and R.V. Klar. 1996. *Ground Magnetic Survey of the Little Cones, Crater Flat, Nevada*. CNWRA 96-002. San Antonio, TX: Center for Nuclear Waste Regulatory Analyses.
- Crowe, B.M., and F.V. Perry. 1989. Volcanic probability calculations for the Yucca Mountain site: Estimation of volcanic rates. *Proceedings Nuclear Waste Isolation in the Unsaturated Zone, Focus '89*. La Grange Park, IL: American Nuclear Society: 326-334.

- Crowe, B.M., F.V. Perry, J. Geissman, L. McFadden, S. Wells, M. Murrell, J. Poths, G.A. Valentine, L. Bowker, and K. Finnegan. 1995. *Status of Volcanic Hazard Studies for the Yucca Mountain Site Characterization Project*. Los Alamos National Laboratory Report LA-12908-MS. Los Alamos, NM: Los Alamos National Laboratory.
- Ferrill, D.A., J.A. Stamatakos, S.M. Jones, B. Rahe, H.L. McKague, R.H. Martin, and A.P. Morris. 1996. Quaternary slip history of the Bare Mountain fault (Nevada) from the morphology and distribution of alluvial fan deposits. *Geology* 24(6): 559–562.
- Fierstein, J., and M. Nathenson. 1992. Another look at the calculation of fallout tephra volumes. *Bulletin of Volcanology* 54: 156–167.
- Fleck, R.J., B.D. Turrin, D.A. Sawyer, R.G. Warren, D.E. Champion, M.R. Hudson, and S.A. Minor. 1996. Age and character of basaltic rocks of the Yucca Mountain region, southern Nevada. *Journal of Geophysical Research* 100(B4): 8,205–8,227.
- Frizzell, V.A. Jr., and J. Shulters. 1990. *Geologic Map of the Nevada Test Site, Southern Nevada*. U.S. Geological Survey Miscellaneous Investigations Map I-2046. Reston, VA: U.S. Geological Survey.
- Glaze, L.S., and S. Self. 1991. Ashfall dispersal for the 16 September 1986 eruption of Lascar, Chile, calculated by a turbulent diffusion model. *Geophysical Research Letters* 18(7): 1,237–1,240.
- Griesmeyer, J.M., and D. Okrent. 1981. Risk management and decision rules for light water reactors. *Risk Analysis* 1: 121–136.
- Global Volcanism Network. 1995. Cerro Negro, Nicaragua. *Bulletin of the Global Volcanism Network* 20(11/12): 2–4.
- Healey, D.L., and C.H. Miller. 1971. *Gravity Survey of the Amargosa Desert Area of Nevada and California*. U.S. Geological Survey Report USGS-474-308. U.S. Geological Survey Technical Letter NTS-99: 30 pp.
- Hill, B.E. 1995. *Expert-Panel Review of CNWRA Volcanism Research Programs*. CNWRA 95-002. San Antonio, TX: Center for Nuclear Waste Regulatory Analyses.
- Hill, B.E., and C.B. Connor. 1996. Volcanic Systems of the Basin and Range *NRC High-Level Radioactive Waste Research at CNWRA, July–December 1995*. B. Sagar, ed. CNWRA 95-02S. San Antonio, TX: Center for Nuclear Waste Regulatory Analyses. 5–1 to 5–21.
- Ho, C.-H. 1991. Time trend analysis of basaltic volcanism at the Yucca Mountain site. *Journal of Volcanology and Geothermal Research* 46: 61–72.
- Jarzemba, M.S., and P.A. LaPlante. 1996. *Preliminary Calculations of Expected Dose from Extrusive Volcanic Events at Yucca Mountain*. IM 5078-771-610. San Antonio, TX: Center for Nuclear Waste Regulatory Analyses.

- Langenheim, V.E., K.S. Kirchoff-Stein, and H.W. Oliver. 1993. Geophysical investigations of buried volcanic centers near Yucca Mountain, southwest Nevada. *Proceedings of the Fourth Annual International Conference on High-Level Radioactive Waste Management*. La Grange Park, IL: American Nuclear Society: 1,840–1,846.
- Langenheim, V.E., and D.A. Ponce. 1995. Depth to Pre-Cenozoic basement in southwest Nevada. *Proceedings of the Sixth Annual International Conference on High-Level Radioactive Waste Management*. La Grange Park, IL: American Nuclear Society: 129–131.
- Link, R.L., S.E. Logan, H.S. Ng, F.A. Rokenbach, and K.-J. Hong. 1982. *Parametric Studies of Radiological Consequences of Basaltic Volcanism*. Sandia National Laboratory Report SAND 81-2375. Albuquerque, NM: Sandia National Laboratory.
- Luhr, J.F., and T. Simkin. 1993. *Paricutin, the Volcano Born in a Mexican Cornfield*. Phoenix, AZ: Geoscience Press.
- McAllister, J.F. 1970. *Geology of the Funeral Creek Borate Area, Death Valley, Inyo County, California*. California Division of Mines and Geology Map Sheet 14. Sacramento, CA: California Division of Mines and Geology.
- McDuffie, S.M., C.B. Connor, and K.D. Mahrer. 1994. A simple 2-D stress model of dike-fracture interaction. *EOS, Transactions of the American Geophysical Union* 75(16): 345.
- McKnight, S.B. 1995. *Geology and Petrology of Cerro Negro Volcano, Nicaragua*. M.S. Thesis. Tempe, AZ: Arizona State University.
- Morris, A., D.A. Ferrill, and D.B. Henderson. 1996. Slip-tendency analysis and fault reactivation. *Geology* 24(3): 275–278.
- Oliver, H.W., D.A. Ponce, and W.C. Hunter. 1995. *Major Results of Geophysical Investigations at Yucca Mountain and Vicinity, Southern Nevada*. U.S. Geological Survey Open-File Report 95-74. Reston, VA: U.S. Geological Survey.
- Parsons, T., and G.A. Thompson. 1991. The role of magma overpressure in suppressing earthquakes and topography: Worldwide examples. *Science* 253: 1,399–1,402.
- Rose, W.I., Jr., S. Bonis, R.E. Stoiber, M. Keller, and T. Bickford. 1973. Studies of volcanic ash from two recent Central American eruptions. *Bulletin Volcanologique* 37: 338–364.
- Self, S., R.S.J. Sparks, B. Booth, and G.P.L. Walker. 1974. The 1973 Heimaey strombolian scoria deposit, Iceland. *Geological Magazine* 111: 539–548.
- Sheridan, M.F. 1992. A Monte Carlo technique to estimate the probability of volcanic dikes. *Proceedings of the Third International Conference on High-Level Radioactive Waste Management*. La Grange Park, IL: American Nuclear Society: 2,033–2,038.

- Smith, E.I., T.R. Feuerbach, and J.E. Faulds. 1990. The area of most recent volcanism near Yucca Mountain, Nevada: Implications for volcanic risk assessment. *Proceedings of the International Topical Meeting on High-Level Radioactive Waste Management*. La Grange Park, IL: American Nuclear Society: 81–90.
- Stock, J.M., J.H. Healy, S.H. Hickman, and M.D. Zoback. 1985. Hydraulic fracturing stress measurements at Yucca Mountain, Nevada, and relationship to regional stress field. *Journal of Geophysical Research* 90 (B10): 8,691–8,706.
- Suzuki, T. 1983. *A Theoretical Model for the Dispersion of Tephra*. D. Shimozuru and I. Yokiyama, eds. Arc Volcanism: Physics and Tectonics. Tokyo, Japan: Terra Scientific Publishing Company: 95–113.
- Suzuki, T. 1985. Analysis of the 1977 tephra of Usu volcano by the turbulent diffusion model. *Bulletin of the Volcanological Society of Japan* 30: 231–251.
- Taylor, P.S., and R.E. Stoiber. 1973. Soluble material on ash from active Central America volcanoes. *Geological Society of America Bulletin* 84: 1,031–1,042.
- TRW Environmental Safety Systems, Inc. 1995. *Total System Performance Assessment—1995: An Evaluation of the Potential Yucca Mountain Repository*. (B00000000-01717-2200-00136). Las Vegas, NV: TRW Environmental Safety Systems, Inc.
- U.S. Department of Energy. 1993. *Study Plan for Study 8.3.1.8.5.1., Characterization of Volcanic Features, Revision 1*. Washington, DC: U.S. Government Printing Office.
- U.S. Department of Energy. 1996a. *Probabilistic Volcanic Hazards Analysis for Yucca Mountain, Nevada*. Civilian Radioactive Waste Management System Management and Operating Contractor BA0000000-1717-2200-00082, Rev. 0. Washington, DC: U.S. Government Printing Office.
- U.S. Department of Energy. 1996b. *Study Plan for Study 8.3.1.8.1.1., Probability of Magmatic Disruption of the Repository, Revision 3*. Washington, DC: U.S. Government Printing Office.
- Walker, G.P.L. 1973. Explosive volcanic eruptions—a new classification scheme. *Geologische Rundschau* 62: 431–446.
- Walker, G.P.L. 1981. Generation and dispersal of fine ash and dust by volcanic eruptions. *Journal of Volcanology and Geothermal Research* 11: 81–92.
- Wilson, M.L., and 24 others. 1994. *Total-System Performance Assessment for Yucca Mountain—SNL Second Iteration (TSPA-1993)*. Sandia National Laboratories Report SAND93-2675. Albuquerque, NM: Sandia National Laboratories.

- Wright, L.A., R.A. Thompson, B.W. Troxel, T.L. Pavlis, E.H. DeWitt, J.K. Otton, M.A. Ellis, M.G. Miller, and L.F. Serpa. 1991. Cenozoic magmatic and tectonic evolution of the east-central Death Valley region, California. M.J. Walawender and B.B. Hanan, eds. *Geological Excursions in Southern California and Mexico, Guidebook for the 1991 Annual Meeting of the Geological Society of America*. San Diego, CA: San Diego State University: 93-127.
- Yogodzinski, G.M., and E.I. Smith. 1995. Isotopic domains and the area of interest for volcanic hazard assessment in the Yucca Mountain area. *EOS, Transactions of the American Geophysical Union* 76(46): F669.

3 STRUCTURAL DEFORMATION AND SEISMICITY

Primary Authors: J.A. Stamatakos, P.S. Justus, D.A. Ferrill, R. Chen, and G.I. Ofoegbu

Technical Contributors: D.P. Cederquist, J.R. Firth, R.V. Klar, H.L. McKague, B.R. Rahe, K.J. Smart, G.L. Stirewalt, and G.W. Wittmeyer

Key Technical Issue Co-Leads: H.L. McKague (CNWRA) and P.S. Justus (NRC)

3.1 INTRODUCTION

Yucca Mountain (YM) lies within the central Basin and Range Province of the western North American Cordillera [see figure 1 of Wernicke (1992), p 554], a region characterized by complex interactions of strike-slip and extensional deformation active since the onset of the Cenozoic 65 m.y. ago. The region is still tectonically active as indicated by Quaternary (including Holocene) faulting, volcanism, and historic seismicity (including the 1992 Little Skull Mountain earthquake). Continuing structural deformation and seismicity at YM and in the Yucca Mountain region (YMR) pose a risk of noncompliance with radiological safety, health, and environmental protection standards because these tectonic processes might modify existing groundwater flow, damage waste packages (WPs), degrade stability of underground openings, and disrupt surface and other preclosure operations including retrievability.

The primary objective of the Structural Deformation and Seismicity (SDS) Key Technical Issue (KTI) is to evaluate structural deformation, seismicity, and related hazards on safe disposal of high-level nuclear waste (HLW) at the proposed YM, Nevada, repository. As part of that task, the SDS KTI evaluates hypotheses outlined in the U.S. Department of Energy (DOE) Waste Containment and Isolation Strategy (WCIS) regarding potential effects of seismicity and structural deformation (U.S. Department of Energy, 1996)¹. Pertinent hypotheses are (i) the amount of movement on faults through the potential repository horizon will be too small to bring waste to the surface and too small and infrequent to significantly impact containment during the next few thousand years and (ii) the severity of ground motion expected in the repository horizon for tens of thousand of years will only slightly increase the amount of rockfall and drift collapse. In addition, the SDS KTI provides critical structural and seismicity information to other KTIs to evaluate the DOE WCIS hypotheses concerning seepage, containment, radionuclide mobilization, radionuclide transport, dilution, and volcanism.

In addition to evaluations of the DOE WCIS hypotheses, the SDS KTI evaluates conclusions regarding SDS in the DOE 1995 Total System Performance Assessment (TSPA-95) (TRW Environmental Safety Systems, Inc., 1995) in preparation for the upcoming TSPA Viability Assessment (TSPA-VA). Notwithstanding tectonic activity of the region, the DOE concluded on page 2-14 in TSPA-95 (TRW Environmental Safety Systems, Inc., 1995) that future consequences of faulting and seismicity will be negligible on release of radionuclides to the accessible environment. The DOE did not explicitly include external events in TSPA-95. Its conclusion about negligible affects of structural deformation and seismicity on total system performance was based primarily on the DOE Probabilistic Seismic Hazard Analysis (PSHA) (Wong et al., 1995) and auxiliary performance assessment (PA) calculations (e.g., Gauthier et al., 1995) in which only a subset of possible externally induced natural phenomena were considered (e.g., WP

¹U.S. Department of Energy. 1996. Highlights of the U.S. Department of Energy's Updated Waste Containment and Isolation Strategy for the Yucca Mountain Site. DOE Concurrence Draft.

rupture or enhanced degradation from faulting and fracture or bulk rock seepage flow, and seismicity-induced water table fluctuations). Moreover, the DOE data used to constrain faulting characteristics were based solely on trenching studies of suspected Quaternary faults in alluvium (Pezzopane, 1995). These estimates are not considered conservative because they yield minimum fault-slip values (Ferrill et al., 1996a). Alternative methods for gauging fault-slip (e.g., apatite fission-tracks, geodetic surveys, alluvial fan studies, and ground magnetic surveys) indicate greater slip-rates than those proposed by the DOE [Ferrill et al. (1996b; 1996c); Stamatakos et al. (1996)²]. In addition, the DOE TSPA-95 did not consider potential effects of faulting and seismicity on disruption of groundwater flow, thermal perturbations, or structural control of magma injection along faults and fractures.

SDS KTI evaluations are also relevant to DOE PSHA, Probabilistic Fault Displacement Hazard Analysis (PFDHA), corresponding deterministic fault-displacement and seismic hazard analyses, and controlled design assumptions concerning faults and fractures. The DOE plans to complete its expert elicitation on PSHA and PFDHA in Fiscal Year 1997 (FY97) and present those findings in early FY98. The PSHA and PFDHA results will be used by DOE for both preclosure design and operation safety decisions as well as input to the TSPA-VA.

SDS has been subdivided by Nuclear Regulatory Commission (NRC) into five subissues that serve as focal points for SDS KTI technical tasks. The first subissue focuses on data, which provide the basis for evaluations of tectonic, structural, and seismological models, DOE hypothesis and assumptions, as well as PSHA and TSPA. The SDS KTI continues to assess and independently evaluate critical SDS data and complete resolution of this issue is not expected in FY97. However, an important component of this subissue was resolved in FY96. Type I faults have been identified based on a deterministic assessment of seismicity in the YMR. Those findings are presented in McKague et al. (1996) and are summarized in section 3.3.4.

The second subissue comprises model validation and verification that provide the basis for the three-dimensional (3D) geologic framework model of the site, methodologies and results of seismic and fault-displacement hazards assessments, and coupled mechanical-thermal-hydrologic-chemical process models. A significant component of SDS KTI work in FY96 related to possible structural control of volcanism Connor et al. (1996a), Conway et al. (1996),³ Connor et al. (1996b), and Stamatakos et al. (1996).⁴ Integration of structural models in volcanic probability models is presented in chapter 2 of this report. The SDS KTI developed hydrological applications in the Center for Nuclear Waste Regulatory Analyses (CNWRA) 3D geologic framework model (Stirewalt and Henderson, 1995a; 1995b; 1996). Technical investigations presented in section 3.3.3 summarize modeling result of faulting and

²Stamatakos, J.A., C.B. Connor, and R.H. Martin. 1996. Quaternary volcanism and basin evolution of Crater Flat, Nevada, from detailed ground magnetic surveys of the Little Cones. *Journal of Geology*. Accepted for publication.

³Conway, F.M., D.A. Ferrill, C.M. Hall, A.P. Morris, J.A. Stamatakos, C.B. Connor, A. Halliday, and C. Condit. 1996. Timing of volcanism along the Mesa Butte fault in the San Francisco Volcanic Field, Arizona, from ⁴⁰Ar/³⁹Ar ages: Implications for the longevity of cinder cone alignments. *Journal of Geophysical Research*. Submitted for publication.

⁴Stamatakos, J.A., C.B. Connor, and R.H. Martin. 1996. Quaternary volcanism and basin evolution of Crater Flat, Nevada, from detailed ground magnetic surveys of the Little Cones. *Journal of Geology*. Accepted for publication.

seismicity along the Bare Mountain fault (BMF) and possible co-seismic links to slip on antithetic YM faults is examined using ABAQUS (v.5.5).

The third subissue centers on alternative conceptual (tectonic) models (ACM). Identification and appropriate use of tectonic models is critical to the overall assessment of SDS effects on proposed repository performance. Tectonic models provide a common reference frame that exposes gaps in data acquisition, deficiencies in data analysis, and a focal point for future investigations. These models provide bounds for probability and consequence analyses and offer a vehicle to link structural and seismological features with other geological processes such as groundwater flow and volcanism. Finally, tectonic models provide a basis for representative abstractions of SDS in TSPA calculations. Results of SDS KTI investigations of the YMR tectonic setting, including analyses of contemporary strain and *in situ* stress, are given in Ferrill et al., 1996,⁵ Rahe et al. (1996),⁶ (Stamatakos and Ferrill, 1996b); and Stamatakos et al. (1996).⁷ On the basis of an Appendix 7 meeting on viable tectonic models held in San Antonio in May 1996, tentative agreement was reached between the DOE, the CNWRA, the State of Nevada, and the United States Geological Survey (USGS) that only 5 of the more than 12 proposed tectonic models for the YMR are supported by existing data. Results of the Appendix 7 meeting are summarized in section 3.3.1. In addition, the potential for additional seismic sources from buried faults implied in two of the five viable models was investigated by analog deformation experiments using a sandbox deformation apparatus. Results of the analog experiments are presented in section 3.3.2.

The fourth subissue relates to potential for disruption of WPs, underground openings, and surface facilities/operations. The SDS KTI completed a detailed review of DOE Topical Report 1 (TR1), *Methodology to Assess Fault Displacement and Vibratory Ground Motion Hazard at Yucca Mountain*, (U.S. Department of Energy, 1994). In the review, the NRC concluded that sufficient information exists to close all comments and resolve the methodology to evaluate seismic hazards at YM. The SDS KTI is also investigating the effects of faulting on repository performance using the faulting module (Stirewalt et al., 1996), a PA code designed to assess WP disruption from faulting within the repository block.

The fifth subissue is concerned with the potential for disruption of flow due to structural deformation or seismicity. The SDS KTI investigated this subissue at two scales of observation. Technical investigations of the role of fractures, faults, and *in situ* stress on regional groundwater flow are summarized in 3.3.5. The evaluation is based in part on dilation-tendency analysis using 3DStress (v.1.2). Results suggest that regional groundwater flow may converge near the eastern boundary of the proposed repository. Local-scale variations in groundwater flow and infiltration resulting from possible dilation of joints and fractures (with concomitant increases in porosity and permeability) in the hangingwall blocks above a series of active normal fault was investigated using UDEC (v.2.01). These results are presented

⁵Ferrill, D.A., A.P. Morris, S.M. Jones, and J.A. Stamatakos. 1996. Geometric, thermal, and temporal constraints on the development of extensional faults at Bare Mountain (Nevada) and implications for seismicity in the Yucca Mountain region. *Geological Society of America Bulletin*. Submitted for publication.

⁶Rahe, B., D.A. Ferrill, and A.P. Morris. 1996. Physical analog modeling of pull-apart basin evolution. *Tectonophysics*. Submitted for publication.

⁷Stamatakos, J.A., C.B. Connor, and R.H. Martin. 1996. Quaternary volcanism and basin evolution of Crater Flat, Nevada, from detailed ground magnetic surveys of the Little Cones. *Journal of Geology*. Accepted for publication.

in section 3.3.6 and show significant dilation of fractures in the hangingwall block after each faulting event.

3.2 OBJECTIVES AND SCOPE OF WORK

The SDS KTI seeks to ensure that significant SDS conditions and hazards are identified, sufficiently understood, fully considered, and used appropriately to evaluate repository performance. This objective requires review and independent confirmation of data, numerical models and alternative conceptual tectonic, structural, and seismic models, and PA, PSHA, and PFDHA calculations. The scope of work includes review of the DOE documents, review of applicable peer-reviewed literature, meeting participation to discuss SDS related issues with the DOE, observation of quality assurance (QA) audits, and independent technical investigations. The independent technical investigations are designed to provide guidance to the NRC on critical SDS licensing issues and associated reviews of upcoming DOE reports, most notably the DOE PSHA and PFDHA, the DOE WCIS strategy, and SDS aspects of the DOE TSPA-VA. Forthcoming issue resolution reports are intended to be an integral programmatic component of the NRC effort.

Technical investigations by the CNWRA are based on geological and geophysical data; numerical, conceptual, and analog models; and deterministic and probabilistic fault and seismic analyses. These investigations provide important and independent results on SDS conditions that can ultimately be linked to iterative PA, PSHA and PFDHA. For example, recent geological and geophysical investigations of the BMF (Ferrill et al., 1996b) indicate fault slip-rates up to one order of magnitude greater than the DOE estimates (Pezzopane, 1995). These values provide independent assessments of faulting in the CNWRA PSHA and PFDHA. These fault slip estimates also provide alternative estimates of faulting in planned PA sensitivity studies of WP disruption using the FAULTING module, which will then feed into the iterative total performance assessment (TPA) calculations.

Issue resolution will be achieved when the following three conditions are met. First, the DOE has collected data of sufficient extent and quality to identify and characterize all significant Quaternary and contemporary SDS conditions and SDS hazards necessary to assess potential repository performance. Second, the DOE has evaluated relevant data and uncertainties and developed alternative conceptual models of the contemporary and projected seismo-tectonic systems and structural geologic features and conditions. Third, the DOE has appropriately integrated these data and concepts into its process models and assessments of future repository performance. SDS KTI work on resolution of the five subissues is so directed that, when resolved, they would provide a technical basis for reasonable assurance that public safety, health, and environmental protection standards will be met.

3.3 SIGNIFICANT TECHNICAL ACCOMPLISHMENTS

3.3.1 Tectonic Models

Staff members from the DOE, the NRC, the Advisory Committee on Nuclear Waste (ACNW), the Nuclear Waste Technical Review Board (NWTRB), the Electric Power Research Institute (EPRI), the CNWRA, the USGS, and the State of Nevada met in San Antonio on May 7-8, 1996 for an Appendix 7⁸ meeting to discuss conceptual tectonic models of the Crater Flat-YM area. The meeting was initiated by

⁸Informal meetings between the staff of NRC and DOE for the purpose of information exchange.

the NRC and the CNWRA to facilitate resolution of this subissue. In this meeting, tectonic models proposed for the YMR were reviewed in the context of the most recent geological and geophysical data. Of the 11 tectonic models proposed, the DOE, the NRC, the CNWRA, USGS, and the State of Nevada informally agreed that only five were presently supported by existing data. Although this agreement on the remaining five models was not unanimous and the participants still disagree on the relative importance of each model, tentative agreement forms the basis for resolution of the subissue related to tectonic models. In addition, there was no general consensus on which models are truly independent and which may be subsets of others.

The SDS KTI refers to the five viable tectonic models as the

- deep detachment fault (12–15 km) model (Ferrill et al., 1996b, figures 2-3, 2-6)
- moderate detachment fault (6–8 km) model (Ferrill et al., 1996b, figures 2-3, 2-6)
- planar faults with internal block deformation model (Janssen, 1995)
- pull-apart basin model Fridrich (1996),⁹ (McKague et al., 1996, figures 4-3, 4-7)
- Amargosa shear model (Caskey and Schweichert, 1992; McKague et al., 1996, figure 4-3)

In a broader sense, these five models can be considered in two general categories. The first three are dominantly related to extensional deformation and the latter two are dominantly related to strike-slip deformation. Moreover, the five models are not mutually exclusive. Locally extensional-dominated deformation (within Crater Flat, for example) can exist within a larger region of transtensional deformation related to a pull-apart basin. In addition, none of the viable tectonic models explicitly supports partitioning Crater Flat into separate magma-probability domains (in which the probability of magma is significantly lower at YM versus Crater Flat) as implied by recent DOE volcanic hazard assessments (e.g., Crowe et al., 1995).

3.3.2 Analog Modeling of Pull-Apart Basins

Of the five viable tectonic models, the pull-apart basin model proposed by the USGS Fridrich (1996)¹⁰ and the Amargosa shear proposed by the State of Nevada (Schweichert, 1989) present the greatest seismogenic risks to overall repository safety and performance. These two models imply significant buried or blind seismic sources in Crater Flat adjacent to YM that are not currently accounted for in PSHA or in plans for repository design and operations. The nature of these risks has been the focus of the CNWRA analog model studies of pull-apart deformation. Specifically, scaled sandbox deformation experiments were conducted as analogs to the geologic evolution of pull-apart basins. From this modeled evolution, changes in seismic risks are inferred. By comparing the analog models to the geometry of faults in Crater Flat and the surrounding region, implicit seismic risks of the pull-apart and Amargosa Shear

⁹Fridrich, C.J. 1996. Tectonic evolution of the Crater Flat Basin, Yucca Mountain region, Nevada. Cenozoic Basins of the Death Valley Region. L. Wright, ed. *Geological Society of America Special Paper*. In press.

¹⁰*Ibid.*

models can be better constrained. Results presented here are a followup to preliminary results of Stamatakos and Ferrill (1996a). A more detailed description of the analog sandbox models and analyses of the evolution of pull-apart basins is given in Rahe et al. (1996).¹¹ Results from this work bear directly on subissues of the SDS KTI associated with (i) data, (ii) model verification, (iii) alternate conceptual models, and (iv) potential for disruption of WPs.

3.3.2.1 Sequential Development of Pull-Apart Basins

Pull-apart basins are structural depressions formed by localized extension along strike-slip fault zones (Burchfiel and Stewart, 1966). In the classic conceptual model of pull-apart basin formation (Burchfiel and Stewart, 1966), pull-apart basins form within the brittle crust above a horizontal detachment in the lower crust. Although active pull-apart basins can exist for millions of years, they are geologically transient features that evolve and eventually become inactive (Zhang et al., 1989). Pull-apart basin evolution can be divided into four steps: incipient, early, early mature, and late mature (figure 3-1).

Incipient pull-apart basins are characterized by initiation of closely spaced normal faults parallel to oblique steps between main strike-slip displacement zones that define the boundaries of a graben or half graben. Motion along faults is partitioned between normal and strike-slip faults in relatively small and unconnected individual fault segments (e.g., Stamatakos and Ferrill, 1996). Strike-slip faults are not recognizable within the pull-apart basin at the surface (figure 3-1a). Earthquake hazards are mitigated by fault segmentation in which rupture is limited to the isolated fault segments (Sibson, 1986). Normal and strike-slip faults are segmented from each other in the incipient and early stages of basin development.

During the early stage (figure 3-1b) basin-bounding normal fault systems are characterized by lateral variations of fault throw that produce localized relay ramps. Pull-apart basins exhibit additional normal faults toward the basin interior inward from the original bounding faults, as well as cross-basin strike-slip faults that cut diagonally across the basin interior (figure 3-1b). Relay ramps are described as accommodating displacement transfer from one fault segment to another, while maintaining continuity between the footwall and hangingwall (Peacock and Sanderson, 1991; Trudgill and Cartwright, 1994). Relay ramps form early in fault system development as individual normal faults increase rupture area and begin to interact, but prior to coalescence of the deformation onto a single through-going strike slip fault. Relay ramps also form along developing sections of normal faults that bound the growing pull-apart basin.

At the early and late mature stages (figures 3-1c and 3-1d), strike-slip and normal faults join to completely bound the pull-apart basin at the surface. Displacement associated with cross-basin faults causes development of a through-going strike-slip fault that defines these stages. This fault cuts through the center of the pull-apart basin, linking the two main strike-slip displacement zones and typically represents continued activity on segments of the original cross-basin faults and formation of new connecting strike-slip fault segments. This linking of main strike-slip displacement zones dramatically enlarges the overall fault area capable of rupture and thus increases potential for large-magnitude earthquakes. Late in this stage, normal faults bounding the outer margins of the basin commonly show a decrease in fault activity. This decrease consistently occurs on normal faults bounding the side of the pull-apart basins experiencing less strike-slip displacement relative to the fixed basement.

¹¹Rahe, B., D.A. Ferrill, and A.P. Morris. 1996. Physical analog modeling of pull-apart basin evolution. *Tectonophysics*. Submitted for publication.

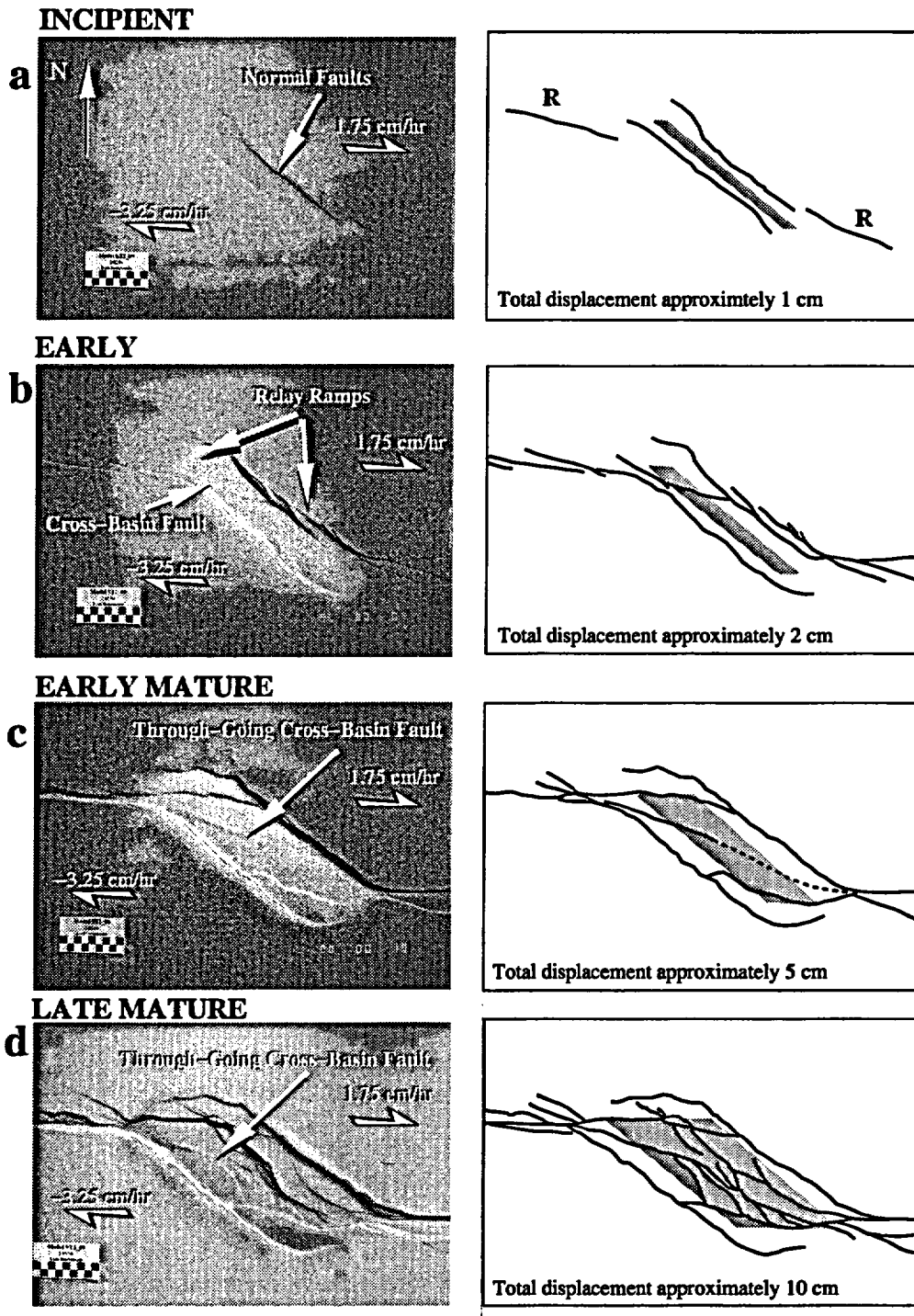


Figure 3-1. Photographs and corresponding line drawings showing evolution of a pull-apart basin from analog modeling experiments. Stages of development are (a) incipient, (b) early, (c) early mature, and (d) late mature. Shaded area in line drawings represents displacement at the base of the basin. R in line drawings are the expected Riedel shear orientation.

The observed evolution of pull-apart basins (e.g., Zhang et al., 1989) is favorably represented by sequential deformation of the CNWRA analog models. In these analog models, cross-basin faults formed as one or two separate small faults with orientations along the Riedel (R) shear orientation, 15° to the main shear direction. In the incipient stage, these cross-basin faults connected the tips (corners) of the basin with the center of the basin-bounding normal faults on the opposite margin of the basin (figure 3-1b). As further strike-slip displacement separated the active tips of the pull-apart basin (corresponds to bends in the controlling fault at depth), the basin widened relative to its length. When the basin reached optimal configuration (with a length-width ratio of about 2.4:1.0), new cross-basin faults (which still formed in a R shear orientation) connected the active tips of the basin (figures 3-1c and 3-1d). These cross-basin faults effectively linked slip on the formerly segmented master strike-slip faults. The result is a single, through-going strike-slip fault system (with a large potential rupture plane and correspondingly large earthquake magnitude) and inactive basin bounding normal faults.

3.3.2.2 Implications to Seismic Hazard Analyses

Results from the analog models reinforce concerns about potential seismic hazards of strike-slip dominated tectonics (Stamatakos and Ferrill 1996; McKague et al., 1996). The primary concern for repository performance is the potential for significant blind seismic sources. Current DOE PSHA analyses do not include the potential for seismicity generated from blind faults (e.g., Wong et al., 1995). In addition, these models predict substantial strike-slip or oblique-slip deformation on most faults related to the pull-apart basin. Yet, in recent paleoseismic investigations that rely on trenching studies in alluvium (e.g., Klinger and Anderson, 1994) only fault throw (the vertical component of slip) is factored into estimates of recurrence and slip rate. The viability of the pull-apart or Amargosa shear models suggests paleoseismic investigations may underestimate fault activity.

The pull-apart model of Fridrich (1996)¹² proposes a highly elongated pull-apart rhombochasm or sphenochasm that extends from northern Crater Flat to the Death Valley-Furnace Creek fault system. This geometry corresponds to the incipient or young stage of pull-apart evolution (figure 3-1) where a significant fraction of deformation is accommodated by bounding normal faults. The master strike-slip faults and cross-basin faults are segmented, and considerable widening of the basin is required (roughly an additional 8 km of right slip on the Death Valley-Furnace Creek fault system) before the cross-basin faults could link the active tips at the corners of the basin. The most significant implication of this model to seismic hazard analyses is the potential of an earthquake on one of the cross-basin faults. These faults would have moderate rupture areas that would yield earthquakes with maximum moment magnitudes (M_m) of 6.6 to 6.8 (McKague et al., 1996). Because of their proximity to YM, however, such earthquakes have the potential to generate relatively large peak accelerations (0.76 g or larger) at the potential repository site (McKague et al., 1996).

In the Amargosa shear model, Schweickert (1989) envisions Crater Flat as a shear zone accommodating right-lateral shear on a proposed buried strike-slip system that trends northwest from southeast of Pahrump to northwest of the Miocene Caldera complex. Although Schweickert (1989) does not explicitly depict the shear zone as a pull-apart, it shares many structural features with a mature stage pull-apart basin. The Amargosa shear zone is interpreted to result from a releasing bend along a strike-slip fault system, and deformation is accommodated by a combination of strike-slip and extensional faulting.

¹²Fridrich, C.J. 1996. Tectonic evolution of the Crater Flat Basin, Yucca Mountain region, Nevada. Cenozoic Basins of the Death Valley Region. L. Wright, ed. *Geological Society of America Special Paper*. In press.

The most significant implication of this model is the potential for a large earthquake near YM. The size of the proposed Amargosa system is comparable to the Death Valley-Furnace Creek fault or to segments of the San Andreas. Thus the Amargosa shear has the potential for earthquakes with $M_m \geq 7.8$. Depending on how close the boundary of the proposed shear zone is located to the repository site, such a large earthquake could produce peak accelerations at the site well in excess of 1.0 g (McKague et al., 1996).

3.3.3 Mechanical (Numerical) Analyses of Faulting at Bare Mountain and Yucca Mountain

Most conventional PSHA estimate peak accelerations by assuming fault length and surface distance to source parameters. Based on these assumptions, paleoseismicity is reconstructed from the mapped trace-length of faults and recurrence estimates from fault-trenching studies. Recent earthquakes in the western United States, however, challenge these assumptions. The 1992 Landers earthquake ruptured along several previously distinct fault segments (with a surface magnitude $M_s=7.6$) that by themselves would not seem capable (based on their mapped trace-length) of generating such a large magnitude earthquake (e.g., Hart et al., 1993; Sieh et al., 1993; Sowers et al., 1994). In addition, the Landers earthquake was part of a coseismic sequence of earthquakes (see Ferrill et al., 1994 for summary) that apparently initiated with the Joshua Tree ($M_s=6.3$) earthquake on April 22, 1992 and terminated with the Little Skull Mountain ($M_s=5.4$) earthquake on June 29, 1992 (Harmsen, 1994). The 1994 Northridge ($M_s=6.9$) earthquake (Hauksson et al., 1995) occurred along a previously unmapped blind fault that did not produce any surface rupture and resulted in anomalously large near-field peak accelerations. The implication of these earthquakes to the potential HLW repository is that the DOE data used in YM PSHA may not accurately reflect future seismicity and thus has relevance to SDS KTI data subissue. Therefore, seismicity data used by the DOE in future PA and in evaluation of the WCIS hypotheses that the severity of ground motions expected in the repository horizon for tens of thousands of years will only slightly increase the amount of rockfall, and drift collapse may not be reasonably conservative. To investigate the significance of this potential data deficiency, mechanical analyses were conducted to simulate fault-slip on BMF. Specifically the following were examined:

- Distribution of fault displacement along the BMF; in particular, the relationship between magnitude of fault displacement at the ground surface (surface fault displacement), average fault displacement, and maximum fault displacement. In developing historical earthquake data based on observations of geologic structures, fault-rupture parameters such as surface fault displacement and rupture length are used in empirical relationships (e.g., Wells and Coppersmith, 1994) to estimate maximum earthquake magnitudes associated with existing faults. In these empirical relationships, however, it is not clear if there are significant differences among the earthquake magnitudes calculated using different fault-rupture parameters, such as fault rupture at depth.
- Distribution of ground-motion amplitudes to determine if the magnitudes of acceleration at the ground surface and at depths of 200–500 m are consistent with assumptions commonly made in developing ground-motion attenuation curves.
- Possibility that slip on the BMF could trigger slip on YM faults and how the potential for triggered slip may vary with the proposed geometry of the YM faults given in the moderate and deep detachment models.

Analyses were based on a model of the Bare Mountain-Yucca Mountain fault system; BMF is interpreted as a listric fault with a detachment at about 12 km depth and the YM faults are steeply dipping faults in the hangingwall (see figure 2-3, p. 2-6, Ferrill et al., 1996b). Two YM faults were modeled in the analyses, representing faults that terminate at either the steeply dipping (YM1) or detachment (YM2) segments of the BMF (figure 3-2). Analyses were conducted using the finite element code ABAQUS (v.5.5). Each fault was modeled as a 100 m thick zone of isotropic and elastic-plastic material with a yield strength defined using the Drucker-Prager failure criterion (e.g., Ofoegbu and Ferrill, 1995) and the surrounding rock mass isotropic and linear-elastic.

Each analysis was conducted in two steps. First, initial static equilibrium was established under a specified initial stress state (based on vertical stress gradient of 25 MPa/km and vertical-to-horizontal stress ratio of 1:0.25), gravitational body force, and boundary restraints. Second, a shear-stress pulse was applied over a selected (~ 2-km) segment of the BMF through dynamic analysis, thereby simulating the release of seismic energy over the selected fault segment (an earthquake) and the response of the model was monitored for about 10 s. The focus of the simulated earthquake (i.e., the fault segment over which the shear-stress pulse was applied) was varied to simulate a shallow-focus earthquake (Case sc01 at 1.5 km depth), an intermediate-focus earthquake (Case sc02 at 6 km depth), a deep-focus earthquake on steep fault segment (Case sc03 at 10 km depth), and another deep-focus earthquake on the detachment segment (Case sc04 at 12 km depth).

Results calculated from the model suggest values of earthquake magnitude based on empirical relationships with surface fault displacement (Wells and Coppersmith, 1994) give satisfactory estimates of potential earthquake magnitudes for moderate to deep sources on steeply dipping faults, but overestimate magnitudes for shallow sources and underestimate magnitudes for low-angle faults (table 3-1). The first two sets of values in table 3-1 are based on Wells and Coppersmith (1994) empirical relationships, whereas the third is based on Hanks and Kanamori (1979). The latter requires evaluation of seismic moment, based in part on the rupture area, A_r . Because A_r cannot be calculated directly from a two-dimensional (2D) model, its value is estimated from data on subsurface fault lengths and down-dip rupture lengths from Wells and Coppersmith (1994). As a result, a range of magnitudes (instead of a single magnitude) is presented for each case. The three methods of earthquake-magnitude calculation give similar values for Cases sc02 and sc03 (intermediate and deep earthquakes on steep-fault), while the magnitude based on surface displacement is too small for Case sc04 (low-angle fault) and too large for sc01 (shallow focus).

The model results also indicate that an earthquake originating on the BMF at a depth of 5 km or more produces larger ground motions at a distance away from the fault (in the YM area in this simulation) than near the surface rupture (in the BM region in this simulation). Figure 3-2 shows seismic energy from a planar source (such as a fault surface) travels away from the source along a path perpendicular to the fault. Because the source is not a point, as assumed in ground-motion attenuation functions, the wave paths are not attenuated spherically. The largest ground-motion amplitudes do not occur at the epicenter (directly above the focus) but at a point near the intersection of the fault normal plane (or line) that passes through the focus of the earthquake and the surface. Thus, maximum ground motions will not necessarily be at the epicenter but could occur a short distance away. For example, the magnitudes of ground acceleration illustrated in figure 3-2 are about 0.2–0.4 g (horizontal) and 0.2–0.5 g (vertical) in the YM area, but smaller than 0.1 g in the immediate vicinity of the surface trace of the BMF. Such a distribution of ground accelerations could not have been predicted using a ground-motion attenuation relationship that estimates maximum ground motions solely on site-to-source distance.

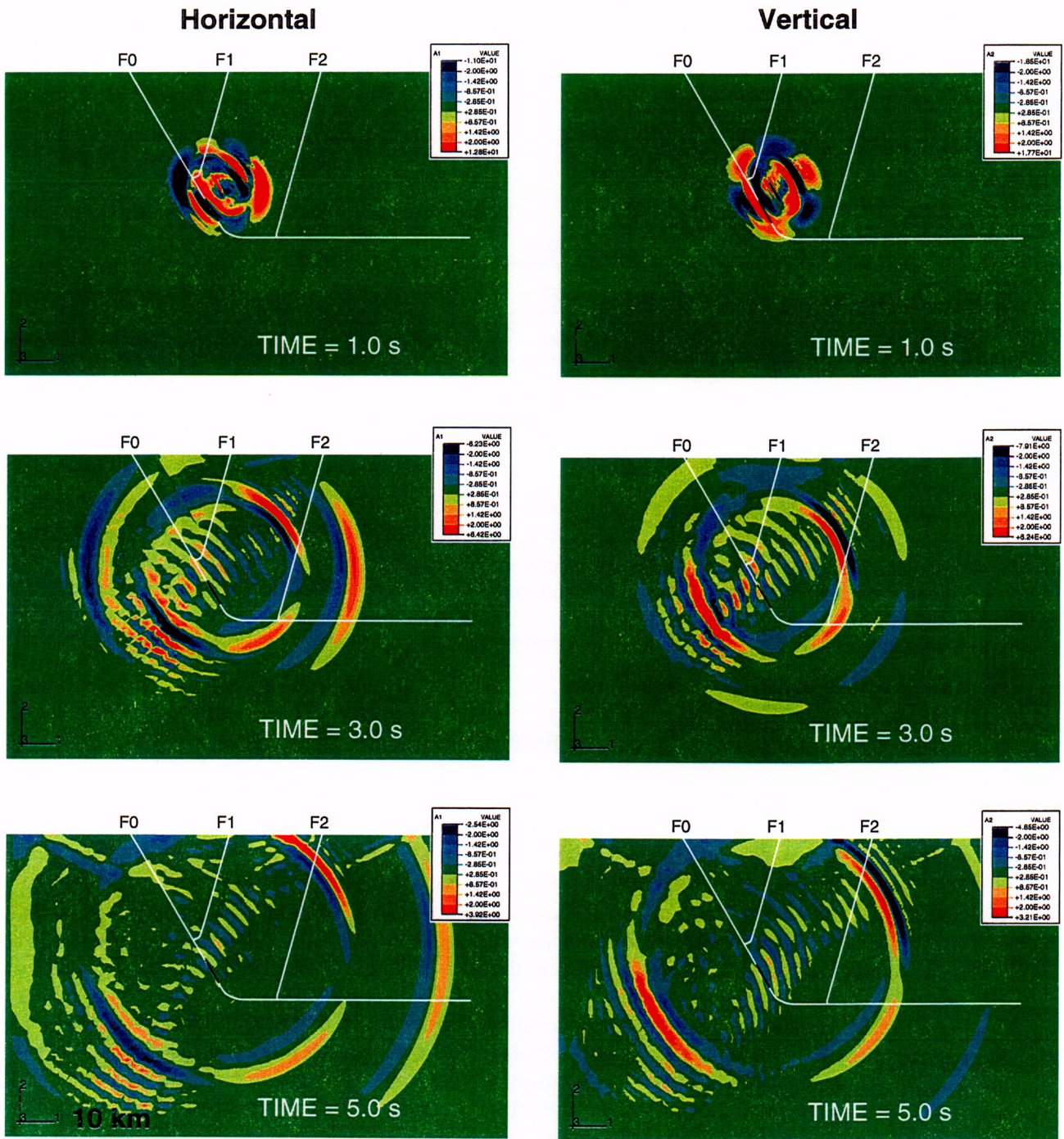


Figure 3-2. Contour of horizontal (left column) and vertical (right column) components of ground accelerations in m/s^2 for model case sc03. Plots are shown for times of one, three, and five seconds after the simulated seismic event. BMF is simulated along with the two subsidiary YM faults (YM1 and YM2). The source zone is shown by the dark line segment on the BMF. For horizontal accelerations, positive is toward the right and negative is toward the left; for vertical accelerations, positive is up and negative is down.

C-02

Table 3-1. BMF displacement, down-dip rupture length, and earthquake magnitudes

Model Case	Fault Displacement (m)			DRL ¹ (km)	Magnitude Based On		
	Surface	Average	Maximum		Surface Displ. ²	DRL ²	Seismic Moment ³
sc01	2.92	1.07	4.00	18.50	6.9	6.7	6.3 to 6.7
sc02	4.12	3.03	11.60	27.68	7.0	7.1	6.9 to 7.2
sc03	2.39	3.08	13.90	26.44	6.9	7.0	6.9 to 7.2
sc04	0.05	0.65	4.43	23.71	5.7	6.9	6.3 to 6.7

¹Down-dip rupture length
²Moment magnitudes calculated from empirical formulas of Wells and Coppersmith (1994)
³Rupture area range calculated from ratio of subsurface rupture length and down-dip rupture width for normal fault data compiled by Wells and Coppersmith (1994). Moment magnitude is calculated from formulas of Kanamori and Anderson (1975) and Hanks and Kanamori (1979)

The model results also suggest that a BMF earthquake may trigger slip on YM faults, but for the modeled geometry of faults the magnitude of triggered slip is small compared to BMF slip. This may be a function of the sharp curvature of the listric portion of the BMF. Previous results from Ofoegbu and Ferrill (1995) suggest the likelihood of triggered slip is greater when the listric geometry of the BMF is more gently curved. For the four simulated earthquake cases (table 3-2), the largest triggered slip of 0.26 m occurs on YM2 (in response to a deep-focus earthquake originating from the steep segment of BMF). The shallow-focus case, sc01, does not induce measurable slip on the YM faults, whereas all other cases trigger slip. This suggests that an earthquake originating on the BMF at a depth of 5 km or more may produce measurable displacement on faults in the YM vicinity.

Collectively, these analyses suggest uncertainty in ground-motion attenuation functions, especially when used for sources in the near-field (i.e., for faults close enough to the site so they no longer can be considered point sources). Although earthquake magnitude estimation based on surface-rupture parameters may be satisfactory, ground accelerations calculated from these magnitudes in conventional ground-motion attenuation curves may underestimate peak ground accelerations at the proposed repository site because they fail to account for asymmetric radiation of seismic energy caused by the geometry of the seismic source. Future effort in the SDS KTI will be directed toward investigating the relationship between ground accelerations calculated in the numerical model and those calculated using empirical ground-motion attenuation relationships.

Table 3-2. Fault displacements on YM faults triggered by slip on BMF

Model Case	Fault F1 (Figure 3-2)		Fault F2 (Figure 3-2)	
	Surface Displacement (m)	Maximum Displacement (m)	Surface Displacement (m)	Surface Displacement (m)
sc01	No Slip	No Slip	No Slip	No Slip
sc02	0.09	0.13	0.04	0.05
sc03	0.02	0.13	0.26	0.26
sc04	0.06	0.10	0.02	0.07

3.3.4 Type I Faults

Adequate PSHA and related faulting and seismic hazard analyses require consideration of only those faults in the YMR posing significant potential risk to long-term waste isolation and short-term safety and retrievability objectives specified in the Title 10 Code of Federal Regulations (CFR) 60.111, 60.112, and 60.113. Identification of these faults is also important to design criteria for the Geologic Repository Operations Area (GROA) that require design of structures, systems, and components so anticipated natural phenomena (e.g., vibratory ground motion or direct repository rupture from slip on active faults) will not interfere with necessary safety functions [10 CFR part 60.131(b) (1)].

The criteria for selecting Type I faults (i.e., those that could affect repository design or performance) are from McConnell et al. (1992). Application of those criteria to the more than 400 faults within a 100 km radius of YM indicates that 52 faults may be considered Type I faults (McKague et al., 1996). McKague et al. (1996) serves as the focus for issue resolution with the DOE regarding Type I faults and provides a technical basis for the NRC evaluation of the DOE submittals. Issue resolution, however, only addresses the effects of seismicity that may be important. It does not include resolution on rates or recurrence of faulting or on faults that may serve as pathways or barriers to groundwater or magma flow, heat, or refluxation.

McKague et al. (1996) reports three main findings. First, the report develops a database of 52 Type I faults. Significant faults not considered Type I faults are the Pagany Wash, Sever Wash, and Yucca Wash faults. Despite having surface areas capable of producing peak accelerations greater than 0.1 g at YM, these faults lack evidence of significant Quaternary slip and have unfavorable orientations for slip in the current stress field. Beatty Wash Scarp is the only remaining Type II fault (i.e., there was insufficient data available to determine whether it is Type I or not) because differing opinions of its origin exist (it may not be a fault). Of the 52 Type I faults, the 24 capable of generating peak accelerations greater than 0.3 at the site all lie within a 10 km radius of YM. Important faults more distant from the potential repository include the BMF, Stagecoach Road, and Rock Valley faults, all capable of generating peak accelerations at YM greater than 0.25 g.

Second, the likelihood for slip within the present *in situ* stress state was estimated. Review of slip tendency for the YMR shows that nearly all faults at YM have relatively high slip tendency values in the current *in situ* stress field, except northwest trending faults. In the current stress state, maximum and intermediate principal stresses have nearly equal magnitudes. Thus, N trending right-lateral strike-slip, NNE trending left-lateral strike-slip faults and NE trending normal faults could slip without significant changes in the regional stress as observed in the aftershock sequence following the 1992 Little Skull Mountain earthquake. In addition, slip tendency analysis performed on several alternative cross sections (drawn across Crater Flat from BM to Jackass Flat) indicate active faults penetrating the entire thickness of the brittle crust pose the most significant potential seismic hazard. In contrast, faults that intersect a detachment at shallower crustal levels (e.g., at ~7 km depth) or where deformation is greatest at the surface and diminishes with depth, have limited potential as seismic hazards.

Third, additional constraints on fault and seismic hazard assessment were evaluated in light of alternative tectonic models and fault scaling relationships. For example, scaling relationship of fault-trace length versus cumulative vertical displacement (throw) indicates that most faults in the YMR fall within the expected range established from fault data sets worldwide. Mapped trace-lengths of the BMF, Windy Wash (WW), and Ghost Dance (GD) faults are anomalous. The mapped trace-length of the BMF is anomalously short for its cumulative offset and thus a longer BMF needs to be considered in future seismic hazard analyses. In contrast, the mapped trace-length of the WW and GD faults are too long for their accumulated throws, suggesting that either the offset estimates are too small or these faults are actually composed of a series of smaller distinct fault segments. If the latter is correct, then maximum moment magnitude and peak accelerations estimated from these faults may presently be overestimated because lengths used in the attenuation functions are too long.

3.3.5 Dilation-Tendency of Faults and Fractures and Implications for Groundwater Flow in the Yucca Mountain Region

Technical questions about the influence of faulting and fractures on groundwater flow relate to SDS KTI subissues involving tectonic models and disruption of flow. In addition, these analyses are critical to the evaluation of the DOE WCIS hypotheses on containment, radionuclide mobilization, radionuclide transport, and dilution.

Groundwater in the volcanic tuffs of YM and in the regional aquifer system consisting of Paleozoic strata is dominantly transmitted through networks of fractures. The fractures in tuff are the products of thermal contraction (cooling), tectonic deformation, and unloading. Fractures in the Paleozoic strata of the regional aquifer system are dominantly from tectonic deformation. Field observations from tuffs at YM suggest that dilation of fractures may change with time and is dependent on the stress field. In general, a propagating extension fracture will terminate against an older extension fracture that is open. An open fracture dissipates the high crack-tip stresses associated with propagating fractures, causing a younger extension fracture (joint) to abut pre-existing fractures. In the case where an earlier fracture is tightly closed due to high normal stress across perfectly matched surfaces or the fracture is healed by a mineral filling (vein), the propagating fracture may continue across the earlier fracture producing a mutually cross-cutting relationship. Faults (shear fractures), however, are typically capable of cutting earlier unfilled joints.

Studies of rock pavements at YM revealed three sets of cooling joints and at least three sets of tectonic joints (Barton and Hsieh, 1989; Barton et al., 1993; Throckmorton and Verbeek, 1995; Sweetkind

and Williams-Stroud, 1995), Sweetkind et al. (1996).¹³ Because cooling joints were the first to form, the fractures of the first set of cooling joints (C1) tend to be relatively long and continuous compared with other fractures. Fractures of the first set of tectonic joints (T1) generally trend N-S, tend to be relatively long and commonly cross cooling joints (e.g., C1). The number of T1 joints appears to be inversely proportional to the number of cooling joints (Throckmorton and Verbeek, 1995). This observation suggests that extensional strain (dilation) may have been locally accommodated by dilatant reactivation of cooling joints rather than formation of new tectonic joints. The most prominent sets of later tectonic joints are the NW-trending T2 set and NE-trending T3 set. T2 and T3 joints typically abut cooling joints and pre-existing (T1) tectonic joint sets.

Dilation-tendency (tendency for dilation in the direction normal to a fracture plane) is by definition high at the time of extension fracture formation. It appears that cooling joints were relatively tightly closed at the time of formation of crossing T1 joints but may have later reopened. Dilatant reactivation of cooling joints would explain the complex abutting relationships with later tectonic joints (e.g., crossing of T1 joints versus abutting of T2 and T3 joints). Furthermore, some cooling joints and early tectonic joints were apparently reactivated as small displacement faults that may have caused formation of ancillary fractures (e.g., T, R, and R' shears) which may explain localized development of additional tectonic fracture sets Sweetkind et al.(1996).¹⁴ Early formed fractures (e.g., cooling joints), or fractures that encounter no barriers to propagation (e.g., T1 joints that cross cooling joints) will typically be the most continuous and may, if open, present preferential pathways for groundwater flow. These may, if open, represent fast pathways for radionuclides, but could also favorably prevent pooling of groundwater around WPs by draining groundwater from the proposed repository horizon.

3.3.5.1 Dilation-Tendency

Fracture aperture depends on fracture dilation, mismatched irregularities on the fracture walls, presence of mineral fillings and coatings or wall-rock material within the fracture, and the resolved normal stress (the stress acting perpendicular to the fracture surface to close the fracture). Fractures within a 3D stress field experience a normal stress determined by the magnitudes and directions of the principal stresses in relation to the plane of the fractures. The ability of a fracture to open (dilate) and transmit fluid is directly related to the normal stress acting across the fracture as well as the fluid pressure. Once formed or opened a change in the stress field can cause the effective normal stress to close the fractures, unless the fractures are propped open (i.e., by fragments of wall rock within the open fracture, precipitated mineral coating on fracture walls, or offset of irregular fracture walls) so that opposing fracture surfaces do not match across the fracture. The magnitude of the normal stress can be computed for surfaces of all possible orientations within a known or hypothesized stress field that can be normalized by comparison with differential stress. Dilation-tendency (T_d) for a surface is defined (Ferrill et al., 1995) as

¹³Sweetkind, D.S., S. Williams-Stroud, and J. Coe. 1996. Characterizing the fracture network in the unsaturated zone at Yucca Mountain, Part 1. Collection and interpretation of geologic data: Case studies. T.E. Hoak and P.K. Blomquist, eds. Fractured Reservoirs: Descriptions, Predictions, and Applications: Rocky Mountain Association of Geologists 1996 Guidebook. In press.

¹⁴*Ibid.*

$$T_d = (\sigma_1 - \sigma_n) / (\sigma_1 - \sigma_3) \quad (3-1)$$

Analysis of dilation-tendency can be used to evaluate populations of existing faults and fractures that may act as pathways for fluid flow. Additionally, dilation-tendency analysis can be used to assess relative risks of magma injection along existing faults. This application is described in chapter 2.

Two factors, with respect to *in situ* stress and fractures, may contribute significantly to anisotropy of transmissivity in fractured rock. First, existing fractures that are at a high angle to the maximum horizontal stress may be preferentially closed by the maximum horizontal stress, thereby reducing transmissivity parallel to the minimum *in situ* stress (Ferrill et al., 1995; Wittmeyer et al., 1994; Wittmeyer and Ferrill, 1994). New fractures will form in orientations parallel (model 1 tensile fractures) or at a relatively low oblique angle (<45°; model 2 shear fractures) to the minimum principal stress. In either case, the *in situ* stress directly affects fracture orientation, fracture aperture, and resulting bulk transmissivity of the rock. Transmissivity will tend to be relatively higher in the plane normal to the minimum principal stress direction. Analysis of dilation tendency of natural fractures in granite at the Juktan underground hydroelectric power plant in northern Sweden (Carlsson and Olsson, 1979) showed close agreement with both measured transmissivity anisotropy and observed groundwater flow into tunnels along fractures (Ferrill et al., 1995).

3.3.5.2 Dilation-Tendency Analysis of Yucca Mountain Area Faults and Fractures

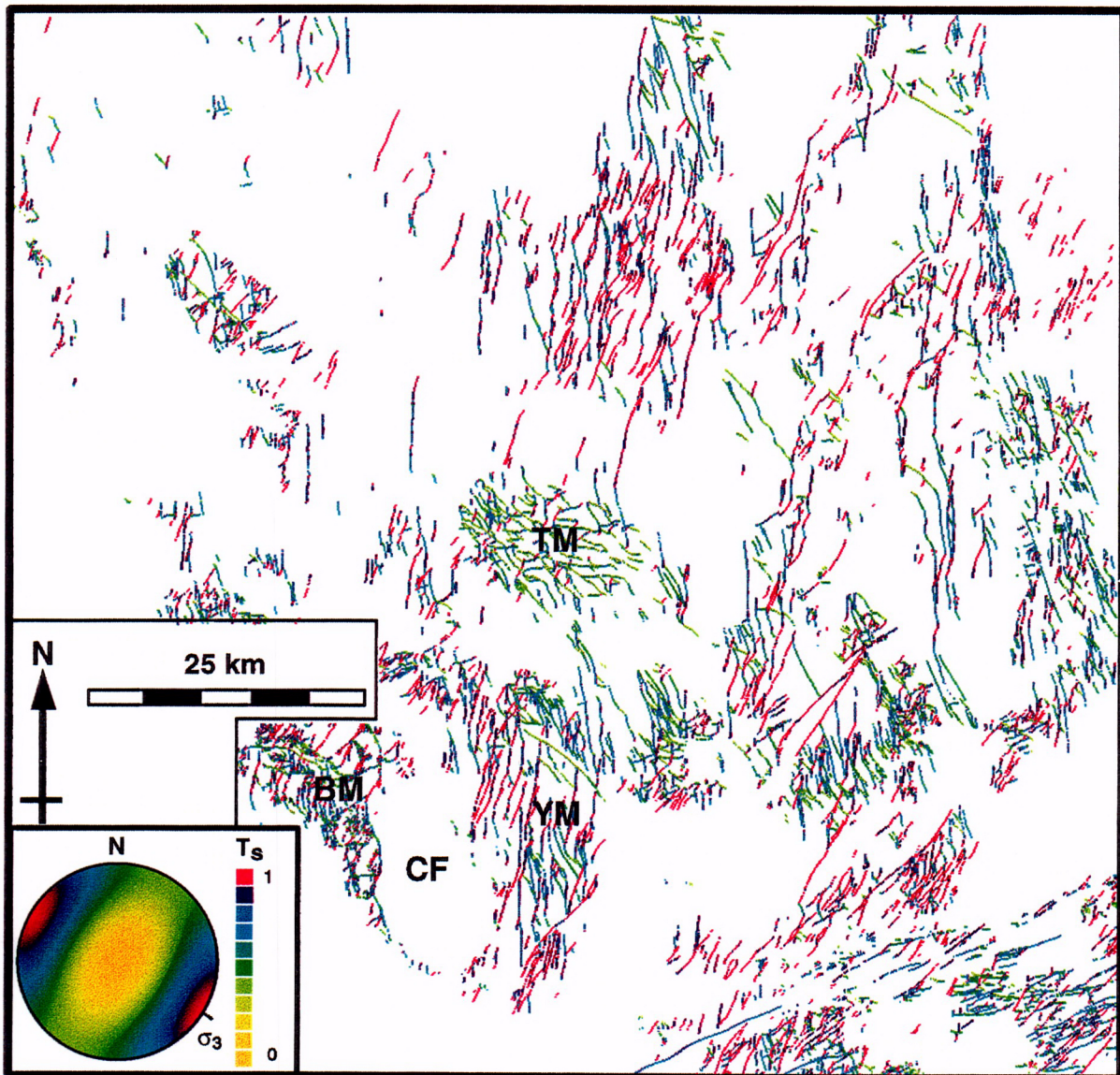
Dilation-tendency analysis of faults and fractures at YM was performed to evaluate the relative likelihood for fractures or faults to dilate in the contemporary stress field. Estimates of contemporary stress in the YM area consistently indicate that the regional minimum principal stress (σ_3) is horizontal and trends W-NW and the maximum horizontal stress (τ_1) is horizontal and trends N-NE (Zoback et al., 1981; Zoback, 1992; Zoback et al., 1992; Stock et al., 1985; Harmsen 1994; Morris et al., 1996). Stress estimates indicate the YM stress regime may be intermediate between a normal faulting regime, typified by vertical σ_1 and a strike-slip faulting regime characterized by vertical σ_2 . Dilation-tendency analysis was performed assuming the maximum principal stress is vertical, the minimum principal stress is horizontal trending 120°, and the intermediate principal stress (maximum horizontal stress) is horizontal and trending 030°. The resulting analyses illustrate that subvertical fractures and faults that trend 030° have the highest dilation-tendency and there is a range of strikes of $\pm 35^\circ$ and dips of between 65° and 90° where fractures have >80 percent of the maximum possible dilation-tendency within the stress field. Dilation-tendency is independent of scale and may apply to small joints or major faults. Dilation-tendency analysis of faults in and around YM illustrates an abundance of N-NE trending faults that have high dilation-tendency (figure 3-3).

3.3.5.3 Sensitivity Analysis of Transmissivity Anisotropy on Groundwater Flow

In developing maps depicting the regional groundwater flow regime for a laterally extensive area, it is usually assumed that flow is perpendicular to potentiometric contours. The direction of flow and driving force (negative gradient of the potentiometric surface), however, are only parallel if the transmissive properties of the aquifer are isotropic or if the driving force is everywhere parallel to either the major or minor semi-axes of the transmissivity tensor. Geologic evidence indicates flow in the aquifers in the YM area is primarily through fractures and faults, some of which have been widened by dissolution

E 500000 m
N 4150574 m

E 600529 m
N 4150574 m



E 500000 m
N 4053301 m

E 600529 m
N 4053301 m

Figure 3-3. Dilation-tendency analysis of faults in and around YM based on fault maps (Frizzell and Schulters, 1990; Monsen et al., 1992; and Sawyer et al., 1995)

in carbonate rocks. Fractured aquifers most commonly have anisotropic transmissivity. The orientation of the horizontal stress ellipse is herein used to analyze the sensitivity of transmissivity anisotropy, assuming that fracture frequency or aperture and therefore transmissivity is affected by the contemporary stress field. Analyses of subregional flow directions were conducted following the approach of Wittmeyer et al. (1994) and Wittmeyer and Ferrill (1994). The subregional potentiometric surface was constructed from the interpreted steady-state water levels measured in and around YM (after Wittmeyer et al., 1995). Contouring the potentiometric surface illustrates the steep hydraulic gradient north and northeast of YM and an area of very low gradient beneath Fortymile Wash and Jackass Flat. In the study area, the saturated zone is within fractured Tertiary tuff and Paleozoic strata, however, the water table is in alluvium at the southern end of Jackass Flat.

A contaminant plume released into the saturated zone beneath the proposed repository site would be expected to move SE away from the potential repository to Jackass Flat and turn south beneath Jackass Flat and migrate to Amargosa Valley. Assuming anisotropic transmissivity in the fractured aquifer (maximum transmissivity parallel to τ_1) flow directions will rotate toward τ_1 . Because of curvature of potentiometric contours at YM, modified flow directions produce local variations in flow direction that may serve to focus or channelize flow. The results illustrate (figure 3-4) that flow pathways in the vicinity of the proposed repository site show a marked convergence near the eastern edge of the proposed repository site. The result has two important implications for performance. First, converging flow near the proposed repository would reduce the area where lateral spreading of released radionuclides would occur, and thus may reduce dilution. Second, a contaminant plume localized along fractures could be exceedingly difficult to recognize and monitor unless a monitoring well was favorably placed directly along a flow pathway. This channelization mechanism is of course highly dependent on existing sets of open fractures, orientation of the stress tensor, and magnitude of the resulting transmissivity anisotropy.

Recent multiwell pumping tests at the C-Well complex (conducted by USGS for the DOE) indicate that the local maximum transmissivity lies along the NW trending axis between wells C-2 and C-3, a distance of 30 m. This is contrary to the results presented here but is not all that surprising because the C-Well test is only indicative of local variations in fracture intensity and orientation. Interpreting hydraulic properties of a fractured aquifer via continuum theory requires fracture density within the test area large enough for the fractured aquifer to be considered a porous medium. At the 30-to-70 m scale of the C-Well complex, there may be too few fractures to validate the results presented previously, which are based on a view of fractures as a continuum. The phenomena described in this section need to be tested at a scale larger than that at the C-Well complex.

3.3.6 Hangingwall Deformation from Normal Faulting—UDEEC (v.2.01) Modeling Calculations

Fault related deformation in fault blocks and fault zones can cause significant changes in fracture aperture, thereby altering porosity, permeability, and hydraulic conductivity. Zhang and Sanderson (1996) studied fluid flow and deformation in regions of jointed rock around extensional faults and observed that during faulting, significant dilation and fluid flow occurred in vertical-subvertical joints in the hangingwall and within the fault zone itself. Because the near surface tectonic setting at YM is characterized by a system of extensional faults (e.g., Scott, 1990), increases in permeability and fluid flow in the hangingwall from normal faulting could facilitate flow of groundwater at YM, especially drainage of perched water. The purpose of SDS KTI work was to investigate this possibility and to evaluate its significance to waste isolation at YM.

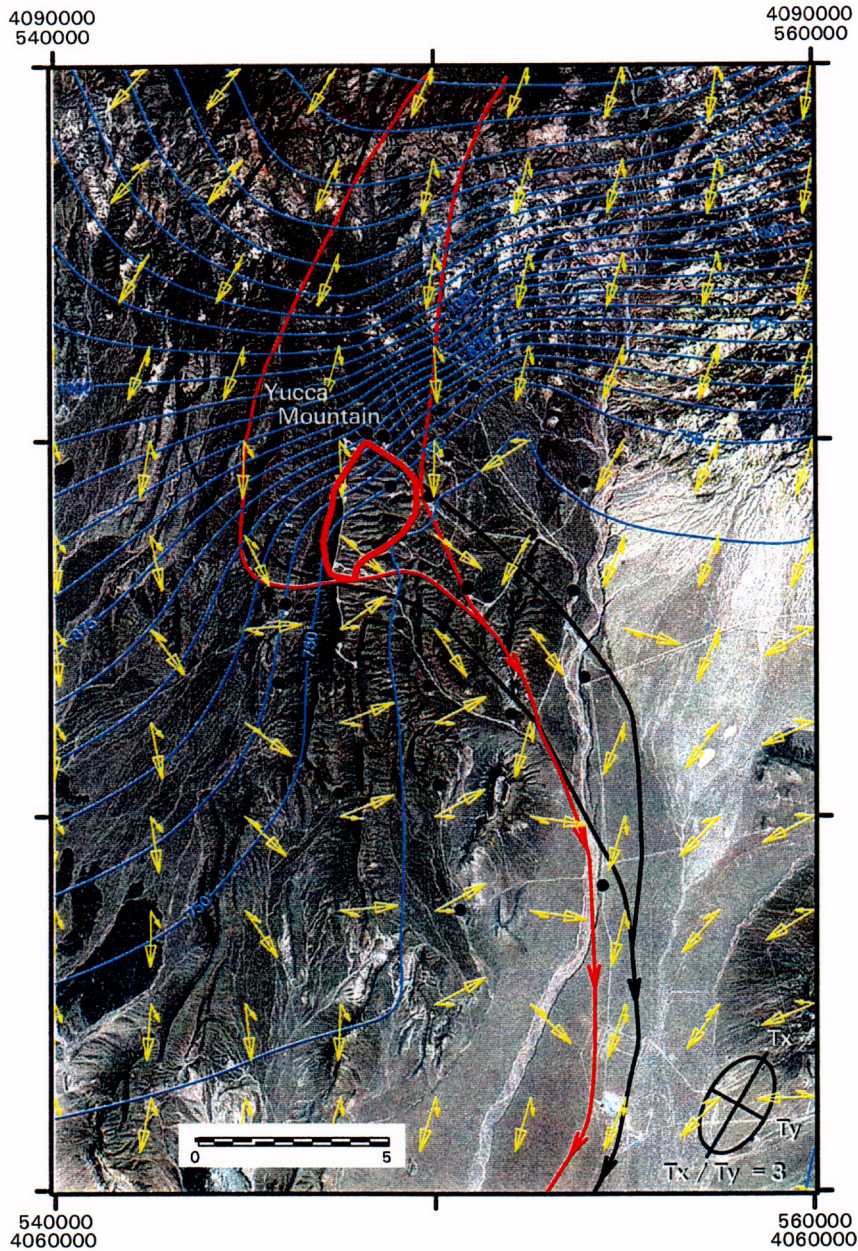


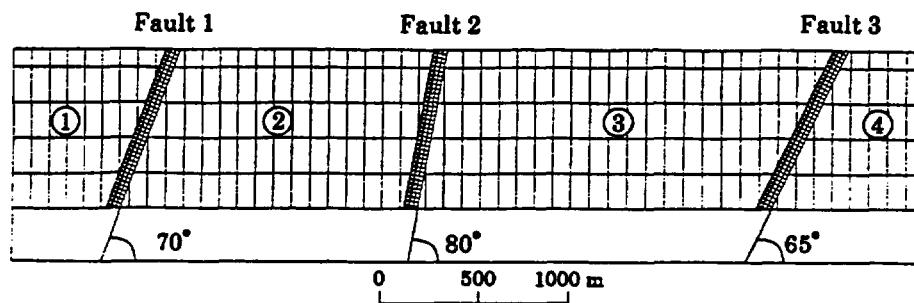
Figure 3-4. Contours representing potentiometric surface based on interpreted steady-state water levels (after Wittmeyer et al., 1995) overlaid on Landsat Thematic Mapper image. Short arrows indicate flow directions (driving force) assuming isotropic transmissivity; long arrows illustrate flow directions assuming a horizontal transmissivity ratio of three ($\tau_x/\tau_y = 3$) with maximum principal transmissivity parallel to the maximum horizontal stress direction. Black dots show well locations.

The 2D models were analyzed using the distinct element code UDEC (v.2.01) (Itasca Consulting Group, Inc., 1993) in which a fracture porosity and fully coupled mechanical-hydraulic analysis is performed assuming impermeable blocks (i.e., water flows through fractures only). The first model was a modification of the 50x40 m rectangular model used by Zhang and Sanderson (1996). The second model was a simple fault model based on an east-west cross section through the proposed repository taken from the CNWRA 3D geological framework model for YM (Stirewalt and Henderson, 1995b). The model configuration consisted of three fault zones and two joint sets (vertical and horizontal at spacings of 100 and 200 m above an unjointed basement (figure 3-5a). The fault zones modeled were analogous to the Solitario Canyon (SC), GD, and Bow Ridge (BR) faults. Each fault is represented as a 75 m wide zone and modeled as a highly fractured zone with two joint sets parallel and perpendicular to the fault zone. Mechanical and hydrologic properties are assumed to be similar to the Topopah Spring welded tuff (Ahola et al., 1996). The *in situ* stresses include vertical stress caused by gravitational loading and horizontal stress related to vertical stress by an assumed Poisson's ratio. Fluid pressure in the model is assumed to be hydrostatic.

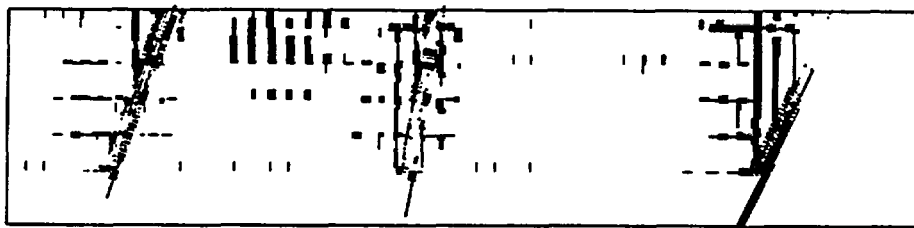
The first model was simulated following the sequence described by Zhang and Sanderson (1996). Simulation of the YM fault model started with an initial stage to achieve steady-state mechanical and hydraulic conditions followed by 1 m displacement of three fault zones in a predefined sequence. Displacement of each fault zone was simulated by allowing vertical movement of the basement beneath the hangingwall region to produce 1 m of slip parallel to the fault zone. Changes in porosity associated with each fault slip were then estimated. Such changes do not reflect porosity changes that may occur in geologic time between successive fault slip events.

Simulation of the first model basically reproduced the results obtained by Zhang and Sanderson (1996). Similar results were also observed in the YM fault model simulation. Figures 3-5b through 3-5d show the distribution of joint apertures after each fault slip in the sequence of BR, GD, and SC, where the thickness of solid lines is proportional to the magnitude of joint aperture. Joint dilation from slip of BR mainly occurred between the GD and SC faults in the hangingwall close to each fault zone and within each fault zone (figure 3-5b). About 100 percent increase in overall porosity was observed in regions between and within the fault zones. Although joint dilation occurred mainly on the vertical joints, some degree of increased dilation was also observed on the horizontal joints. Slip of GD resulted in greater dilation of fractures and joints in the areas between fault zones and within GD and SC faults (figure 3-5c). The combined effect of slip on the BR and GD faults resulted in a more than 150 percent increase in porosity. Slip of SC fault mainly increased joint apertures in its hangingwall with little change in its footwall (figure 3-5d). The calculations only address the potential for change immediately following a normal earthquake. Other processes that could reduce porosity, such as fracture filling or the compressive effects of *in situ* stresses, are not considered.

Two additional simulations were conducted with 1 m slips of each fault in the sequences, GD-SC-BR and SC-GD-BR, to study the effects of slip sequence on dilation. Both these scenarios resulted in more aperture dilation in the area between GD and SC faults and less aperture dilation in the area between GD and BR faults and along horizontal joints. In summary, fault-slip appears to increase joint apertures, especially along vertical joints and existing fault zones in the hangingwall of the fault zone that slipped. The amount and location of fracture dilation also appear to be sensitive to different slip sequences. The resulting magnitude and distribution of joint apertures change depending on relative locations of the fault zones. Further analyses need to be performed to better understand faulting-induced aperture changes. These include investigations of the (i) effect of fault zone structure and irregularities in fault geometry; (ii) inclusion of stratigraphic information specific to YM, especially existing joint patterns in each thermal-



(a) Model Geometry and Mesh



(b) After slip on Fault 3 only



(c) Slip on Fault 2 after slip on Fault 3



(d) Slip on Fault 1 after slip on Faults 2 and 3

Figure 3-5. Geometry of YM fault used in UDEC (v.2.01) modeling. (a) Model consists of three fault zones, SC, GD, and BR faults and two regional joint sets (vertical and horizontal) above an unjointed basement. Cross section shows location and thickness of joints (solid lines) after 1 m slip of the BR fault, (b) after 1 m slip of the GD fault, and (c) after 1 m slip of the SC fault (d).

mechanical unit; (iii) modeling of unsaturated flow to simulate drainage of perched water; and (iv) effects of a significantly large population of fractures and joints in the model. In addition, the methods in which fault slip and the associated boundary conditions were applied needs to be explored further to more closely simulate fault slip that occur *in situ*.

3.3.7 Summary

Technical investigations by the SDS KTI addressed components of all five subissues deemed essential to resolution of the SDS KTI primary objective—evaluation of the effects of SDS and related hazards on safe disposal of HLW at the proposed YM repository. Technical work presented in this report represents significant progress toward resolution of these five subissues. Activities summarized in this chapter include overviews of the identification of Type I faults (McKague et al., 1996) and identification of viable conceptual tectonic models of the YMR. In addition, technical investigations on (i) analog models of pull-apart basins, (ii) numerical modeling of faulting at BM and YM, (iii) dilation-tendency analysis of faults and fractures and implications for groundwater flow in the YMR, and (iv) hangingwall deformation from normal faulting are presented.

To facilitate resolution of the ACM subissue, the NRC and the CNWRA convened an Appendix 7 meeting on May 7-8, 1996 with technical representatives from the DOE, USGS, ACNW, NWTRB, EPRI, and the State of Nevada. A dozen tectonic models proposed for the YMR were reviewed in terms of the most recent geological and geophysical data. Informal agreement among meeting participants was reached that five models are presently supported by the existing data, although agreement on the five models is not unanimous and the participants still differ on the relative importance of each model. Of these five models, the two proposed by representatives of the State of Nevada and the USGS [Crater Flat (CF) is interpreted as a pull-apart basin] pose the greatest seismic risk because of the potential for blind or buried faults not currently accounted for in the DOE PSHA.

The CNWRA investigations examined development of pull-apart basins through a series of analog sandbox experiments constructed to simulate strike-slip deformations like those proposed for Death Valley and CF. Results of the experiments show that evolution of pull-apart basins can be characterized in four stages (incipient, early, early mature, and late mature). The relative level of seismic hazard potential appears to vary significantly during this evolutionary sequence. Greatest risk is during the mature stage. The cross-basin faults can be linked directly with the master strike-slip fault forming a single, thoroughgoing structure with the potential for large-magnitude earthquakes. Comparisons of the analog models to the tectonic models show that the so-called Amargosa Shear model (Schweickert, 1989) presents the greatest potential seismic risk. In that model, CF is envisioned as a right-lateral (clockwise) shear zone very similar to a mature pull-apart basin. Proposed concealed faults beneath CF would be capable of earthquakes with maximum magnitudes in excess of $M_m=7.8$ (McKague et al., 1996). In contrast, the sphenochasm model Fridrich (1996)¹⁵ would best correspond to an incipient or early mature pull-apart and thus would present a less hazardous alternative to the Amargosa Shear model. However, even in this tectonic model, the potential for seismicity on concealed cross-basin faults near the repository remains an important consideration in PSHA.

¹⁵Fridrich, C.J. 1996. Tectonic evolution of the Crater Flat Basin, Yucca Mountain region, Nevada. Cenozoic Basins of the Death Valley Region. L. Wright, ed. *Geological Society of America Special Paper*. In press.

Identification of only those faults in the YMR that pose significant potential risk to repository performance (i.e., Type I faults) is an integral component of an adequate PSHA. The SDS KTI has identified 52 Type I faults from the more than 400 faults within a 100 km radius of YM (McKague et al., 1996). This analysis provides guidance to the NRC for resolution of this aspect of the data subissue and for upcoming review and comment on the DOE PSHA. In addition to the criteria in NUREG-1451 (McConnell et al., 1992), McKague et al. (1996) used an analysis of fault slip from 3DStress (v.1.2) to assess the seismic potential of faults within the current, *in situ* stress state.

Finite element modeling using ABAQUS (v.5.5) was performed to investigate seismicity and faulting along the BMF. Results indicate that earthquake magnitudes estimated from surface offsets are reasonably representative for moderately deep earthquakes on steeply dipping portions of the fault plane but appear to overestimate magnitudes of shallow earthquakes and underestimate magnitudes of deep earthquakes on low-angle segments of the fault. The models also suggest that for the assumed deep detachment geometry with narrowly confined listric curvature, slip on the BMF does not produce appreciable compensatory slip on YM faults. The most significant result of the modeling is that radiation patterns of seismic energy may be anisotropic so that the largest ground-motion amplitudes do not occur at the epicenter but at a point between the epicenter and the intersection of a line or plane normal to the fault-plane originating at the earthquake focus and extending to the surface. Given the geometry of an east-dipping BMF, peak accelerations may be highest near YM for an earthquake at BM because seismic energy from slip on the BMF at depth radiates to the surface towards YM. The implication of this result is that predicted ground accelerations derived from traditional attenuation functions may significantly underestimate expected peak accelerations from sources in the near-field (near the fault).

Dilation-tendency analysis was used to evaluate the potential effect of horizontal stress on groundwater flow. Modeling indicates that flow pathways converge near the eastern boundary of the proposed repository site. Implications of this result are (i) convergence would limit lateral spreading of any contaminated plume near the site, thereby reducing dilution, and (ii) a plume localized along fractures, like the one predicated in the models, would be difficult to recognize and assess in PA calculations. The models show that localization along fractures is highly sensitive to the orientation of existing fracture sets relative to the orientation of horizontal stress. These results suggest that dilution may be reduced, limiting dilution as a favorable condition as indicated in the DOE WCIS (U.S. Department of Energy, 1996).¹⁶

Models of YM faulting were also analyzed using the distinct element code UDEC (v.2.01) to investigate the possibility that normal faulting could alter groundwater flow patterns in the hangingwall blocks above active normal faults. Impermeable blocks that restricted flow to fractures and joints were modeled. To simulate conditions at YM, the models contained three faults (GD, SC, and BR) with a geometry derived from the CNWRA 3D geologic framework model and two sets of orthogonal fractures (horizontal and vertical). Deformation was modeled as a series of faulting events on the three faults. Results from the analysis showed significant changes in porosity in selected regions between the fault zones and within the fault zones themselves. Dilation mainly occurred in vertical joints and fractures, although some dilation of horizontal joints was also observed. Changes in porosity were sensitive to the order in which faults slipped. The greatest porosity changes occurred with combined slip on the GD and BR faults. Slip on the SC fault increased fracture dilation in its hangingwall with little change in its footwall (i.e., the hangingwall blocks of the GD and BR faults).

¹⁶U.S. Department of Energy. 1996. Highlights of the U.S. Department of Energy's Updated Waste Containment and Isolation Strategy for the Yucca Mountain Site. DOE Concurrence Draft.

3.4 ASSESSMENT OF PROGRESS TOWARD MEETING OBJECTIVES

3.4.1 Resolution of Main Key Technical Issue

Significant progress was made by the NRC and the CNWRA staffs toward meeting the main SDS KTI objective. These investigations included field geological and geophysical studies that help to constrain the viable tectonic models and tectonic processes in the YMR, laboratory studies that constrained ages and rates of deformation, analyses of fault coverages that identified potential performance affecting faults, as well as laboratory studies and numerical analysis that provide insight into possible styles of deformation in the YMR. These investigations, independently and in combination, reduced uncertainties and provided the basis for issue resolution with the DOE.

Progress within the SDS KTI treated several needs: (i) communication with the DOE on site characterization during prelicensing, (ii) evaluation of the DOE progress toward resolving issues critical to supporting license application, and (iii) preparation for review of a license application for YM. It has been necessary for the SDS KTI to act proactively to ensure these needs are treated, given the constraints arising from the DOE schedule and prioritization. The Appendix 7 meeting on alternative conceptual tectonic models demonstrates that this proactive approach is mutually beneficial to the DOE and the NRC. The meeting resulted in a common recognition that more than half the proposed conceptual tectonic models for the YM geologic setting are not presently supported by geologic evidence. The five remaining models significantly reduce and simplify conceptualization of YMR tectonics.

Alternatively, there is greater difficulty in proactively treating numerical modeling of tectonic processes, especially as they relate to performance. The consequences of structural deformation and seismicity on performance are often indirect. As a result, they received limited treatment in early PAs which, unfortunately, were used to argue that consequences of structural deformation and seismicity are negligible. Focused technical investigations of structural and seismic processes reported here provide compelling evidence that such processes need to be considered within the limited expenditure of resources.

Progress toward resolution of the following five subissues is a prerequisite to resolution of the main issue.

1. **Data.** The preliminary identification of Type I faults using the NUREG-1451 (McConnell et al., 1992) methodology resolved a component of this subissue. The DOE has also compiled preliminary identification of Type I faults (Whitney, 1996). The SDS KTI staff is prepared to discuss with the DOE its seismic source term database and resolve this component of this subissue. Conceptual models also provided insight into adequacy of data sets. For example, several viable tectonic models suggest unidentified (blind) faults that are not in fault data sets. Tectonic models discussed with the DOE at the Appendix 7 meeting and evaluation of pull-apart scale model experiments at the CNWRA generated important information on potential blind seismic sources of large-magnitude earthquakes and blind faults.
2. **Model (numerical) validation and verification.** The SDS KTI independently evaluated sensitivity of ground motion to seismic attenuation models and is prepared to move toward issue resolution as appropriate. The SDS KTI modeled groundwater flow anisotropy using fracture aperture changes in changing *in situ* stress fields as a surrogate for bulk transmissivity. The methodology of using dilation-tendency analysis in groundwater studies is a pioneering effort by the CNWRA,

and the SDS KTI is prepared to assimilate the results of PA calculations. In light of the Type I fault report (McKague et al., 1996), analysis of BM-YM fault connectivity, considerations of strike-slip dominant tectonic models, and upgrading SEISM 1.1 code, the SDS KTI staff is prepared to present input on PSHA and PFDHA to the DOE at its FY97 workshops on PSHA.

3. **ACMs.** The Appendix 7 meeting on Alternative Tectonic Models (ATMs) was an important step toward resolution of this subissue on identification of viable tectonic models for the YMR. The DOE and the NRC appear to agree that five ACMs are presently supported by existing data. Much of that data was generated from the CNWRA field, laboratory, and numerical studies of the YMR tectonic setting and associated tectonic processes.
4. **Potential for disruption of WP, underground openings and surface facilities/operations.** The DOE postponed its consideration of disruptive processes and events scenarios from TSPA-95 (TRW Environmental Safety Systems, Inc., 1995) to TSPA-VA. The NRC and the CNWRA staffs are presently using the FAULTING module to evaluate potential breaching of WPs by faulting, including sensitivity studies of faulting on alternative estimates of faulting activity (Ferrill et al., 1996b; Pezzopane, 1995).
5. **Potential for disruption of flow.** Sensitivity of transmissivity to the *in situ* stress field YM area was investigated by the SDS KTI with input from the Unsaturated and Saturated Flow Under Isothermal Conditions (USFIC) KTI. In addition, effects of fault displacement on joint aperture in the hangingwall and footwall of a normal fault were investigated. Preliminary results indicate measurable changes in fracture and joint aperture in the hangingwall. Analysis of anisotropic flow as a result of the interaction of the *in situ* stress and fractures provided insight into the potential for convergence of flow near the eastern edge of the potential repository which could lead to useful quantifications of dilution. Future work will focus on developing more complex and detailed models with the intent of assessing the sensitivity of porosity changes to both variations in faulting parameters (slip and recurrence) and fracture intensity, orientation, and distribution.

3.4.2 Evaluation of the U.S. Department of Energy Testable Hypotheses

The DOE based the organization, management, and explanations of its rationale for testing and analyses of total system performance on 15 testable hypotheses (U.S. Department of Energy, 1996).¹⁷ Two hypotheses that fall within the purview of this KTI are potential disruptive processes and events (faulting and seismicity) that the DOE intends to analyze for effects on the predicted doses to the public (described in section 3.1). These hypotheses are: "The amount of movement of faults through the repository horizon will be too small to bring waste to the surface, and too small and infrequent to significantly impact containment during the next few thousand years," and "The severity of ground motion expected in the repository horizon for tens of thousands of years will only slightly increase the amount of rockfall and drift collapse."

The first hypothesis is being directly tested by the NRC and the CNWRA using the FAULTING module. Preliminary calculations of cumulative fault displacements based on even the most conservative

¹⁷U.S. Department of Energy. 1996. Highlights of the U.S. Department of Energy's Updated Waste Containment and Isolation Strategy for the Yucca Mountain Site. DOE Concurrence Draft.

slip rate estimates indicate that faults acting alone will produce insufficient displacement to transport waste to the surface in the next ten thousand years. The significance of faulting on containment, however, has not yet been evaluated. Results will be described in the NRC detailed review of TSPA-95 (TRW Environmental Safety Systems, Inc., 1995) in FY97.

The second hypothesis is being evaluated in part by this KTI. Preliminary analyses described in sections 3.3.2, 3.3.3, and 3.3.4 indicate that the potential severity of ground motion could be higher than currently considered by the DOE. Results will be presented to the DOE in FY97 in issue resolution status reports on identification of tectonic models and Type I faults, and in the DOE workshops on PSHA, where CNWRA staff have been invited to participate.

3.4.3 Evaluation of Selected U.S. Department of Energy Assumptions

The DOE controlled design assumption #23 concerning subsurface fault standoff is being evaluated in part by this KTI (i.e., location of Type I faults, main trace of faults, characteristics of GD fault). The DOE notes that to the extent practical, repository openings will be located to avoid Type I faults. For unavoidable Type I faults that intersect emplacement drifts, the DOE plans to allow 15 m standoff from the edge of the fault zone to the nearest WP. Avoidance is assumed to be adequate by using a 60 m offset from the main trace of a fault at the proposed repository level. They further note that a 120 m standoff should be used on the west side of the GD fault because the Exploratory Studies Facility (ESF) Topopah Spring main drift will be excavated before the GD fault characteristics are fully investigated (Controlled Design Assumption Document Rev. 2, 12/19/95, B00000000-01717-4600-0032, p 6-24).

Selection of particular standoff distances is an issue to be resolved jointly with the SDS, Container Life and Source Term, USFIC, Evolution of the Near-Field Environment, and Repository Design and Thermal-Mechanical Effects (RDTME) KTIs. Faults that are not Type I and fractures that may be fast pathways in some scenarios may need to be considered by the DOE for avoidance or setback. This KTI considers the subissue of identification of Type I faults will be resolved in FY97.

The DOE assumption concerning future seismic effects on flow was not explicitly evaluated in FY96. The DOE states that increases in water table elevation due to seismic effects can be bounded at 20-30 m, which should have no adverse impact on performance (U.S. Department of Energy, 1996)¹⁸. Field measurements from past worldwide occurrences of water table fluctuation in response to seismic events are well known (Ofoegbu et al., 1995). Work in progress at the CNWRA relating slip and dilation-tendency to flow bears on this assumption and will be reported in FY97.

The DOE hypotheses concerning future faulting and fracturing effects on flow is in the early stage of evaluation by computer modeling at the CNWRA (section 3.3.7 and 3.3.8). The DOE states that hydrologic characteristics of faults and fractures at YM represent cumulative effect of numerous tectonic events and thus, they consider that future events are unlikely to significantly change those hydrologic

¹⁸U.S. Department of Energy. 1996. Highlights of the U.S. Department of Energy's Updated Waste Containment and Isolation Strategy for the Yucca Mountain Site. DOE Concurrence Draft.

characteristics (U.S. Department of Energy, 1996)¹⁹. Quantitative analyses of the potential change of fracture characteristics, such as numerical analysis of fracture aperture changes resulting from faulting (section 3.3.5), do not necessarily support this DOE hypothesis. Significant changes in the hydrologic characteristics may result from a single tectonic event. Thus, the DOE hypothesis is valid only for those characteristics that can be shown to result from cumulative events and not simply result from the latest tectonic event(s). Additionally, the hypothesis does not consider the potential effects on flow driven through fractures by an internal thermal source. The characteristics of faults/fractures to heat transport and consequent refluxation remain to be evaluated.

3.5 INTEGRATION WITH OTHER KEY TECHNICAL ISSUES

Preliminary review of geophysical data and discussions with USGS, the State of Nevada, and others at the Appendix 7 meeting on alternative tectonic models for YM indicate that CF and Yucca Flat lie in the same structural domain with no obvious indication of different magma probability zones beneath CF and YMR. Numerical modeling of the intersection of a rising magma with a weak fault zone suggest that any future magmatism would be controlled by moderate to steeply dipping faults. These activities support Igneous Activity KTI contentions of structural controls and probability of volcanism. Refinement of tectonic models based on resolution of crustal geophysical survey data may help constrain uncertainties about the deeper crustal structural controls on magma generation, flow, and transport in the Crater Flat-YM area. Improved understanding of deep seated faults and crustal zones of accommodation of uplift and subsidence have implications for probability, location, and consequences of future volcanism. In addition, the identification of Type I faults and development of the FAULTING module for the TSPA analysis provided input into the role of structural deformation and seismicity on the potential for waste package failure.

Collection, review, and analysis of the DOE data on fracture origin, length, aperture characteristics, and orientation were started in FY96. Such data will contribute to the sensitivity and bounding calculations of hydrologic flow in the saturated and unsaturated zones in both the near- and far-field regions surrounding the proposed repository. Analysis of fracture patterns with 3DStress suggest concentration of flow along the east side of YM and thus provides an important constraint for the USFIC KTI. The SDS KTI will also continue to provide structural analyses of DOE ESF-wall and surface-outcrop fracture and fault mapping.

Finally, a number of SDS KTI activities are near completion for integration of the PA KTI, including development of the FAULTING module software, review and redefinition of the lithostratigraphic columns of the subregions of the TSPA repository model, and additional development and modifications to the 3D geologic framework model. This work was accomplished with input from the USFIC, RDTME, and Total System Performance Assessment and Integration (TSPAI) KTIs.

3.6 REFERENCES

Ahola, M.P., R. Chen, H. Karimi, S.M. Hsiung, and A.H. Chowdhury. 1996. *Parametric Study of Drift Stability in Jointed Rock Mass, Phase I: Discrete Element Thermal-Mechanical Analysis of Unbackfilled Drifts*. CNWRA 96-009. San Antonio, TX: Center for Nuclear Waste Regulatory Analyses.

¹⁹U.S. Department of Energy. 1996. Highlights of the U.S. Department of Energy's Updated Waste Containment and Isolation Strategy for the Yucca Mountain Site. DOE Concurrence Draft.

- Barton, C.C., and P.A. Hsieh. 1989. Physical and hydrologic flow properties of fractures: Field Trip Guidebook T385: 28th International Geologic Congress. Washington, DC: *American Geophysical Union* 36.
- Barton, C.C., E. Larsen, W.R. Page, and T.M. Howard. 1993. *Characterizing Fractured Rock for Fluid-Flow, Geomechanical, and Paleostress Modeling: Methods and Preliminary Results from Yucca Mountain, Nevada*. U.S. Geological Survey Open-File Report 93-269. Reston, VA: U.S. Geological Survey.
- Burchfiel, B., and J. Stewart. 1966. "Pull-apart" origin of the central segment of Death Valley, California. *Geological Society of America Bulletin* 77: 439-442.
- Carlsson, A., and T. Olsson. 1979. Hydraulic conductivity and its stress dependence. *Proceedings, Organization for Economic Cooperation and Development and International Atomic Energy Agency, 1979*. Paris, France: 249-259.
- Caskey, S.J., and R.A. Schweickert. 1992. Mesozoic deformation in the Nevada Test Site and vicinity: Implications for the structural framework in the Cordilleran and thrust belt and tertiary extension north of the Las Vegas Valley. *Tectonics* 11: 1,314-1,331.
- Connor C.B., R.H. Martin, P.G. Hunka, D.B. Henderson, and R.V. Klar. 1996a. *Ground Magnetic Survey of the Little Cones, Crater Flat, Nevada*. CNWRA 96-002. San Antonio, TX: Center for Nuclear Waste Regulatory Analyses.
- Connor, C.B., J.A. Stamatakos, D.A. Ferrill, and B.E. Hill. 1996b. Integrating structural models into probabilistic volcanic hazard analyses: An example from Yucca Mountain, Nevada. *Geological Society of America Abstracts with Program 1996 Annual Meeting*. Boulder, CO: Geological Society of America: 28: 192.
- Crowe, B.M., F.V. Perry, J. Geissman, L. McFadden, S. Wells, M. Murrell, J. Poths, G.A. Valentine, L. Bowker, and K. Finnegan. 1995. *Status of Volcanic Hazard Studies for the Yucca Mountain Site Characterization Project*. Los Alamos National Laboratory Report LA-12908-MS. Los Alamos, NM: Los Alamos National Laboratory.
- Ferrill, D.A., S.R. Young, G.L. Stirewalt, A.P. Morris, and D.B. Henderson. 1994. Tectonic processes in the central Basin and Range region. *NRC High-Level Radioactive Waste Research at CNWRA January-June 1994*. B. Sagar, ed. CNWRA 94-01S. San Antonio, TX: Center for Nuclear Waste Regulatory Analyses: 139-160.
- Ferrill, D.A., A.P. Morris, D.B. Henderson, and R.H. Martin. 1995. Tectonic processes in the central Basin and Range region. *NRC High-Level Radioactive Waste Research at CNWRA July-December 1994*. B. Sagar, ed. CNWRA 95-01S. San Antonio, TX: Center for Nuclear Waste Regulatory Analyses: 121-139.

- Ferrill, D.A., J.A. Stamatakos, and A.P. Morris. 1996a. Structural controls of progressive deformation of the Yucca Mountain (Nevada) region. *Geological Society of America Abstracts with Program 1996 Annual Meeting*. Boulder, CO: Geological Society of America: 28: 192.
- Ferrill, D.A., G.L. Stirewalt, D.B. Henderson, J.A. Stamatakos, A.P. Morris, K.H. Spivey, and B.P. Wernicke. 1996b. *Faulting in the Yucca Mountain Region: Critical Review and Analyses of Tectonic Data from the Central Basin and Range*. NUREG/CR-6401. Washington, DC: Nuclear Regulatory Commission.
- Ferrill, D.A., J.A. Stamatakos, S.M. Jones, B. Rahe, H.L. McKague, R.H. Martin, and A.P. Morris. 1996c. Quaternary slip history of the Bare Mountain fault (Nevada) from the morphology and distribution of alluvial fan deposits. *Geology* 24: 559–562.
- Frizzell, V.A., and J. Shulters. 1990. *Geologic Map of the Nevada Test Site, Southern Nevada*. U.S. Geological Survey Miscellaneous Investigations Series, Map I-2046, Scale 1:100,000. Denver, CO: U.S. Geological Survey.
- Gauthier, J.H., M.L. Wilson, D.J. Borns, and B.W. Arnold. 1995. Impacts of seismic activity on long-term repository performance at Yucca Mountain. *Methods of Seismic Hazard Evaluation, Focus '95*. Las Vegas, NV: American Nuclear Society: 159–168.
- Hanks, T.C., and H. Kanamori. 1979. A moment-magnitude scale. *Journal of Geophysical Research* 84: 2,348–2,350.
- Harmsen, S.C. 1994. The Little Skull Mountain earthquake of 29 June 1992: Aftershock focal mechanisms and tectonic stress field implications. *Bulletin of the Seismological Society of America* 84: 1,484–1,505.
- Hart, E.W., W.A. Bryant, and J.A. Treiman. 1993. Surface faulting associated with the June 1992 Landers earthquake, California. *California Geology* 46(1): 10–16.
- Hauksson, E., L.M. Jones, and K. Hutton. 1995. The 1994 Northridge earthquake sequence in California: Seismological and tectonic aspects. *Journal of Geophysical Research* 100: 12,335–12,355.
- Itasca Consulting Group, Inc. 1993. *UDEC Version 2.0 User's Manual*. Minneapolis, MN: Itasca Consulting Group.
- Janssen, B. 1995. *Numerical Modelling of Extension of the Earth's Crust with Example from the Basin and Range, United States*. Ph.D. Dissertation. Shasburg, France: l'Universite' Louis-Pasteur de Strasburg.
- Kanamori, H., and D.L. Anderson. 1975. Theoretical basis of some empirical relations in seismology. *Bulletin of the Seismological Society of America* 65: 1,073–1,096.
- Klinger, R.E., and L.W. Anderson. 1994. Topographic profiles and their implications for late Quaternary activity of the Bare Mountain Fault, Nye County, Nevada. *Geological Society of America Abstracts with Program 1994 Annual Meeting*. Seattle, WA: Geological Society of America 26(2): A-63.

- McConnell, K.I., M.E. Blackford, and A.K. Ibrahim. 1992. *Staff Technical Position on Investigations to Identify Fault Displacement Hazards and Seismic Hazards at a Geologic Repository*. NUREG-1451. Washington, DC: Nuclear Regulatory Commission.
- McKague, H.L., J.A. Stamatakos, and D.A. Ferrill. 1996. *Type I Faults in the Yucca Mountain Region*. CNWRA 96-007. San Antonio, TX: Center for Nuclear Waste Regulatory Analyses.
- Monsen, S.A., M.D. Carr, M.C. Reheis, and P.A. Orkild. 1992. *Geologic Map of Bare Mountain, Nye County, Nevada*, U.S. Geological Survey Miscellaneous Investigations Series, Map I-2201, Scale 1:24,000. Denver, CO: U.S. Geological Survey.
- Morris, A.P., D.A. Ferrill, and D.B. Henderson. 1996. Slip-tendency analysis and fault reactivation. *Geology* 24: 275-278.
- Nuclear Regulatory Commission. 1996. *Disposal of High-Level Radioactive Waste in Geologic Repository. Title 10, Energy, Part 60 (10 CFR Part 60)*. NUREG-1451. Washington, DC: U.S. Government Printing Office.
- Ofoegbu, G.I., and D.A. Ferrill. 1995. *Finite Element Modeling of Listric Normal Faulting*. CNWRA 95-008. San Antonio, TX: Center for Nuclear Waste Regulatory Analyses.
- Ofoegbu, G.I., S. Hsuing, A.H. Chowdhury, and J. Philip. 1995. *Field Site Investigations: Effects of Mine Seismicity on Groundwater Hydrology*. NUREG/CR-6283. Washington, DC: Nuclear Regulatory Commission.
- Peacock, D., and D. Sanderson. 1991. Displacements, segment linkage and relay ramps in normal fault zones. *Journal of Structural Geology* 13: 721-733.
- Pezzopane, S.K. 1995. *Preliminary Table of Characteristics of Known and Suspected Quaternary Faults in the Yucca Mountain Region*. U.S. Geological Survey Administrative Report. Reston, VA: U.S. Geological Survey.
- Sawyer, D.A., R.R. Wahl, J.C. Cole, S.A. Minor, R.J. Laczniak, R.G. Warren, C.M. Engle, and R.G. Vega. 1995. *Preliminary Digital Geological Map Database of the Nevada Test Site Area, Nevada*. U.S. Geological Survey Open-File Report 95-0567. Scale 1:100,000. Denver, CO: U.S. Geological Survey.
- Schweickert, R.A. 1989. Evidence for a concealed strike-slip fault beneath Crater Flat, Nevada. *Geological Society of America Abstracts with Program 1989 Annual Meeting*. Denver, CO: Geological Society of America 28: 21.
- Scott, R.B. 1990. Tectonic setting of Yucca Mountain, southwest Nevada. Basin and Range extensional tectonics near the latitude of Las Vegas, Nevada. B.P. Wernicke, ed. *Geological Society of America Memoir* 176: 251-282.

- Sibson, R. 1986. Rupture interaction with fault jogs. S. Das, J. Boatwright, and C. Scholz eds., *Earthquake Source Mechanics*. Washington, DC. American Geophysical Union Geophysical Monograph 37(6): 157–167.
- Sieh, K., L. Jones, E. Hauksson, K. Hudnut, D. Eberhart-Phillips, T. Heaton, S. Hough, K. Hutton, H. Kanamori, A. Lilje, S. Lindvall, S.F. McGill, J. Mori, C. Rubin, J.A. Spotila, J. Stock, H.K. Thio, J. Treiman, B. Wernicke, and J. Zachariassen. 1993. Near-field investigations of the Landers earthquake sequence, April to July, 1992. *Science* 260: 171–176.
- Sowers, J.M., J.R. Unruh, W.R. Lettis, and T.D. Rubin. 1994. Relationship of the Kickapoo fault to the Johnson Valley and Homestead faults, San Bernadino County, California. *Bulletin of the Seismological Society of America* 84(3): 532–536.
- Stamatakos, J.A., and D.A. Ferrill. 1996a. Tectonic processes in the Central Basin and Range region. *NRC High-Level Radioactive Waste Research at CNWRA July–December 1995*. B. Sagar, ed. CNWRA 95-02S. San Antonio, TX: Center for Nuclear Waste Regulatory Analyses: 6–1 to 6–25.
- Stamatakos, J.A., and D.A. Ferrill. 1996b. Kinematic constraints of central Basin and Range tectonism from paleomagnetic and fission track studies at Bare Mountain, Nevada. *Geological Society of America Abstracts with Program 1996 Annual Meeting*. Denver CO: Geological Society of America: 28: 125.
- Stirewalt, G.L., and D.B. Henderson. 1995a. A preliminary three-dimensional geological framework model for Yucca Mountain. *Proceedings of the Sixth Annual International Conference on High-Level Radioactive Waste Management*. La Grange Park, IL: American Nuclear Society: 16–118.
- Stirewalt, G.L., and D.B. Henderson. 1995b. *A Three-Dimensional Geological Framework Model for Yucca Mountain, Nevada, with Hydrologic Application: Report to Accompany 1995 Model Transfer to the Nuclear Regulatory Commission*. CNWRA 94-023. San Antonio, TX: Center for Nuclear Waste Regulatory Analyses.
- Stirewalt, G.L., and D.B. Henderson. 1996. Development of three-dimensional hydrostratigraphic models for the potential high-level radioactive waste repository site at Yucca Mountain, Nevada. *Association of Engineering Geologists 39th Annual Meeting Program and Abstracts*. Bryan, TX Association of Engineering Geologists: 67–68.
- Stirewalt, G.L., S.M. McDuffie, and R.D. Manteufel. 1996. A consequence analysis module to simulate fault displacement in the repository block at Yucca Mountain. *Proceedings of the Topical Meeting on Methods of Seismic Hazard Evaluation: Focus '95*. Las Vegas, NV: American Nuclear Society. 169–177.
- Stock, J.M., J.H. Healy, S.H. Hickman, and M.D. Zoback. 1985. Hydraulic fracturing stress measurements at Yucca Mountain, Nevada, and relationship to regional stress field. *Journal of Geophysical Research* 90: 8,691–8,706.

- Sweetkind, D.S., and S. Williams-Stroud. 1995. Controls on the genesis of fracture networks, Paintbrush Group, Yucca Mountain, Nevada. *EOS, Transactions, American Geophysical Union* 76: F597.
- Throckmorton, C.K., and E.R. Verbeek. 1995. *Joint Networks in the Tiva Canyon and Topopah Spring Tuffs of the Paintbrush Group, Southwestern, Nevada*. U.S. Geological Survey Open-File Report 95-2. Denver, CO: U.S. Geological Survey.
- Trudgill, B., and J. Cartwright. 1994. Relay-ramp forms and normal-fault linkages, Canyonlands National Park, Utah. *Geological Society of America Bulletin* 106: 1,143–1,157.
- TRW Environmental Safety Systems, Inc. 1995. *Total System Performance Assessment—1995: An Evaluation of the Potential Yucca Mountain Repository*. (B00000000-01717-2200-00136). Las Vegas, NV: TRW Environmental Safety Systems, Inc.
- U.S. Department of Energy. 1994. *Methodology to Assess Fault Displacement and Vibratory Ground Motion at Yucca Mountain*. DOE Topical Report 1, YMP/TR-002-NP. Washington, DC: U.S. Department of Energy.
- Wells, D., and K. Coppersmith. 1994. New empirical relationships among magnitude, rupture length, rupture width, rupture area, and surface displacement. *Bulletin of the Seismological Society of America* 84: 974–1,002.
- Wernicke, B. 1992. Cenozoic extensional tectonics of the U.S. Cordillera. The Cordilleran Orogen: Conterminous U.S. B.C. Burchfiel, P.W., Lipman, and M.L. Zoback, eds. *The Geology of North America G-3*. Boulder, CO: *Geological Society of America*: 553–581.
- Whitney, J.W. 1996. *Seismo Tectonic Framework and Characterization of Faulting at Yucca Mountain, Nevada*. Denver, CO: U.S. Geological Survey.
- Wittmeyer, G.W., and D.A. Ferrill. 1994. Effect of contemporary regional stress on the anisotropy of transmissivity in fractured rock aquifers. *EOS, Transactions, American Geophysical Union* 75:(44): 258.
- Wittmeyer, G.W., W.M. Murphy, and D.A. Ferrill. 1994. Regional hydrologic processes of the Death Valley Region. *NRC High-Level Radioactive Waste Research at CNWRA, January–June 1994*. San Antonio, TX: B. Sagar, ed. CNWRA 94-01S. Center for Nuclear Waste Regulatory Analyses: 189–212.
- Wittmeyer, G., R. Klar, G. Rice, and W. Murphy. 1995. *The CNWRA Regional Hydrogeology Geographic Information System Database*. CNWRA 95-009. San Antonio, TX: Center for Nuclear Waste Regulatory Analyses.
- Wong, I.G., S.K. Pezzopane, M. Mengas, R.K. Green, and R.C. Quittmeyer. 1995. Probabilistic seismic hazard analyses of the exploratory studies facility at Yucca Mountain, Nevada. *Methods of Seismic Hazard Evaluation, Focus '95*. Las Vegas, NV: American Nuclear Society. 51–63.

- Zhang, P., B. Burchfiel, S. Chen, and Q. Deng. 1989. Extinction of pull-apart basins. *Geology* 17: 814–817.
- Zhang, Z., and D.J. Sanderson. 1996. Numerical modeling of the effects of fault slip on fluid flow around extensional faults. *Journal of Structural Geology* 18: 109–119.
- Zoback, M.L. 1992. First- and second-order patterns of stress in the lithosphere: The World Stress Map Project. *Journal of Geophysical Research* 97(B8): 11,703–11,728.
- Zoback, M.L., R.E. Anderson, and G.A. Thompson. 1981. Cenozoic evolution of the state of stress and style of tectonism of the Basin and Range Province of the western United States. *Philosophical Transactions of the Royal Society of London A300*: 407–434.
- Zoback, M.L., and 36 Project participants. 1992. World Stress Map—maximum horizontal stress orientations. *Journal of Geophysical Research* 87(B8).

4 EVOLUTION OF THE NEAR-FIELD ENVIRONMENT

Primary Authors: P.C. Lichtner, R.T. Pabalan, N. Sridhar, W.M. Murphy, B.W. Leslie, and P.J. Angell

Technical Contributors: P.J. Angell, B.W. Leslie, P.C. Lichtner, W.M. Murphy, R.T. Pabalan, and N. Sridhar

Key Technical Issue Co-Leads: N. Sridhar (CNWRA) and B.W. Leslie (NRC)

4.1 INTRODUCTION

The U.S. Department of Energy (DOE) updated Waste Containment and Isolation Strategy (WCIS) for the proposed repository at Yucca Mountain (YM)¹ has the primary goals of near-complete containment of radionuclides within waste packages (WPs) for several thousand years and acceptably low annual doses to a member of the public living near the site. Among the system attributes recognized in this strategy to be most important in accomplishing these goals are the rate of seepage of water into the proposed repository, WP life time (containment), release rate of radionuclides from breached WPs, and radionuclide transport through engineered and natural barriers. The objective of the Evolution of the Near-Field Environment (ENFE) Key Technical Issue (KTI) is to evaluate these attributes as they relate to the transient near-field environment and provide bounding calculations of near-field environmental conditions for use in total system performance assessment (TSPA) calculations.

The near field is that portion of the proposed repository where physical and chemical properties have been altered by the proposed repository construction operations and radioactive waste emplacement affecting performance of the proposed repository (Wilder, 1993a). The spatial extent of the near-field environment varies depending on the specific process considered. For example, the near-field environment can extend to a considerable distance from the waste emplacement horizon if transport of radionuclides is considered, whereas the processes of importance to spent fuel dissolution occur in a much smaller region.

Expected near-field environmental processes for the proposed YM repository were reviewed previously (Glassley, 1986; Murphy, 1991; Wilder, 1993a,b). However, these evaluations were focused on the older Site Characterization Plan (SCP) design of the engineered barrier system (EBS) involving borehole emplacement of a thin (12.5 mm), single-walled container (U.S. Department of Energy, 1988). Recently, a new WP design called the Advanced Conceptual Design (ACD) has evolved involving thick (120 mm), multiple-wall containers (TRW Environmental Safety Systems, Inc., 1996b). The emplacement geometry has also changed from a vertical borehole concept to a horizontal drift concept. The DOE thermal loading strategy also has evolved, with the aim of higher thermal loading to create a longer dryout period. Processes affecting the near-field environment and WP performance must be considered in light of changes in the EBS design. For example, the effect of gamma radiolysis on corrosion of container materials is unimportant because of shielding provided by the thick overpacks. On the other hand, effects of corrosion of outer overpack on the corrosion of inner overpack must be considered in

¹U.S. Department of Energy. 1996. *Highlights of the U.S. Department of Energy's Updated Waste Containment and Isolation Strategy for the Yucca Mountain Site*. DOE Concurrence Draft. July 1996. Washington, DC: U.S. Department of Energy.

the new design. Similarly, the large volume of iron containing material is expected to affect the radionuclide transport processes through generation of colloids and secondary iron-containing minerals. Also, the higher thermal load expected in the new design may extend the spatial scale of the near-field environment. The present report focuses on the ACD concept in evaluating the processes affecting the near-field environment. Baseline conditions prior to proposed repository construction and waste emplacement have been described extensively in previous reports (Wilder, 1993a,b; U.S. Department of Energy, 1988).

This chapter describes sensitivity analyses of the near-field environment conditions conducted through use of the computer code MULTIFLO, auxiliary analyses of pH changes due to cement-water interactions, and assessment of the viability of microbial organisms and effects in the near-field environment. The focus of these technical accomplishments, and this chapter, is the subissues concerning containment, radionuclide mobilization, and radionuclide transport.

The ENFE KTI has been divided into four subissues directly linked to four system attributes (seepage, containment, radionuclide mobilization, and radionuclide transport) of the DOE WCIS.² One subissue within the ENFE KTI addresses three of the DOE hypotheses within the seepage attribute: (i) limited fracture flow at the proposed repository depth (Hypothesis #2); (ii) capillary retention reduces seepage into the drifts (Hypothesis #3); and (iii) bounds can be placed on thermally-induced changes in seepage rates (Hypothesis #4). However, in FY96 the ENFE KTI did not address the subissue related to seepage. The second ENFE subissue will evaluate the DOE hypothesis of slow corrosion at low humidity within the DOE containment attribute (Hypothesis #7). Evaluating the DOE hypothesis that radionuclide release from waste forms due to surface area exposed, dissolution, colloid formation, and microbial activity will be low (Hypothesis #9) is the focus of the third ENFE subissue. The final ENFE subissue focuses on the DOE hypothesis that transport properties of both engineered and natural barriers will significantly reduce radionuclide concentration (Hypothesis #10).

Each of the ENFE subissues has been addressed during FY96 activities in a multidisciplinary evaluation conducted of near-field processes and the evolution of the near-field environment at YM (Angell et al., 1996). An objective of this review was to judge the sensitivity of proposed repository performance to near-field environmental effects, and a set of subjective prioritized recommendations was provided as an overview and justification for the technical work described in this chapter. Two primary system characteristics significant to performance were identified in the near-field evaluation report (Angell et al., 1996). Coupled thermal-hydrological-geochemical processes were concluded to have the greatest priority. These processes will have big effects on the near-field environment; they will affect proposed repository performance by having dominant effects on containment, release, and radionuclide transport; and predicting these effects will be difficult. The chemistry of the near field will evolve as a result of thermal-hydrologic-geochemical processes associated with heat output of radioactive waste. Chemical composition of water in the near field that could come in contact with the WP, including its oxidation state, pH, chloride concentration, and other compositional variables, is important to the WP life time and radionuclide release from the EBS. Chemistry of the near field could also be important for transport of radionuclides through its impact on speciation, sorption, and coprecipitation of radionuclides. In addition, chemical changes in the near field could affect fracture permeability and the rate of seepage into drifts.

²U.S. Department of Energy. 1996. *Highlights of the U.S. Department of Energy's Updated Waste Containment and Isolation Strategy for the Yucca Mountain Site*. DOE Concurrence Draft. July 1996. Washington, DC: U.S. Department of Energy.

Another important system characteristic is the effect of engineered materials on the near-field environment. Large amounts of container materials, cementitious materials, waste form materials, and their alteration products will have strong effects on the near-field environment. Uncertainties in the properties and behavior of these materials under proposed repository conditions make predictions of performance difficult. Nevertheless, expected processes such as the influence of cementitious materials on water chemistry, the effects of container alteration products on radionuclide transport, and the role of secondary products of waste form materials on radionuclide releases indicate that engineered materials will be significant to performance.

Three other issues were identified in the near-field evaluation report to be of lower priority (Angell et al., 1996). Microbiology is of concern because of uncertainty with regard to its potential effects. Radiolysis can affect radionuclide speciation and release. Also, near-field rock stability under long-term conditions of elevated temperature is uncertain.

4.2 OBJECTIVES AND SCOPE OF WORK

The objective for the ENFE KTI is to conduct activities that will lead to resolution of subissues within the KTI using both proactive and reactive approaches. Resolving the ENFE KTI and its subissues will require evaluating the range of near-field environment (temperature, saturation, and chemical composition) that may result from the interactions of emplaced waste and other materials introduced during proposed repository operations with the host rock and fluids at YM. The breadth of reactive work during FY96 included evaluation of the DOE preliminary near-field environment report (Wilder, 1993a,b), an audit review of the DOE assumptions of the near-field environment used in TSPA-95 (Baca and Brient, 1996; TRW Environmental Safety Systems, Inc., 1995), and evaluating the extent to which the DOE heater tests could be used to constrain the range of expected near-field geochemical conditions. These reactive activities evaluated the information and its relationship to the DOE WCIS hypotheses.³ In addition, the reactive tasks provided constraints that focused technical work accomplished in the ENFE KTI during FY96 on aspects of the subissues that lead to issue resolution.

Proactive work during FY96 focused on development of computer modeling capabilities that allow sensitivity analyses to be conducted on the near-field environment conditions, auxiliary analyses of pH changes due to cement-water interaction, and evaluation of the viability and effects of microbial organisms in the near field. Field work under this KTI focused on collection and analysis of altered rock samples in the vicinity of YM. These samples are being examined in the laboratory to determine the patterns and characteristics of mineral alteration. Observations will be used to support predictive modeling of chemical alteration of the near-field environment. Laboratory efforts during FY96 for the ENFE KTI focused on study of the viability of microbial organisms under expected near-field conditions. These experiments form the basis for resolving the subissue on the importance of microbial organisms on radionuclide mobilization.

The development of the MULTIFLO code (Seth and Lichtner, 1996; Lichtner and Seth, 1996), and the cement-water and microbial organism studies, provide the NRC the capability and information necessary to evaluate the DOE assumptions on processes and parameters used in TSPA. These technical

³U.S. Department of Energy. 1996. *Highlights of the U.S. Department of Energy's Updated Waste Containment and Isolation Strategy for the Yucca Mountain Site*. DOE Concurrence Draft. July 1996. Washington, DC: U.S. Department of Energy.

activities also allow evaluation of the assumptions used by DOE to support the hypotheses in WCIS. Thus, each of these proactive activities has or will contribute (when completed in FY97) to subissue resolution within the ENFE KTI and in other KTIs.

4.3 SIGNIFICANT TECHNICAL ACCOMPLISHMENTS

4.3.1 Sensitivity Analyses Using MULTIFLO

4.3.1.1 Introduction

Model calculations of the redistribution of moisture resulting from emplacement of nuclear waste at the proposed YM high-level waste (HLW) site in Nevada indicate that heat produced from the decay of fission products contained in the waste creates a dryout zone surrounding the proposed repository with enhanced zones of saturation above and below the proposed repository horizon caused by condensation of water (Buscheck and Nitao, 1993; Pruess and Tsang, 1993). The degree of dryness and time to rewet the proposed repository depends on the heat load of radioactive waste and hydraulic properties of the host rock.

As a result of evaporation, condensation, and flow during heating of the proposed repository, salinity and pH may increase in the near-field region. The amount of water that can be evaporated depends on initial saturation and porosity of the rock and water flow toward the WPs. Salts could form on the WP and in the near field as a result of evaporation (Walton, 1993). High pH fluids could react with the silicate host rock producing calcium silicate hydrates (CSHs) and could affect sorption characteristics, porosity, and permeability of the host rock. Precipitation of minerals on fracture surfaces could limit the effect of retardation of radionuclides by matrix diffusion. At high thermal loads, concentrations in dissolved species such as chloride and elevation in the pH are expected to occur near the boiling front surrounding the proposed repository. In regions of condensation, a reduction in concentration is expected due to dilution. In addition, an inverted fluid density gradient will occur below the proposed repository leading to unstable conditions. A further complication is that the boiling front is predicted to change continuously in position in response to the changing thermal load as waste decays with time. Prediction of such effects can only be achieved with models that couple thermal, hydrologic, and chemical (THC) processes.

Few models have been presented that account for THC coupled processes (White, 1995). Robinson⁴ carried out a two-dimensional calculation using a repository scale model with a single component, SiO₂. Robinson⁵ concluded that the dryout zone could be extended due to changes in permeability and porosity caused by precipitation and dissolution of quartz. However, the permeability-porosity relation used by Robinson⁶ seems questionable. He associated a six order of magnitude change in permeability with a variation in porosity from 0.09 to 0.13. No attempt was made to estimate changes in pH and salinity due to evaporation and condensation processes.

⁴Robinson, B. 1994. *Status of Coupled Thermohydrologic/Geochemical Modeling*. Presented at the DOE/NRC Technical Exchange Meeting. Las Vegas, NV: November 9, 1994.

⁵*Ibid.*

⁶*Ibid.*

Current codes that describe coupled thermal-hydrologic processes, such as TOUGH, TOUGH2, VTOUGH, FEHM, and NUFT (Pruess, 1987; Nitao, 1989, 1996; Zyvoloski et al., 1992), do not include multicomponent chemistry suitable for describing rock-water interaction or the effects on solution chemistry due to evaporation and condensation processes. Reaction path codes, such as EQ3/6 (Wolery, 1992), that provide sophisticated descriptions of chemical interaction, do not include explicitly spatial-dependent processes. The code MULTIFLO, developed under the ENFE KTI, provides the capability to model THC processes for multicomponent-multiphase systems in one, two, or three spatial dimensions (Lichtner and Seth, 1996; Seth and Lichtner, 1996).

4.3.1.2 Description of the Code MULTIFLO

MULTIFLO sequentially couples two-phase fluid flow and reactive transport of aqueous and gaseous species. It is composed of two modules: Mass and Energy TRANsport (METRA), a two-phase fluid flow code; and General Electrochemical Migration (GEM), a reactive transport code that takes into account multicomponent chemical reactions involving aqueous, gaseous, and mineral species. METRA and GEM may each be run in stand-alone mode or in coupled mode. In coupled mode, METRA is called first to compute the pressure, temperature, saturation state, and liquid and gas velocities for a single time step. These quantities are then fed to GEM to solve the reactive transport equations in a partially saturated medium. The equivalent continuum model (ECM) is used by METRA to represent the interaction between fractures and matrix. GEM accounts for reactions within the aqueous and gas phases assuming local chemical equilibrium and ion-exchange and kinetic reaction with minerals. Thermodynamic data are provided by an equivalent form of the EQ3/6 database data0.com.r16 applicable for temperatures to 300 °C (Wolery, 1992).

4.3.1.3 Application to the Proposed Nuclear Waste Repository at Yucca Mountain, Nevada

Using the code MULTIFLO, predictions of solution composition, temperature, saturation, and mineral reaction for the proposed YM HLW are based on a moderate heat loading of 80 MTU/acre. With this heat load, a liquid phase is always present. The YM host rock is modeled as pure quartz with an initial volume fraction of 90 percent and a porosity of 10 percent. The ECM is used to represent interaction between fractures and matrix. The chemical model for the aqueous solution used in the calculations consists of 7 primary species and 14 secondary species as listed in table 4-1. The initial fluid composition is presented in table 4-2, abstracted from J-13 groundwater sampled from the saturated zone at YM (Harrar et al., 1990). The unsaturated zone water has even higher concentrations of dissolved solids than the saturated zone water and, therefore, even higher concentrations than predicted here would occur due to evaporation. Calcite and tobermorite precipitate as secondary alteration products. Effective rate constants for quartz, calcite, and tobermorite were chosen to approximate local equilibrium. Material properties of the host rock used in the calculation were taken from Pruess and Tsang (1993).

4.3.1.4 Results

Results are presented for a one-dimensional calculation using MULTIFLO along a vertical line through the center of the proposed repository. The proposed repository horizon is located 375 m below the ground surface and 225 m above the water table. An initial heat load of 80 MTU/acre assuming 26-yr-old spent fuel was used in the calculation with a decaying heat load corresponding to the average WP used in TSPA-95 (TRW Environmental Safety Systems, Inc., 1995). The temperature profile plotted as a function of distance above the water table is shown in figure 4-1 for times ranging from 10 to 10,000 yr. The maximum temperature obtained for this heat load is approximately 130 °C. The deflection

Table 4-1. Chemical species used in MULTIFLO calculations

Primary Species	Other Aqueous Species	Minerals	Gases
Ca ²⁺	OH ⁻	Quartz (SiO ₂)	CO ₂ (g)
Na ⁺	CO ₂ (aq)	Calcite (CaCO ₃)	
K ⁺	CO ₃ ²⁻	Tobermorite (Ca ₅ Si ₆ H ₂₁ O _{27.5})	
H ⁺	CaCO ₃ (aq)		
SiO ₂ (aq)	CaHCO ₃ ⁺		
HCO ₃ ⁻	CaOH ⁺		
Cl ⁻	CaCl ₂ (aq)		
	NaHCO ₃ (aq)		
	NaCl(aq)		
	NaOH(aq)		
	KCl(aq)		
	H ₃ SiO ₄ ⁻		
	H ₂ SiO ₄ ²⁻		

in the temperature profile at approximately 100 °C indicates the presence of a heat pipe.

The corresponding liquid saturation profile is shown in figures 4-2(a) and (b). Above and below the proposed repository horizon regions of enhanced saturation form and expand with time. In these regions, the pore spaces become almost fully saturated during the period of relative dryness at the proposed repository horizon. The saturation state is a dynamic condition caused by continuous evaporation of liquid drawn toward the proposed repository by capillary forces and gravity above the repository horizon and by condensation farther away in cooler regions. Within the heat pipe region the velocity of water vapor is approximately 1,600 times faster than the liquid velocity.

The pH profile is shown in figures 4-2(c) and (d) and the chloride concentration in figures 4-3(a) and (b). The pH increases to values above 10 as CO₂ degasses from the liquid phase at evaporation fronts above and below the

proposed repository horizon. The increase in pH is a consequence of degassing of CO_{2(g)} according to the reaction



The pH decreases at the condensation fronts above and below the proposed repository horizon. The chloride concentration increases by over a factor of 10 from its ambient value at the evaporation front. At the condensation fronts the chloride concentration decreases from its ambient value because the condensing liquid is devoid of salts. Quartz and calcite dissolve in the condensate zones and precipitate in the regions of evaporation. Tobermorite (Ca₅Si₆H₂₁O_{27.5}) precipitates in the high pH region.

Concentrations of total and free SiO_{2(aq)} are shown in figure 4-3(c) and (d). At high pH, H₃SiO₄⁻ becomes the dominant silica species. The reaction rate for quartz is shown in figures 4-4(a) and (b) at two different times: 25 and 250 yr. A positive value indicates precipitation and a negative value dissolution. Regions of dissolution and precipitation move with the evaporation and condensation zones. This minimizes change in porosity and variations in permeability at any point. Minimal change in porosity are predicted over the height of the rock column during simulation time.

The pH and chloride concentration corresponding to different thermal heat loads are indicated in figures 4-4(c) and (d). A time of 25 yr was chosen because complete dryout occurs at longer times for the 100 MTU/acre heat load. The increase in chloride concentration due to evaporation could have important consequences on corrosion rates of the steel overpack and the stainless steel inner liner. Carbon steel becomes passivated at $\text{pH} > 8$. However, pitting becomes important for chloride concentrations $\geq 3 \times 10^{-3} \text{ M}$ at $\text{pH} \sim 8.4$ if the corrosion potential is greater than the repassivation potential. The repassivation potential is a function of temperature and chloride concentration, and the corrosion potential is a function of temperature, pH, and dissolved oxygen concentration. For Alloy 825, there is no effect on repassivation potential due to pH in the range $2 \leq \text{pH} \leq 12$. Pitting becomes important for a chloride concentration $\geq 10^{-2} \text{ M}$. Future work will consider more realistic host rock compositions and extend the calculation to two spatial dimensions. Including feldspars can be expected to affect the pH and provide a supply of silica and other cations which could lead to precipitation of salts such as halite. The results of calculations of the kind presented here can be used to provide bounding estimates of chloride concentration, pH, and other variables in total system performance models and to provide constraints for sensitivity analyses for container life, source term, and radionuclide transport.

Table 4-2. Initial fluid composition corresponding to that of J-13 well water

Species	Concentration, Molality
Ca^{2+}	2.9×10^{-4}
Na^{+}	2×10^{-3}
K^{+}	1.4×10^{-4}
HCO_3^{-}	2.7×10^{-3}
$\text{SiO}_2(\text{aq})$	1.1×10^{-3}
Cl^{-}	1.8×10^{-4}
pH = 6.9	

4.3.2 Effects of Manmade Materials: Cement-Water Interactions

An important aspect of the evolution of the near-field environment is the interaction of groundwater with cementitious materials that could affect WP corrosion and waste form alteration, radioelement speciation, dissolution/precipitation, sorption/desorption reactions, and radionuclide transport. Cementitious materials will be introduced during the construction of the nuclear waste proposed repository primarily in roadways and as ground support for the estimated 228,000 m of proposed repository excavation (TRW Environmental Safety Systems, Inc., 1996a). Roadways for construction and emplacement, particularly for ramps and service mains, will include concrete inverts, stabilized and strengthened by grouting and overlain by reinforced cast-in-place concrete caps. Cementitious materials for ground support may exist as (i) shotcrete or fibercrete (as full or partial circle structural lining); (ii) grout (typically to encapsulate and secure rock bolts, but also to consolidate and strengthen the rock mass); and (iii) concrete lining (pre-cast or cast-in-place, with or without reinforcement). Concrete may also be used for WP pedestals (TRW Environmental Safety Systems, Inc., 1996a).

Cements are fine-grained, high surface area materials containing soluble phases [e.g., CSH gels], metastable with respect to crystalline CSHs. These properties make the materials potentially reactive in the near-field environment and could significantly alter near-field geochemistry. Pore fluids in contact with hydrated cementitious materials are characterized by alkaline pH (> 10) conducive to precipitation of radionuclides, including transuranics (Glasser et al., 1985; Atkins et al., 1990). Cement hydration products can also provide sorption sites that could aid in retarding radionuclide migration (Atkins et al., 1990; 1991) from the EBS to the host rock. In addition, alkaline conditions can provide an environment resulting in formation of a tightly adhering passive film on carbon steel overpack which protects it from uniform corrosion.

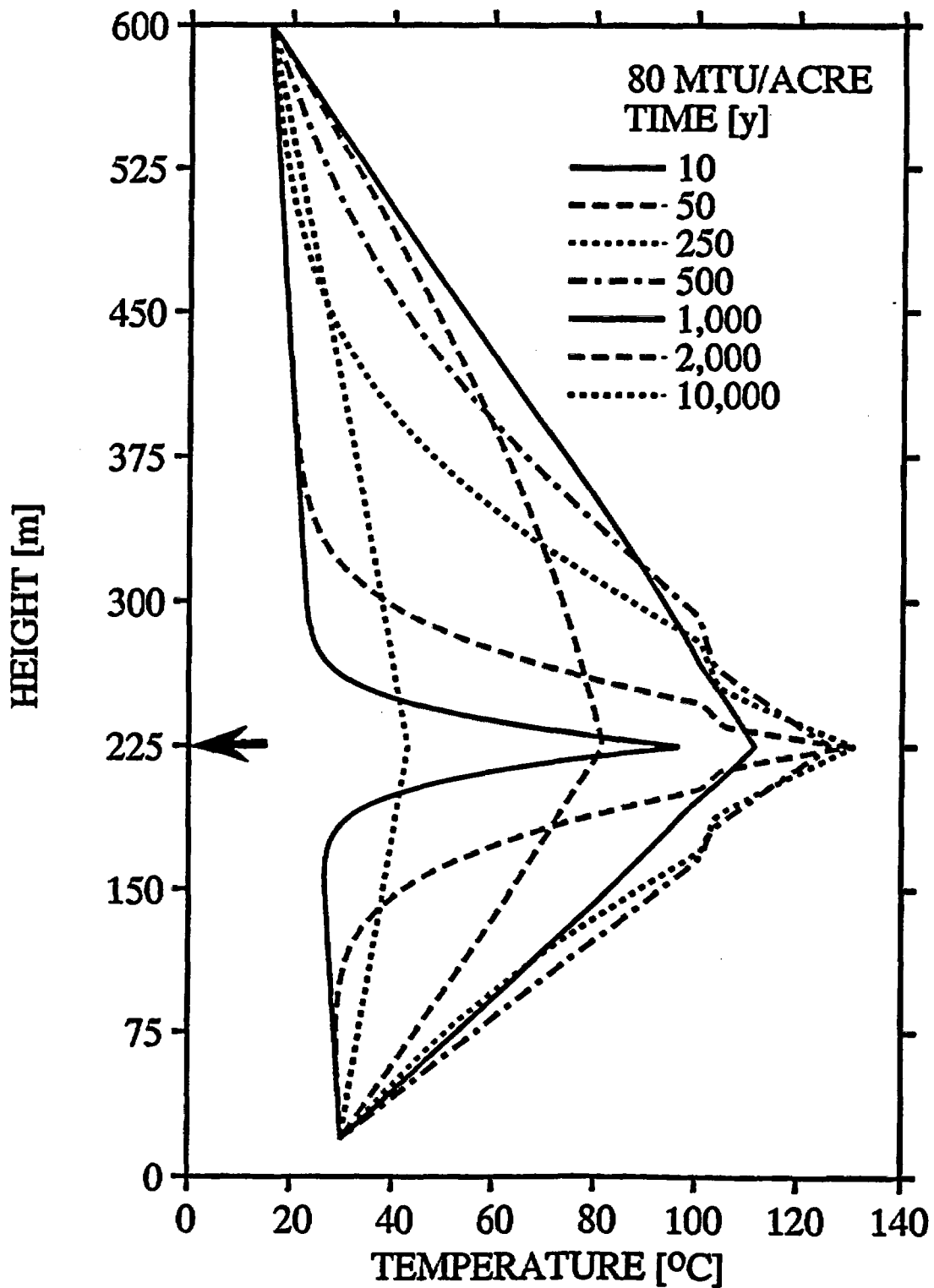


Figure 4-1. Temperature plotted as a function of distance above the water table at times ranging from 10 to 10,000 yr. The arrow depicts the horizon of the proposed repository.

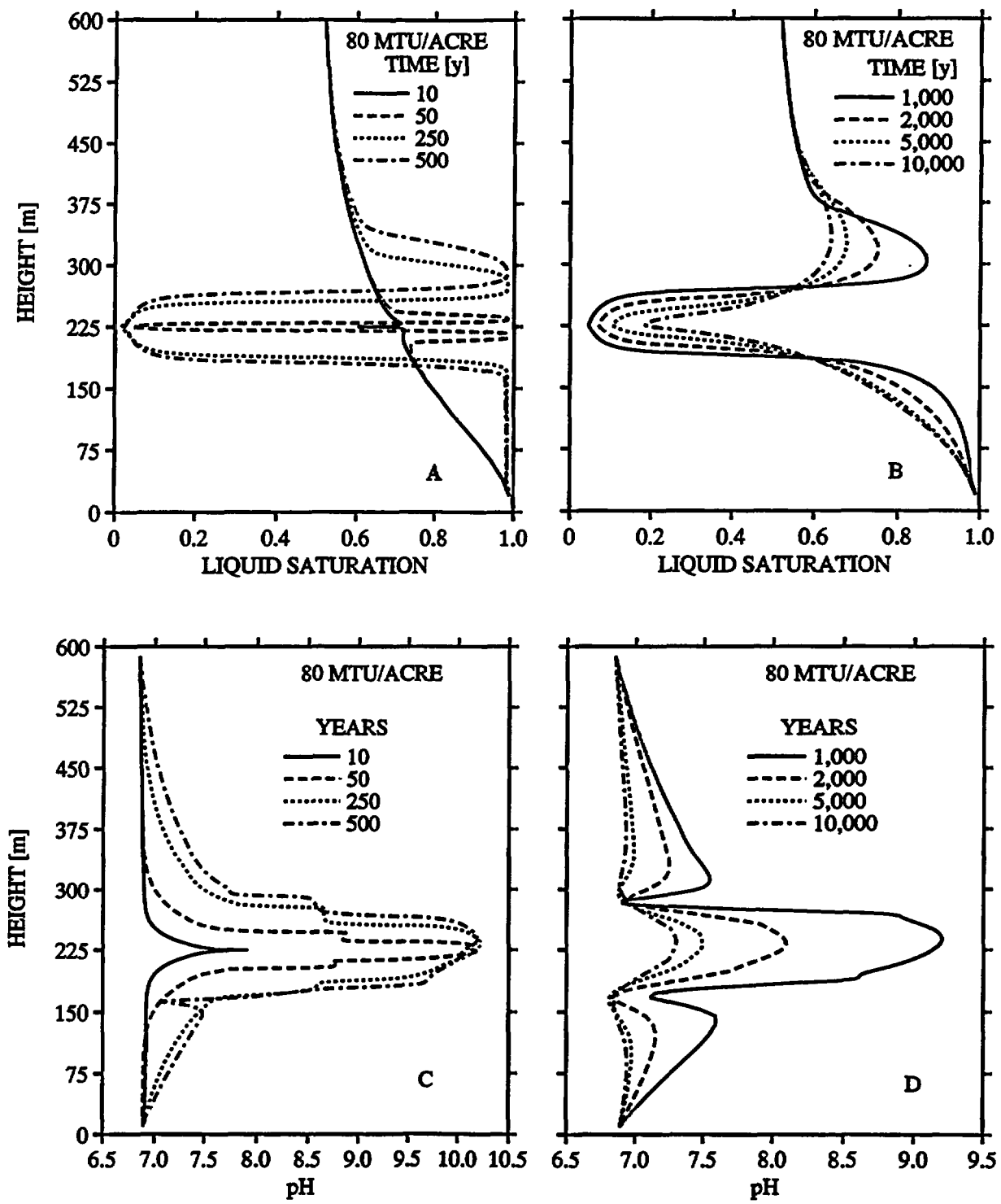


Figure 4-2. Liquid saturation [(a) and (b)] and pH [(c) and (d)] plotted as a function of distance above the water table at times ranging from 10 to 10,000 yr

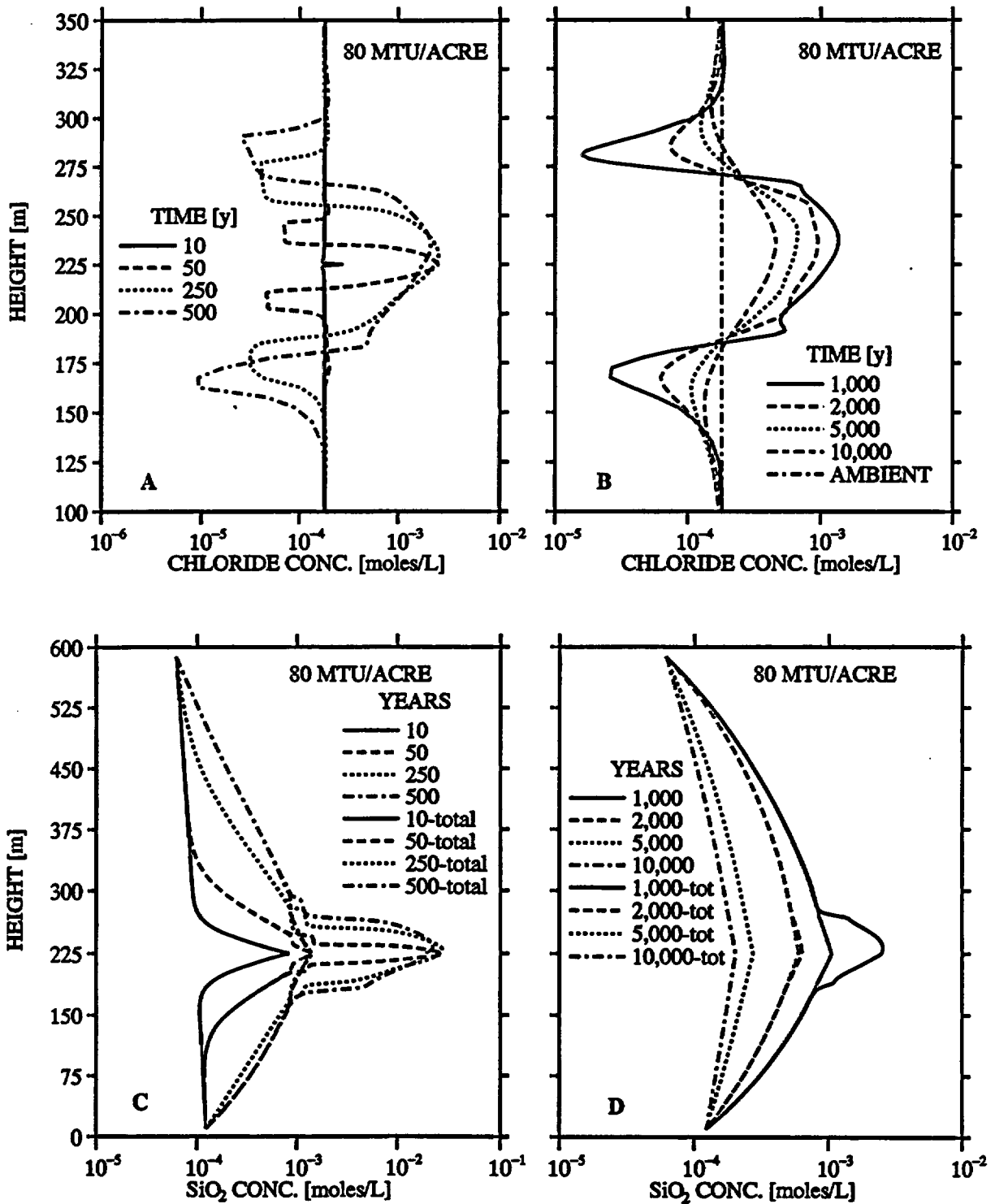


Figure 4-3. Chloride [(a) and (b)] and silica concentration [(c) and (d)] plotted as a function of distance above the water table at times ranging from 10 to 10,000 yr

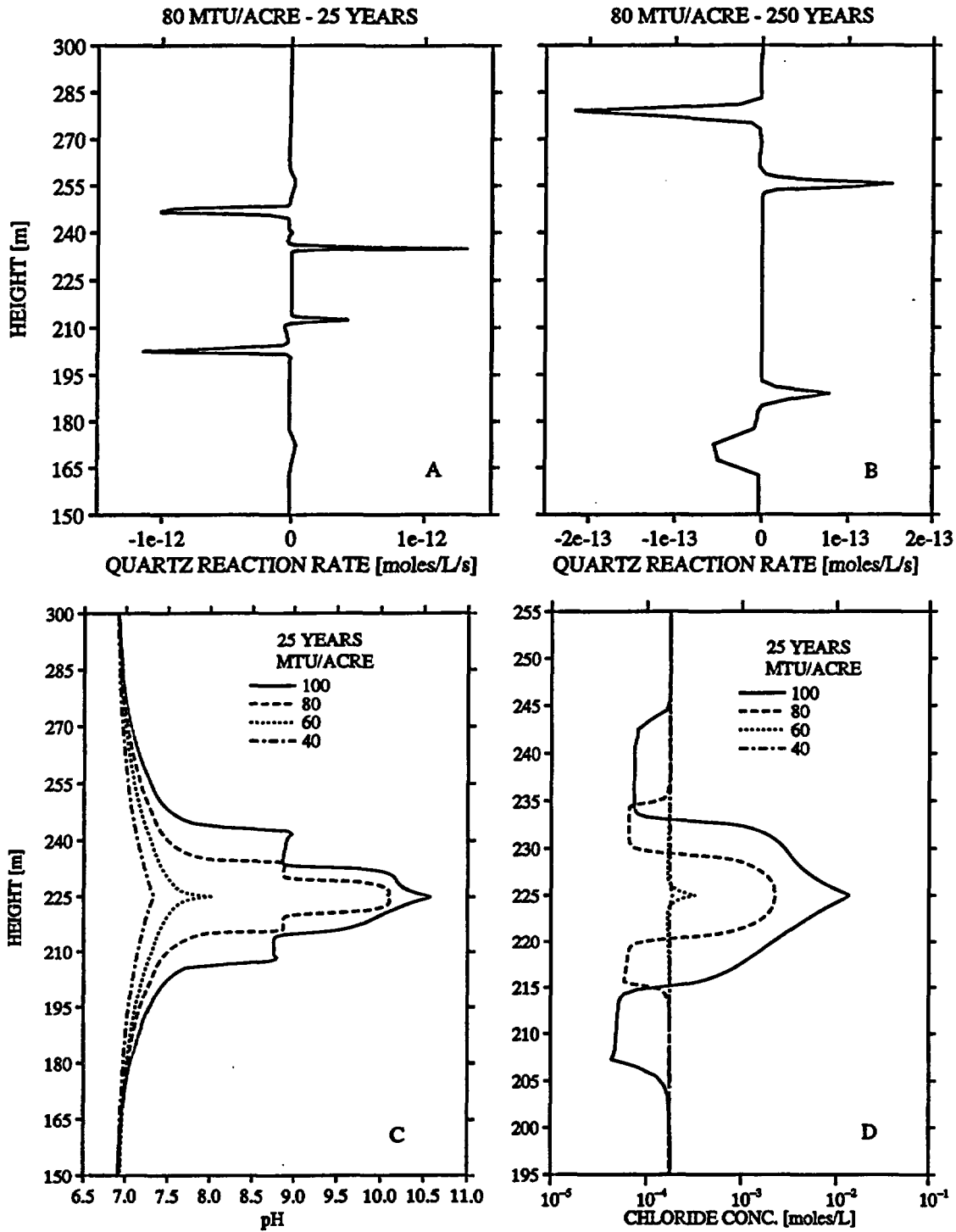


Figure 4-4. Reaction rate of quartz [(a) and (b)] for times of 25 and 250 yr for a repository heat load of 80 MTU/acre, and pH and chloride concentration [(c) and (d)] at 25 yr for heat loads of 40, 60, 80, and 100 MTU/acre plotted as a function of distance above the water table. Note differences in the vertical scale.

Alkaline conditions can be detrimental to the stability of nuclear waste glass and mineral components of the geologic barrier. Experiments by Heimann (1988) indicated that cement/glass interaction leads to accelerated dissolution/alteration of nuclear waste glass compared to a system without cement. Minerals common at YM such as clinoptilolite, mordenite, and montmorillonite, which is also an important component of bentonite backfill material, become unstable at high pH (Komarneni and Roy, 1983; Angus et al., 1983). Mineral alteration due to alkaline solutions and precipitation of secondary phases could affect the sorptive and retardation ability of the geologic barrier and its hydraulic properties (porosity and permeability). Results from U and Np sorption experiments discussed in chapter 5 illustrate the strong dependence of actinide sorption on pH. For example, at atmospheric $p\text{CO}_2$ conditions, U(6+) sorption decreases by four orders of magnitude from pH ~6 to pH ~9 and Np(5+) sorption decreases by more than two orders of magnitude from pH ~8 to pH ~10. The release of radionuclides from the container and from the EBS could be affected by cement/water interactions. Lichtner and Eikenberg (1995) analyses indicated that interaction between a hyperalkaline plume released from a cement-based radioactive waste repository and a marl host rock could result in a rapid decrease in porosity of the host rock several meters from the repository due to precipitation of secondary phases. This study also indicated that porosity could increase at the interface of the marl host rock and the cement due to mineral dissolution. Precipitation of calcite would also occur as the low CO_2 -high Ca cement pore waters mixed with the ambient fluids containing high CO_2 concentrations (Steeffel and Lichtner, 1994). Another important consideration is the durability of rock bolts encapsulated with cementitious grout and of shotcrete planned to be used in emplacement drifts for ground support. The durability of these ground supports may be weakened by cement/tuff reactions and increase the likelihood of rock falls that could damage the waste containers. In addition, carbon steel can undergo localized corrosion or cracking if the external environment is alkaline. As indicated in chapter 5, localized corrosion of carbon steel overpack may occur in the form of pitting or crevice corrosion when the external environment is moderately alkaline (pH ~8 to 10), and stress corrosion cracking can occur in a $\text{HCO}_3^-/\text{CO}_3^{2-}$ environment at a pH of about 10 and when the corrosion potential reaches a critical value.

To address the consequences of cementitious materials in the near field, one must be able to predict changes in near-field chemistry as caused by cementitious materials, particularly with respect to solution pH, a key parameter controlling radionuclide sorption/transport, mineral dissolution/precipitation, waste form degradation, and container corrosion. These predictions are possible for near ambient temperature conditions using available hydration models, geochemical equilibrium codes, and thermodynamic data for cement phases (e.g., Berner, 1992; Atkins and Glasser, 1992; Reardon, 1992).

Simulations of cement/water interactions were conducted as part of this KTI using the equilibrium code SIMUL developed by Reardon (1992). Compositions of porewaters in equilibrium with hydrated Type II Portland cement were calculated. This type of cement is used in the production of concrete inverts for the ESF⁷ and is likely to be the predominant type of cement material used for proposed repository construction. The calculations were based on composition data for anhydrous Type II Portland cement [table 4-3, Clifton et al. (1991)] assuming a water/cement ratio of 0.38 and a setting time of 90 d. The setting time is used in the Reardon (1992) model to estimate the degree of hydration of each cement component and the bound water content as a function of time, whereas the water/cement ratio determines the amount of water available in the system and influences the calculated concentration of aqueous species. A water/cement ratio of 0.38 is the value used in production of concrete inverts for the

⁷N. O'Connor. 1996. Personal Communication.

ESF. A setting time (90 d) greater than the value used in constructing the concrete inverts (28 d)⁸ was assumed for the simulation to partially account for further hydration reactions which occur over time.

Porewater chemical composition predicted to be in equilibrium with CSH gel, portlandite, brucite, ettringite, and hydrogarnet, the principal phases present at later stages of cement hydration (Reardon, 1992), is shown in table 4-4. CSH has a variable Ca/Si ratio and is the principal binding phase in Portland cements. The predicted hyperalkaline pH (13.9) of the pore fluid arises from the preferential partitioning of Na and K into the aqueous phase due to the absence of solid phase controls on these elements in a mature cement. Although Na and K concentrations in the cement material are low (table 4-3), these are dominant cations in the pore fluid. Due to charge balance constraints, Na⁺ and K⁺ concentrations must be balanced by an equivalent concentration of anions, predominantly OH⁻. Alkali content of the cement paste determines the pH of porewater and influences the solubility of other phases in cementitious material.

Table 4-3. Composition of Type II Portland cement (taken from Clifton et al., 1991)

Oxide Component	Weight Percent
SiO ₂	21.0
Al ₂ O ₃	4.4
Fe ₂ O ₃	3.1
CaO	63.5
MgO	3.4
SO ₃	2.94
Na ₂ O	0.26
K ₂ O	0.50
Loss on Ignition	1.00

The major influence of alkalis on porewater chemistry and mineral solubilities could be short-lived if advection and diffusion processes dilute the concentration of alkalis. Where alkali concentration is small, porewater pH is buffered by dissolution of portlandite (Atkins and Glasser, 1992; Reardon, 1992; Berner, 1992). The predicted composition of porewater in equilibrium with alkali-free Type II Portland cement is given in table 4-5, indicating a pH of 12.5. Eventual depletion of portlandite causes the pore fluid pH to decrease from 12.5 to approximately 11, controlled by the incongruent dissolution of the CSH gel, particularly the Ca/Si ratio of the gel (Berner, 1992). When dissolution of CSH is complete, the pH of the cement pore fluid continues to decrease to a value approaching that of the groundwater.

The pH of water from tuffaceous aquifers at YM and vicinity falls in the range 7 to 9.2, with most samples in the 7 to 8 range (Kerrisk, 1987). The large difference in chemical potential between groundwater and pore fluid in cementitious materials provides a driving force for reactions between the two systems. These reactions will lead to a range of water chemistries that need to be considered in evaluating the performance of waste containers and the transport of radionuclides.

Several models have been developed to predict the evolution of pH in cementitious low- and intermediate-level waste repositories (e.g., Berner, 1987). A study by Atkinson et al. (1989) indicated that interaction of groundwater typical of a clay environment with cement could maintain a pH above about 10.5 for a time period on the order of a few hundred thousand years under the low flow rates assumed in that study. At those pH conditions, passive film formation would protect carbon steel, a material proposed as an overpack for HLW containers, unless high concentrations of chloride, sulfate,

⁸N. O'Connor. 1996. Personal Communication.

Table 4-4. Predicted solid and porewater composition for hydrated Type II Portland cement with initial composition given in table 4-3: water/cement ratio of 0.38 and setting time of 90 d. Solute concentrations are millimolal. Solid quantities are in millimoles per kilogram of water in the cement paste [total of bound and unbound water].

Species	Concentration mmol/kg H ₂ O	Activity Coefficient	Solid Phase	Log Saturation Index
OH ⁻	1.06 × 10 ⁻³	0.682	Brucite	0
Ca ²⁺	0.67	0.018	Portlandite	0
Mg ²⁺	6.61 × 10 ⁻⁷	0.038	Etringite	0
MgOH ⁺	6.47 × 10 ⁻⁶	0.436	CSH Gel	0
Na ⁺	584	0.636	Hydrogarnet	0
K ⁺	763	0.719	Amorphous Silica (SiO ₂)	-5.32
Al(OH) ₄ ⁻	0.23	0.524	Sepiolite [Mg ₄ Si ₆ O ₁₅ (OH) ₂ · 6 H ₂ O]	-11.01
H ₃ SiO ₄ ⁻	0.223	0.504	Gibbsite [Al(OH) ₃]	-2.88
H ₂ SiO ₄ ²⁻	6.61	0.060	Calcite (CaCO ₃)	-9.2
SO ₄ ²⁻	136	0.048	Gypsum (CaSO ₄ · 2 H ₂ O)	
Brucite [Mg(OH) ₂]	1.33 × 10 ⁺³	1.000	Syngenite [K ₂ Ca(SO ₄) ₂ · H ₂ O]	-2.38
Portlandite [Ca(OH) ₂]	1.19 × 10 ⁺⁴	1.000	Monosulfate (Ca ₄ Al ₂ O ₆ SO ₄ · 12 H ₂ O)	-1.09
Etringite [Ca ₆ Al ₂ O ₆ (SO ₄) ₃ · 32 H ₂ O]	299	1.000	Arcanite (K ₂ SO ₄)	-0.93
CSH Gel (x CaO · SiO ₂ · x H ₂ O, x = Ca/Si)	7.25 × 10 ⁺³	1.000	Glaserite [K ₃ Na(SO ₄) ₂]	-1.79
Hydrogarnet [Ca ₃ Al ₂ (OH) ₁₂]	1.1 × 10 ⁺³	1.000		
pH	13.88			
Ionic Strength (mole/Kg H ₂ O)	1.49			
Bound H ₂ O	66.60%			
Ca/Si _{CSH}	1.03			

Table 4-5. Predicted solid and porewater composition for hydrated alkali-free Type II Portland cement. Solute concentrations are millimolal. Solid quantities are in millimoles per kilogram of water in the cement paste [total of bound and unbound water].

Species	Concentration mmol/kg H ₂ O	Activity Coefficient	Solid Phase	Log Saturation Index
OH ⁻	42.2	0.682	Brucite	0
Ca ²⁺	21.1	0.018	Portlandite	0
Mg ²⁺	3.54 × 10 ⁻⁵	0.038	Ettringite	0
MgOH ⁺	8.61 × 10 ⁻⁵	0.436	CSH Gel	0
Al(OH) ₄ ⁻	5.82 × 10 ⁻³	0.524	Hydrogarnet	0
H ₃ SiO ₄ ⁻	1 × 10 ⁻³	0.504	Amorphous silica	-6.03
H ₂ SiO ₄ ²⁻	4.29 × 10 ⁻⁴	0.060	Sepiolite	-15.47
SO ₄ ²⁻	2.75 × 10 ⁻²	0.048	Gibbsite	-2.88
Brucite	1.33 × 10 ⁺³	1.000	Gypsum	-2.68
Portlandite	6.54 × 10 ⁺³	1.000	Monosulfate	-1.14
Ettringite	314	1.000	Calcite	-6.35
CSH Gel	7.25 × 10 ⁺³	1.000		
Hydrogarnet	1.08 × 10 ⁺³	1.000		
pH	12.48			
Ionic Strength (mole/kg H ₂ O)	0.0634			
Bound H ₂ O	66.90%			
Ca/Si _{CSH}	1.76			

and/or carbonate are present which could lead to localized corrosion. However, results of current models of cement/water interactions are highly dependent on the assumptions used, particularly the reliance of pH evolution on solubility and persistence of a CSH gel known to be thermodynamically metastable. The same study by Atkinson et al. (1989) indicated that if recrystallization of the CSH gel occurred in the long term, lower pH could result due to the lower solubility of the crystalline CSH phases. If groundwater pH is buffered in the range 8 to 10 by crystalline CSH phases, localized corrosion or stress corrosion cracking of carbon steel overpack may be enhanced and adversely affect performance of the

waste canister. The possibility of CSH recrystallization is high in an HLW repository due to the long timeframe involved and the elevated temperatures imposed by radioactive decay heat from emplaced nuclear wastes. Even modest temperature excursion to 55 °C for 6 to 12 mo can result in partial transformation of CSH gel to more stable, though poorly crystallized, phases such as jennite and tobermorite (Atkins and Glasser, 1992). Thus, modeling of cement/near-field interactions in an HLW repository must consider the likelihood that cement chemistry is dominated by phases other than those present in the initial material.

The effects of cementitious materials on the evolution of the near-field environment at YM are difficult to quantify because of uncertainties in the amount that will be used in the estimated 228,000 m³ of excavation. Although an estimate of 560,000 m³ of shotcrete for ground support was reported (Bruton et al., 1993) based on the SCP (U.S. Department of Energy, 1988), mostly competent ground has been encountered during construction of the Exploratory Studies Facility (ESF). Although qualitative information regarding effects of cementitious materials on the near-field environment can be derived using chemical models for cement/water interactions, a detailed analysis specific to the proposed YM repository environment will require specific information regarding inventory and location of these materials.

4.3.3 Effect of Microorganisms in the Near Field

Horn and Meike (1995) concluded that microorganisms are potentially important in three areas relative to proposed repository performance at YM: (i) alteration of groundwater and host rock chemistry, (ii) corrosion of the EBS, and (iii) mobility of radionuclides. Another important factor of microbial action on the evolution of the near field is its potential to affect flow of water both in the matrix and in fractures. It is known that growth of bacteria and the resultant production of exopolymeric substances can lead to a decrease in the porosity of tuff and other rocks. This effect on porosity can affect transport of radionuclides away from the proposed repository and water flow to containers and waste forms. Microbial plugging of pores and fractures could prevent resaturation of the proposed repository following dryout and could also increase the time necessary to achieve dryout. The DOE has partially characterized the microbiology of the proposed YM repository site. This survey showed that a number of microorganisms that could have an impact on the proposed repository are present at the site. However, this limited survey looked for a partial list of microorganisms, focusing particularly on those implicated in microbial corrosion processes. The current or anticipated level of activity of those organisms has not been addressed.

The Center for Nuclear Waste Regulatory Analyses (CNWRA) studies concentrated on the viability of a natural population following exposure to various temperatures to determine whether the proposed repository will be self sterilizing due to heating by the waste. A sample of tuff obtained from the proposed repository horizon at YM was cored providing an undisturbed sample which was crushed and a 2–4-mm-size fraction collected. Samples of crushed tuff were heated to various temperatures for 200 hr and bacterial viability assessed. A Gram-positive spore former maintained viability at temperatures to 120 °C for the extended time exposures and showed variable viability for shorter 150 °C exposures. Only aerobic heterotrophic bacteria were screened in this study. With a heat load of 83 MTU, the maximum predicted temperature is 130 °C. Therefore, these results indicate that microorganisms can survive over short periods in the near-field environment, although probably not on the containers themselves. Later, when suitable conditions prevail, they can become active. Although these bacteria have not been fully characterized, it is possible that as Gram-positive spore formers producing acid from glucose and capable of anaerobic growth, they are members of the genus *Clostridium*. This group of

bacteria is often associated with MIC due to the ability to produce organic acids. They are also a common isolate from corroded pipes. These isolates produce extracellular polymeric substances potentially affecting hydraulic properties of the host rock and other near-field components.

Two factors have been suggested to limit the effects of microbiological organisms on the performance of the EBS and proposed repository (TRW Environmental Safety Systems, Inc., 1996b):

- (i) Diffusion of oxygen destabilizes anaerobic conditions needed by obligate anaerobes. This argument neglects anaerobic niches known to form in the environment in oxidizing conditions. For example, Lee et al. (1993) demonstrated that formation of a biofilm on a surface can lead to conditions necessary for anaerobic sulfate reducing bacteria to grow.
- (ii) The level of oxidizable sulfur species found at the proposed repository horizon is insufficient to maintain bacteria such as Thiobacilli. A potentially important area is the microbial degradation of concrete. Milde et al. (1993) first reported microbially induced degradation (MID) of concrete in a Hamburg sewer system. They were able to link the degradation to the action of Thiobacilli, a group of bacteria capable of oxidizing sulfur compounds to sulfuric acid. Recently, Hamilton et al. (1996) surveyed a number of large concrete structures above ground which showed evidence of severe degradation. They identified many sites with severe degradation that also had high numbers of Thiobacilli; in each case, they identified a source of reducible sulfur. The DOE site characterization has shown that Thiobacilli are present but not a suitable supply of sulfur. However, potentially large amounts of sulfate are available from Portland cement.

Although the action of the Thiobacilli on MID of concrete is potentially limited by lack of oxidizable sulfur, potential corrosive action on steel may be important. *Thiobacillus ferrooxidans* is a unique member of the Thiobacilli that can obtain energy autotrophically from the oxidation of iron without an organic carbon source, using carbon dioxide instead. Again, its action on the canisters is limited at elevated temperatures. Literature on this bacteria reports its growth in pure planktonic cultures. Under these conditions, it is known to be acidophilic requiring low pH. However, biofilm cells are distinct from the physiology of planktonic cultures. Therefore, the CNWRA experiments are determining whether *T. ferrooxidans* can grow and oxidize iron at the pH anticipated in the proposed repository.

4.4 SUMMARY OF TECHNICAL ACCOMPLISHMENTS

THC coupled processes were examined using the MULTIFLO code. The code was used to assess the range of near-field environmental conditions as a function of areal mass loading. Calculations show that significant changes in pH and salinity could occur with moderate thermal loading of the proposed repository. With increasing heat load, higher concentrations of dissolved solutes are expected. At the extreme case of complete dryout, salts are expected to precipitate during the heating regime and dissolve during the cooling phase as the proposed repository rewets. It is expected that for the higher heat loads, when complete dryout occurs, an evaporite deposit will form in the near field with the deposition of salts occurring throughout the dryout zone in the near-field region. The effect of this evaporite deposition on fluid composition during the rewetting stage is being investigated.

One of the main limitations of the present calculation is the use of the ECM. In this model, the fractured porous medium is represented as a single average continuum. Capillary equilibrium is assumed

to be maintained between the fracture and matrix. As a consequence of this assumption, it is not possible for flow to take place in the fracture network without the matrix becoming fully saturated at the same time. This assumption of the model is fundamental to the formation of a capillary barrier sandwiched between zones of enhanced moisture content and the proposed repository horizon preventing liquid water from reaching the waste during the heating regime. Consequently, gravity driven flow such as dripping, which may be an important process for container life and source term, can not be described within the confines of the ECM. Alternate conceptualizations, such as multiple interacting continua, may provide a better description of fracture flow. Verification or validation of the THC coupling may be attempted through an analysis of field samples at YM originating from paleohydrothermal sources. Field samples have been collected and are being analyzed. Alternatively, idealized laboratory experiments may be performed if suitable methods of accelerating the processes can be found and the results compared to model predictions for validating models. However, these have not been attempted in FY96.

The effects of cementitious materials on near-field environment has been estimated using available data mainly at near-ambient temperatures. However, considerable uncertainties exist regarding the stability of the CSH gel phase that may determine the pH of the fluid contacting the cement. If the gel phase recrystallizes at higher temperatures, the pH may not attain as high a value as calculated from room temperature data. It is also important to couple these essentially static calculations with a transport model such as MULTIFLO to estimate the spatial extent of the change in pH due to cement-water interactions.

The investigation of microbiological activity has shown that bacterial colonies native to the host rock at YM are viable even after exposure to 120 °C. However, their activity and the effects on near-field environment through interaction with cementitious materials may be limited by the absence of oxidizable sulfur species.

4.5 ASSESSMENT OF PROGRESS TOWARD MEETING OBJECTIVES

The completion of the ENFE evaluation report (Angell et al., 1996) enabled a prioritization of those aspects of the evolution of the near-field environment that are likely to affect the attributes of the DOE WCIS. Completion of the ENFE evaluation report (Angell et al., 1996) also prepared the ENFE KTI team to review the two near-field DOE synthesis reports (mineralogy/petrology and near-field environment), which are anticipated to be released in FY97, and the DOE TSPA-95 effort (TRW Environmental Safety Systems, Inc., 1995). Development of computer modeling capabilities allowed sensitivity analyses of the near-field environment to be determined and projection of expected THC effects for the DOE heater tests. These sensitivity analyses will be used to address DOE hypotheses related to low corrosion, mobilization of radionuclides, and slow transport. In addition, sensitivity analyses results will be directly incorporated in the NRC detailed TSPA-95 review effort. Both the cement-water interaction study and the laboratory microbial investigations focused on aspects of the near-field environment important to performance (Angell et al., 1996), that support resolution of subissues, and that address DOE hypotheses related to low corrosion and slow transport. Cement-water calculations provide an upper limit on the pH of fluids significantly higher than that used by the DOE in TSPA-95 (TRW Environmental Safety Systems, Inc., 1995) and provides for a basis to resolve the appropriate range of environmental conditions to use in performance calculations. The microbial studies provide a scientific basis for determining the importance of microbial interactions on radionuclide transport and a footing to resolve this aspect of the limited radionuclide transport subissue. In general, studies of these issues

address overall performance because near-field conditions affect the rate of container corrosion, alteration of waste forms and radionuclide release, and transport of radionuclides through the near field.

No new subissues for this KTI were discovered during FY96 as a result of the ENFE team effort. However, two aspects of existing subissues were brought to light as being currently under-emphasized in the ENFE effort. The importance of fractures on the transport of fluids needs to be evaluated for staff to resolve the ENFE subissue of low infiltration into emplacement drifts. In addition, the importance of man-introduced materials, such as cementitious materials, has been demonstrated to be an important control of fluid chemistry. However, the impacts of degradation of the WP including the waste have not been incorporated into determining importance to the evolution of the chemistry of the near-field environment. The ENFE subissue addressing the DOE hypothesis of low seepage into the emplacement drift requires answering the question of what are the changes in fracture permeability due to interactions of fluids with the rock matrix and fractures. Two lines of evidence suggest the importance of resolving this question.

- (i) The MULTIFLO modeling effort and modeling completed by the Thermal Effects on Flow (TEF) KTI indicate the formation of a heat pipe. Geologic evidence of fossil heat pipes has been recently interpreted to indicate downward flow of liquid condensate within vapor-filled fractures.⁹
- (ii) High pH fluids derived from interaction with cementitious material have been suggested to affect the porosity and permeability of the interacting host rock (Steeffel and Lichtner, 1994).

For the case of the proposed repository, both evaporative processes and fluid interaction with cementitious material will drive fluids to a high pH. The net result of the high pH will be to strengthen the importance of water rock interaction and its consequences on hydrologic characteristics of the fractures. To help resolve this subissue, hydrologic models for near-field interactions, other than ECMs, will be required. The ENFE subissue addressing the DOE hypothesis of limited radionuclide transport from the EBS to the host rock requires definition of the bounding environmental factors affecting radionuclide transport from the EBS. At present, the importance of the degradation of the WP and release from the source have not been incorporated into evaluation of bounding conditions. Completion of the EBSPAC module in the Container Life and Source Term (CLST) KTI should allow for some estimates of possible bounding geochemical conditions to be determined.

4.6 INTEGRATION WITH OTHER KEY TECHNICAL ISSUES

Development and beta testing of the MULTIFLO code required input and assistance from the TEF and Total System Performance Assessment and Integration (TSPAI) KTI teams. The assistance provided by other teams include specifying information that the model would need to provide to the other KTIs and providing boundary conditions for beta testing the model.

Output from the ENFE KTI for FY96 are predominately related to development of the MULTIFLO computer code. The MULTIFLO code is the basis for many of the thermal analyses currently being conducted under the TEF KTI. Calculations performed using MULTIFLO are also being

⁹S. Ingebritsen. 1996. Personal Communication.

used as input in the EBSPAC calculation of CLST by the CLST KTI team. Currently, these codes are not directly linked. Additionally, the METRA part of the MULTIFLO code is being used by the Repository Design and Thermal-Mechanical Effects (RDTME) KTI to benchmark temperature calculations performed using an effective conductivity model. The temperature calculations from the effective conductivity model are then being used in the EBSPAC.

Two subissues, low infiltration into emplacement drifts and radionuclide transport, will need additional effort to approach resolution. Currently under the ENFE KTI implementation plan, ENFE does not obtain input from the Structural Deformation and Seismicity (SDS) KTI. To complete an analysis of the importance of fractures on the evolution of the near field will require input from the SDS of a simplified or abstracted model of faults and their geometry. Discussions with the SDS team to refine the informational needs of the ENFE KTI have been initiated. Bounding the chemical composition of near-field pore fluids will require increased interactions with the CLST team. Currently, the degradation products of the engineered barrier and waste form and importance to pore fluid chemistry have not been factored into efforts to bound near-field fluid chemistry. Finally, the linkage and pathway between information generated in the ENFE sensitivity analyses and the actual input needs of the TSPA team should be refined.

In support of the TSPA KTI, sections of TSPA-95 (TRW Environmental Safety Systems, Inc., 1995) related to near-field environment were reviewed with particular attention to an evaluation of the dependence of the results of performance calculations on geochemical characteristics of the near field. In general, this review concluded that important near-field characteristics are fairly well recognized in qualitative descriptions of model development. However, minimal recognition of these characteristics was employed in the performance calculations.

4.7 REFERENCES

- Angell, P., J.A. Apps, G.A. Cragolino, S.-M. Hsiung, P.C. Lichtner, W.M. Murphy, R.T. Pabalan, D.A. Pickett, N. Sridhar, S.A. Stothoff, and D.R. Turner. 1996. *Evolution of the Near-Field Environment in the Proposed High-Level Waste Repository at Yucca Mountain, Nevada*. W.M. Murphy, ed. CNWRA Letter Report. San Antonio, TX: Center for Nuclear Waste Regulatory Analyses.
- Angus, M.J., C.E. McCulloch, R.W. Crawford, F.P. Glasser, and A.A. Rahman. 1983. Kinetics and mechanism of the reaction between Portland cement and clinoptilolite. *Advances in Ceramics* 8. G.G. Wicks and W.A. Ross, eds. Columbus, OH: Nuclear Waste Management: American Ceramic Society: 429-440.
- Atkins, M., and F.P. Glasser. 1992. Application of Portland cement-based materials to radioactive waste immobilization. *Waste Management* 12: 105-131.
- Atkins, M., J. Cowie, F.P. Glasser, T. Jappy, A. Kindness, and C. Pointer. 1990. Assessment of the performance of cement-based composite material for radioactive waste immobilization. *Scientific Basis for Nuclear Waste Management XIII Symposium Proceedings*. M. Oversby and P.W. Brown, eds. Pittsburgh, PA: Materials Research Society: 176: 117-127.

- Atkins, M., F.P. Glasser, and A. Kindness. 1991. Phase relations and solubility modelling in the CaO-SiO₂-Al₂O₃-MgO-SO₃-H₂O system: For application to blended cements. *Scientific Basis for Nuclear Waste Management XIV Symposium Proceedings*. T. Abrajano, Jr. and L.H. Johnson, eds. Pittsburgh, PA: Materials Research Society: 212: 387-394.
- Atkinson, A., N.M. Everitt, and R.M. Guppy. 1989. Time dependence of pH in a cementitious repository. *Scientific Basis for Nuclear Waste Management XII Symposium Proceedings*. W. Lutze and R.C. Ewing, eds. Pittsburgh, PA: Materials Research Society: 127: 439-446.
- Baca, R.G., and R.D. Brient. 1996. *Total System Performance Assessment 1995 Audit Review*. CNWRA Letter Report. San Antonio, TX: Center for Nuclear Waste Regulatory Analyses.
- Berner, U.R. 1987. Modelling porewater chemistry in hydrated Portland cement. *Scientific Basis for Nuclear Waste Management X Symposium Proceedings*. J.K. Bates and W.B. Seefeldt, eds. Pittsburgh, PA: Materials Research Society: 44: 319-330.
- Berner, U.R. 1992. Evolution of pore water chemistry during degradation of cement in a radioactive waste repository environment. *Waste Management* 12: 201-219.
- Bruton, C.J., A. Meike, B.E. Viani, S. Martin, and B.L. Phillips. 1993. Thermodynamic and structural characteristics of cement minerals at elevated temperature. *Proceedings of the Topical Meeting on Site Characterization and Model Validation (Focus '93)*. La Grange Park, IL: American Nuclear Society: 150-156.
- Buscheck, T.A., and J.J. Nitao. 1993. The analysis of repository-heat-driven hydrothermal flow at Yucca Mountain. *Proceedings of the Fourth Annual International Conference on High-Level Radioactive Waste Management*. La Grange Park, IL: American Nuclear Society: 1: 847-867.
- Clifton, J.R., L.I. Knab, E.J. Garboczi, and L.X. Xiong. 1991. *Chloride Ion Diffusion in Low Water-to-Solid Cement Phases*. NUREG/CR-5727. Washington, DC: Nuclear Regulatory Commission.
- Glasser, F.P., M.J. Angus, C.E. McCulloch, D. Macphee, and A.A. Rahman. 1985. The chemical environment in cements. *Scientific Basis for Nuclear Waste Management VIII Symposium Proceedings*. C.M. Jantzen, J.A. Stone, and R.C. Ewing, eds. Pittsburgh, PA: Materials Research Society: 44: 849-858.
- Glassley, W.E. 1986. *Reference Waste Package Environment Report*. UCRL-53726. Livermore, CA: Lawrence Livermore National Laboratory.
- Hamilton, M.A., R.D. Rogers, R. Veeh, and M. Zolynski. 1996. Evaluation of microbially-influenced degradation of massive concrete structures. *Scientific Basis for Nuclear Waste Management XIX Symposium Proceedings*. W.M. Murphey and D.A. Knecht, eds. Pittsburgh, PA: Materials Research Society: 412: 469-474.

- Harrar, J.E., J.F. Carley, W.F. Isherwood, and E. Raber. 1990. *Report of the Committee to Review the Use of J-13 Well Water in Nevada Nuclear Waste Storage Investigations*. UCID-21867. Livermore, CA: Lawrence Livermore National Laboratory.
- Heimann, R.B. 1988. Interaction of cement and radioactive waste forms in multicomponent systems tests at 200 °C, Part 2: Mineralogical changes of cement. *Cement Concrete Research* 18: 554–560.
- Horn, J.M., and A. Meike. 1995. *Microbial Activity at Yucca Mountain*. UCRL-ID-122256. Livermore, CA: Lawrence Livermore National Laboratory.
- Kerrisk, J.F. 1987. *Groundwater Chemistry at Yucca Mountain, Nevada, and Vicinity*. LA-10-29-MS. Los Alamos, NM: Los Alamos National Laboratory.
- Komarneni, S., and D.M. Roy. 1983. Hydrothermal interactions of cement or mortar with zeolites or montmorillonites. *Scientific Basis for Nuclear Waste Management VI Symposium Proceedings*. D.G. Brookins, ed. Pittsburgh, PA: Materials Research Society: 15: 55–62.
- Lee, W., Z. Lewandowski, M. Morrison, W.G. Characklis, R. Avci, and P.H. Nielsen. 1993. Corrosion of mild steel underneath aerobic biofilms containing sulfate-reducing bacteria, Part II: At high dissolved oxygen concentration. *Biofouling* 7: 217–239.
- Lichtner, P.C., and J. Eikenberg. 1995. *Propagation of a Hyperalkaline Plume into the Geological Barrier Surrounding a Radioactive Waste Repository*. PSI 95-01. Wurenlingen, Switzerland: Paul Scherrer Institute.
- Lichtner, P.C., and M.S. Seth. 1996. *User's Manual for MULTIFLO: Part II—MULTIFLO 1.0 and GEM 1.0. Multicomponent–Multiphase Reactive Transport Model*. CNWRA 96-010. San Antonio, TX: Center for Nuclear Waste Regulatory Analyses.
- Milde, K., W. Sand, W. Wolff, and E. Bock. 1993. Thiobacilli of the corroded concrete walls of the Hamberg sewer system. *Journal of General Microbiology* 129: 1,327–1,333.
- Murphy, W.M. 1991. Performance assessment perspectives with reference to the proposed repository at Yucca Mountain, Nevada. *Proceedings from the Technical Workshop on Near-Field Performance Assessment for High-Level Waste*. Madrid, Spain: Swedish Nuclear Fuel and Waste Management Co.: 11–12.
- Nitao, J.J. 1989. *V-TOUGH—An Enhanced Version of the TOUGH Code for the Thermal and Hydrologic Simulation of Large-Scale Problems*. UCID-21954. Livermore, CA: Lawrence Livermore National Laboratory.
- Nitao, J.J. 1996. *Reference Manual for the NUFT Flow and Transport Code, Version 1.0*. UCRL-ID-113J20. Livermore, CA: Lawrence Livermore National Laboratory.
- Pruess, K. 1987. *TOUGH User's Guide*. LBL-20700. Berkeley, CA: Lawrence Berkeley Laboratory.

- Pruess, K., and Y. Tsang. 1993. Modeling of strongly heat-driven flow processes at a potential high-level nuclear waste repository at Yucca Mountain, Nevada. *Proceedings of the Fourth Annual International Conference on High-Level Radioactive Waste Management*. La Grange Park, IL: American Nuclear Society: 1: 568-575.
- Reardon, E.J. 1992. Problems and approaches to the prediction of the chemical composition in cement/water systems. *Waste Management* 12: 221-239.
- Seth, M.S., and P.C. Lichtner. 1996. *User's Manual for MULTIFLO: Part I—METRA 1.0 β , Two-Phase Nonisothermal Flow Simulator*. CNWRA 96-005. San Antonio, TX: Center for Nuclear Waste Regulatory Analyses.
- Steeffel, C., and P.C. Lichtner. 1994. Diffusion and reaction in rock matrix bordering a hyperalkaline fluid-filled fracture. *Geochimica et Cosmochimica Acta* 58: 3,595-3,612.
- TRW Environmental Safety Systems, Inc. 1995. *Total System Performance Assessment—1995: An Evaluation of the Potential Yucca Mountain Repository*. B00000000-01717-2200-00136. Las Vegas, NV: TRW Environmental Safety Systems, Inc.
- TRW Environmental Safety Systems, Inc. 1996a. *Mined Geologic Disposal System Advanced Conceptual Design Report. Volume II of IV, Repository*. B00000000-01717-5705-00027. Rev. 00. Las Vegas, NV: TRW Environmental Safety Systems, Inc.
- TRW Environmental Safety Systems, Inc. 1996b. *Mined Geologic Disposal System Advanced Conceptual Design Report. Volume III of IV, Engineered Barrier Segment/Waste Package*. B00000000-01717-5705-00027. Rev. 00. Las Vegas, NV: TRW Environmental Safety Systems, Inc.
- U.S. Department of Energy. 1988. *Site Characterization Plan, Yucca Mountain Site, Nevada Research and Development Area, NV*. DOE/RW-0199. Washington, DC: Office of Civilian Radioactive Waste Management: U.S. Department of Energy.
- Walton, J.C. 1993. Effects of evaporation and solute concentration on presence and composition of water in and around the waste package at Yucca Mountain. *Waste Management* 13: 293-301.
- White, S.P. 1995. Multiphase nonisothermal transport of systems of reacting chemicals. *Water Resources Research* 31: 1,761-1,772.
- Wilder, D.G. 1993a. *Preliminary Near-Field Environment Report. Vol. I: Technical Bases for EBS Design*. UCRL-LR-107476. Livermore, CA: Lawrence Livermore National Laboratory.
- Wilder, D.G. 1993b. *Preliminary Near-Field Environment Report. Vol. II: Scientific Overview of Near-Field Environment and Phenomena*. UCRL-LR-107476. Livermore, CA: Lawrence Livermore National Laboratory.

Wolery, T.J. 1992. *EQ3/6, A Software Package for Geochemical Modeling of Aqueous Systems: Package Overview and Installation Guide. Version 7.0.* UCRL-MA-110662. Part 1. Livermore, CA: Lawrence Livermore National Laboratory.

Zyvoloski, G., Z. Dash, and S. Kelkar. 1992. *GEHMN 1.0: Finite Element Heat and Mass Transfer Code.* LA-12062-MS. Rev. 1. Los Alamos, NM: Los Alamos National Laboratory.

5 CONTAINER LIFE AND SOURCE TERM

Primary Authors: G.A. Cragnolino, S. Mohanty, T.M. Ahn, H.K. Manaktala, D.S. Dunn, P.J. Angell, W.M. Murphy, and N. Sridhar

Technical Contributors: B.J. Davis, S. Larose, Y.-M. Pan, and R.A. Rapp

Key Technical Issue Co-Leads: N. Sridhar (CNWRA) and K.C. Chang (NRC)

5.1 INTRODUCTION

The U.S. Department of Energy (DOE) updated Waste Containment and Isolation Strategy (WCIS) for the proposed repository at Yucca Mountain (YM)¹ has the primary goals of near-complete containment of radionuclides within waste packages (WPs) for several thousand years and acceptably low annual doses to a member of the public living near the site. Among the system attributes recognized in this strategy to be most important in accomplishing these goals are the WP life time (containment), rate of release of radionuclides from breached WPs, and radionuclide transport through engineered and natural barriers. The objective of the Container Life and Source Term (CLST) Key Technical Issue (KTI) is to evaluate these attributes independently and provide input to the performance assessment (PA) of the overall proposed repository.

Several subissues have been delineated within the CLST KTI that directly address the DOE WCIS. These include (i) evaluation of methodologies for extrapolating short-term laboratory data to long-term performance, (ii) evaluation of factors affecting waste form alteration products and the release of radionuclides, (iii) determining the effect of long-term thermal exposure and mechanical loads on the mechanical stability of the container materials, (iv) assessing the effect of microbiological organisms on the performance of container materials, and (v) performing sensitivity analyses on the effects of thermal loading, near-field environment, and galvanic coupling on container life using the Engineered Barrier System Performance Assessment Code (EBSPAC). The DOE performed a probabilistic analysis of container life in TSPA-95 using the Waste Package Degradation (WAPDEG) code. Similar methodologies may be used in the DOE viability assessment (VA) through TSPA-VA. The sensitivity analyses performed in this KTI will enable the Nuclear Regulatory Commission (NRC) and the Center for Nuclear Waste Regulatory Analyses (CNWRA) staffs to evaluate methodologies used by DOE in TSPA-95 and compare the container life cumulative distribution curves predicted by EBSPAC and WAPDEG. These analyses will also facilitate the evaluation of the significance of these subissues to the overall system performance.

The major component of the Engineered Barrier System (EBS) is the WP, which includes the waste form [spent fuel (SF) and vitrified waste], fuel cladding, filler, canisters [multi-purpose canister (MPC) and pour canister], and disposal overpacks. In addition to the WP, the EBS consists of backfill, concrete inverts, emplacement pedestals, drip shields, and other components used in the proposed repository construction. Some components affect the waste containment indirectly through their effects on near-field environment (e.g., concrete inverts, rock bolts), while other components affect containment

¹U.S. Department of Energy. 1996. *Highlights of the U.S. Department of Energy's Updated Waste Containment and Isolation Strategy for the Yucca Mountain Site*. DOE Concurrence Draft. July 1996. Washington, DC: U.S. Department of Energy.

directly (e.g., overpacks, cladding). Evaluation of the components of EBS that affect containment and radionuclide release directly is considered in this KTI.

Several WP designs have been proposed by the DOE over the history of the proposed YM repository program. Of these designs, the canistered fuel design is considered the primary choice (TRW Environmental Safety Systems, Inc., 1996). In this design, either 21 pressurized water reactor (PWR) or 40 boiling water reactor (BWR) SF assemblies are contained in a type 316L stainless steel MPC (3.5-cm wall thickness) in which a fuel basket, probably made of borated stainless steel, provides criticality control and enhances heat transfer. The MPC is surrounded by an inner overpack made of a corrosion-resistant alloy (2.5-cm wall thickness), in turn contained in an outer overpack made of a corrosion-allowance material (10-cm wall thickness). The proposed outer length of such a WP is 5.682 m and the outer diameter is 1.802 m. The total surface area is about 37 m² and the loaded weight is about 65,000 Kg. Alternate designs include WP for uncanistered fuel (no MPC), small canistered fuel (12 PWR or 24 BWR SF assemblies), and vitrified reprocessed waste. A list of candidate materials for the overpacks is shown in table 5-1 with the materials that are the primary choices in the present design indicated. In addition to providing an independent evaluation of containment for specific materials in the present WP and radionuclide release from the EBS, the CLST KTI addresses the appropriateness of predictive methodologies which are generally applicable to a wide variety of materials.

5.2 OBJECTIVES AND SCOPE OF WORK

This KTI has three objectives:

- (i) Evaluate the scope and quality of the DOE WP program and WP design
- (ii) Conduct sensitivity analyses on performance of the EBS in relation to uncertainties in conceptual models and data
- (iii) Provide input to the PA of the overall repository

To accomplish the first objective, the DOE planning documents on the WP program and Total System Performance Assessment (TSPA)-95 (TRW Environmental Safety Systems, Inc., 1995) calculations were reviewed. The second objective is being accomplished through detailed evaluations of specific failure processes and incorporation of abstracted models in the EBSPAC. The third objective will be accomplished through the incorporation of EBSPAC as a source term module into the NRC/CNWRA Total Performance Assessment (TPA) code.

This section of the annual report describes some of the sensitivity analyses of WP performance through the use of EBSPAC, a detailed evaluation of dry oxidation and thermal embrittlement of the outer steel overpack, the applicability of the repassivation potential concept for long-term prediction of inner overpack performance, and some of the factors affecting radionuclide release from SF. Some of these detailed analyses have already been abstracted in EBSPAC. The integration between this KTI and some of the other KTIs is briefly described.

Table 5-1. Candidate materials in the advanced conceptual design (TRW Environmental Safety Systems, Inc., 1996)

Component	Materials	
	Primary	Alternate
Inner Overpack	Alloy 825 (UNS N08825)	<u>Ni-Base Alloys</u> Alloy C-22 (UNS N06022) Alloy G-30 (UNS N06030) Alloy C-4 (UNS N06455) Alloy G-3 (UNS N06985) Alloy N08221 (Not in commercial production) <u>Ti-Base Alloys</u> Grade 12 (UNS R53400) Grade 16 (UNS R52402)
Outer Overpack	ASTM A516, Grade 55 Carbon Steel (UNS K01800)	<u>Fe-Base Alloys</u> ASTM A27 Grade 70-40 (UNS J02501) cast steel ASTM A387 Grade 22 (UNS K21590) alloy steel <u>Cu-Base Alloys</u> 90-10 CuNi (UNS C70600) 70-30 CuNi (UNS C71500) <u>Ni-Base Alloy</u> Alloy 400 (UNS N04400)
Outer Overpack, HLW Glass	70-30 CuNi (UNS C71500)	

5.3 SIGNIFICANT TECHNICAL ACCOMPLISHMENTS

5.3.1 Sensitivity Analyses Using the Engineered Barrier System Performance Assessment Code

The overall strategy for EBSPAC development consists of concurrent development of detailed analyses or models of physical and physicochemical processes affecting WP performance and abstraction of these models for incorporation into EBSPAC. Models and computational approaches used previously in SOTEC (Sagar et al., 1992) and SCCEX (Cragolino et al., 1994) codes have been incorporated with appropriate modifications in the current version of EBSPAC (Mohanty et al., 1996).

Sensitivity analyses provide an adequate methodology to evaluate the relative importance of certain processes and the associated variables or parameters on the performance of WPs. Although detailed conceptual and numerical models exist for many corrosion and mechanical failure processes, material specific parameters for these models, that should be adapted to the conditions prevailing in a repository under partially saturated conditions, are scarce. These parameters are obtained through reviews

of published literature and information reported by the DOE, combined with data obtained in the experimental investigations program conducted within this KTI. In some cases, lack of reliable data for a given parameter justifies the use of sensitivity analyses as a tool to evaluate the need for acquiring new data.

In EBSPAC, Version 1.0 β (Mohanty et al., 1996), only the largest canistered fuel WP design for 21 PWR or 40 BWR SF assemblies in a horizontal drift emplacement, as currently envisioned by the DOE (TRW Environmental Safety Systems, Inc., 1996), was considered. As a set of external calculations to EBSPAC, the thermal model provides the temperature distribution as a function of time and position within the EBS as well as in the surrounding geosphere. The temperature and relative humidity (RH) at the WP surface as functions of time are used to predict the conditions that affect the occurrence and rate of corrosion of the WP and the subsequent release of radionuclides. The chemical composition, pH, and oxygen concentration of the fluid able to come in contact with the WP is determined by the environment model, where the evaporative effects produced by heat released by radioactive decay are considered.

Below a critical value of RH, air oxidation of steel is modeled as the dominant process for the steel overpack. Mechanical failure as a result of thermal embrittlement of the steel promoted by long-term exposure to temperatures above 150 °C is evaluated at each time step. If the RH is higher than the critical value, the occurrence of aqueous corrosion of the steel overpack is evaluated. No distinction is made in EBSPAC between humid air corrosion and aqueous corrosion because both processes are governed by the same fundamental principles. The corrosion models calculate the rates of uniform and localized corrosion. The corrosion process at any given time depends on the corrosion potential and the critical potential required to initiate a particular localized corrosion process. Following penetration of the outer container, electrical contact of the inner and outer container through the presence of an electrolyte path such as that provided by modified groundwater promotes galvanic coupling assuming that metallic contact always exists between both containers. The galvanic coupling model evaluates whether penetration of the inner container by localized corrosion is possible; otherwise, uniform corrosion or mechanical fracture becomes the predominant failure mechanism because the inner container becomes protected against localized corrosion.

Once penetration of the inner container occurs, the RH criterion is applied to determine whether air oxidation or aqueous dissolution of SF is the subsequent process to be evaluated. Air oxidation of SF leads to gaseous release of C-14 predominantly from the fuel cladding, whereas I-129, Cl-36, and C-14 are released as gases from the fuel pellets and the pellet/cladding gap. In Version 1.0 β of EBSPAC, aqueous release of radionuclides from SF only includes congruent releases with solubility constraints of the radionuclides contained in the irradiated UO₂ matrix. Only the bathtub model is used in Version 1.0 β of EBSPAC, although dripping of modified groundwater on the SF will be implemented in future versions. Aqueous releases are treated only as dissolution rate limited release or solubility limited release.

EBSPAC performs deterministic calculations for a single cell, not for the overall repository, through two separate, distinctive parts. One part deals with WP failure calculations and the other, essentially a separate code, with release calculations; no feedback exists from the release part into the failure part. The release code includes the incorporation of radionuclide decay, generation of daughter products in the chains, temporal variation of inventory in the WP, and spatial variations in the properties of the surrounding material. However, the degree of complexities incorporated varies from model to model to accomplish necessary simplifications while ensuring conservatism in calculations of radionuclide release.

As an example of the capabilities of the EBS-PAC, a set of calculations was performed to demonstrate the effect of galvanic coupling on the failure time of the WP. In Version 1.0 β of EBS-PAC a simplified approach is used to account for galvanic coupling effects between the inner and the outer overpacks. The corrosion potential of the galvanic couple formed when the wall of the outer container is penetrated by a pit, $E_{\text{corr}}^{\text{WP}}$, is estimated by using experimentally measured values of the potential of the bimetallic couple, E_{couple} , for a well-defined area ratio between both components. Then $E_{\text{corr}}^{\text{WP}}$ is determined through a linear combination of E_{corr} of the outer overpack, as calculated by the code at the time of its through-wall penetration, and E_{couple} , according to the following expression

$$E_{\text{corr}}^{\text{WP}} = (1 - \eta)E_{\text{corr}} + \eta E_{\text{couple}} \quad (5-1)$$

where η is the efficiency of the galvanic coupling with the condition $0 \leq \eta \leq 1$. A value of E_{couple} equal to $-0.46 \text{ V}_{\text{SHE}}$ was adopted on the basis of results reported by Scully and Hack (1984) for a galvanic couple made of steel and alloy 625 (a nickel-base alloy similar in electrochemical behavior to alloy 825) with an area ratio 1:1 and exposed to sea water. The values adopted for the different parameters needed to calculate E_{corr} and those establishing the dependence of the critical potentials with chloride concentration and temperature are reported elsewhere (Mohanty et al., 1996). A chloride concentration of 0.3 mol/L has been used in this set of calculations, instead of 3×10^{-3} mol/L as provided by MULTIFLO calculations (Mohanty et al., 1996), to attain failure within the 10,000-yr simulation period for $\eta = 0$.

Figure 5-1 shows the WP failure time as a function of the galvanic coupling efficiency for two values of the areal mass loading (AML), currently a repository design variable. The calculations correspond to the thermal model cases (Mohanty et al., 1996) in which neither ventilation is assumed during the initial 100 yr operations period nor backfill after permanent closure. It is seen that at 80 MTU/acre, which is close to the value adopted by the DOE in TSPA-95 for the high thermal loading case, η has an important effect on the WP failure time, which increases abruptly from 2,736 yr to more than 10,000 yr (the simulation time) for η values close to 0.2. A similar effect is observed at 40 MTU/acre where failure time increases from 472 yr to more than 10,000 yr for η values just above 0.08. On the contrary, no effect of η is found at 20 MTU/acre, a case where failure time is greater than 10,000 yr regardless of the value of η . If galvanic coupling is completely ineffective ($\eta = 0$), the shortest failure time occurs at the intermediate AML (40 MTU/acre). The wetting time is also the shortest at the intermediate AML, but the differences in failure times are only explainable by the effect of temperature on the initiation of localized corrosion. The wetting times, corresponding to a critical value of RH equal to 65 percent, are 153, 50, and 2,336 yr for 20, 40, and 80 MTU/acre, respectively.

Although penetration by localized corrosion of the outer container occurs in a few hundred years, as illustrated in figure 5-2, for 20 MTU/acre, only slow passive dissolution of the inner alloy 825 container takes place subsequently because E_{corr} is lower than the critical potential for localized corrosion at the relatively low temperatures encountered at this low AML. In this case, the inner container is undermined just after 10,000 yr. In summary, the critical potential above which localized corrosion occurs increases with a decrease in temperature so the likelihood of localized corrosion for a given chemical environment decreases with a decrease in AML. At high AML, WP remains dry for a long period, and the container life is long. These two competing factors lead to a minimum container life at

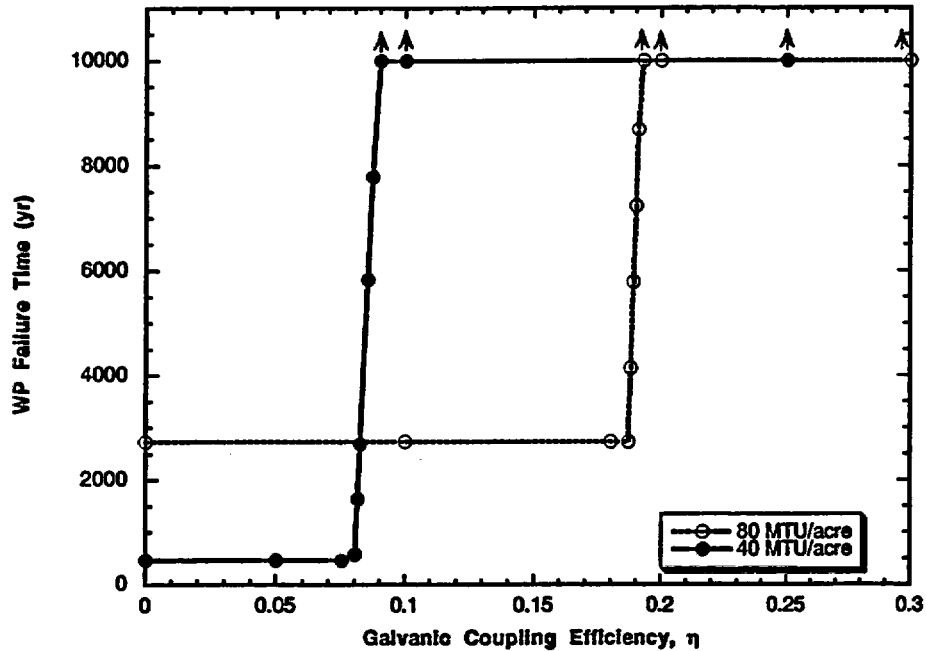


Figure 5-1. Effect of galvanic coupling on the waste package failure time for two values of areal mass loading in the absence of ventilation and backfilling. Arrows indicate no failure within the simulation time (10,000 yr).

an intermediate AML. If efficient galvanic coupling occurs, container life can be greater than 10,000 yr, independent of the AML value. Additional sensitivity analyses currently being accomplished with Version 1.0 β of EBSPAC include the effect on the failure time of varying several parameters of interest such as chloride concentration and critical RH, among others.

5.3.2 Thermal Embrittlement of Carbon Steel

Depending upon the thermal loading strategy, WP materials can be exposed to temperatures well above 100 °C for thousands of years. In addition, backfilling can induce a sharp increase in temperature of the WP surface above 100 °C, followed by a gradual decrease with time.² In the DOE TSPA-95 (TRW Environmental Safety Systems, Inc., 1995), no consideration was given to the effect of prolonged exposures at these temperatures on material stability and specific mechanical properties. Thermal embrittlement is related to the well-known phenomenon of temper embrittlement that affects tempered low-alloy steels as a result of isothermal heating or slow cooling within the temperature range of 325 to 575 °C. Temper embrittlement is a major concern to the integrity of engineering components that operate within that critical temperature range and also to heavy section components that are slowly cooled through the critical temperature range after heat treatment or welding operations. Examples of such components

²Manteufel, R.D. 1996. Effects of ventilation and backfill on an underground nuclear waste repository. *International Journal of Heat and Mass Transfer*. Accepted for publication.

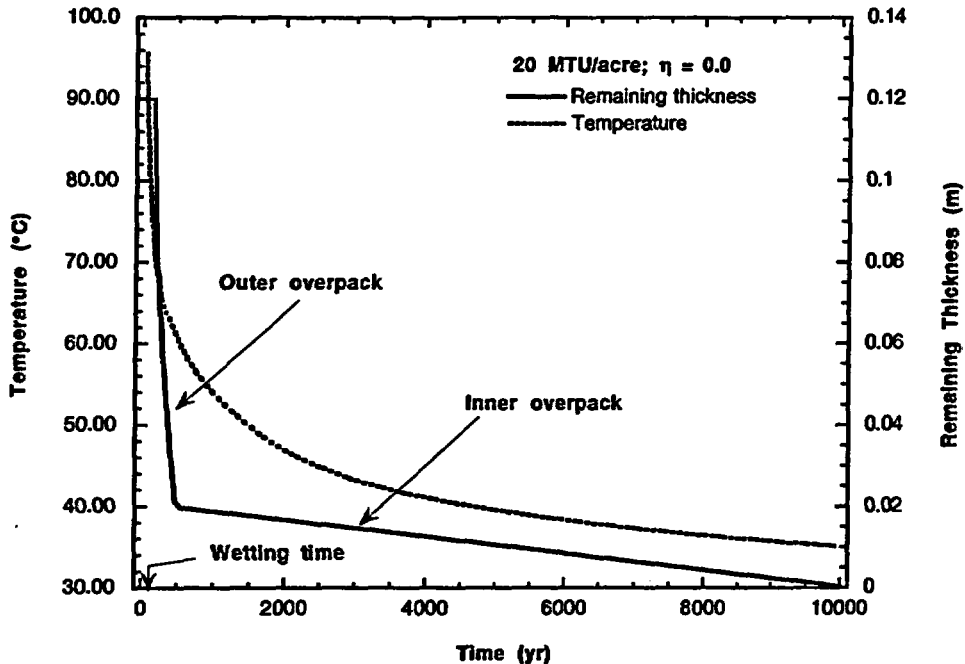


Figure 5-2. Temperature of the waste package and remaining wall thickness as a function of time for the lowest areal mass loading in the absence of galvanic coupling

are pressure vessels and turbine rotors. This phenomenon leads to a shift in the ductile-brittle transition temperature (DBTT), as shown schematically in figure 5-3, where the variation of the impact fracture energy for notched specimens is represented as a function of test temperature. However, the potential for embrittlement of carbon and low-alloy steels at temperatures lower than 300 °C as a result of extended exposures (hundreds to thousands of years) expected under repository conditions has never been experimentally investigated (Cragnolino et al., 1996). Lack of information is undoubtedly related to the extended times that could be required to induce the occurrence of this phenomenon, if it occurs, at these relatively low temperatures.

Temper embrittlement occurs when impurities originally present in the steel, such as Sb, Sn, P, Si, and As, segregate along prior austenite grain boundaries during exposure to temperatures ranging from 300–600 °C. Of these elements, P is the most common embrittling element found in commercial low-alloy steels. According to Briant and Banerji (1983), this detrimental role of P is a consequence of the following facts: (i) it segregates during austenitization and tempering, as well as during aging; (ii) it segregates rapidly even at low temperatures; and (iii) its concentration in commercial steels is usually greater than that of other embrittling elements. In importance, P is followed by Sn and Si, since Sb and As are not generally present in sufficiently large quantities in commercial steels. The segregation of P promotes fracture of notched specimens upon impact and leads to a change in the low-temperature fracture mode from transgranular cleavage to intergranular fracture.

By reviewing the available literature on temper embrittlement of low-alloy steels (Cragnolino et al., 1996), useful thermodynamics and kinetics expressions based on the segregation model originally developed by McLean (1957) were found for predicting long-term behavior at lower temperatures. These expressions have been successfully applied to the diffusion and segregation of P following long-term aging

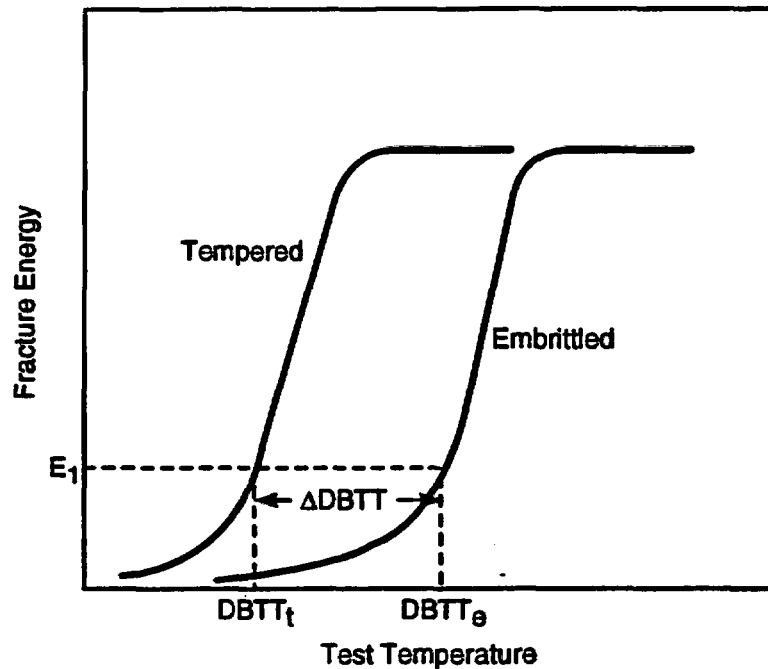


Figure 5-3. Schematic diagram of the effect of embrittlement on the ductile-brittle transition temperature as a function of test temperature

(20,000 hr) at temperatures above 300 °C in steels such as A508 and A533B which are used as pressure vessel materials in nuclear power plants (Druce et al., 1986; Hudson et al., 1988). The grain boundary P segregation and the embrittlement data for alloy A533B are clearly correlated via a linear relationship shown in figure 5-4 (Druce et al., 1986). On the basis of Druce's work, it is estimated that P concentrations above 0.06 weight percent may lead to noticeable embrittlement.

Although McLean's model can be used for predicting the segregation kinetics of P as applied by Druce et al. (1986) to pressure vessel steels, the prediction is primarily dependent on the validity of certain critical modeling parameters, such as the diffusion coefficient for P in steels. The diffusion coefficient of P was evaluated through a compilation of high temperature diffusion data for iron and various steels from the literature, from which the following Arrhenius expression was derived

$$D(\text{cm}^2/\text{s}) = 0.017 \exp \left[\frac{-179.22(\text{kJ}/\text{mol})}{RT} \right] \quad (5-2)$$

Thus, kinetics of phosphorous segregation to grain boundaries at temperatures prevailing at the WP overpack can be predicted. A sensitivity analysis was performed by varying the diffusion coefficient, as depicted in figure 5-5. A significant P enrichment can be attained at lower temperatures (200 °C) but longer times.

It was also found that an important metallurgical factor controlling the degree of embrittlement is grain size (Wada and Hagel, 1976; Lonsdale and Flewitt, 1978; Ucisik et al., 1978). The degree of embrittlement has been evaluated in various studies by comparing base materials and welds, as well as the associated heat affected zones (HAZs) using weldments or simulated microstructures. It appears that

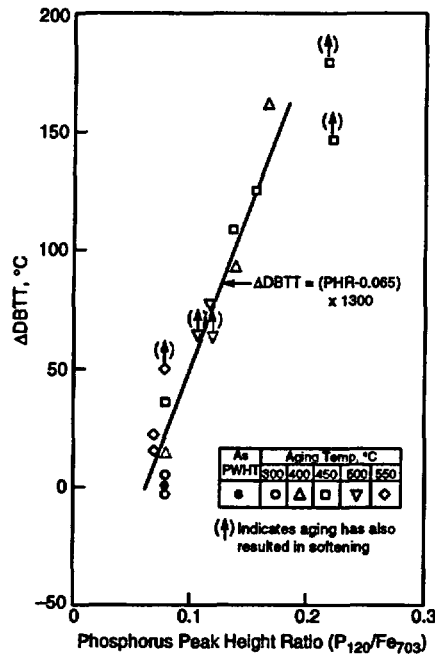


Figure 5-4. Embrittlement as a function of phosphorus segregation in A 533B-Class 1 simulated coarse-grained heat affected zone (Druce et al., 1986)

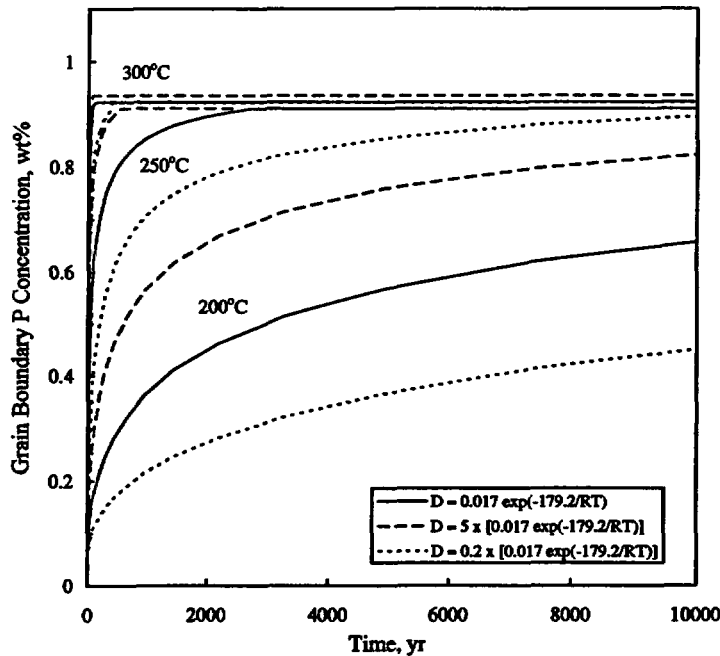


Figure 5-5. Grain boundary concentration of phosphorus at various temperatures calculated on the basis of the values of the diffusion coefficient given by Eq. (5-2) and upper and lower bounds obtained at each temperature by multiplying such values by 5 and 0.2, respectively

welds are less susceptible than the base metal, but coarse grain microstructures developed in the HAZ could be significantly more embrittled than the base metal (Tavassoli et al., 1984). Empirical equations relating embrittlement with chemical composition of steels have been developed, in which the effect of alloying elements and detrimental impurities is included (i.e., Watanabe et al., 1974; Bruscato, 1970; Newhouse, 1972; Viswanathan and Bruemmer, 1985). It should be noted that significant variability has been reported for components made from the same nominal grade of pressure vessel steel. Correlations used to estimate fracture toughness, K_{IC} , by using values of impact energy obtained with Charpy V-notched specimens (i.e., Iwadata et al., 1985; Rolfe and Novak, 1970) have also been compiled (Cragolino et al., 1996).

The concern about susceptibility to thermal embrittlement of some candidate materials for the WP outer disposal overpack can be reduced through appropriate selection of the chemical composition of steel or processing techniques. There are two potentially promising processing methods: (i) reducing the amount of P in the steel through a two-step process combining the basic oxygen furnace (BOF) and the ladle refining furnace (LRF) process (Kusuhara et al., 1980), and (ii) adding small but controlled amounts of Al and B accompanied by reductions in Si content (Nakanishi et al., 1984).

Based on review of the literature, it is concluded that low-alloy steels, such as A387 Grade 22, and eventually C-Mn steels, such as A516 Grade 55, may be susceptible to a substantial degradation in toughness as a consequence of long-term thermal aging at repository temperatures anticipated for the high heat-loading concept (i.e., >200 °C). The investigation also revealed that low-alloy steels are more susceptible to thermal embrittlement than plain carbon steels. Therefore, it is preferable to use plain carbon steels if thermal embrittlement is the only consideration. However, it is preferable to use low-alloy steels to resist humid-air and aqueous corrosion, which may become more significant under low thermal loading strategy. Hence, selection of outer overpack must involve a balance between these considerations and the thermal loading strategy.

5.3.3 Dry Oxidation of Carbon Steel Overpack

Under dry conditions of an RH of less than 65 percent, one degradation mode of the outer steel container is dry oxidation caused by the interaction with gaseous oxygen in air. The proposed YM repository site is considered buffered with air. Currently, the DOE postulates that dry oxidation of the outer container would be negligible for the Mined Geological Disposal System planned at the YM repository site leading to penetrations of 0.40, 0.86, and 1.84 μm , after 100, 1,000, and 10,000 yr at 200 °C (Stahl, 1993). In FY96, a preliminary report was prepared to evaluate this dry oxidation (Ahn, 1996). A detailed review of the state of knowledge regarding dry oxidation of carbon and low-alloy steel was performed independently by Professor R.A. Rapp, Ohio State University (Larose and Rapp, 1996) under a CNWRA contract. This section summarizes the conclusions from these reports.

A preliminary analysis of localized oxidation was conducted at the NRC, focusing predominantly on iron-base alloys with significant alloy content (Ahn, 1996). At temperatures above 600 °C, iron-base alloys often show localized dry oxidation (Shida and Moroishi, 1992; Otsuka and Fujikawa, 1991; Newcomb and Stobbs, 1991; Tasovac et al., 1989; Mayer and Smeltzer, 1973). This localized oxidation is normally much deeper than uniform oxidation. The extrapolated values suggest thin (at most 100 μm at 200 °C) penetration by localized dry oxidation. However, simple extrapolations may underestimate the real penetration. Dry oxidation can be more localized than that observed above 600 °C for noncandidate alloys. Lower concentration of alloying elements and lower performance temperature can be the main

cause for this further localization in candidate alloys. Additionally, if all metal ions, mobile at high temperatures, are essentially frozen under repository conditions, oxygen will be the main mobile species. Consequently, oxidation can be deeper as promoted by oxygen diffusion compared with the oxidation by metal diffusion. On the other hand, if iron oxides formed at lower temperatures are protective to a certain extent, there would be less localized oxidation. Extreme diffusion calculations show that oxygen can penetrate through the 10-cm container wall in less than 10,000 yr at both 150 and 200 °C. The consequences of this penetration may include (i) container breach, and (ii) easy mechanical failure of container by localized oxidation or by (atomic or gaseous) oxygen embrittlement. The reasonableness of the extreme diffusion calculations need to be assessed through further literature evaluation or focused experiments.

Larose and Rapp (1996) undertook a more detailed examination of the potential for dry oxidation at repository temperatures, with a specific focus on candidate overpack steels (C-Mn and low-alloy steels). As a baseline, the thermodynamics and kinetics of pure iron oxidation were considered. Thermodynamics of the Fe-O system from room temperature to 1,600 °C was used to understand the oxide phases important within the small temperature range of interest to the repository. The literature on oxidation of iron or steel at temperatures beyond 567 °C is not considered relevant because the stable oxide phase at low oxygen fugacities beyond this temperature is wüstite, corresponding to Fe_{1-y}O , which is slightly deficient in Fe (Muan and Osborne, 1965). At lower temperatures, the oxide scale on iron has two phases, an inner magnetite (Fe_3O_4) and an outer hematite (Fe_2O_3) phase. The kinetics of oxide growth at temperatures below 567 °C are dictated by cation diffusion outwards not by oxygen transport inwards. Grain boundaries in the oxide scale are known to influence the diffusivities in oxides, but the values are not known at the temperatures of interest. Oxidation of pure iron between 400 and 550 °C is especially affected by delamination of the scale due to condensation of cation vacancies at the metal-oxide interface. The oxidation rate of steel at low temperatures increases with the carbon content in steel. At 250 °C, carbon steels containing 0.2 weight percent carbon are expected to lose about 4 μm in thickness, while steels containing 2.25 weight percent chromium and 1 weight percent molybdenum (another candidate container material) are expected to undergo a thickness loss of about 3 μm in 1,000 yr at the same temperature. They concluded that because low-temperature oxidation in carbon and low-alloy steels following a parabolic rate law is controlled by outward diffusion of iron rather than inward diffusion of oxygen, intergranular penetration of oxide would not be significant. The discrepancies between these two analyses of dry oxidation need to be resolved through further investigation.

5.3.4 Long-Term Corrosion Prediction

As reported in chapter 4, modeling of the evolution of the near-field environment has shown that the saturation increases above and below the repository horizon and the chemistry of this saturated zone water is alkaline. Such conditions can promote the passivation of carbon steel (Pourbaix, 1974). In addition, the presence of small amounts of chloride in the groundwater is well known for promoting localized attack (pitting or crevice corrosion) on carbon steel, typically considered a corrosion-allowance-type material (Szkłarska-Smiałowska, 1986; Marsh et al., 1985). Finally, the presence of microbiological organisms can alter the local environment adjacent to the WP and accelerate the corrosion rate.

Activities in the CLST KTI focused on developing a methodology to predict localized corrosion initiation and propagation. Localized corrosion is assumed to occur when E_{corr} of the overpack is greater than the repassivation potential E_{rp} . In the last year, efforts at the CNWRA emphasized measuring the E_{rp} of ASTM A516 grade 60 carbon steel, which is similar to the candidate outer overpack material, and

alloy 825, a candidate inner overpack material, in a wide range of test solutions. The data generated from these tests are used in EBSPAC to predict container life time. Long-term testing of alloy 825 is conducted to determine if E_{tp} is a conservative parameter for predicting localized corrosion.

5.3.4.1 Effect of Solution Composition on Repassivation Potential for A516 Grade 60 and Alloy 825

Measurement of the E_{tp} for A516 grade 60 was performed using cyclic potentiodynamic polarization (CPP) tests in solutions containing 3×10^{-4} to 5 M chloride and a total carbonate concentration of 0.012 M as sodium carbonate (Na_2CO_3) and sodium bicarbonate (NaHCO_3). The carbonate/bicarbonate ratio was adjusted for each test solution to obtain a solution pH of 9.0. These solutions were deaerated with 99.999 percent N_2 . Tests were conducted at both 65 and 95 °C. The test procedure used was similar to that given by ASTM G-61 (American Society for Testing and Materials, 1995) and details provided in a previous report (Sridhar et al., 1995).

The CPP scans exhibited significant hysteresis characteristic of pitting or localized attack. Observation of the specimens using a $70\times$ stereoscope revealed that all specimens exhibited some shallow pitting along with uniform corrosion. The E_{tp} for ASTM A516 Grade 60 was found to be

$$E_{tp} = -620.3 + 0.47T + (-95.2 + 0.88T) \log [Cl^-] \quad (5-3)$$

where T is the temperature in °C and the chloride concentration is expressed in molar units.

Previously, acquired CPP test data for alloy 825 specimens along with crevice repassivation potential data reported by Tsujikawa and Okayama (1990) were similarly analyzed. However, for this material, pitting corrosion was not observed at chloride concentrations lower than 3×10^{-3} M. In addition, E_p was not found to be a function of temperature. The regression equation for E_{tp} at temperatures above 50 °C is

$$E_{tp} = 422.8 - 4.1T + (-64 - 0.8T) \log [Cl^-] \quad (5-4)$$

The previous expressions were incorporated in EBSPAC, Version 1.0 β (Mohanty et al., 1996) as the electrochemical basis for evaluating WP failure time in conjunction with calculations of E_{corr} .

5.3.4.2 Long-Term Testing of Alloy 825

Potentiostatic tests with alloy 825 specimens were conducted over 2 yr to gain further confidence in the use of E_{tp} for long-term prediction of container life. The test apparatus and procedures have been previously described (Sridhar et al., 1995; Dunn et al., 1996). Tests were conducted in 1,000 ppm (0.028 M) chloride solutions at 95 °C. The electrochemical parameters, such as potential, current density, E_{corr} , etc., were continuously monitored and the specimens were periodically inspected for signs of localized corrosion.

Results of the long-term tests are shown in figure 5-6 where specimens that exhibited localized corrosion are indicated by solid symbols. It is apparent from this figure that the initiation of crevice

corrosion occurs much more readily than that of pitting corrosion. Also, the time necessary to initiate localized corrosion decreases as the potential of the specimen increases. No localized attack was observed in potentiostatic tests conducted at potentials lower than E_{pp} , as depicted by the open symbols in figure 5-6.

To further verify that the initiation of localized corrosion requires as a condition that E_{corr} becomes greater than E_{pp} , a test under naturally exposed conditions (open-circuit potential) is being conducted in an aerated 1,000 ppm Cl^- solution. The results of this test, shown in figure 5-7, indicate that E_{corr} is highly variable but in general tends to become more noble with time. On two occasions, as indicated in the figure, E_{corr} was found to be greater than E_{pp} for brief periods. At the conclusion of these test intervals, localized corrosion in the form of crevice corrosion on the mill-finished surface was observed. However, since E_{corr} did not remain above E_{pp} for an extended period, the depth of the localized attack was shallow.

5.3.5 Effects of Microbial Growth on High-Level Nuclear Waste Containers

Microbially influenced corrosion (MIC) is currently acknowledged as a phenomenon that may affect the performance of high-level waste (HLW) containers. It was shown in chapter 4 that microbial populations can survive exposures to temperatures on the order of 120 °C for short periods. However, they become active only when the temperature decreases, upon reintroduction of water and nutrients. Although there is no consensus on the detailed mechanisms involved, MIC is recognized as a modification of abiotic localized corrosion (Thierry and Sand, 1995). It was shown in section 5.3.4 that localized corrosion in abiotic media occurs when E_{corr} exceeds E_{pp} . Microbiological organisms can adversely affect the susceptibility to localized corrosion of a material by either increasing E_{corr} (called ennoblement) or decreasing the E_{pp} . In the present program, two materials were used to examine these two processes: (i) type 316L stainless steel representing a typical corrosion-resistant alloy, and (ii) A 516 carbon steel representing a corrosion-allowance material. Classically, bacteria involved in MIC have been divided into three broad phenotypic groups: (i) acid producers (APB), (ii) sulfate reducers (SRB), and (iii) iron oxidizers (IOB) (Little et al., 1991). The DOE research has concentrated on and identified bacteria representative of each of these phenotypic groups as part of the natural flora at the proposed HLW repository site at YM (Pitonzo et al., 1996).

Microbial biofilms are known to grow in environments where growth nutrients are present only at growth limiting levels (Costerton et al., 1995). Bacteria are able to grow due to the efficiency with which biofilms are capable of scavenging available nutrients. Many of the accepted mechanisms of MIC involve the oxidation or reduction of nutrients releasing corrosive metabolic products, such as reduced sulfur species and acids, as well as products of the oxidation or reduction of various other species, including metal cations that can potentially alter E_{pp} or E_{corr} . These metabolic products can then be concentrated in the surface area covered by the bacteria leading to localized concentration cells. It is therefore necessary to determine what reactions are important to the container life and which are possible at the repository site under anticipated near-field environmental conditions.

The MIC research at the CNWRA has used the model bacterium *Shewanella putrefaciens*, a thiosulfate reducing bacteria (TRB), that was originally isolated from a corroded oil supply line. *S. putrefaciens* is capable of using a number of terminal electron acceptors (TEA) including oxygen, iron

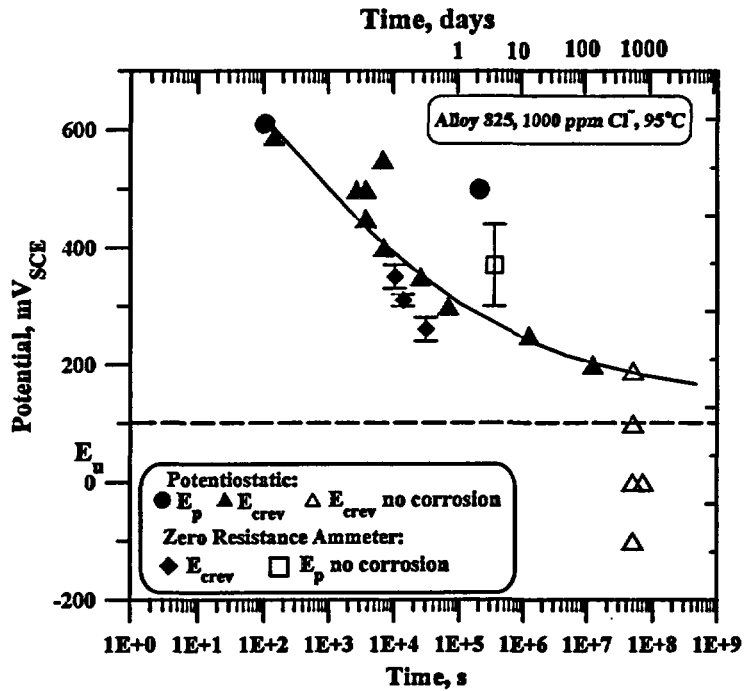


Figure 5-6. Effect of potential on initiation and repassivation of localized (pitting and crevice) corrosion of alloy 825 in 1,000 ppm Cl⁻ solution at 95 °C using potentiostatic and zero resistance ammeter measurements

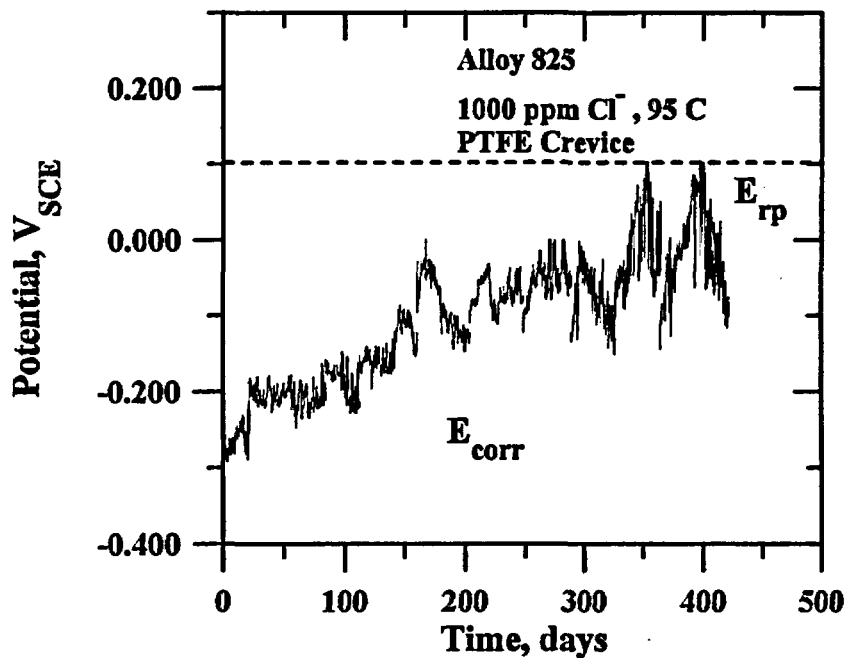


Figure 5-7. Corrosion potential of alloy 825 (creviced specimen) as a function of time in an air saturated 1,000 ppm Cl⁻ solution at 95 °C

(III), nitrate, manganese dioxide, and thiosulfate. Various MIC processes are linked to the microbial reduction of many of these compounds. By modifying the metabolic pathways of this bacterium and, hence, the metabolic products, their effects on E_{corr} and E_{tp} can be examined independently. Multiple electrode probes were exposed to *S. putrefaciens* grown in batch reactors where the medium composition was altered to promote the use of various TEAs. The experimental procedures have been reported elsewhere (Angell et al., 1996).

S. putrefaciens produced no ennoblement under the conditions so far examined on 316L stainless steel. *S. putrefaciens* grown under aerobic conditions, with oxygen as the TEA, caused a small increase in E_{corr} with no evidence of localized corrosion. The addition of either nitrate or thiosulfate (2 mM) to the medium caused essentially no change to E_{corr} under aerobic conditions because oxygen is the preferential TEA. When oxygen is removed and the bacteria is cultured in anaerobic conditions *S. putrefaciens* will continue to grow by reducing whatever other TEA has been selected. Nitrate used as the anaerobic control again showed there was little variation on E_{corr} and no evidence of localized corrosion, with the metal exhibiting only passive behavior.

The reduction of thiosulfate resulting in the production of sulfide had little effect on E_{corr} that remained well below E_{tp} as measured by cyclic polarization in abiotic conditions in the same medium with thiosulfate, but no metabolic sulfide. However, visual inspection revealed pitting on a number of specimens. EIS confirmed these results with the appearance of two time constants on the Bode and Nyquist plots. It is suggested that this is due to localized breakdown of the passive film on the 316L specimen. This may appear to contradict the findings in abiotic environments that E_{corr} had to exceed E_{tp} to initiate localized corrosion. However, it is possible that E_{tp} in the biotic solution was lower than that in the abiotic solution. While relatively low levels of thiosulfate (2 mM), added to simulate the metabolic product of this bacterium, had little effect on E_{tp} in abiotic solutions, there was evidence of localized attack in biotic solutions. It is postulated that bacteria are able to concentrate their metabolic products at specific sites leading to localized areas where the chemistry could be significantly different from the bulk solution leading to localized changes in E_{tp} . This hypothesis is currently being evaluated experimentally. This finding, if verified, is of significance for the prediction of the effects of MIC on container life. Whereas groundwater in the vicinity of the proposed repository site at YM has 25 ppm sulfate, microbial action could lead to a micro-environment with a possible sulfide concentration in the range of the reported values of 10^{-2} M necessary to induce pitting (Newman et al., 1982). It should also be noted that the ratio of sulfide to chloride is an important factor in localized pitting.

5.3.6 Factors Affecting Radionuclide Release from Spent Fuel

Studies of the behavior of SF in the proposed repository at YM have advanced on several fronts. An analysis of literature on dry oxidation and fracturing of SF (Ahn, 1995a) concluded that volume changes due to oxidation causes fracturing. Dry oxidation and fracturing enhance the potential for radionuclide releases because of increases in surface area, solid state diffusion of relatively volatile radionuclides, and subsequent dissolution or colloid formation under aqueous conditions. The rate of dry oxidation may depend on diffusion of oxygen in the SF matrix or reaction kinetics. Diffusion limited oxidation is slow on a 10,000-yr time scale, and oxidation reaction kinetics decrease strongly with decreasing temperature so that higher oxides (i.e., greater than UO_2) may not form below 150 °C under dry conditions.

Dissolution of SF releases highly soluble and gaseous species and may generate colloids of low solubility radioelements (Ahn, 1995b). Secondary solid phases form in SF dissolution tests, but they may not be protective with regard to oxidative dissolution of SF. Colloids form during oxidative dissolution of SF and can form by nucleation in supersaturated solutions, dispersion (physical breakup), or sorption of radioelements on existing colloids. Many uncertainties persist regarding the stability and mobility of colloids, resulting in uncertainties on the significance of colloids to the source term.

Natural analog, experimental, and thermodynamic studies indicate that the properties of secondary uranyl minerals will control the source term for uranium and minor, low solubility radioelements incorporated in these phases in the proposed repository at YM. Uranophane, a common hydrated calcium uranyl silicate, is a preponderant uranyl mineral at the Nopal I natural analog site (and elsewhere) (Pearcy et al., 1994). Similarities between this site and YM and the common enrichment in Ca of secondary minerals at YM suggest that uranophane will significantly affect the performance of the repository. Nevertheless, uncertainties in the properties of uranophane preclude accurate predictions of its role. Experimental studies were initiated to determine fundamental thermodynamic properties of uranophane. Obtaining appropriate materials has been a significant challenge. Attempts to separate adequately pure uranophane from geologic samples failed because of its fine grain size and intimate intergrowths with other minerals. Efforts succeeded to synthesize a phase from chemical reagents that has the structure (based on x-ray diffraction data) and stoichiometric chemical composition of uranophane. This phase is being used in solubility experiments and was intended for use in future studies of actinide (Np and/or Pu) coprecipitation studies.

5.3.7 Future Developments

EBSPAC was developed to conduct PAs of the EBS taking into consideration the need to evaluate the failure of the WP and subsequent release of radionuclides. EBSPAC will be incorporated into the TPA code as the source term module.

With minor modifications, EBSPAC is applicable to various designs of the EBS that involve different thermal and environmental conditions, distinct types of SF combinations, and dissimilar overpack materials and WP designs. Alterations in the radionuclide composition, including chains, can be accommodated by modifying the radionuclide input data file. However, the current version of the code needs additional modifications to be used for the vitrified HLW.

To keep the source term calculation simple, EBSPAC focuses on a single cell. However, post- and pre-processors can be written to integrate EBSPAC as a source term module into the TPA code for overall PA studies. It should be noted that this version of EBSPAC has been developed mainly as framework for future improvements. Depending upon available resources and in order of priority, these developments include

- Implementation of the results of MULTIFLO calculations to obtain a better description of the evolution of the chemical composition and variables of the near-field environment, such as pH and f_{O_2} , as a function of temperature and time. Future MULTIFLO calculations will address the definition of the near-field environment at the drift scale, including the effects of various heat loads, host rock compositions, and initial fluid compositions.

- Incorporation of more developed corrosion models for the description of wet/dry periods, including the effect of through-wall penetrations of various sizes on the outer container and their related influence on galvanic coupling effects, as well as the consideration of stress corrosion cracking models.
- Improvement of the mechanical failure model through appropriate implementation of the methodology described for analysis of thermal embrittlement of the steel outer overpack.
- Incorporation of a SF dissolution rate-limited model to address the release of relatively soluble radionuclides such as Tc-99, I-129, Np-237, and Cs-135 and implementation of simplified models to account for colloidal transport of the actinides.
- Evaluation of the effect of partially failed containers on radionuclide release, including the influence of partially failed MPC and cladding.
- Determination of the effects of uranyl silicates as potential secondary alteration products of SF in the presence of high-silica concentration groundwater anticipated to be encountered by the WP because these alteration products could play an important role in enhancing the dissolution of SF and the release of radionuclides.
- Consideration of variable water infiltration into the EBS that will require modification of modules where liquid release calculations are performed to have a full implementation of the effect of time varying flow rate on radionuclide release from SF.
- Incorporation of cladding failure models, including creep, localized corrosion, and delayed hydride cracking.
- Consideration of criticality as a result of the degradation of the WP, water intrusion, and geometry changes due to instability of basket materials.
- Evaluation of radionuclide release from vitrified HLW.

The principal steps for development of a complete assessment of the potential for thermal embrittlement of the outer steel overpack are (i) predicting the level of grain boundary P segregation using acceptable models; (ii) estimating the toughness degradation of the steel using the relationship between P segregation and the degree of embrittlement as measured by DBTT parameter; (iii) combining the previous steps for estimating the variation of toughness, ΔDBTT , with time; (iv) calculating the evolution of fracture toughness, K_{IC} , with time using an appropriate K_{IC} -CVN correlation; and (v) calculating the change in the critical crack size, a_{cr} , as K_{IC} changes with time using fracture mechanics. A successful thermal stability assessment would require sufficient information for the specific material conditions to fully define both the segregation model parameters and the embrittlement potencies.

The results of these activities would provide the NRC with a better understanding of the potential for thermal embrittlement of overpack materials due to long-term aging. These studies are needed to support sensitivity analyses and to address uncertainties in models [i.e., applicability of Guttman and McLean theory to C-Mn steels (Guttman and McLean, 1979)], parameters (i.e., coefficient diffusion of P in steels), and data (i.e., correlations between ΔDBTT and K_{IC}). A more

complete evaluation of the embrittlement of steel overpacks under repository conditions will provide staff with the knowledge base needed to assess adequacy of the DOE treatment of this potential failure mode.

Some additional work may be needed to attain a complete assessment of the potential for intergranular oxidation of steel in dry air because discrepancies in mechanistic interpretations may lead to different estimates of intergranular penetration of oxide. However, this phenomenon may not affect the performance of the steel overpack as inferred by extrapolating data obtained in the temperature range of 400 to 576 °C to predict the behavior at repository temperatures. Long-term testing of alloy 825, extended for about 30 mo seems to indicate that E_{rp} is a robust parameter to assess the performance of the inner overpack. It is expected that the continuation of these tests during FY97 and FY98 would be valuable to confirm the validity of the current observations. In this regard, it is important to emphasize that the DOE should conduct a critical assessment of the relevance of using initiation potentials for localized corrosion, instead of repassivation potentials, as valid parameters to predict WP performance.

To date, the DOE has paid little attention to MIC; in TSPA-95 reference was made to MIC but it was not accounted for in the current models. The only work seen is a preliminary report in the form of an extended abstract (Pitonzo et al., 1996). These authors looked at the effect of axenic and mixed cultures of bacteria isolated from YM on the corrosion rate of 1020 carbon steel. A mixed culture of IOB, APB, and SRB was the only one to show significant corrosion rates (1.3 mm yr^{-1}). This rate was three to four times that of the abiotic control. Due to the limited nature of this abstract, it is difficult to fully relate the results to the waste repository.

5.4 ASSESSMENT OF PROGRESS TOWARD MEETING OBJECTIVES AND PATHS TO RESOLUTION

One of the objectives in the CLST KTI is being achieved through the development of EBSPAC to evaluate the failure of WPs and ultimately the release of radionuclides from the EBS. The technical description and user's manual for Version 1.0 β of EBSPAC was recently issued (Mohanty et al., 1996). Preliminary calculations conducted using EBSPAC Version 1.0 β clearly indicate there are two parameters of greatest importance to container life: (i) the AML, which determines the WP temperature and the RH as well as the chemical composition of the near-field environment; and (ii) the degree of galvanic coupling between the outer carbon steel overpack once it is breached and the inner nickel-base alloy overpack, which determines the failure time of the WP inner overpack. Additional sensitivity analyses will be needed to complete the goal of assessing the influence of other dominant environmental and materials factors on WP life and hence, the potential for radionuclide release within the initial thousands of years after repository closure.

With the incorporation of a probabilistic driver, Version 1.0 β of EBSPAC can be used to conduct an independent review of the container life cumulative distribution functions (CDFs) presented by the DOE in TSPA-95. As noted previously, models and computational approaches used in SOTEC (Sagar et al., 1992) and SCCEX (Cragolino et al., 1994) codes were incorporated with appropriate modifications in the current version of EBSPAC. In addition, the development of EBSPAC benefited from the data obtained in the experimental investigation program conducted within this KTI. The critical potentials used in EBSPAC for assessing the susceptibility to localized corrosion of ASTM A516 steel and alloy 825 have been generated in this program in conjunction with data extracted from the open literature. Experimental confirmation is now available indicating that E_{rp} , as measured in relatively short tests, is a reliable parameter for evaluating the long-term susceptibility to localized corrosion.

In TPSA-95, the DOE did not address the potential for mechanical failure of the carbon steel overpack due to thermal embrittlement. The propensity to thermal embrittlement of the outer steel overpack was evaluated through a review of the literature (Cragnolino et al., 1996). Calculations indicate that thermal embrittlement susceptibility could be significant only at WP temperatures exceeding 200 °C over extended periods (thousands of years). Sources of uncertainties in the degree of embrittlement related to uncertainties in models, parameters, or data have been identified, but additional work could be necessary following appropriate sensitivity analyses. Based on the current assessment, there is a need to determine the DOE design parameters prior to resolving this issue.

Different interpretations have been developed regarding the mechanisms of dry oxidation of steels (Ahn, 1996; Larose and Rapp, 1996) which lead to different values of oxide penetration by extrapolating high-temperature data. Nevertheless, it can be concluded, at least for C-Mn steels, that this phenomenon is not a matter of primary concern. Limited investigation can lead to a complete resolution of this issue.

Experimental work at the CNWRA on MIC demonstrated that localized corrosion of corrosion-resistant materials such as type 316L stainless steel can occur in the presence of *S. Putrefaciens*. The effect cannot be attributed to an increase in E_{corr} but to a decrease in E_{rp} that can be due to the concentration of metabolic products such as sulfide in localized areas of the metal surface. These results combined with observations reported by Pitonzo et al. (1996) of the existence of several species of bacteria responsible for MIC failures as part of the natural flora in the proposed site at YM confirm the need for a complete assessment of the effects of MIC on WP failure. The possibility of microorganism influence on radionuclide release from the EBS should be addressed.

5.5 INTEGRATION WITH OTHER KEY TECHNICAL ISSUES

The evaluation of thermal embrittlement of the outer overpack steel required knowledge of the container temperature as a function of time. This was provided by the temperature calculations performed in the Repository Design and Thermal-Mechanical Effects (RDTME) KTI using an effective conductivity approach.

Calculation of the time required to form an aqueous condensate film on the WP (time to wetting) is necessary to evaluate container life. Time to wetting is a function of the RH, calculated in the RDTME KTI. Results were provided to EBSPAC as a table.

Initiation of localized corrosion is dependent on the chloride concentration and pH of the aqueous solution contacting the WP. MULTIFLO calculations have been performed in the Evolution of the Near-Field Environment KTI on a repository scale to determine the spatial and temporal distribution of these variables. Results of MULTIFLO calculations have not been directly incorporated in the current version of EBSPAC. However, these calculations formed the basis for assumptions regarding the chemistry of the environment contacting the containers in EBSPAC.

Preliminary calculations were performed regarding failure of overpack materials and dispersion of radionuclides due to magmatic activity. For this purpose, the high temperature creep and stress rupture properties of the overpack materials were considered. The grain-size distribution of SF pellets, as affected by prior oxidation, was considered for determining the dispersion of radionuclides. These results were provided to the Igneous Activity KTI for consequence analyses.

EBSPAC is envisioned as a source term module to be incorporated in the NRC/CNWRA TPA code and reflects a significant activity integrated with the TSPA and Integration (TSPAI) KTI. Since EBSPAC is designed in a modular fashion to calculate container life and radionuclide release separately, evaluation of the CDFs of container life in TSPA-95 can be made using EBSPAC. Additionally, EBSPAC can assess the importance of factors such as thermal loading strategy on container life and source term, which will assist in the sensitivity analyses performed in the TSPAI KTI.

5.6 REFERENCES

- Ahn, T.M. 1995a. *Dry Oxidation and Fracture of LWR Spent Fuels*. NUDOC Accession Number: 9512220279. Washington, DC: Nuclear Regulatory Commission.
- Ahn, T.M. 1995b. *Long-Term Kinetic Effects and Colloid Formations in Dissolution of LWR Spent Fuels*. NUDOC Accession Number: 9508030112. Washington, DC: Nuclear Regulatory Commission.
- Ahn, T.M. 1996. *Dry Oxidation of Waste Package Materials*. NUDOC Accession Number: 9607290014. Washington, DC: Nuclear Regulatory Commission.
- Angell, P., D.S. Dunn, and G.A. Cragolino. 1996. Effect of microbial action on the corrosion potential of austenitic alloy containers for high-level waste. *Scientific Basis for Nuclear Waste Management XIX Symposium Proceedings*. W.M. Murphy and D.A. Knecht, eds. Pittsburgh, PA: Materials Research Society: 412: 539-546.
- American Society for Testing and Materials. 1995. *G-61-86, Standard Test Method for Conducting Cyclic Potentiodynamic Polarization Measurements for Localized Corrosion Susceptibility of Iron-, Nickel-, or Cobalt-Based Alloys*. Vol. 3.02. Philadelphia, PA: American Society for Testing and Materials.
- Briant, C.L., and S.K. Banerji. 1983. Intergranular fracture in ferrous alloys in nonaggressive environments. *Treatise on Materials Science and Technology. Volume 25: Embrittlement of Engineering Alloys*. C.L. Briant and S.K. Banerji, eds. New York, NY: Academic Press: 21-58.
- Bruscato, R. 1970. Temper embrittlement and creep embrittlement of 2 1/4Cr-1Mo shielded metal-arc weld deposits. *Welding Research Supplement* 49: 148s-156s.
- Costerton, J.W., Z. Lewandowski, D.E. Caldwell, D.R. Korber, and H.M. Lappin-Scott. 1995. Microbial biofilms. *Annual Review of Microbiology* 49: 711-746.
- Cragolino, G.A., N. Sridhar, J. Walton, R. Janetzke, T. Torng, J. Wu, and P. Nair. 1994. "Substantially Complete Containment"—Example Analysis of a Reference Container. CNWRA 94-003. San Antonio, TX: Center for Nuclear Waste Regulatory Analyses.
- Cragolino, G.A., H.K. Manaktala, and Y-M. Pan. 1996. *Thermal Stability and Mechanical Properties of High-Level Radioactive Waste Container Materials: Assessment of Carbon and Low-Alloy Steels*. CNWRA 96-004. San Antonio, TX: Center for Nuclear Waste Regulatory Analyses.

- Druce, S.G., G. Gage, and G. Jordan. 1986. Effect of ageing on properties of pressure vessel steels. *Acta Metallurgica* 34: 641-652.
- Dunn, D.S., G.A. Cragnolino, and N. Sridhar. 1996. Localized corrosion initiation, propagation, and repassivation of corrosion resistant high-level nuclear waste container materials. *CORROSION/96*. Paper No. 97. Houston, TX: NACE International.
- Guttmann, M., and D. McLean. 1979. Grain boundary segregation in multicomponent systems. *Interfacial Segregation*. W.C. Johnson and J.M. Blakely, eds. Metals Park, OH: American Society for Metals: 261-350.
- Hudson, J.A., S.G. Druce, G. Gage, and M. Wall. 1988. Thermal ageing effects in structural steels. *Theoretical and Applied Fracture Mechanics* 10: 123-133.
- Iwadate, T., J. Watanabe, and Y. Tanaka. 1985. Prediction of fracture toughness K_{IC} of 2 1/4Cr-1Mo pressure vessel steel from Charpy V-notch test results. *Flaw Growth and Fracture*. ASTM-STP 631. Philadelphia, PA: American Society for Testing and Materials: 493-506.
- Kusuhara, Y., T. Sekine, T. Enami, and H. Ooi. 1980. BOF-LRF refined ultralow phosphorous 2.25Cr-1Mo steel plate of low temper embrittlement susceptibility. *Proceedings of the Fourth International Conference on Pressure Vessel Technology*. London, U.K.: Institute of Mechanical Engineers.
- Larose, S., and R.A. Rapp. 1996. *Review of Low-Temperature Oxidation of Carbon Steels and Low-Alloy Steels for Use as High-Level Radioactive Waste Package Materials*. San Antonio, TX: Center for Nuclear Waste Regulatory Analyses.
- Little, B., P. Wagner, and F. Mansfeld. 1991. Microbiologically influenced corrosion of metals and alloys. *International Materials Review* 36: 253-272.
- Lonsdale, D., and P.E.J. Flewitt. 1978. The role of grain size on the ductile brittle transition of a 2.25 pct Cr-1 pct Mo steel. *Metallurgical Transactions* 9A: 1,619-1,623.
- Marsh, G.P., K.J. Taylor, I.D. Bland, C. Wescott, P.W. Tasker, and S.M. Sharland. 1985. Evaluation of localized corrosion of carbon steel overpacks for nuclear waste disposal in granite environments. *Scientific Basis for Nuclear Waste Management IX Symposium Proceedings*. L.W. Werme, ed. Pittsburgh, PA: Materials Research Society: 59: 421-428.
- Mayer, P., and W. Smeltzer. 1973. Internal oxidation and decarburization properties of an Fe-1w/oMn and Fe-1w/oC alloy in carbon dioxide-carbon monoxide atmosphere at 1000 °C. *Canadian Metallurgical Quarterly* 12: 23-34.
- McLean, D. 1957. *Grain Boundaries in Metals*. London, U.K.: Oxford Press.

- Mohanty, S., G.A. Cragnolino, T. Ahn, D.S. Dunn, P.C. Lichtner, R.D. Manteufel, and N. Sridhar. 1996. *Engineered Barrier System Performance Assessment Code: EBSPAC Version 1.0 β , Technical Description and User's Manual*. CNWRA 96-011. San Antonio, TX: Center for Nuclear Waste Regulatory Analyses.
- Muan, A., and E.F. Osborn. 1965. *Phase Equilibria Among Oxides in Steelmaking*. Reading, MA: Addison-Wesley Publishing Company, Inc.
- Nakanishi, M., S. Watanabe, and J. Furusawa. 1984. On the improvement of ductility and toughness in welded joints of Al-B treated thick plates for pressure vessels. Paper No. 42. *International Conference on the Effects of Residual, Impurity, and Microalloying Elements on Weldability and Weld Properties*. Cambridge, U.K.: The Welding Institute.
- Newcomb, S., and W. Stobbs. 1991. The effects of a grain boundary on the compositional fluctuations inherent in the oxidation of Fe-10Cr-34Ni. *Oxidation of Metals* 35: 69-88.
- Newhouse, D.L. 1972. Temper embrittlement study of nickel-chromium-molybdenum-vanadium rotor steels, I: Effects of residual elements. *Temper Embrittlement of Alloy Steels*. STP 499. Philadelphia, PA: American Society for Testing and Materials: 3-36.
- Newman, R.C., H.S. Isaacs, and B. Alman. 1982. Effects of sulfur compounds on the pitting behavior of type 304 stainless steel in near-neutral chloride solutions. *Corrosion* 38: 216-265.
- Otsuka, R., and H. Fujikawa. 1991. Scaling of austenitic stainless steels and nickel-base alloys in high-temperature steam at 973 K. *Corrosion* 47: 240-248.
- Pearcy, E.C., J.D. Prikryl, W.M. Murphy, and B.W. Leslie. 1994. Alteration of uraninite from the Nopal I deposit, Peña Blanca District, Chihuahua, Mexico, compared to degradation of spent nuclear fuel in the proposed U.S. high-level nuclear waste repository at Yucca Mountain, Nevada. *Applied Geochemistry* 9: 713-732.
- Pitonzo, B., P. Castro, P. Amy, D. Bergman, and D. Jones. 1996. Microbially-influenced corrosion capability of Yucca Mountain bacterial isolates. *Proceedings of the Seventh Annual International Conference on High-Level Radioactive Waste Management*. La Grange Park, IL: American Nuclear Society and New York, NY: American Society of Civil Engineers: 12-18.
- Pourbaix, M. 1974. *Atlas of Electrochemical Equilibria in Aqueous Solutions*. Houston, TX: National Association of Corrosion Engineers: 307-321.
- Rolfe, S.T., and S.R. Novak. 1970. Slow-bend K_{IC} testing of medium-strength high-toughness steels. *Review of Developments in Plain-Strain Fracture Toughness Testing*. ASTM-STP 463. Philadelphia, PA: American Society for Testing and Materials: 124-159.
- Sagar, B., R.B. Codell, J. Walton, and R.W. Janetzke. 1992. *SOTEC: A Source Term Code for High-Level Nuclear Waste Geologic Repositories User's Manual: Version 1.0*. CNWRA 92-009. San Antonio, TX: Center for Nuclear Waste Regulatory Analyses.

- Scully, J.R., and H.P. Hack. 1984. Galvanic corrosion prediction using long- and short-term polarization curves. *CORROSION/84*. Paper No. 34. Houston, TX: National Association of Corrosion Engineers.
- Shida, Y., and T. Moroishi. 1992. Effect of aluminum and titanium additions to Fe-21%Cr-32%Ni on the oxidation behavior in an impure helium atmosphere at high temperatures. *Oxidation of Metals* 37: 327-348.
- Sridhar, N., G.A. Cragnolino, and D.S. Dunn. 1995. *Experimental Investigations of Failure Processes of High-Level Nuclear Waste Container Materials*. CNWRA 95-010. San Antonio, TX: Center for Nuclear Waste Regulatory Analyses.
- Stahl, D. 1993. *Waste Package Corrosion Inputs*. CRWMS M&O Interoffice Correspondence. Las Vegas, NV: TRW Environmental Safety Systems, Inc.
- Szklarska-Smialowska, Z. 1986. *Pitting Corrosion of Metals*. Houston, TX: National Association of Corrosion Engineers: 224-231.
- Tasovac, A., R. Marković, and Ž. Štrbački. 1989. Comparative investigation of some austenitic chromium-nickel steels in hot air. *Materials Science and Engineering A120*: 229-234.
- Tavassoli, A.A., A. Bougault, and A. Bisson. 1984. The effect of residual elements on the temper embrittlement susceptibility of large A508, Class 3, vessel forgings. Paper No. 43. *International Conference on the Effects of Residual, Impurity, and Microalloying Elements on Weldability and Weld Properties*. Cambridge, U.K.: The Welding Institute.
- Thierry, D., and W. Sand. 1995. Microbially influenced corrosion. *Corrosion Mechanisms in Theory and Practice*. P. Marcus and J. Oudar, eds. New York, NY: Marcel Dekker, Inc.: 457-499.
- TRW Environmental Safety Systems, Inc. 1995. *Total System Performance Assessment—1995: An Evaluation of the Potential Yucca Mountain Repository*. B00000000-01717-2200-00136. Las Vegas, NV: TRW Environmental Safety Systems, Inc.
- TRW Environmental Safety Systems, Inc. 1996. *Mined Geologic Disposal System Advanced Conceptual Design Report. Vol. III of IV. Engineered Barrier Segment/Waste Package*. B00000000-01717-5705-00027. Rev. 00. Las Vegas, NV: TRW Environmental Safety Systems, Inc.
- Tsujikawa, S., and S. Okayama. 1990. Repassivation method to determine critical conditions in terms of electrode potential, temperature and NaCl concentration to predict crevice corrosion resistance of stainless steels. *Corrosion Science* 31: 441-446.
- Ucisik, A.H., C.J. McMahon, Jr., and H.C. Feng. 1978. The influence of intercritical heat treatment on the temper embrittlement susceptibility of P-doped Ni-Cr steel. *Metallurgical Transactions* 9A: 321-329.

- Viswanathan, R., and S.M. Bruemmer. 1985. In-service degradation of toughness of steam turbine rotors. *Transactions of the ASME. Journal of Engineering Materials and Technology* 107: 316-324.
- Wada, T., and W.C. Hagel. 1976. Effect of trace elements, molybdenum, and intercritical heat treatment on temper embrittlement of 2 1/4Cr-1Mo steel. *Metallurgical Transactions 7A*: 1,419-1,426.
- Watanabe, J., Y. Shindo, Y. Murakami, T. Adachi, S. Ajiki, and K. Miyano. 1974. Temper embrittlement of 2 1/4Cr-1Mo pressure vessel steel. *29th Petroleum Mechanical Engineering Conference*. New York, NY: American Society of Mechanical Engineers.

6 THERMAL EFFECTS ON FLOW

Primary Authors: R.T. Green, A.C. Bagtzoglou, R.D. Manteufel, P.C. Lichtner, and G.I. Ofoegbu

Technical Contributors: R. Chen, M.E. Hill, S.M. Hsiung, K.M. James, M.A. Muller, G.I. Ofoegbu, and G. Rice

Key Technical Issue Co-Leads: A.H. Chowdhury (CNWRA) and J.A. Pohle (NRC)

6.1 INTRODUCTION

Prediction of thermally driven redistribution of moisture through partially saturated, fractured porous media caused by the emplacement of heat-generating high-level radioactive waste (HLW), with acceptable uncertainty, is the focus of the Thermal Effects on Flow (TEF) Key Technical Issue (KTI). Redistribution of moisture driven by heat may result in extended periods of dryness in the proposed repository during either the period of high heat or during cooling. Also, redistribution of moisture driven by heat could result in channeling moisture toward waste packages (WP). Thus, it is necessary to understand the spatial and temporal effects of the thermal load on temperature as well as liquid and gas phase flux in the vicinity of the proposed repository to have confidence in predictions of containment and long-term waste isolation. The U.S. Department of Energy (DOE) is developing a waste containment and isolation strategy to demonstrate that waste can be contained and isolated at the proposed Yucca Mountain (YM) site. The DOE strategy defines attributes of the disposal system deemed important to containment and isolation. DOE has identified hypotheses that address attributes to be evaluated within this KTI. Three of these hypotheses are: (i) there will be low humidity at the WP surface; (ii) there will be low percolation flux and limited fracture flow at repository depth; and (iii) thermally induced flux can be bounded. Evaluating these hypotheses necessitates understanding thermally driven flow of moisture through partially saturated and fractured porous media. This KTI was divided into three resolvable subissues in pursuit of this understanding: (i) is the DOE thermal testing program sufficient to assess the likelihood of gravity driven refluxing occurring in the near field, (ii) is the DOE thermal modeling approach adequate for assessing the nature and bounds of thermally induced flux in the near field, and (iii) will the DOE thermal loading strategy result in thermally induced flux in the near field and humidity at the WP surface to meet the performance objectives? Resolution of these subissues will establish the knowledge base necessary to predict, with acceptable uncertainty, thermally driven redistribution of moisture through partially saturated fractured porous media. The DOE hypotheses can then be evaluated using these predictive capabilities.

The FY96 activities of TEF KTI reported herein address all three subissues. In section 6.2, these activities and results are discussed to assess the extent the subissues have been resolved through FY96.

6.2 OBJECTIVES AND SCOPE OF WORK

The objective of this KTI is to understand heat and mass transfer through geologic materials to predict thermally driven redistribution of moisture through partially saturated fractured porous media at the proposed repository with acceptable uncertainty. Specific laboratory-scale experiments, analysis of existing field-scale test results, and predictive numerical modeling are being conducted to achieve this objective. Planned work has been prioritized to identify tasks whose resolution is both achievable within available resources and that will lead to significant reduction in uncertainty. Tasks designed to reduce uncertainties in these subissues in FY96 are both reactive and proactive: (i) review and evaluate the DOE

thermohydrology program, including the DOE peer review activity; (ii) benchmark test computer codes; (iii) provide sensitivity analyses; and (iv) evaluate conceptual models. Pursuit of these four activities were relevant to the first two subissues in the TEF KTI. The third subissue, will DOE thermal loading strategy result in thermally induced flux in the near field and humidity at the WP surface to meet the performance objectives, will be resolved using information gained during the resolution of the first two subissues.

Review and evaluation of the DOE thermohydrology program included (i) review of a DOE peer review team (PRT) report, (ii) the DOE response to PRT recommendations, (iii) PRT comments to the DOE response to PRT recommendations, (iv) attendance at an Appendix 7 meeting on Exploratory Studies Facility (ESF) thermal testing including site visit, and (v) participation in a DOE/Nuclear Regulatory Commission (NRC) ESF video conference. This activity also included a presentation to the Advisory Committee on Nuclear Waste on thermal-hydrological coupled processes.

Benchmark testing (i.e., code-to-code comparisons) was conducted of DOE and NRC thermohydrologic codes. The DOE codes, TOUGH2 and FEHM were tested against the NRC codes CTOUGH and MULTIFLO. The TOUGH2 and FEHM codes are currently being used to support Total System Performance Assessments (TSPAs) while CTOUGH and MULTIFLO are being used by the Center for Nuclear Waste Regulatory Analyses (CNWRA) in reviewing the DOE TSPAs. Various test problems were used to (i) compare and contrast code capabilities, (ii) identify and understand any significant differences that may arise, and (iii) assess robustness and computational efficiencies of the codes.

Work performed in regard to sensitivity analysis included the effects of (i) backfill on temperature and saturation; (ii) media properties on prediction of moisture redistribution at proposed repository scale; (iii) ventilation on rock dryout and drift relative humidity; (iv) geologic structure and features on the evolution of perched water body; and (v) geologic structure and media hydrologic properties on temperature and saturation. Temperature and saturation at the WP will influence the integrity of the canister. Once released from the WP, transport of radionuclides will be influenced by thermally driven moisture at and below the repository horizon.

6.3 SIGNIFICANT TECHNICAL ACCOMPLISHMENTS

6.3.1 Review and Evaluation of the Department of Energy Thermohydrology Program

The purpose of the review of the DOE thermohydrology program was to provide an independent evaluation of the DOE Yucca Mountain Site Characterization Office (YMSCO) Thermohydrologic Testing and Modeling Program. This review was conducted to evaluate whether the DOE thermohydrologic program would enable the DOE to conservatively predict thermally driven flow at the proposed repository with acceptable uncertainty. In particular, the central question is: will the DOE program provide the information necessary to resolve the subissues identified in the TEF KTI? For this review, it was assumed that information regarding the YMSCO Thermohydrologic Testing and Modeling Program contained in previous DOE reports was superseded by data in three recent documents and supported by information provided during an Appendix 7 meeting and a DOE/NRC ESF video conference meeting. The three documents are: (i) PRT Record Memorandum Report and Recommendations submitted to the DOE in January, 1996, (ii) the DOE response to PRT recommendations distributed in July 1996, and (iii) the PRT comments to the DOE response to PRT recommendations dated July 30, 1996. No additional documents regarding this review process have been released by DOE as of September 1996.

Further insight into the YMSCO Thermohydrologic Testing and Modeling Program was gained during the DOE/NRC Appendix 7 meeting on July 24, 1996 and during the quarterly DOE/NRC ESF video conference meeting September 12, 1996. The Appendix 7 meeting on thermal testing was held at YM and included a visit to the ESF and thermal alcove experiments. Results of this review were submitted to the NRC as a letter report in September 1996 and are summarized here.

The review concluded that the DOE YMSCO Thermohydrologic Testing and Modeling Program, as represented in the information available for this review, adequately addresses most, but not all critical relevant technical issues. It was noted in the PRT report, and supported here, that the discontinuance of surface based hydrologic testing may result in unacceptably high uncertainty in infiltration estimates. The importance of acceptable predictions of infiltration rates is manifested in thermohydrologic flow models whose predictions are highly sensitive to prescribed infiltration rates at the upper boundary. It was also noted in both reports that the DOE does not have plans to evaluate the conceptual models as rigorously as needed to ensure that their analyses provide conservative and acceptably accurate predictions of proposed repository performance. It is possible that heater tests designed for conditions different from those expected at the proposed repository may provide misleading results. Results from a field-scale heater test with an excessively high thermal load may support an equivalent continuum model (ECM) conceptual model, however, the ECM might not accurately incorporate important moisture redistribution mechanisms, such as refluxing and dripping, that would be experienced under repository conditions. For example, a drift-scale heater conducted with drift wall temperatures $> 200\text{ }^{\circ}\text{C}$ could conceivably minimize the potential for reflux dripping from the drift ceiling. The heater test would thereby concur with ECM conceptual models which do not predict dripping, a mechanism not yet predicted in any analyses, but which has been observed in previous heater tests (i.e., Climax, G-tunnel, and the road tunnel near Superior, AZ). Analyses of WP integrity and radionuclide transport from the WP may not be conservative if thermally driven moisture flow near the WP is not conservatively modeled (Pruess and Tsang, 1993, 1994). In future precicensing interactions with DOE, the potential benefits of a spatially variable thermal load for the drift-scale heater test will be suggested as a way to test for the potential of this mechanism.

In neither the PRT report nor the DOE response to the PRT report was it demonstrated that DOE bounding assumptions and analyses of the thermo-hydrological-chemical (THC) processes are conservative. At high thermal loads, significant concentrations in dissolved species such as chloride and elevation in pH can be expected to occur near the boiling front surrounding the repository (Walton, 1993). As a consequence corrosion rates and sorption properties of the host rock will be affected. Prediction of such effects can only be achieved with models which adequately couple THC processes (Lichtner and Seth, 1996). The current codes mentioned by the PRT and DOE (TOUGH, TOUGH2, VTOUGH, FEHM, and NUFT) do not include chemistry suitable for describing rock-water interaction and the effects on solution chemistry due to evaporation and condensation processes. An additional code mentioned in the DOE response, GIMRT/OS3D, is a fully saturated code that does not include two-phase fluid flow. The code EQ3/6, a geochemical reaction path model, does not appear adequate for the analysis either, although use of this code was recommended by the PRT. This is because the problem to be solved is fundamentally a moving boundary problem. Reaction fronts will not remain stationary with time and therefore, it is difficult to see the utility of using EQ3/6 which does not incorporate fluid transport to model such processes. Analyses which omit critical THC processes may not be conservative. It is important that the DOE YMSCO Thermohydrological Testing and Modeling Program be designed to address these and the above mentioned issues.

6.3.2 Benchmark Testing of Computer Codes

Thermohydrologic codes used by the DOE and NRC/CNWRA were assessed through benchmark testing (i.e., code-to-code comparisons) and the results were used to (i) compare and contrast code analysis capabilities, (ii) identify and understand any significant differences that may arise, and (iii) assess robustness and computational efficiencies of the codes. Benchmark testing (Baca and Seth, 1996) included four general thermohydrologic codes: TOUGH2, FEHM, CTOUGH, and MULTIFLO. The TOUGH2 and FEHM codes are actively being used by DOE contractors, while the CTOUGH and MULTIFLO codes are being used by the NRC/CNWRA. The benchmark testing of these four thermohydrologic codes was conducted using two sets of computational test cases. Each set of cases consisted of one- and two-dimensional (2D) simulations of isothermal and nonisothermal flow involving both porous and fractured-porous media systems. In general, the benchmark testing showed that three of the four codes tested (TOUGH2, CTOUGH, and MULTIFLO) appear to possess sufficient capability to simulate some of the hydrologic and thermohydrologic conditions expected to be important at the proposed HLW repository at YM. In all the test cases considered, it was found that the numerical results produced by these three thermohydrologic codes agreed. The primary differences were in computational efficiency and it was found the MULTIFLO code was substantially faster than the other codes. FEHM solved most of the test cases and the numerical results agreed adequately well with results of the other three codes. However, the FEHM code that was tested experienced computational difficulties in two test cases due to prohibitively large execution times that occurred as a result of repetitive reductions of the time step; one with high infiltration rates and the other with flow in fracture-porous media. The overall results of the benchmarking study suggest that the use of distinct thermohydrologic codes by DOE and NRC will not lead to contentious methodology issues.

6.3.3 Sensitivity Analysis

A robust, accurate two-phase numerical simulator was needed to perform a sensitivity analysis of thermally driven flow through partially saturated fractured porous rock. Therefore, the first task of this analysis was to evaluate and select a two-phase numerical simulator to be used in predictive modeling. Results from previously conducted scoping analyses using C-TOUGH (Lichtner, 1994) were compared with similar analyses predicated on an ECM performed using MULTIFLO, a multicomponent, multiphase, nonisothermal reactive transport code developed at the CNWRA (Seth and Lichtner, 1996). MULTIFLO proved to be more efficient and capable in these and other comparative analyses (Baca and Seth, 1996) and was selected as the two-phase simulator in the sensitivity analyses. In addition, TOUGH2 (Pruess, 1991), a two-phase simulator used by the DOE contractors, is used to provide an independent comparison of MULTIFLO results and to assess a dual continuum conceptual model. Limited use of DCM-3D (Updegraff et al., 1991) has been initiated to test an alternative conceptual model of matrix/fracture interactions. Other than this limited testing, however, all simulation of thermally driven moisture through partially saturated fractured rock that was performed as part of this KTI was accomplished using an ECM conceptual model and computed with MULTIFLO. Although limitations in the ECM have been recognized, future analysis will also use the ECM with MULTIFLO until an acceptable model or code is identified.

Sensitivity analyses were conducted to assess the importance of variations in thermal loading schemes, drift engineering design, backfill material, hydraulic properties, and geologic structures and features. Effects are presented in terms of predicted temperature and saturation. Results from these analyses were used to address the subissue to identify the nature and bounds of thermally induced flux in the near field. Moisture conditions at the WP will affect canister integrity and thermally driven moisture flow at and below the proposed repository horizon will affect radionuclide transport.

6.3.3.1 Effects of Backfill on Temperature and Saturation

Engineered barriers such as backfill may play a role in containing waste and inhibiting radionuclide transport by providing structural control of near field rock movements, deterring human entry, and creating a diversionary path for episodic water intrusions. In addition, the selective use of backfill material with a low thermal conductivity has been considered as a proactive procedure to engineer the hydrothermal conditions near the WP (Buscheck et al., 1995).

A series of simulations was performed with the MULTIFLO code to evaluate the effects of backfill on temperature and saturation at the WP and the drift wall. The evaluation included assessments of: (i) backfill versus no backfill materials, (ii) effect of saturation of the backfill materials, and (iii) effect of the thermal conductivity of backfill materials. A vertically oriented, 2D numerical model spanning from ground surface to the water table was used for these analyses. The model was configured with six hydrostratigraphic layers similar to that used in the 1995 DOE Total System Performance Assessment (TSPA-95) (TRW Environmental Safety Systems, Inc., 1995). Each layer was represented as a uniform equivalent continuum combining the effects of matrix and fractures (Klavetter and Peters, 1986). The vertical boundaries were no heat or fluid flow. The surface and water table were established as constant temperature and pressure boundaries. The upper boundary was assigned a uniform, steady infiltration rate of 0.3 mm/yr as was used in TSPA-95 (TRW Environmental Safety Systems, Inc., 1995). The WPs are assumed to be initially stored in open drifts. After 100 yr, the drift voids are filled with backfill material. The assigned package spacing equates to an areal power density of 83 MTU/Ac. The model geometry, property values, and heat load are consistent with TSPA-95 (TRW Environmental Safety Systems, Inc., 1995).

The temperature effect of emplacing backfill materials into a drift 100 yr after emplacement of 30 yr old spent fuel is illustrated in figure 6-1. Before the backfill is emplaced, temperature in the drift at the surface of the WP increases steadily for approximately 50 yr then declines as the waste decays. Immediately after emplacement of the backfill materials, the temperature in the drift decreases by 15 °C from evaporation of pore water in the backfill (in this case, the initial saturation of the backfill was assumed to be 0.5). After the pore water of the backfill materials is evaporated, the backfill acts as an insulator and the temperature at the WP increases by about 10 °C above its pre-emplacment level. Temperatures elevated due to the insulating effect of the backfill persist for about 1,500 yr.

The effects of variable saturation of the backfill were examined for initial backfill saturations of 0.01, 0.5, and 0.99 compared to measured *in situ* Topopah Spring Welded (TSw) saturations that vary from about 0.5 to 0.99. The saturation of backfill material will be affected by drying mechanisms associated with the manner in which the backfill materials are mined, transported, stored, and possibly processed. Analysis for initial saturations of 0.01, 0.5, and 0.99 provide the range of possibilities that could be encountered. Increased saturation in the backfill causes temporary lower temperatures after emplacement, however, after 10–20 yr there is negligible difference in the predicted temperatures or saturations (figure 6-2).

It has been asserted by the DOE (Buscheck et al., 1995) that emplaced backfill material with low thermal conductivity will elevate the WP temperature, decrease the drift wall temperature, and decrease the extent of the boiling isotherm with the advantageous effect that water condensed above the drifts will be more easily shed away and downward from the WP. Analyses were conducted within the TEF KTI to evaluate this assertion. Initially, a literature search was conducted to collate existing measurements and estimates for thermal conductivity values of geologic units at YM. Most of the measurements were made on intact rock whereas backfill materials will most certainly be crushed or

Effect of Backfill on Temperature (83 kW/Ac)

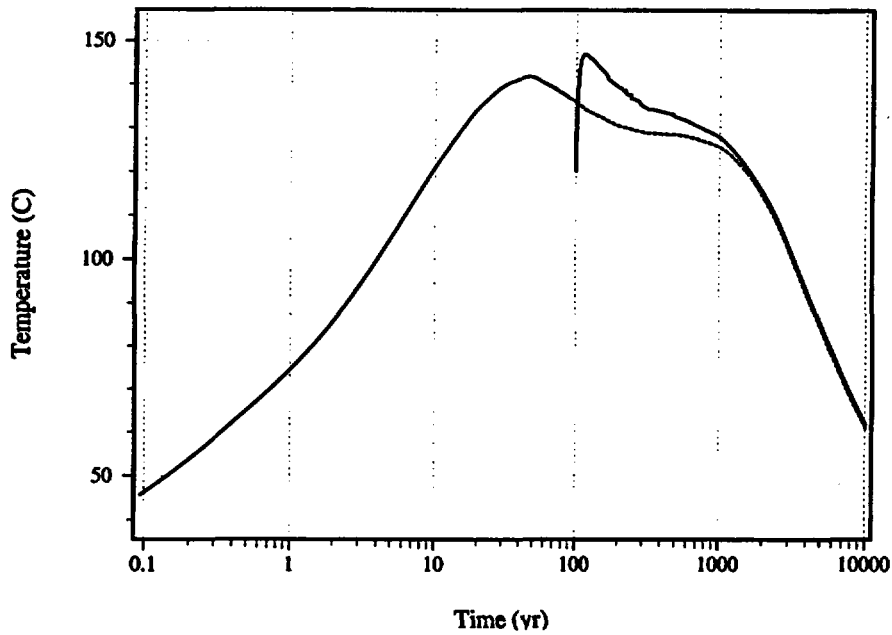


Figure 6-1. Effects of backfill on temperature at the waste package; dotted line denotes no backfill

Effects of Initial Saturation of Backfill (83 kW/Ac)

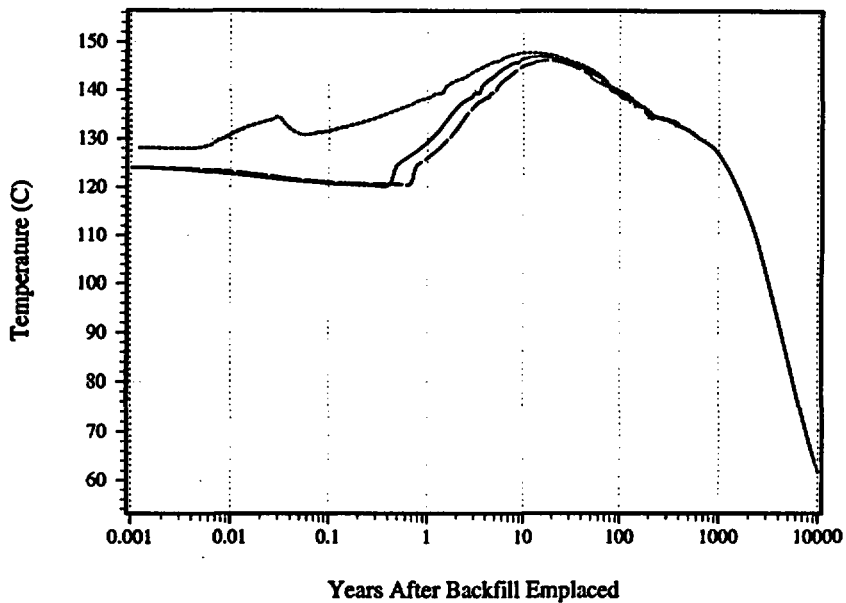


Figure 6-2. Waste package temperature as a function of initial saturation of backfill for initial saturations of 0.01 (dotted line), 0.5 (solid line), and 0.99 (dashed line)

granulated. For this reason, a steady-state laboratory apparatus was assembled to measure the bulk thermal conductivity of crushed rock over a range of temperatures and saturations. Using reasonable estimates of thermal conductivity identified in the literature search and laboratory testing, numerical analyses were then conducted to assess the relative effect of backfill materials exhibiting different values for thermal conductivity, K_r . Following is a discussion of this assessment.

Previous studies that measured and/or estimated the thermal conductivities of the thermal-mechanical units at YM have been conducted by Lappin (1980), Lappin et al. (1982), Sass and Lauchenbruch (1982), Lappin and Nimick (1985), Nimick and Lappin (1985), and Sass et al. (1988). Nimick (1990a,b) rejects most of the thermal conductivity values obtained in the aforementioned investigations because of uncertainties and errors cited by authors or their peers. The DOE Reference Information Base (RIB) (U.S. Department of Energy, 1993) cites Nimick (1990a,b) measured and estimated values of thermal conductivity for the thermal-mechanical units at YM. The DOE RIB values for thermal conductivity by Nimick are, therefore, assumed to be most representative of the thermal-mechanical units at YM. The classification of the thermal-mechanical units at YM used by Nimick is compared to that used in TSPA-95 (TRW Environmental Safety Systems, Inc., 1995) in table 6-1. The measured and estimated values of thermal conductivity values obtained by Nimick (1990a,b) and referenced in the RIB are presented in table 6-2.

To date, measurements of thermal conductivities at steady-state conditions are not available for bulk crushed samples collected from YM (Wilson et al., 1994). To gain a better understanding of the parameters that may affect these estimates, laboratory measurements of the thermal conductivity were made of crushed tuff materials, such as those being considered for use as backfill at the proposed repository. A steady-state thermal conductivity apparatus was constructed to measure the thermal conductivity of bulk rock samples. A schematic diagram of the apparatus is shown in figure 6-3. The cell accepts 1.35 m³ of sample material and will accommodate dry to fully saturated samples over a temperature range of 10 to 230 °C, although only dry samples were measured for temperatures in excess of 100 °C.

Preliminary thermal measurements were performed on welded tuff collected from the Apache Leap Test Site (ALTS). Core samples from ALTS were broken, crushed, and sieved into a fraction consisting of very angular to subangular rock pieces between 1.6 and 4 cm in diameter. The crushed tuff was dried for two days at 90 °C then loaded into the thermal conductivity cell. A total of six measurements was conducted on the same sample, although the sample was more tightly packed in tests 2 through 6 than in test 1 (the cell contained about 0.1 m³ more rock in tests 2–6). As expected, thermal conductivity of the more tightly packed sample increased from 0.246 to 0.266 W/m-K, with all other variables remaining constant.

Measurements were also performed to determine if thermal conductivity is sensitive to variations in the temperature of the boundaries of the sample. Heat flux was controlled by varying the temperature difference between the top and bottom aluminum plates (e.g., increasing or decreasing the temperature of the heater or heat sink or both). The heat flux was varied from 20.74 to 115.80 W/m² and the average temperature varied from 26.41 to 66.93 K. Thermal conductivity is illustrated in figure 6-4 as a function of temperature. Although subtle, there is a linear relationship between temperature and thermal conductivity. Test 1, which was loosely packed, departs slightly from this linear relationship. In all of the test runs, the sample attained thermal equilibrium within a few days. Results of these preliminary measurements are presented in table 6-3.

Table 6-1. Classification of thermal-mechanical units at Yucca Mountain

Nimick (1990a,b)		TSPA-95 (TRW Environmental Safety Systems, Inc., 1995)	
Unit	Depth ¹ (m)	Unit	Depth (m)
TCw	0-60	TCw	0-95
PTn	60-125	PTn	95-148
TSw1	125-300	TSw	148-482
TSw2	300-400		
TSw3	400-420	TSv	474-482
CHn1	420-570	CHnv	482-563
CHn2	570-590	CHnz	563-684
CHn3	590-600		
¹ approximations			

Table 6-2. Measured and estimated values of thermal conductivity, κ_t

Formation	κ_t at <i>In Situ</i> Saturation (W/m-K)	κ_t Ambient Saturation Not Indicated (W/m-K)	κ_t Saturated (W/m-K)	κ_t Dry (W/m-K)
TCw	1.59-1.73 ¹			1.51-1.64 ¹
PTn	1.55-1.67 ¹	1.68-1.94 ²		
TSw	1.59-2.18 ¹		1.6-2.1 ²	1.58-2.36 ²
TSv	1.26-1.28 ¹	1.20-2.09 ²		
CHnv	0.84-1.21 ¹	1.17-1.44 ²		
CHnz	1.26-1.57 ¹		1.16-1.83 ²	0.54-.076 ²
¹ Estimated values				
² Measured values				

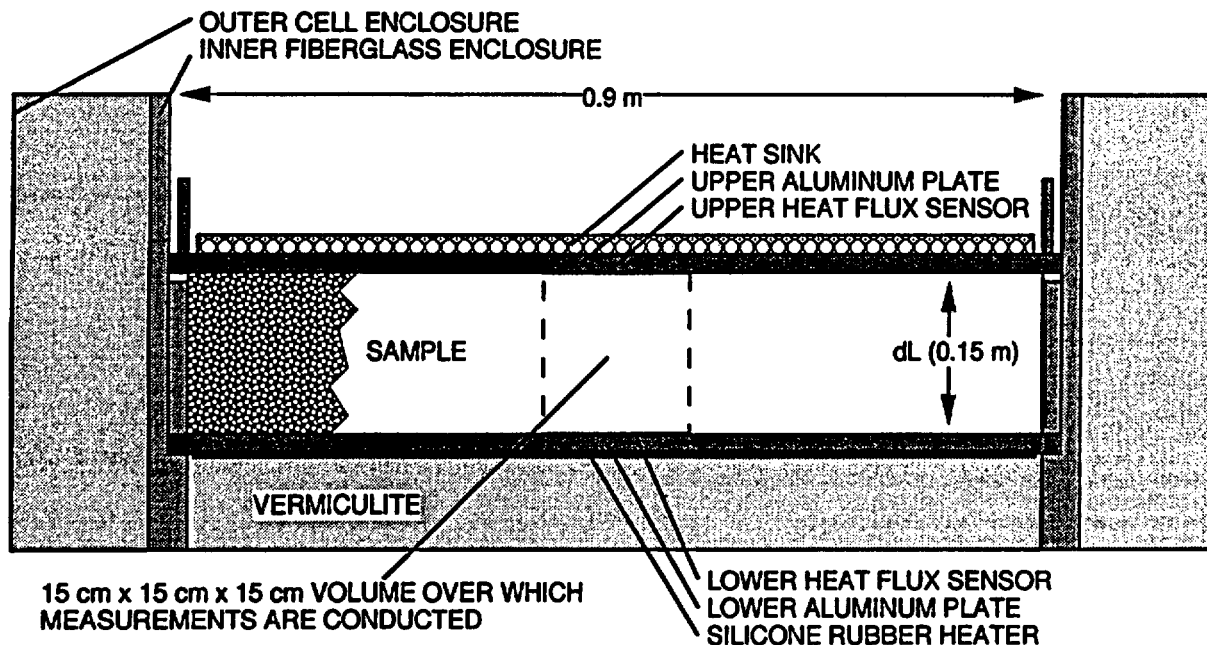


Figure 6-3. Schematic of bulk thermal conductivity measurement apparatus

The numerical model used in analyses to assess the effect of the thermal conductivity of backfill materials was similar to that used in the previous backfill analyses. The time history of WP temperature with backfill thermal conductivities of 0.2, 0.6, 2.0, and 10.0 W/m-K is illustrated in figure 6-5. The first three thermal conductivities are similar to those of tuff backfill materials and intact tuff. The high value of 10 W/m-K exceeds the thermal conductivities of common geologic materials but approaches a value equivalent to radiative heat transfer through air over short distances. This figure indicates that backfill with a lower thermal conductivity acts as an insulator and results in higher WP temperatures; higher conductivity backfill acts as a conductor and can lower WP temperatures. This effect is most pronounced immediately emplacement of the backfill and gradually becomes insignificant with time as temperatures and heat after flux diminish. It is interesting to note that although backfill thermal conductivity affects temperature at the WP, it has little effect on temperature at the drift wall. Temperature at the WP, roof, sidewall, and within the pillar are illustrated in figure 6-6 for a backfill thermal conductivity of 0.2 W/m-K. This figure shows that the temperature at locations other than the WP do not differ significantly with change in thermal conductivity of the backfill. Similarly, backfill thermal conductivity has no appreciable effect on saturation near the drift wall.

Thermal Conductivity

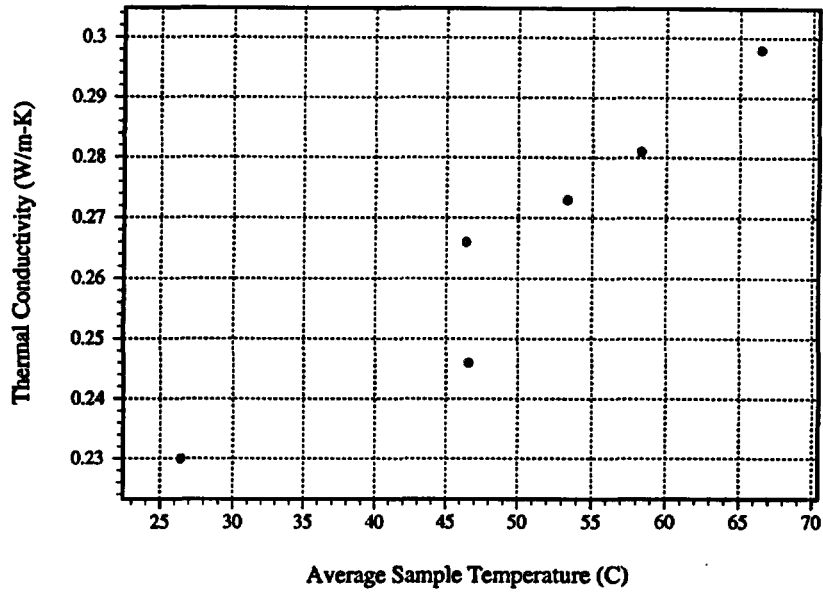


Figure 6-4. Thermal conductivity of dry bulk tuff from the Apache Leap Test site as a function of temperature

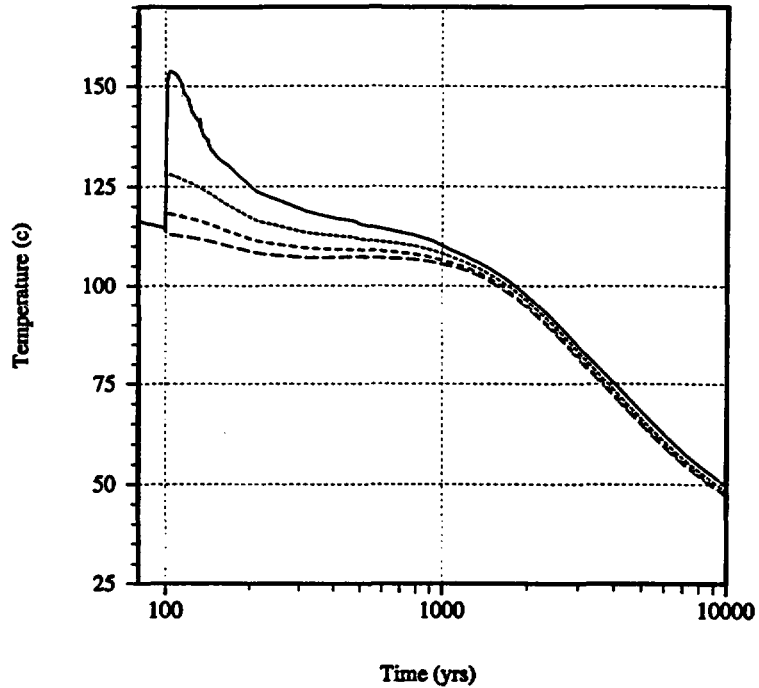


Figure 6-5. Waste package temperature as a function of backfill thermal conductivity of 0.2 (solid line), 0.6 (dotted line), 2.0 (short dash), and 10.0 W/m-K (long dash)

Table 6-3. Unsaturated thermal conductivity measurements of ALTS tuff. Uncertainties in the thermal conductivity values were calculated based on errors in sample thickness, temperature measurement, and accuracy of the heat flux sensors.

Test Number	Temperature of Top Plate (°C)	Temperature of Bottom Plate (°C)	Average Sample Temperature (°C)	Heat Flux (Q) (W/m ²)	Thermal Conductivity (K _T) (W/m-K)
1	23.14	70.00	46.57	75.52	0.246±0.026
2	23.35	69.40	46.38	80.36	0.266±0.028
3	39.94	76.60	58.27	67.59	0.281±0.029
4	40.42	92.44	66.43	101.75	0.298±0.031
5	20.98	85.66	53.22	115.80	0.273±0.029
6	19.53	33.28	26.41	20.74	0.230±0.024

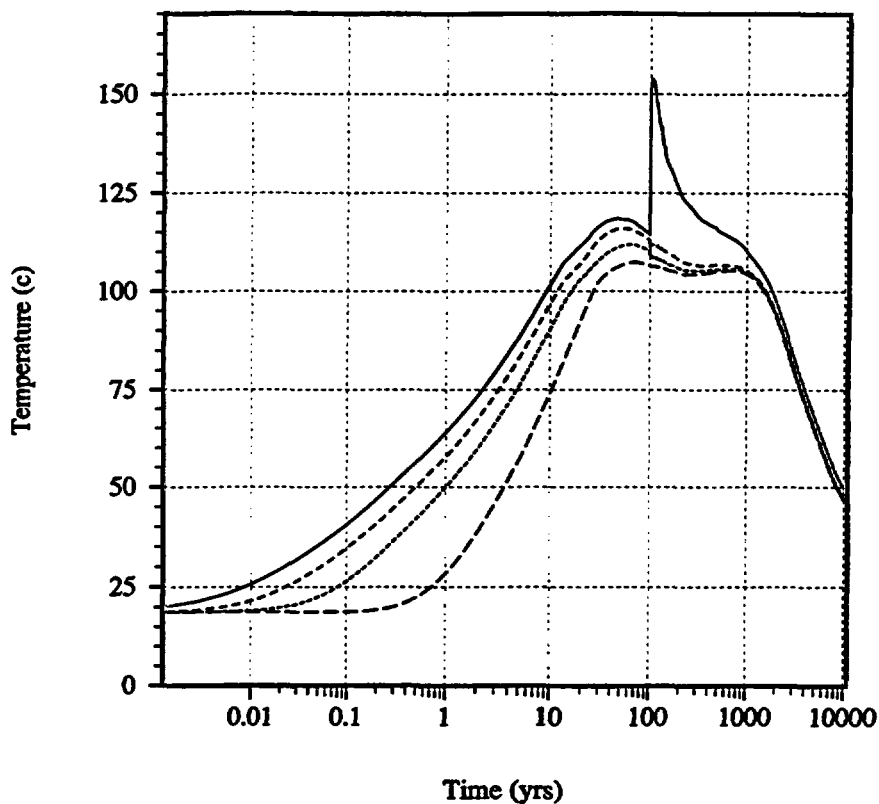


Figure 6-6. Temperature at waste package (solid line), drift roof (dotted line), drift sidewall (short dash), and pillar center (long dash) for backfill with a thermal conductivity of 0.2 W/m-K

6.3.3.2 Effect of Media Properties on Prediction of Moisture Redistribution at Yucca Mountain

Variations in the hydraulic properties of partially saturated porous media can have significant effects on the redistribution of moisture driven by heat generated from HLW emplaced at the proposed geologic repository at YM. The objective of this part of the sensitivity analysis was to evaluate the hydraulic conditions at YM for different, yet reasonable, homogeneous hydraulic property values assigned to the Paintbrush Tuff (PTn) and Calico Hills (CHnv) units located above and below the proposed repository horizon, respectively, in the presence of heat-generating HLW. The six-layer model is similar to that described in the backfill simulations. Model description and basecase properties were taken from TSPA-95 (TRW Environmental Safety Systems, Inc., 1995). Details of the analyses can be found in Green (1996).

In this analysis, the importance of media property values was assessed by how saturation and hydraulic conductivity, $K(\theta)$, are affected in the presence of heat-generating waste at the proposed HLW repository. The hydraulic properties of the PTn and CHnv units were varied to determine their effect on saturation. Saturation of the units alone is of limited use, however, knowledge of saturation and the saturation/pressure relationship of a medium allows calculation of $K(\theta)$, a direct indication of flow rates or groundwater travel times, because the flow of groundwater and any radionuclides released from WP would probably be downward, hydraulic conditions in the unsaturated units below the repository, particularly the CHnv, are of greatest interest.

It was found that saturation of the PTn and CHnv units could be increased from 0.2–0.3 to near full saturation by decreasing either the van Genuchten α or n parameters or by decreasing permeability (van Genuchten, 1980). In general, emplacement of the heat source resulted in negligible moisture change in the PTn, some moisture increase in the CHnv, and significant redistribution of moisture in the tuff units between the PTn and CHnv units in all cases studied. However, there is considerable variability in unsaturated hydraulic conductivity, $K(\theta)$, of CHnv depending on the properties assigned to PTn and CHnv (table 6-4). In particular, $K(\theta)$ for the CHnv directly below the proposed repository decreased by a factor of 10^2 at 100 and 1,000 yr and by 10^4 at 10,000 yr after the onset of heating when the hydraulic properties of the PTn and the CHnv were varied from values given in TSPA-95 (TRW Environmental Safety Systems, Inc., 1995) to values selected from the 1993 DOE Total System Performance Assessment (TSPA-93) report (Wilson et al., 1994). Consequently groundwater flow through the CHnv below the proposed repository would be significantly less if hydraulic properties taken from the TSPA-93 (Wilson et al., 1994) are found to be more appropriate than TSPA-95 (TRW Environmental Safety Systems, Inc., 1995) values. The wide range of values predicted for $K(\theta)$ indicate the large uncertainty (i.e., a factor of 10^2 to 10^4) associated with these calculations.

6.3.3.3 Effects of Ventilation on Rock Dryout and Drift Humidity

The most recent proposed repository designs call for an extended time period up to 150 yr before permanent closure of the proposed repository (TRW Environmental Safety Systems, Inc. 1993, 1994). During this preclosure period, it will be necessary to ventilate the subsurface facility to permit inspection and observation. If ventilation is employed over such a long time, some heat and groundwater will be removed from the facility. The removal of heat will reduce the peak WP temperature and the removal of groundwater will create a drier, less-corrosive environment. Even after permanent closure, ventilation may have some long lasting effects. In most earlier analyses, the proposed repository was assumed to be sealed and both heat and groundwater were conserved within the mountain for thermohydrologic calculations. Motivated by the changing designs, this analysis addresses the effects of ventilation on temperature reduction and groundwater removal. If ventilation is found to have a significant

Table 6-4. Saturation and unsaturated hydraulic conductivity (m/s) in CHnv at 100, 1,000, and 10,000 y for TSPA-95 (TRW Environmental Safety Systems, Inc., 1995) basecase and TSPA-93 (Wilson et al., 1994)

Case	100 yr		1,000 yr		10,000 yr	
	θ	K(θ)	θ	K(θ)	θ	K(θ)
TSPA-95	0.25	1.03e-9	0.28	1.89e-9	0.18	3.51e-10
TSPA-93	0.21	1.46e-11	0.24	2.55e-11	0.07	5.46e-14

impact on the WP environment, then it may be incorporated in future designs and TSPAs (Nuclear Regulatory Commission, 1995; TRW Environmental Safety Systems, Inc., 1995).

During the construction and operation of the proposed repository, ventilation will be used to provide oxygen to workers. Current designs call for a minimum ventilation capacity of 125 m³/s of air for normal operations and a maximum of nearly 600 m³/s for cooling if needed (TRW Environmental Safety Systems, Inc., 1994). The potential for groundwater removal is great because of increased underground temperatures (i.e., more moisture can be contained in a cubic meter of air when temperatures are increased). But because the permeability of the subsurface rock is low for liquid flow, the groundwater will not readily flow into the drifts. A reasonably conservative approach is to assume that the groundwater is immobile and does not flow to the drift walls. The groundwater in the host rock will vaporize *in situ* as if a vaporization front penetrates into the medium. After being vaporized, the water can flow due to gas pressure differences or by molecular diffusion. The gaseous permeability of a fractured rock mass is generally orders of magnitude greater than the liquid permeability so that small pressure gradients can motivate significant amounts of gas flow. At this time, the gradient in gas pressure was neglected because ventilation can strongly affect gas pressures in the drift. Ventilation could be used to maintain low gas pressures in the drift, hence drawing vapor into the drift and increasing groundwater mechanism. Hence, this work underestimates the removal of groundwater due to ventilation.

In this work, a drift-scale model was used to predict the three-dimensional (3D) transient temperature field in the vicinity of an emplacement drift. The model extends from the ground surface to the proposed repository horizon (~350 m below the ground surface and ~250 m above the water table) to 750 m below the water table. The model consisted of seven homogenous but distinct layers of rock whose thermal properties were based on Wilson et al. (1994) that are primarily from DOE (1993). The spacing between WP along a drift and the spacing between parallel drifts affect the areal mass loading (AML). To study the effects of ventilation, an intermediate AML of 40 MTU/acre was used. In the model, heat flux applied to the drift wall was reduced to compensate for heat removed by sensible heating of the ventilated air and latent heating of the vaporized groundwater. Figure 6-7 shows three thermal sources histories considered. The reference case (first scheme) has no ventilation. The other two cases are considered to evaluate the potential effects from increased heat removal by ventilation and are discussed in Manteufel (1996). In all three cases the drift has been filled with backfill materials 150 yr after the onset of heating and there is no additional ventilation.

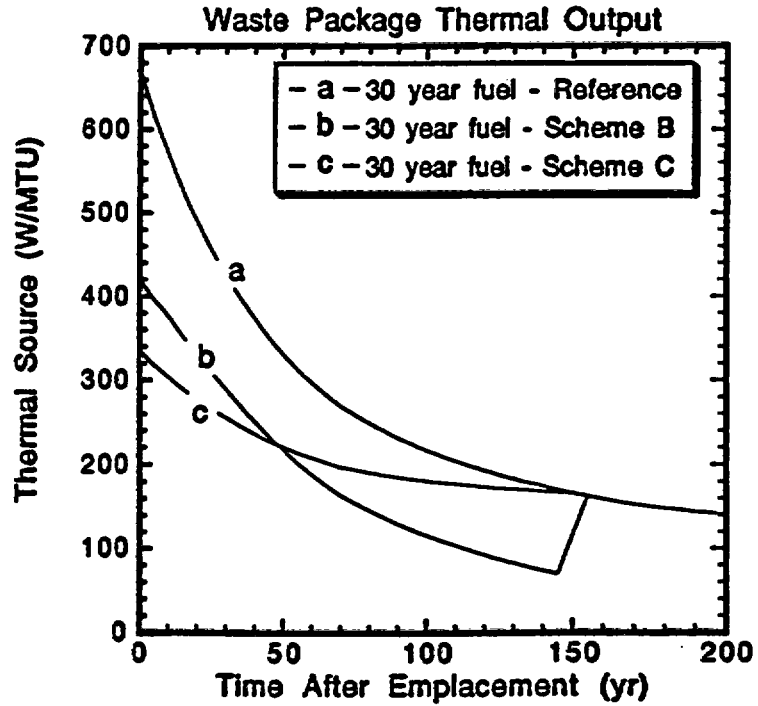


Figure 6-7. Thermal output of waste package for no ventilation (reference scheme, 30 yr old fuel) and two ventilation schemes

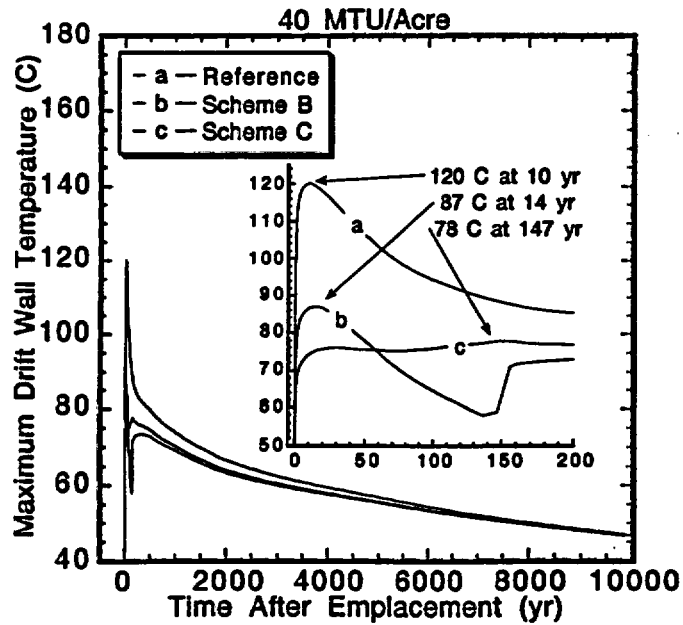


Figure 6-8. Maximum drift wall temperature for three schemes

Figure 6-8 illustrates maximum drift wall temperatures to 10,000 yr. Both ventilation cases have a strong effect on the wall temperature to 150 yr. Without ventilation, the maximum temperature is 120 °C at 10 yr. With ventilation, the temperature is either 33 °C lower (87 °C at 14 yr) or 42 °C lower (78 °C at 147 yr). Both ventilation schemes moderate the wall temperature over time. Scheme C gives the most steady temperature profile with the maximum wall temperature maintained about 75 °C for at least the first 200 yr. The long-term effects are less significant between schemes. After 1,000 yr the wall temperatures are within 10 °C for all schemes and the differences continue to diminish with time.

A model was also developed to predict the rate and extent of dryout. The model is based on immobile groundwater that is locally vaporized. This model is reasonably conservative and is expected to predict the minimum rate of dryout. Other mechanisms and features that would enhance dryout are not included such as lower gas pressures in the drift and the existence of fractures through which vapor can more readily flow into the drift. Both schemes produced nearly the same wall temperatures and about the same dryout. The dryout is diffusion limited hence, the position of the vaporization front scales with the square root of time. This implies the vapor mass flux into the drift scales as the inverse of the square root of time. Over 150 yr, the extent of dryout is predicted to be about 4 to 5 m for either ventilation scheme.

In summary, these results suggest that ventilation during the first 150 yr can moderate underground temperatures. For two hypothetical yet plausible ventilation schemes, the maximum drift wall temperature was 87 °C at 14 yr and 78 °C at 147 yr as compared with 120 °C at 10 yr without ventilation. In addition to extracting heat, ventilation provides a removal mechanism for water vapor. The extent of dryout was about 4 to 5 m over 150 yr for both cases. This suggests that ventilation can be an effective thermal management tool in addition to AML (drift and WP spacing) and age of waste. In future prelicensing interactions with the DOE, it will be suggested that the possible benefits of long-term ventilation be explored.

6.3.3.4 Effects of Geologic Structure and Features on the Evolution of Perched Water Bodies

The formation of perched water bodies either above, within, and below the proposed repository horizon can potentially cause, at some point in time, liquid water to contact or elevated humidity to exist near waste canisters. The exposure of WP to water could in turn increase the rate of waste canister failure resulting in greater releases of radionuclides. In general, perched water bodies tend to be transient features formed where there is a contrast in hydrologic properties (Freeze and Cherry, 1979). Contrasts may result from differences at boundaries between various ash flows and also by low hydraulic conductivity strata being adjacent to more permeable and conductive strata along structural features such as faults or other persistent discontinuities. YM is dissected by numerous faults (Frizzell and Shulters, 1990), thus substantially increasing the probability of locally saturated conditions occurring.

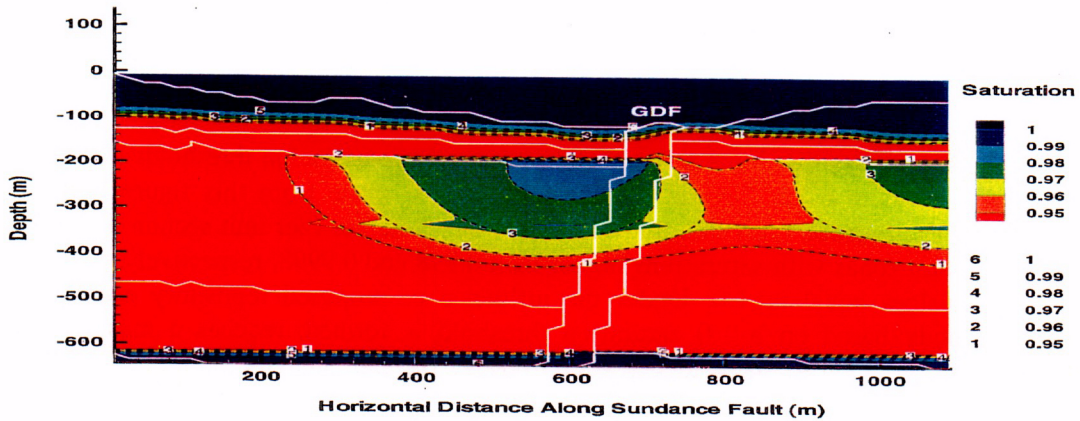
It has been hypothesized that in the vicinity of the proposed repository rock drying by repository heat may cause perched water zones to form. This process involves vaporization of water around the proposed repository. It is expected that water vaporized by radiogenic heat will move away from the waste canisters until it reaches a location where the rock temperature is low enough to permit condensation. If the condensed water encounters low permeability material, rock water saturations may increase and form a perched zone. These multiphase flow conditions and their effects on the formation and dissipation of perched water bodies could significantly affect the performance of waste canisters in a repository. Sensitivity analyses have been performed using MULTIFLO to simulate the evolution of perched water bodies in the presence of heat-generating HLW at YM. As an initial component to these analyses, the presence of pre-existing perched water bodies at YM was first assessed. Second, the further evolution of perched water induced by multiphase conditions was numerically simulated.

The geographical area considered for this analysis is the vicinity of the intersection of Ghost Dance fault (GDF) and Sundance fault in the proposed repository area of the YM site. The modeled area is a north-facing, 2D vertical section along the Sundance Fault, 1,100 m wide by 650 m deep, taken from the CNWRA Geological Framework Model (GFM). Note that the effects of the Sundance Fault are not considered in these analyses. The area of interest is above the water table and primarily updip of GDF. GFM includes lithostratigraphy, hydrostratigraphy, and geologic structure (Stirewalt et al., 1994; Stirewalt and Henderson, 1995) of the YM region. Lithostratigraphy and geologic structure are based on surface geologic maps of the site (Scott and Bonk, 1984). Subsurface geology is constrained by borehole data from the DOE site characterization activities (e.g., Flint and Flint, 1990) and through construction of balanced cross sections. Thermal and hydrologic property values assigned to the matrix of each of the different lithostratigraphic units were assumed homogeneous and isotropic. Data used in this study were adopted from TSPA-95 (TRW Environmental Safety Systems, Inc., 1995). The GDF was modeled only as a geological boundary, without any specific properties assigned. If the GDF acted as a conduit to flow, the formation of a perched water zone updip of the fault may be suppressed. Future work will address the behavior of the flow system taking into consideration fault properties. The lithostratigraphic units represented in the model are (from top to bottom): (i) Tiva Canyon Welded (TCw), (ii) PTn, (iii) TSw 1,2,3, (iv) CHn, and (v) Prow Pass Welded (PPw).

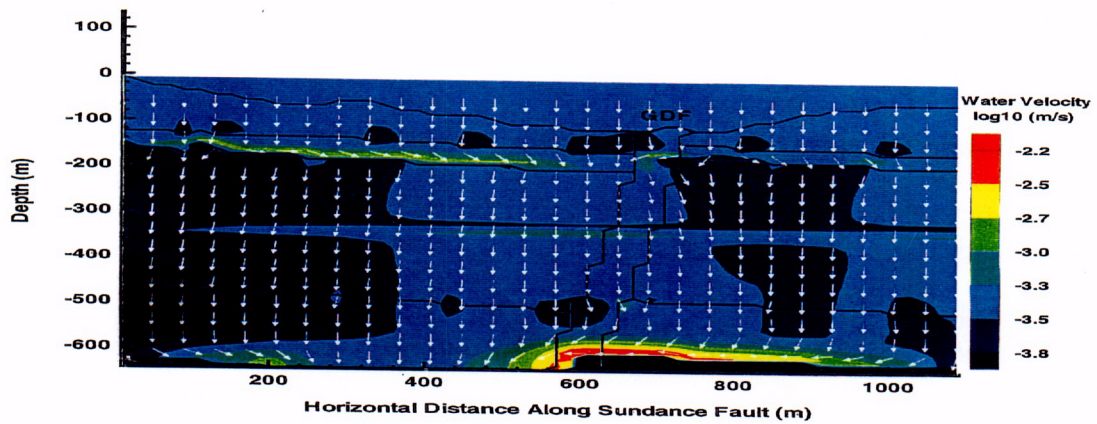
The spatial mesh of this model is rectangular with a $\Delta x=20$ -m and $\Delta z=10$ -m (x and z are horizontal and vertical directions respectively). The left and right boundaries are no-flow, the top boundary is constant flux, and the bottom boundary is a water table condition. A uniform initial saturation value of 0.25, corresponding to the bubbling pressure for most YM units, was assigned to the entire modeled region. Initial conditions were based on a constant flux rate of 0.3 mm/yr, similar to TSPA-95 (TRW Environmental Safety, Systems, Inc., 1995). Solution of the transient flow equation under isothermal conditions produced pressure head results, transformed to saturation values. These saturations indicated the presence of existing perched water zones. At various points in time, the volume of moisture within zones with saturation equal to or in excess of an *a priori* selected saturation value (typically 0.998, 0.9998, and 1.00) was then calculated, thus providing the time variation of the perched water volume.

Under the influence of a constant surface flux of 0.3 mm/yr and isothermal conditions, the flow system exhibits the following behavior. The PTn unit, having a high permeability, allows water to flow freely down through it. When the water encounters the TSw unit with low permeability, downward flow is inhibited. This causes the water to be channelled downdip in the PTn until it reaches the GDF. The footwall of the fault has been uplifted so that the PTn in the hangingwall is juxtaposed against the relatively impermeable TSw unit in the footwall of the fault. This produces a trap where water begins to accumulate producing a perched water zone. As it continues to accumulate, some water percolates slowly downward through the TSw unit, extending the perched water body well into the TSw unit. The perched body continues to grow as long as inflowing water exceeds the rate at which water percolates through the TSw. The simulated perched zone attains a steady-state condition characterized by high saturation values (i.e., 0.99 and higher) immediately updip of the GDF (figure 6-9a).

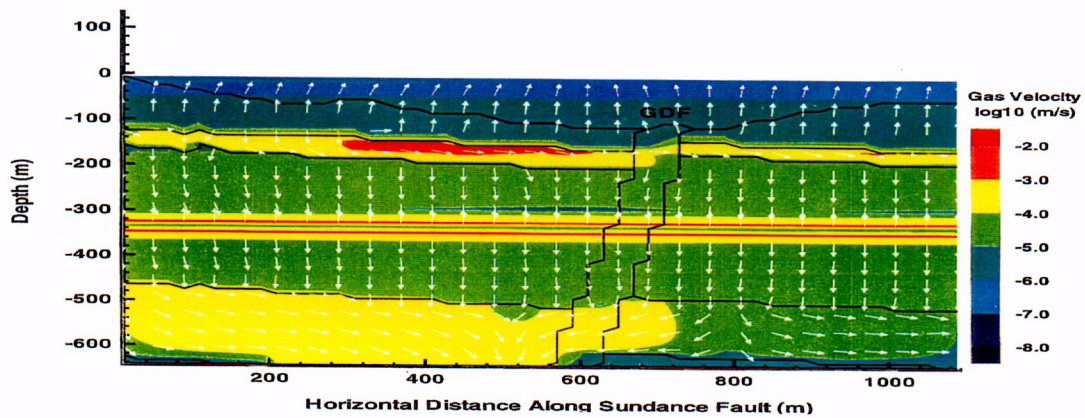
The isothermal results were used as the initial condition for the nonisothermal analysis. A uniform thermal load of 83 MTU/acre was applied over the entire simulated repository (1,100 m long by 10 m thick) at a depth of 340 m below the top boundary. The time history of the heat load was taken from TSPA-95 (TRW Environmental Safety Systems, Inc., 1995). In less than one yr after the onset of heating, the thermal effects of the proposed repository are manifested by increased saturation and liquid and gas phase velocities within the proposed repository horizon (figure 6-9a,b,c). These effects are amplified beneath the area of highest saturation values predicted for prerepository conditions. As time progresses, a high saturation zone develops at the proposed repository horizon, immediately updip of the GDF. The



(a)



(b)



(c)

Figure 6-9. Results of nonisothermal flow analyses after 1 yr of repository heating with isothermal analyses steady-state results as initial conditions. Solid white lines represent the geologic structure and topographic relief, (a) Saturation, dashed black lines correspond to steady-state saturation values obtained from isothermal analyses; (b) liquid-phase velocity; and (c) gas-phase velocity.

C-05

size of the perched water volume increases with time, reaches a maximum value at about 100 yr (figure 6-10), starts decreasing under the influence of elevated temperatures, and is no longer evident by 250 yr (figure 6-11). The proposed repository eventually dries out completely by 1,000 yr.

The time varying volume of perched water for three saturation thresholds (0.998, 0.9998, and 1.00) is shown in figure 6-12. Several observations can be made from this figure. First, though the isothermal analyses produced high saturations giving water volumes (per unit section thickness) of 7,500 and 4,800 m³ within zones with saturations higher than 0.998 and 0.9998, respectively, there was no zone with saturation values equal to 1.0. Under the influence of proposed repository heating, however, a perched water body based on a 1.0 saturation threshold is formed, reaches a maximum volume of 4,000 m³ after 100 yr, and dissipates totally after 1,000 yr. Similar behavior is exhibited by the other two threshold saturations with the exception that the maximum volume occurs around 45 yr followed by an abrupt decrease in the volume. The abrupt decrease in volume for both the 0.998 and 0.9998 saturation values is attributed to condensation effects caused by the thermal pulse having been reached and moved beyond the area of high saturation under isothermal conditions.

It is also worth noting that even though the multiphase effects of proposed repository heating are rapidly propagated throughout the model domain, a long time is required for the thermohydrologic system to return to its preheating state. As illustrated in figure 6-13, this difference is easily seen in the comparison of the liquid phase velocity magnitude contours and direction vectors after a period of 10,000 yr with those simulated for preexisting isothermal conditions (figure 6-9b).

Model results were examined to understand the physical phenomena associated with formation of perched water bodies in the vicinity of the proposed repository under nonisothermal conditions. The introduction of heating causes general movement of gas (water vapor) away from the proposed repository area, whereas water movement directional patterns remain essentially the same as were established prior to proposed repository heating. The combined effect of water accumulation and gas expulsion leads to the development of full saturation, first in the preheating zone of highest saturation. The volume of the full saturation zone initially increases with time and later migrates downwards to a depth of about 360–400 m that is below the proposed repository level. Thereafter, the saturation zone begins to break up and eventually disappears.

Results calculated in this sensitivity analysis indicate that the initial effect of proposed repository heating (under the condition of steady averaged infiltration) can lead to increased water saturation within the proposed repository area. Such increased saturation may result in sustained perched water volumes that grow in size within the first 100 yr of proposed repository heating and begin to dissipate thereafter. The specific effects of such perched water zones on the total system performance have not yet been assessed, however, elevated saturated levels at the proposed repository horizon could affect WP corrosion rates and subsequent radionuclide transport.

6.3.3.5 Effects of High Permeability Features on Temperature and Saturation

Numerical analyses were conducted to assess what effect a zone of higher permeability intersecting the drift would have on the thermohydrology of the drift. This effect was assessed for temperature, saturation, and relative humidity within the drift and at the drift wall. The model extended vertically from the ground surface to the water table and horizontally from the center line of the drift to the mid-distance separating drifts. Rock mass was represented as an ECM. Material properties were taken from TSPA-95 (TRW Environmental Safety Systems, Inc., 1995). Initial conditions were determined for

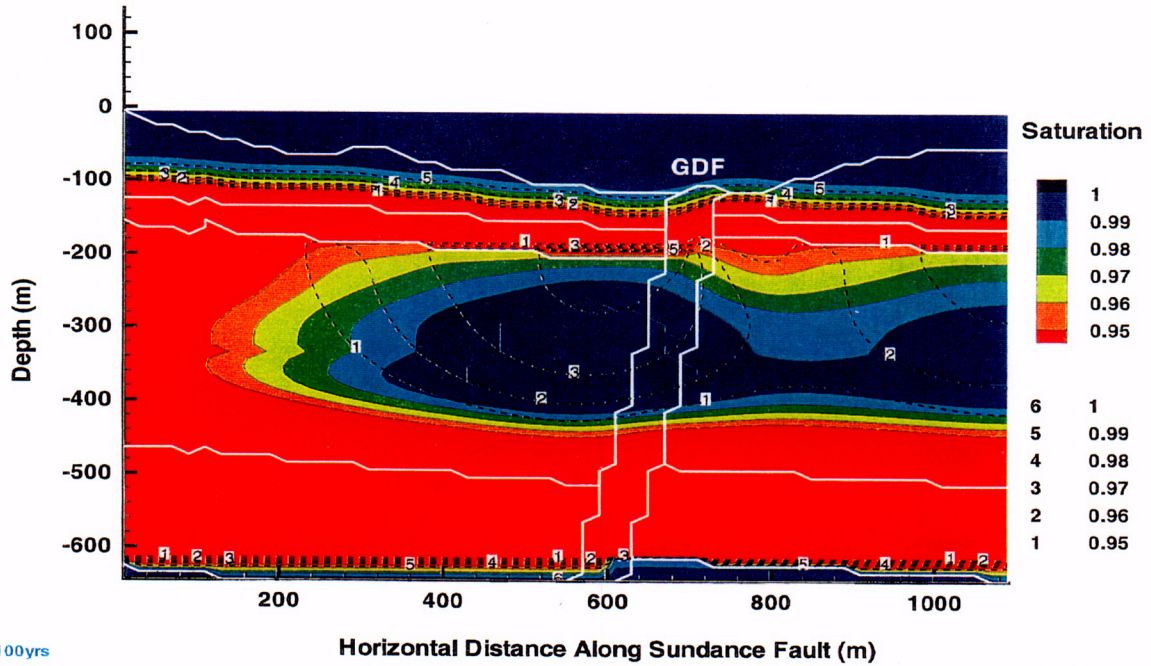


Figure 6-10. Saturation after 100 yr of heating. Dashed black lines correspond to steady-state saturation values obtained from isothermal analyses.

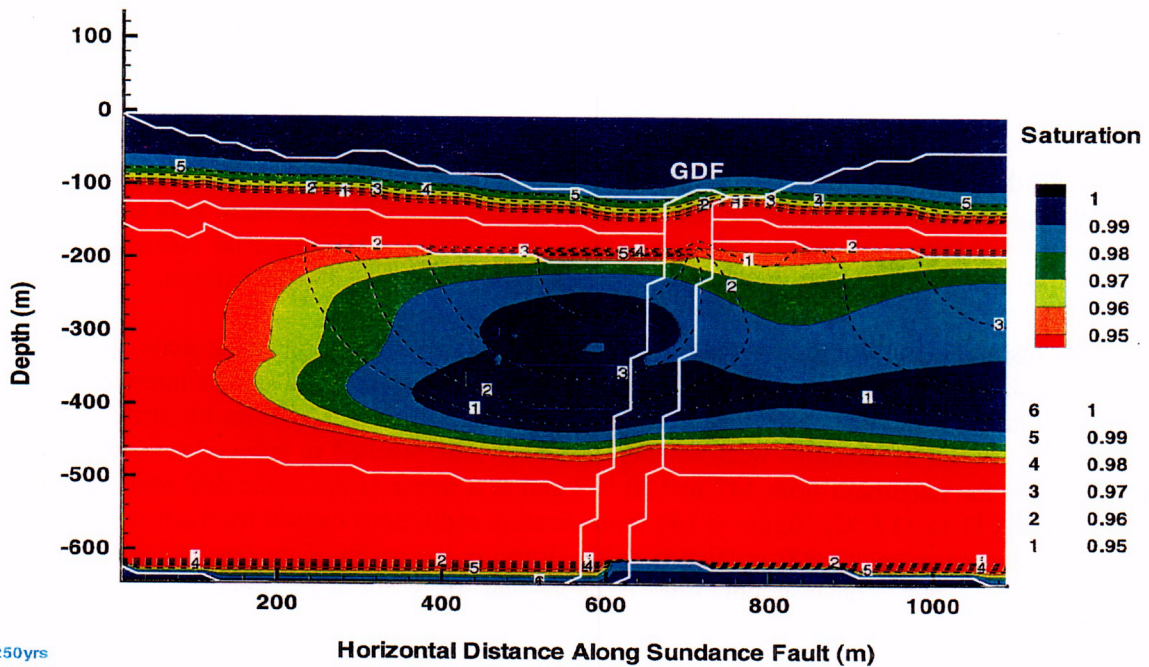


Figure 6-11. Saturation after 250 yr of heating. Dashed black lines correspond to steady-state saturation values obtained from isothermal analyses.

C-06

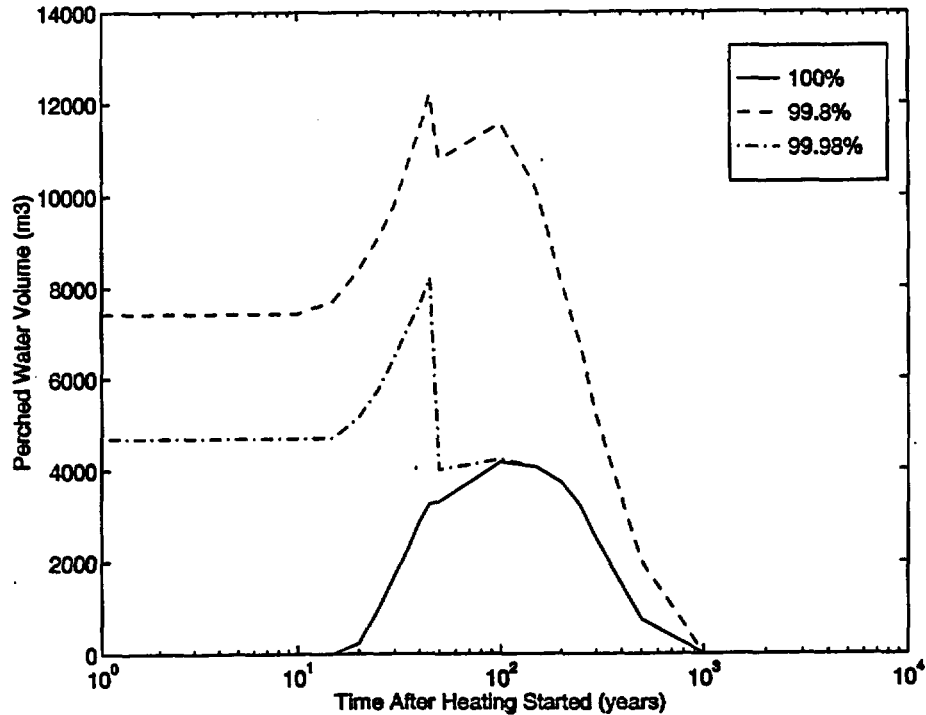


Figure 6-12. Time history of water volume for parts of the domain with saturations higher or equal to 0.998, 0.9998, and 1.00

a uniform infiltration rate of 0.3 mm/yr applied at the upper boundary. Fracture zones that extended from ground surface to the water table and intersected the drifts were simulated. Fracture zone widths varied from 1 to 140 cm. The fracture zones were assigned permeabilities a factor of five greater than that assigned to the matrix of the TSw and a factor of ten less than the permeability assigned to fractures in the TSw. An exponentially decaying heat load with an AML of 83 MTU/acre was assigned to the WP. The void of the drift was initially left empty then filled with backfill material 100 yr after the onset of heating. The MULTIFLO code (Seth and Lichtner, 1996) was used in all analyses.

Simulations conducted with ECM properties assigned to the rock mass were compared to similar simulations but with vertically oriented fracture zones of variable widths intersecting the drift. In general, simulations with fracture zones allowed gas and heat to escape from the drift more easily than was experienced for simulations with no fracture zone. This resulted in reduced temperatures at the WP (a decrease in the maximum from 147 to 120 °C) and to a lesser extent at the drift wall (a decrease in the maximum of 131 to 117 °C) (figure 6-14). Temperature reductions caused by fracture zones persisted at the WP for approximately 3,000 yr (figure 6-15). Varying the width of the fracture zone to about 20 cm indicated that the reduction in temperature is dependent on width of the fracture zone. Increases in the fracture zone width greater than 20 cm however, did not result in any additional decrease in temperature. For example, the 25 °C decrease in temperature at the WP and the 15 °C temperature decrease at the drift wall for a 20 cm wide fracture zone were approximately the same as predicted for fracture zones that vary in width from 20 to 140 cm (figure 6-14). The cause of the slight increase in temperature predicted for fracture zones greater than 80 cm was not identified but may have resulted from excessively coarse numerical discretization.

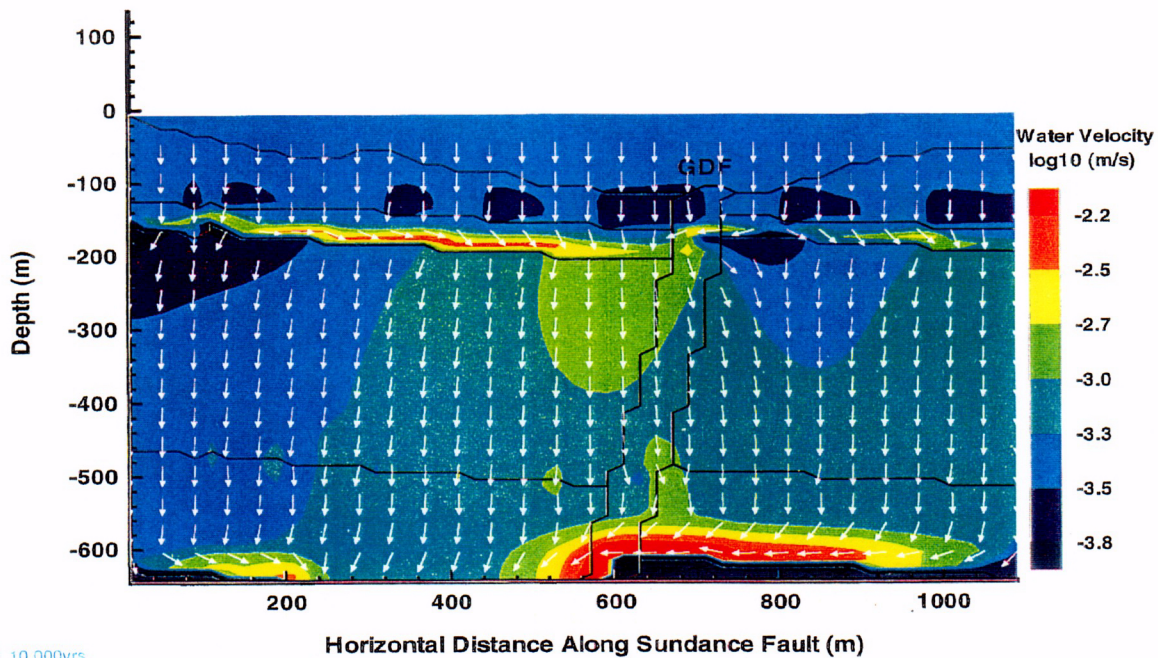


Figure 6-13. Liquid-phase velocity magnitude contours and direction vectors at 10,000 yr

The results of this analysis are consistent with analyses by Buscheck and Nitao (1995), both indicating that the high permeable features that intersect the drift result in lower temperatures at both the WP and at the drift wall. Although a 15 to 25 °C drop in drift wall temperature may not seem consequential, particularly relative to the high level of uncertainty associated with the predictions, temperature decreases from 131 to 117 °C at the drift wall can have added significance. Lower drift wall temperatures permit refluxing waters to approach more closely to the drift wall before vaporizing. There is also the added possibility of liquid water being present near the drift wall at temperatures greater than 100 °C as a result of elevated salt content and capillary pressure. These effects combine to increase the potential for flow down fractures near the drift wall and dripping into the drift, possibly onto WP. Water dripping onto canisters heated to above 100 °C has been experienced during field-scale heater tests in heater tests at G-tunnel, Climax, and at the Apache Leap Test site. Based on these observations, the effect of high permeability features such as these should be considered when evaluating the validity of conceptual models and performing assessments of various thermal loading strategies.

6.3.3.6 Summary of Sensitivity Analyses

Results from the previous sensitivity analyses provide some insight to the importance of thermal and hydraulic properties, geologic features, and their attendant impact on heat and mass transfer mechanisms. Use of backfill materials is found to affect the temperature and saturation within the drift and within the first few meters of rock near the drift. The transient magnitude of these effects has been quantitatively determined, thus contributing to the subissues of the TEF KTI, namely assessing the bounds of thermally induced flux in the near field and humidity at the WP surface. In addition, the knowledge gained will be useful to future reviews of the DOE thermohydrology program.

Peak Temperature at 83 kW/Ac

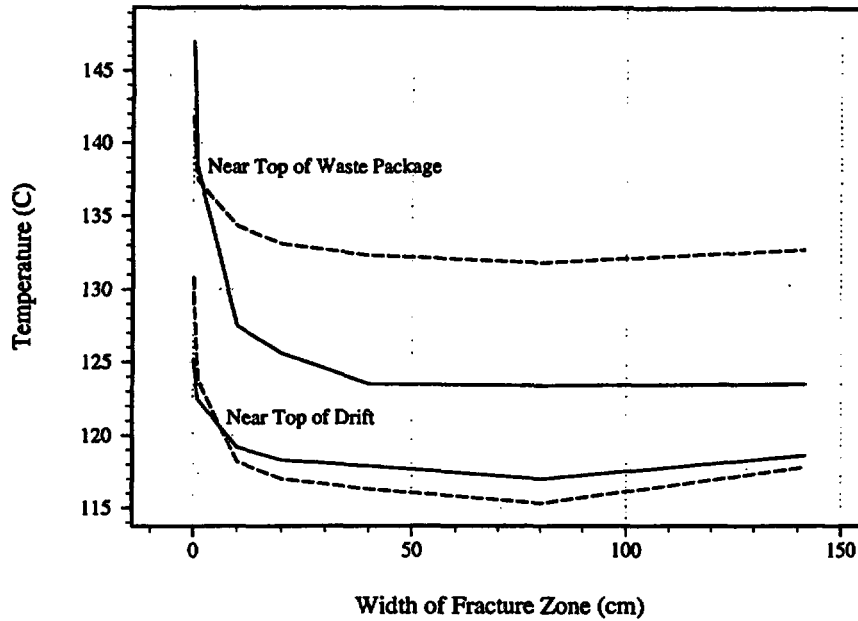


Figure 6-14. Maximum temperature before backfill (dashed line) and after backfill (solid line) at waste package and drift roof as a function of width of a vertically oriented fracture zone intersecting drift

Effect of Fracture Zone on Temperature (83 kW/Ac)

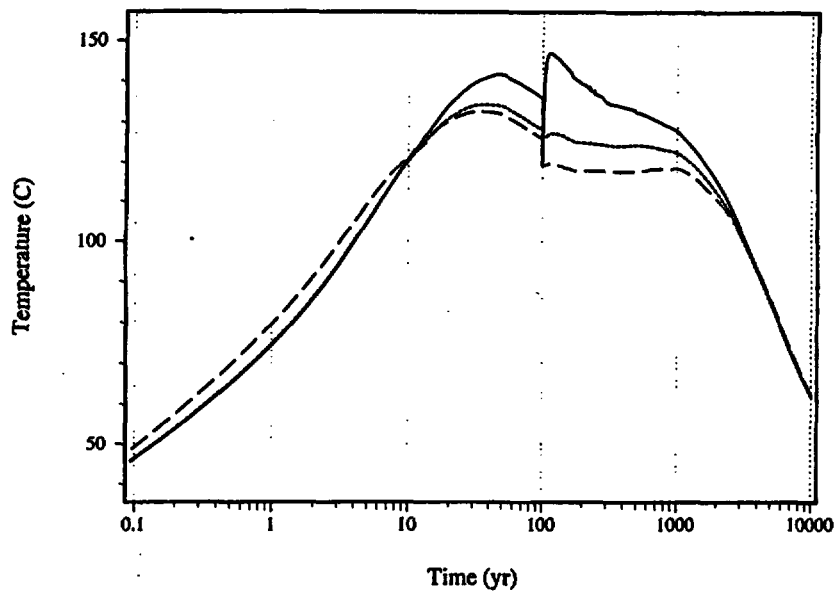


Figure 6-15. Maximum waste package temperature with no fracture (solid line), a 10-cm wide fracture zone (dotted line), and a 140-cm wide fracture zone (dashed line)

The hydraulic properties of two stratigraphic units, the PTn and CHnv, have proved to have a significant effect on flow of water below the repository horizon, in particular, flow through the CHnv. Similarly, ventilation through the drift and geologic features and structures with hydraulic properties different from the rock matrix could have a significant effect on temperature, saturation, and relative humidity within the drift and within the first few meters of rock near the drift. This information contributes directly to the subissue that addresses the bounds of thermally induced flux in the near field.

6.4 ASSESSMENT OF PROGRESS TOWARD MEETING OBJECTIVES

The results of activities conducted in the TEF KTI during FY96 contributed to the reduction of uncertainties associated with the subissues listed in section 6.1. Work was prioritized to identify tasks whose resolution is both achievable within available resources and able to provide significant reduction in uncertainty relative to committed resources. Tasks designed to reduce uncertainties in these subissues in FY96 are both reactive and proactive: (i) review and evaluate the DOE thermohydrology program, including the DOE peer review activity; (ii) benchmark testing of computer codes; (iii) provide sensitivity analyses; and (iv) evaluate conceptual models.

Review and evaluation of the DOE thermohydrology program included review of a DOE PRT, the DOE response to peer review recommendations, the peer review response to the DOE response to PRT recommendations, attendance at an Appendix 7 meeting on ESF thermal testing including site visit, and participation at a DOE/NRC ESF video conference. The review concluded that the DOE Thermohydrologic Testing and Modeling Program, as represented in the information available for this review, does not adequately address several technical issues. It was noted in this review and in PRT recommendations that the DOE has not demonstrated that it has plans to evaluate the alternative conceptual models as rigorously as needed. It is possible that heater tests designed for conditions different from those expected at the proposed repository may provide misleading results. For example, results from a heater test with an excessively high heat load (e.g., one that results in drift wall temperature > 200 °C) may support an ECM conceptual model since high drift wall temperatures (i.e. > 200 °C) could limit the occurrence of reflux dripping into the drift. However, potential difficulties could arise because the ECM might not accurately incorporate important moisture redistribution mechanisms, such as refluxing and dripping, that would be experienced under proposed repository conditions. Additionally, neither the PRT report nor the DOE response to PRT recommendations recognize the potential significance of thermal-hydrological-chemical coupled effects. It was noted that the discontinuance of surface based hydrologic testing may result in unacceptably high uncertainty in infiltration estimates at YM. It is important the DOE Thermohydrological Testing and Modeling Program be designed to address these issues. The comments and recommendations made on the DOE thermohydrology testing and modeling program will provide input to the basis for the resolution in FY97 of the subissue on the sufficiency of the DOE thermal testing program to assess the likelihood of gravity driven refluxing occurring in the near field.

Sensitivity and numerical scoping analyses helped identify the relative importance of specific types of information that contribute to the evaluation of thermally driven moisture through partially saturated fractured rock. It was observed that the emplacement, initial saturation, and thermal conductivity of backfill may be important during those times of the heating period when WP temperatures are high. Conceptual uncertainty regarding the effect of backfill materials has been reduced in the sense of delineating cause and effect relationships, however, the full effect of drift ventilation is not fully resolved. Analyses indicated that selective use of geologic materials that exhibit particularly low thermal conductivities can elevate WP temperatures and decrease drift wall temperatures. The hydraulic

characteristics of particular key geologic units, namely the nonwelded PTn and CHnv whose properties are inherently different from the welded tuffs most common at YM, can have a significant effect on flow through the nonwelded units below the proposed repository horizon (i.e. reasonable variations in hydraulic properties assigned to the PTn and CHnv can result in a factor of 10^4 change in the unsaturated hydraulic conductivity of the CHnv). In summary, these sensitivity analyses identified the relative importance of specific features of the proposed repository site and design. These will provide additional input to the basis for the resolution in FY97 of the subissue on the sufficiency of the DOE thermal testing program to assess the likelihood of gravity driven refluxing occurring in the near field.

Results from a repository-scale model that assumes a constant infiltration rate of 0.3 mm/yr and geologic structure but assumes that each of the hydrostratigraphic units is homogeneous and represented by a uniform matrix continuum indicated that the initial effect of repository heating can lead to increased water saturation within the proposed repository area. Such increased saturation may result in sustained perched water volumes that grow in size within the first 100 yr of proposed repository heating and begin to dissipate thereafter.

The DOE thermohydrologic codes TOUGH2 and FEHM were benchmark tested against the NRC/CNWRA codes CTOUGH and MULTIFLO. In general, the benchmark testing showed that three of the four codes tested (TOUGH2, CTOUGH, and MULTIFLO) appear to possess sufficient capability to simulate the wide range of hydrologic and thermohydrologic conditions expected to be important at the proposed HLW repository at YM. The primary differences noted were in computational efficiency and it was found that the MULTIFLO code was substantially faster than the other codes. The fourth code, FEHM, experienced computational difficulties in two test cases; one with high infiltration rates and the other with flow in fracture-porous media. This testing has provided confidence that the use of distinct thermohydrologic codes will not produce contentious methodology issues.

There remain two areas that still contribute to the uncertainty in resolving the subissues in the TEF KTI. There remain high levels of uncertainty regarding the effects of heterogeneities and geologic structure on thermally driven moisture movement, even though some insight has been gained in this area. A second major contributor to the high level of uncertainty in this KTI is the absence of evidence to support a particular conceptual model that is adequately representative of the heat and mass transfer mechanisms present in partially saturated fractured porous rock. These two areas are target areas of future studies and evaluations for resolution in FY98 of the subissue on the adequacy of the DOE thermal modeling approach for assessing the nature and bounds of thermally induced flux in the near field.

6.5 INTEGRATION WITH OTHER KEY TECHNICAL ISSUES

Information gained in the conduct of the TEF KTI is provided to other KTIs. Similarly information from other KTIs contribute to the information base from which the TEF KTI is resolved. Included here is a summary of the integration of the TEF KTI with other KTIs.

The Unsaturated and Saturated Flow Under Isothermal Conditions (USFIC) KTI provided initial saturation conditions and infiltration boundary conditions to the TEF KTI. Techniques for modeling fault hydraulic properties and flow in fractured medium that are being developed in the TEF KTI will be provided to the USFIC KTI for modeling of isothermal flow. The Structural Deformation and Seismicity KTI provided updated hydrostratigraphy and structural features information to the TEF KTI.

The TEF KTI provided to the Container Life and Source Term KTI updated values of waste package temperature, saturation distributions, and relative humidity for use in EBSPAC analysis. Similarly, the TEF KTI provided to the Evolution of the Near-Field Environment KTI updated values of temperature, saturation distribution, and relative humidity in the near field. Fracture aperture changes calculated by the Repository Design and Thermal-Mechanical Effects KTI were provided to the TEF KTI for use in these sensitivity analyses.

The TEF KTI provided thermohydrologic analyses to the Total System Performance Assessment and Technical Integration KTI for the audit review of TSPA-95 (TRW Environmental Safety Systems, Inc., 1995) and will provide additional information for the detailed review and input to the TSPA code. Specifically, the TEF KTI provided time-dependent waste package temperature and relative humidity at the waste package for proposed repository AMLs.

6.6 REFERENCES

- Baca, R.G., and M.S. Seth. 1996. *Benchmark Testing of Thermohydrologic Computer Codes*. CNWRA 96-003. San Antonio, TX: Center for Nuclear Waste Regulatory Analyses.
- Buscheck, T.A., and J.J. Nitao. 1995. *Thermal-Hydrological Analysis of Large-Scale Thermal Tests in the Exploratory Studies Facility at Yucca Mountain*. UCRL-ID-121791. Livermore, CA: Lawrence Livermore National Laboratory.
- Buscheck, T.A., J.J. Nitao, and L.D. Ramspott. 1995. Localized dryout: An approach for managing the thermal-hydrological effects of decay heat at Yucca Mountain. *Proceedings of the XIX International Symposium on the Scientific Basis for Nuclear Waste Management*. Pittsburgh, PA: Materials Research Society.
- Flint, L.E., and A.L. Flint. 1990. *Preliminary Permeability and Water-Retention Data for Nonwelded and Bedded Tuff Samples, Yucca Mountain Area, Nye County, Nevada*. U.S. Geological Survey Open-File Report 90-569. Denver, CO: U.S. Geological Survey.
- Freeze, A.R., and J.A. Cherry, 1979. *Groundwater*. Englewood Cliffs, NJ: Prentice-Hall.
- Frizzell, V.A., Jr., and J. Shulters. 1990. *Geologic Map of the Nevada Test Site, Southern Nevada*. U.S. Geological Survey Miscellaneous Investigations Series Map I-2046, Scale 1:100,000. Denver, CO: U.S. Geological Survey.
- Green R.T. 1996. The effect of media properties on prediction of moisture redistribution at a high-level nuclear waste repository. *Proceedings of the Seventh Annual International Conference on High-Level Radioactive Waste Management*. La Grange, Park, IL: American Nuclear Society.
- Green, R.T., G. Rice, and K.A. Meyer. 1995. *Hydraulic Characterization of Hydrothermally Altered Nopal Tuff*. NUREG/CR-6356. Washington, DC: Nuclear Regulatory Commission.
- Klavetter, E.A., and R.R. Peters. 1986. *Estimation of Hydrologic Properties of an Unsaturated, Fractured Rock Mass*. SAND84-2642. Albuquerque, NM: Sandia National Laboratory.

- Lappin, A.R. 1980. *Thermal Conductivity of Silicic Tuffs: Predictive Formalism and Comparison with Preliminary Experimental Results*. SAND80-0769. Albuquerque, NM: Sandia National Laboratories.
- Lappin, A.R., and F.B. Nimick. 1985. *Bulk and Thermal properties of the Functional Tuffaceous Beds in Boreholes USW G-1, UE-25a#1, and USW G-2, Yucca Mountain, Nevada*. SAND82-1434. Albuquerque, NM: Sandia National Laboratories.
- Lappin, A.R., R.G. van Buskirk, D.O. Enniss, S.W. Butters, F.M. Prater, C.S. Muller, and J.L. Bergosh. 1982. *Thermal Conductivity, Bulk Properties, and Thermal Stratigraphy of Silicic Tuffs from the Upper Portion of Hole USW-G1, Yucca Mountain, Nye County, Nevada*. SAND81-1873. Albuquerque, NM: Sandia National Laboratories.
- Lichtner, P.C. 1994. *Multi-Phase Reactive Transport Theory*. CNWRA 94-018. San Antonio, TX: Center for Nuclear Waste Regulatory Analyses.
- Lichtner, P.C., and M. Seth. 1996. Multiphase-multicomponent nonisothermal reactive transport in partially saturated porous media: Application to the Proposed Yucca Mountain HLW Repository. *Proceedings of the International Conference on Deep Geologic Disposal of Radioactive Waste. Canadian Nuclear Society, September 16-19*. Winnipeg, Manitoba, Canada: 3-133-3-142.
- Manteufel, R.D. 1996. Groundwater removal near heat dissipating waste packages. *International Conference and Engineering Exhibition*. New York, NY: American Society of Mechanical Engineers.
- Nimick, F.B. 1990a. *The Thermal Conductivity of the Topopah Spring Member at Yucca Mountain, Nevada*. SAND86-0090. Albuquerque, NM: Sandia National Laboratories.
- Nimick, F.B. 1990b. *The Thermal Conductivity of Seven Thermal/Mechanical Units at Yucca Mountain, Nevada*. SAND88-1387. Albuquerque, NM: Sandia National Laboratories.
- Nimick, F.B., and A.R. Lappin. 1985. *Thermal Conductivity of Silicic Tuffs from Yucca Mountain and Ranier Mesa, Nye County, Nevada*. SAND83-1711J. Albuquerque, NM: Sandia National Laboratories.
- Nuclear Regulatory Commission. 1995. *Phase 2 Demonstration of the NRC's Capability to Conduct a Performance Assessment for a High-Level Waste Repository*. NUREG-1464. Washington, DC: Nuclear Regulatory Commission.
- Pruess, K. 1991. *TOUGH2. A General Purpose Numerical Simulator for Multiphase Fluid and Heat Flow*. LBL-29400. Berkeley, CA: Lawrence Berkeley Laboratory.
- Pruess, K., and Y. Tsang. 1993. Modeling of strongly heatdriven flow processes a potential high-level nuclear waste repository at Yucca Mountain, Nevada. *Fourth International High-Level Radioactive Waste Management Conference*. La Grange Park, IL: American Nuclear Society.

- Pruess, K., and Y. Tsang. 1994. Thermal modeling for a potential high-level nuclear repository at Yucca Mountain, Nevada. LBL35381. Berkeley, CA: Lawrence Berkeley Laboratory.
- Sass, J.H., and A.H. Lachenburch. 1982. *Preliminary Interpretation of Thermal Data from the Nevada Test Site*. U.S. Geological Survey Open-File Report 82-9730. Washington, DC: United States Geologic Survey.
- Sass, J.H., A.H. Lachenburch, W.W. Dudley, Jr., S.S. Priest, and R.J. Monroe. 1988. *Temperature, Thermal Conductivity, and Heat Flow near Yucca Mountain, Nevada*. U.S. Geological Survey Open-File Report 87-649. Washington, DC: United States Geologic Survey.
- Scott, R.B., and J. Bonk. 1984. *Preliminary Geologic Map (1:12,000 scale) of Yucca Mountain, Nye County, Nevada, with Geologic Cross Sections*. U.S. Geological Survey Open-File Report 84-494. Denver, CO: U.S. Geological Survey.
- Seth, M.S. and P.C. Lichtner. 1996. *User's Manual for MULTIFLO: Part 1 Metra 1.0 Beta*. CNWRA 96-005. San Antonio, TX: Center for Nuclear Waste Regulatory Analyses.
- Stirewalt, G.L., and D.B. Henderson. 1995. A preliminary three-dimensional geological framework model for Yucca Mountain. *Proceedings of the Sixth Annual International Conference on High-Level Radioactive Waste Management*. La Grange Park, IL: American Nuclear Society: 116–118.
- Stirewalt, G., B. Henderson, and S. Young. 1994. *A Preliminary Three-Dimensional Geological Framework Model for Yucca Mountain, Nevada: Report to Accompany Model Transfer to the Nuclear Regulatory Commission*. CNWRA 94-023. San Antonio, TX: Center for Nuclear Regulatory Analyses.
- TRW Environmental Safety Systems, Inc. 1993. *FY93 Thermal Loading Systems Study Final Report*. B00000000-01717-57-5-00013 Rev. 01. Las Vegas, NV: TRW Environmental Safety Systems, Inc.
- TRW Environmental Safety Systems, Inc. 1994. *Initial Summary Report for Repository/Waste Package Advanced Conceptual Design*. B00000000-0-5705-00015 Rev. 00. Las Vegas, NV: TRW Environmental Safety Systems, Inc.
- TRW Environmental Safety Systems, Inc. 1995. *Total System Performance Assessment—1995: An Evaluation of the Potential Yucca Mountain Repository*. B00000000-01717-2200-00136. Las Vegas, NV: TRW Environmental Safety Systems Inc.
- Updegraff, C.D., C.E. Lee, and D.P. Gallegos. 1991. DCM-3D: *A Dual-Continuum, Three-Dimensional, Groundwater Flow Code for Unsaturated, Fractured, Porous Media*. NUREG/CR-5536. Washington, DC: Nuclear Regulatory Commission.
- U.S. Department of Energy. 1993. *Yucca Mountain Site Characterization Project Reference Information Base*. YMP/93-02. Las Vegas, NV: U.S. Department of Energy.

- U.S. Geological Survey. 1981. *Subsurface-Water Flow and Solute Transport—Federal Glossary of Selected Terms*. Subsurface-Water Glossary Working Group, Ground-Water Subcommittee, Interagency Advisory Committee on Water Data. Washington, DC: U.S. Geological Survey.
- van Genuchten, M.Th. 1980. A closed-form equation for predicting the hydraulic conductivity of unsaturated soils. *Soil Science Society of America Journal* 44: 892–898.
- Wang, J.S.Y., and T.N. Narasimhan. 1986. *Hydrologic Mechanisms Governing Partially Saturated Fluid Flow in Fractured Welded Units and Porous Nonwelded Units at Yucca Mountain*. LBL-21022. Berkeley, CA: Lawrence Berkeley Laboratory.
- Walton, J.C. 1993. Effects of evaporation and solute concentration on presence and composition of water in and around the waste package at Yucca Mountain. *Waste Management*: 13: 293–301.
- Wilson, M.L., J.H. Gauthier, R.W. Barnard, G.E. Barr, H.A. Dockery, E. Dunn, R.R. Eaton, D.C. Guerin, N. Lu, M.J. Martinez, R. Nilson, C.A. Rautman, T.H. Robey, B. Ross, E.E. Ryder, A.R. Schenker, S.A. Shannon, L.H. Skinner, W.G. Halsey, J.D. Gansemer, L.C. Lewis, A.D. Lamont, I.R. Triay, A. Meijer, and D.E. Morris. 1994. *Total-System Performance Assessment for Yucca Mountain—SNL Second Iteration (TSPA—1993) Volume 2*. SAND93-2675. Albuquerque, NM: Sandia National Laboratories.